

***Development of Rodent In Vivo Models:  
Neuroinflammation and Neurodegeneration  
relevant to Alzheimer's Disease***

A dissertation submitted for the higher degree of PhD by:

**Perdita Lucy Pugh BSc (Honours)**

**School of Psychology, Cardiff University**

(Sponsored by GlaxoSmithKline)

**2007**

UMI Number: U584909

All rights reserved

INFORMATION TO ALL USERS

The quality of this reproduction is dependent upon the quality of the copy submitted.

In the unlikely event that the author did not send a complete manuscript and there are missing pages, these will be noted. Also, if material had to be removed, a note will indicate the deletion.



UMI U584909

Published by ProQuest LLC 2013. Copyright in the Dissertation held by the Author.  
Microform Edition © ProQuest LLC.

All rights reserved. This work is protected against  
unauthorized copying under Title 17, United States Code.



ProQuest LLC  
789 East Eisenhower Parkway  
P.O. Box 1346  
Ann Arbor, MI 48106-1346

**SUMMARY OF THESIS: POSTGRADUATE RESEARCH DEGREES**

<b>STUDENT ID NUMBER:</b>	0325956
<b>CANDIDATE'S LAST NAME:</b>	PUGH
<b>CANDIDATE'S FIRST NAME(S):</b>	PERDITA LUCY
<b>SCHOOL:</b>	PSYCHOLOGY
<b>TITLE OF DEGREE:</b>	Please circle appropriate value EdD, EngD, DSW, DClinPsy, DHS, MCh, Md, MPhil, MPhil/PhD, MScD by Research, <b>PhD</b> Other, please specify .....
<b>FULL TITLE OF THESIS</b>	DEVELOPMENT OF RODENT IN VIVO MODELS: NEUROINFLAMMATION AND NEURODEGENERATION RELEVANT TO ALZHEIMERS DISEASE

STUDENT ID NUMBER: 0325956

**SUMMARY OF THESIS:**

Alzheimer's disease (AD) is characterised by A $\beta$  plaque formation, neuroinflammation and neurodegeneration. Current therapies for AD do not modify disease progression; therefore, putative anti-inflammatory and neuroprotective agents need to be assessed in rodent in vivo models that demonstrate robust and reproducible markers of neuroinflammation and neurodegeneration. This thesis interrogated the development of in vivo models comprising markers of neuroinflammation and neurodegeneration in rodent brain. The overview describes innate immunity focusing on lipopolysaccharide (LPS) as a standard immunostimulant followed by a review of AD and beta amyloid (A $\beta$ ). Current rodent in vivo models of LPS or A $\beta$ -induced neuroinflammation or neurodegeneration are also examined. Chapters 2 and 3 describe the novel application of Luminex<sup>®</sup> suspension bead array systems for the detection of LPS-induced cytokine and other intracellular proteins in brain tissue. Intraperitoneal LPS modulated interleukin (IL)-1 $\beta$ , phosphorylated (p)-I $\kappa$ B $\alpha$ , p-p38 kinase and p-JNK protein and intracerebroventricular LPS increased IL-1 $\beta$ , IL-1 $\alpha$  and tumour necrosis factor (TNF) - $\alpha$  protein in rat brain. Cytokine protein in rat brain was abrogated by dexamethasone and the  $\alpha$ 2-adrenoceptor antagonist, fluparoxan. Subsequent chapters investigate more disease relevant models of A $\beta$ -induced neuroinflammation and neurodegeneration detected by immunohistochemistry, Taqman or Luminex<sup>®</sup> techniques. Chapter 4 discussed the assessment, by western blotting, of A $\beta$  forms expelled from apparatus commonly used to inject solutions into rodent brain tissue and identifying the most consistent method of A $\beta$  delivery. Subsequent studies revealing inconsistent neurotoxicity but robust neuroinflammation following intra-hippocampal injection of A $\beta$  were described. Final chapters focus on neuroinflammation and neurodegeneration following peripheral insult (LPS or the noradrenergic neurotoxin, DSP-4) to amyloid precursor protein (APP) / presenilin 1 (PS1) transgenic mice. Peripheral administration of LPS or DSP-4 modulated markers of neuroinflammation and did not initiate neurodegeneration. The implications of the current data on the future development of in vivo models are discussed in the final chapter.

## *Abstract*

Neuroinflammation and neurodegeneration in brain tissue are prominent features in the progression of Alzheimer's disease (AD). In the assessment of putative therapies for AD, rodent in vivo models that demonstrate robust markers of neuroinflammation and neurodegeneration are crucial. Previous detection of neuroinflammation in vivo has largely relied upon immunohistochemical evidence of microglial and astrocytic activation or measurement of cytokine mRNA in rodent brain. Observing neurodegeneration in response to beta amyloid protein (A $\beta$ ) in vivo is limited. Reports of exogenous A $\beta$  induced neurotoxicity are inconsistent and a majority of APP and APP/PS1 mutant mouse lines, unless presenting intraneuronal A $\beta$  deposition, do not exhibit overt neurodegeneration. This thesis explores the development of rodent in vivo models of neuroinflammation and degeneration and, the investigation of markers of neuroinflammation and neurodegeneration in brain tissue following intraperitoneal (IP) or intracerebroventricular (ICV) injection of lipopolysaccharide (LPS), intra-hippocampal (IH) injection of synthetic A $\beta$ 1-42 or IP administration of LPS or the noradrenergic neurotoxin DSP-4 to the APP/PS1 mutant mouse line, TASTPM.

Novel application of a Luminex<sup>®</sup> suspension bead array system for the detection of LPS-induced proteins in brain tissue found that IP LPS induced increases in IL-1 $\beta$ , p-I $\kappa$ B $\alpha$ , p-p38 and p-JNK protein and ICV LPS induced increases in IL-1 $\beta$ , IL-1 $\alpha$  and TNF- $\alpha$  protein in rat brain tissue, which was abrogated by dexamethasone and the  $\alpha$ 2-adrenoceptor antagonist, fluparoxan. IH A $\beta$ 1-42 injection via Hamilton syringe, confirmed by western blotting to provide consistent delivery of A $\beta$ 1-42 into brain tissue, resulted in a small but variable increase in neurodegeneration but significant neuroinflammation. In TASTPM mice, IP injection of LPS or DSP-4 altered cytokine protein levels and DSP-4 modulated expression of GFAP and A $\beta$  plaque load. Neither challenge induced neurodegeneration in TASTPM brain tissue. These data and recent published reports suggest peripheral insults such as LPS or DSP-4 to APP or APP/PS1 mice may only affect pre-existing neuropathology, a possibility that merits further investigation. Variability in A $\beta$ 1-42-induced

neurotoxicity following IH injection indicates that damage caused by exogenous A $\beta$  may not provide a sufficient window of neuronal cell death suitable for screening neuroprotective agents. The data described here has implications on future development of models of neuroinflammation and neurodegeneration for screening putative therapeutic strategies for AD.

## *Acknowledgements*

I would like to thank all my colleagues at GlaxoSmithKline, Harlow, particularly the pharmacology & physiology team, for all their advice and support throughout the duration of my Ph.D and Martin Vidgeon-Hart for his perseverance in reading my first drafts. I also extend my gratitude to the laboratory animal sciences team at GlaxoSmithKline for providing care to the animals and to Simon Bate and Gemma Leeson for all their help and advice with the statistical analysis.

Thank you to my academic supervisor, Mark Good, for his guidance and encouragement during the writing of this thesis.

To all of my friends and family, I appreciate all the patience and understanding over the past few years, especially Sharlin – we have discussed Ph.Ds for so long, I promise we will find other topics of conversation!

Finally, Dave, No more long evenings and weekends on your own! Thank you for your tireless understanding and unwavering belief in me. Where would I be without you?

# Contents

<b>Abstract</b> .....	<b>1</b>
<b>Acknowledgements</b> .....	<b>3</b>
<b>Contents</b> .....	<b>4</b>
<b>List of figures</b> .....	<b>13</b>
<b>List of Tables</b> .....	<b>21</b>
<b>Abbreviations</b> .....	<b>22</b>
<b>CHAPTER 1: General Introduction</b> .....	<b>26</b>
<b>1.1 Overview of thesis</b> .....	<b>26</b>
<b>1.2 Innate immunity</b> .....	<b>26</b>
1.2.1 Effector cells of innate immunity.....	27
1.2.2 Cytokines .....	28
1.2.2.1 Cytokine Families .....	29
1.2.3 Cytokine transcription.....	31
1.2.4 Signal transducing pathways.....	32
1.2.4.1 Involvement of p38 pathway in inflammation.....	33
1.2.4.2 Involvement of JNK pathway in inflammation.....	34
1.2.4.3 Involvement of ERK pathway in inflammation.....	34
1.2.5 The hypothalamic-pituitary-adrenal (HPA) axis.....	35
1.2.5.1 Cytokine-induced glucocorticoid production.....	35
1.2.5.2 Glucocorticoid (GC) modulation of cytokine induction .....	36
1.2.6 Lipopolysaccharide (LPS).....	37
1.2.6.1 LPS: Mechanism of action .....	37
1.2.6.2 Communication between periphery and CNS.....	38
1.2.7 Detection of cytokine expression.....	39
1.2.7.1 Cytokine protein detection using xMAP® technology .....	40
1.2.7.2 Advantages of using xMAP® technology .....	42
1.2.7.3 Detection of LPS-induced cytokine protein in brain tissue .....	42
<b>1.3 Alzheimer's disease (AD)</b> .....	<b>43</b>

1.3.1	Epidemiology .....	43
1.3.2	Early-onset Familial AD (FAD) .....	44
1.3.3	Sporadic AD (SAD) .....	44
1.3.4	Beta Amyloid (A $\beta$ ) .....	46
1.3.4.1	Amyloid precursor protein (APP) .....	46
1.3.4.2	A $\beta$ : mechanism of action .....	47
1.3.4.3	Role of different A $\beta$ forms in neurotoxicity .....	50
1.3.5	Neurodegeneration in AD .....	51
1.3.6	Neuroinflammation in AD .....	52
1.3.6.1	Cell-mediated inflammation .....	52
1.3.6.2	Cytokines .....	53
1.3.6.3	Chemokines .....	54
1.3.6.4	Other markers of neuroinflammation .....	54
1.3.7	Anti-inflammatory agents as disease modifying therapy for AD .....	54
1.4	<i>Neuroinflammation and neurodegeneration in preclinical models</i> .....	55
1.4.1	LPS – in vivo models .....	55
1.4.1.1	LPS-induced neuroinflammation .....	55
1.4.1.2	LPS-induced neurodegeneration .....	56
1.4.2	A $\beta$ – Exogenous in vivo models .....	57
1.4.2.1	Exogenous A $\beta$ -induced neuroinflammation .....	57
1.4.2.2	Exogenous A $\beta$ -induced neurodegeneration .....	57
1.4.3	A $\beta$ – Endogenous in vivo models – Transgenic mice .....	59
1.4.3.1	Endogenous amyloid-induced neuroinflammation .....	59
1.4.3.2	Endogenous amyloid-induced neurodegeneration .....	60
1.5	<i>Thesis Objectives</i> .....	61

**CHAPTER 2: Peripheral administration of LPS – an in vivo model of neuroinflammation? .....** 62

2.1	<i>Introduction</i> .....	62
2.1.1	Glucocorticoid (GC) modulation and inflammation .....	62
2.1.2	P38 $\alpha$ inhibition and inflammation .....	63
2.1.3	$\alpha$ 2-adrenoceptor antagonism and inflammation .....	64
2.1.4	Chapter Aims .....	65
2.2	<i>Materials &amp; Methods</i> .....	66
2.2.1	Materials .....	66
2.2.2	Animals .....	66
2.2.3	Drug administration .....	66

2.2.4	Sample collection .....	67
2.2.5	Cytokine protein determination.....	67
2.2.5.1	Sample preparation.....	67
2.2.5.2	Luminex <sup>®</sup> suspension bead array – cytokine analysis .....	68
2.2.6	Phosphoprotein determination .....	69
2.2.6.1	Sample preparation.....	69
2.2.6.2	Total protein assay .....	69
2.2.6.3	Luminex <sup>®</sup> suspension bead array – phosphoprotein analysis .....	69
2.2.7	Nitric Oxide Assay.....	70
2.2.8	Quantification of cortical mRNA expression - TaqMan.....	71
2.2.9	Data Analysis .....	72
2.3	<i>Protocols</i> .....	73
2.3.1	Study 1: Timecourse of cytokine protein induction.....	73
2.3.2	Study 2: Cytokine protein detection throughout brain tissue.....	73
2.3.3	Study 3: Effect of Dexamethasone on cytokine expression.....	73
2.3.4	Study 4: Cytokine mRNA and intracellular protein expression .....	74
2.3.5	Study 5: Effect of p38 inhibition and $\alpha$ 2 adrenoceptor antagonism on cytokine expression.....	74
2.4	<i>Results</i> .....	74
2.4.1	Study 1: Timecourse of cytokine protein in brain and plasma.....	74
2.4.1.1	Cytokine protein in brain .....	74
2.4.1.2	Cytokine protein in plasma .....	77
2.4.2	Study 2: Cytokine protein throughout brain tissue .....	78
2.4.2.1	Cytokine protein in brain .....	78
2.4.2.2	Cytokine protein in plasma .....	81
2.4.3	Study 3: Effect of Dexamethasone on cytokine expression.....	82
2.4.3.1	Cytokine mRNA changes in frontal cortex.....	82
2.4.3.2	Cytokine protein in brain .....	84
2.4.3.3	Cytokine protein in plasma .....	86
2.4.4	Study 4: Cytokine mRNA and intracellular protein expression .....	87
2.4.4.1	LPS-induced mRNA expression in frontal cortex .....	87
2.4.4.2	LPS-induced intracellular protein phosphorylation .....	89
2.4.4.3	LPS-induced plasma nitrite.....	91
2.4.5	Study 5: Effect of p38 inhibition and $\alpha$ 2 adrenoceptor antagonism on cytokine expression.....	91
2.4.5.1	Cytokine protein in brain .....	91
2.4.5.2	Cytokine protein in plasma .....	96

2.4.5.3	LPS-induced plasma nitrite .....	99
2.5	<i>Discussion</i> .....	100
2.5.1	Detection of cytokine protein in brain and plasma .....	100
2.5.2	Communication of peripheral inflammation to the brain.....	100
2.5.3	Pharmacological manipulation of cytokine protein in brain tissue.....	103
2.5.3.1	Glucocorticoid treatment - dexamethasone.....	103
2.5.3.2	$\alpha$ 2-adrenoceptor antagonism - fluparoxan.....	104
2.5.3.3	P38 inhibition – GW569293 .....	104

**CHAPTER 3: Central administration of LPS – confirming anti-inflammatory activity in brain tissue .....** 107

3.1	<i>Introduction</i> .....	107
3.1.1	Intracerebroventricular (ICV) injection .....	108
3.1.2	Evidence of central cytokine induction by ICV LPS.....	108
3.1.3	Chapter Aims .....	109
3.2	<i>Materials &amp; Methods</i> .....	109
3.2.1	Materials.....	109
3.2.2	ICV cannulation .....	109
3.2.3	Drug administration .....	110
3.2.4	ICV administration and cytokine determination.....	110
3.2.5	Data Analysis .....	111
3.3	<i>Protocols</i> .....	111
3.3.1	Study 6: Pre-treatment of dexamethasone or GW569293: 20 $\mu$ g ICV LPS 111	
3.3.2	Study 7: Pretreatment of dexamethasone: 5 $\mu$ g ICV LPS.....	112
3.3.3	Study 8: Pretreatment of fluparoxan or GW569293: 5 $\mu$ g ICV LPS ....	112
3.4	<i>Results</i> .....	112
3.4.1	Study 6: Pre-treatment of dexamethasone or GW569293: 20 $\mu$ g ICV LPS 112	
3.4.1.1	Cytokine protein in brain .....	112
3.4.1.2	Cytokine protein in plasma .....	113
3.4.2	Study 7: Pretreatment of dexamethasone: 5 $\mu$ g ICV LPS.....	117
3.4.2.1	Cytokine protein in brain .....	117
3.4.2.2	Cytokine protein in plasma .....	119
3.4.3	Study 8: Pretreatment of fluparoxan or GW569293: 5 $\mu$ g ICV LPS ....	120
3.4.3.1	Cytokine protein in brain .....	120

3.4.3.2	Cytokine protein in plasma .....	123
3.5	<i>Discussion</i> .....	124
3.5.1	Central vs. peripheral cytokine response .....	124
3.5.2	Central efficacy of peripherally administered anti-inflammatory agents 125	
3.5.2.1	Glucocorticoid treatment - Dexamethasone.....	125
3.5.2.2	$\alpha 2$ adrenoceptor antagonism - Fluparoxan .....	126
3.5.2.3	P38 inhibition - GW569293 .....	127
3.5.3	The limitations of in vivo LPS-induced neuroinflammation models...	128
 <b>CHAPTER 4: Injection of A<math>\beta</math>1-42 into the brain of the adult rat: neurodegeneration &amp; neuroinflammation.....</b>		
4.1	<i>Introduction</i> .....	130
4.1.1	Delivery of A $\beta$ into the rodent brain.....	130
4.1.2	A $\beta$ aggregation process.....	131
4.1.3	Western blot analysis of A $\beta$ 1-42 forms .....	132
4.1.4	Chapter Aims .....	132
4.2	<i>Materials &amp; Methods</i> .....	133
4.2.1	Materials.....	133
4.2.2	A $\beta$ 1-42 preparation .....	133
4.2.3	Gel analysis of amyloid samples.....	133
4.2.4	Intra-hippocampal (IH) direct injection surgery .....	134
4.2.5	Sample collection .....	135
4.2.6	Immunohistochemistry.....	135
4.2.6.1	Primary antibody staining .....	136
4.2.6.2	Quantification of immunohistochemical staining .....	137
4.2.6.3	Detection of fibrillar A $\beta$ .....	137
4.2.7	Data Analysis .....	137
4.3	<i>Protocols</i> .....	138
4.3.1	Study 9: Western blot analysis of the expulsion of the A $\beta$ 1-42 fragment from apparatus.....	138
4.3.1.1	Lowest concentration of aggregated A $\beta$ 1-42 used in vivo .....	138
4.3.1.2	Oligomeric A $\beta$ 1-42 using minipump .....	138
4.3.1.3	Concentrations of A $\beta$ 1-42 used in vivo to induce neurotoxicity.	139
4.3.2	Study 10: A $\beta$ 1-42 in 0.35% acetonitrile/0.1M PBS.....	139
4.3.3	Study 11: A $\beta$ 1-42 in 0.035% acetonitrile/0.1M PBS or 0.1M PBS alone	
	139	

4.3.4	Study 12: A $\beta$ 1-42 vs. A $\beta$ 42-1 in 0.1M PBS alone .....	140
4.4	<i>Results</i> .....	140
4.4.1	Study 9: Western blot comparison of A $\beta$ 1-42 preparations for direct hippocampal injection .....	140
4.4.1.1	A $\beta$ 1-42 expulsion: polypropylene tubing and Hamilton syringe.	140
4.4.1.2	Oligomeric A $\beta$ 1-42 using minipump .....	140
4.4.1.3	Concentrations of A $\beta$ 1-42 used in vivo to induce neurotoxicity.	143
4.4.2	Study 10: IH A $\beta$ 1-42 (1nmol) in 0.35% acetonitrile/0.1M PBS.....	145
4.4.2.1	Presence of amyloid .....	145
4.4.2.2	Neurodegeneration .....	145
4.4.2.3	Neuroinflammation .....	148
4.4.3	Study 11: IH A $\beta$ 1-42 (1nmol) in 0.035% acetonitrile/0.1M PBS or 0.1M PBS alone .....	149
4.4.3.1	Presence of amyloid .....	149
4.4.3.2	Neurodegeneration .....	150
4.4.3.3	Neuroinflammation .....	152
4.4.4	Study 12: IH A $\beta$ 1-42 (1nmol) vs. A $\beta$ 42-1 (1nmol) in 0.1M PBS alone	154
4.4.4.1	Presence of amyloid .....	154
4.4.4.2	Neurodegeneration .....	156
4.4.4.3	Neuroinflammation .....	158
4.5	<i>Discussion</i> .....	159
4.5.1	Delivery of A $\beta$ 1-42 forms into rodent brain .....	159
4.5.2	Presence of A $\beta$ in brain tissue following intra-hippocampal injection	160
4.5.3	A $\beta$ - induced neurodegeneration .....	161
4.5.4	A $\beta$ 1-42 - induced neuroinflammation.....	162

**CHAPTER 5: Single and repeated administration of LPS to TASTPM APP/PS1 overexpressing mice .....** 165

5.1	<i>Introduction</i> .....	165
5.1.1	Peripheral infection in AD .....	166
5.1.2	LPS administration to APP (&PS1) overexpressing mice .....	166
5.1.3	The TASTPM APP/PS1 overexpressing transgenic mouse model.....	167
5.1.4	Chapter Aims .....	168
5.2	<i>Materials &amp; Methods</i> .....	168
5.2.1	Animals .....	168
5.2.2	Materials.....	168

5.2.3	Treatment .....	169
5.2.4	Sample collection .....	169
5.2.5	Cytokine protein determination.....	169
5.2.5.1	Sample preparation.....	169
5.2.5.2	Luminex <sup>®</sup> suspension bead array – cytokine analysis .....	170
5.2.6	A $\beta$ ELISA .....	170
5.2.7	Immunohistochemistry.....	171
5.2.7.1	Amyloid (1E8) Staining .....	172
5.2.7.2	NeuN .....	172
5.2.7.3	GFAP Staining .....	172
5.2.7.4	Macrophage (CD68) Staining .....	172
5.2.7.5	Quantification of A $\beta$ plaque deposition, neuronal cell loss and GFAP	173
5.2.8	Data Analysis .....	173
5.3	<i>Protocols</i> .....	173
5.3.1	Study 13: Acute administration of LPS in TASTPM mice.....	173
5.3.2	Study 14: Inflammation and neurodegeneration following repeated LPS administration in TASTPM mice.....	174
5.4	<i>Results</i> .....	174
5.4.1	Study 13: Acute LPS administration of TASTPM mice.....	174
5.4.1.1	Cytokine protein in brain .....	174
5.4.1.2	Cytokine protein in plasma .....	181
5.4.2	Study 14: Repeated LPS administration of TASTPM mice .....	185
5.4.2.1	Cytokine protein in brain at 48 hours.....	185
5.4.2.2	Cytokine protein in plasma at 2.5hrs .....	185
5.4.2.3	Cytokine protein in plasma at 48hrs .....	188
5.4.2.4	Cell-mediated neuroinflammation .....	189
5.4.2.5	A $\beta$ load.....	191
5.4.2.6	NeuN .....	193
5.5	<i>Discussion</i> .....	196
5.5.1	LPS induced neuroinflammation - APP/PS1 transgenic mice .....	196
5.5.2	Modulation of A $\beta$ load by LPS – APP/PS1 transgenic mice.....	198
5.5.3	LPS induced neurodegeneration – APP/PS1 transgenic mice .....	199
 <b>CHAPTER 6: Repeated DSP-4 administration to TASTPM APP/PS1 transgenic mice.....</b>		
6.1	<i>Introduction</i> .....	201

6.1.1	Role of NA in neuroinflammation & neurodegeneration .....	201
6.1.2	Depletion of NA following DSP4 administration.....	202
6.1.3	Chapter Aims .....	203
6.2	<i>Materials &amp; Methods</i> .....	203
6.2.1	Animals .....	203
6.2.2	Materials.....	204
6.2.3	Treatment .....	204
6.2.4	Sample collection.....	204
6.2.5	Ex-vivo neurochemistry- HPLC .....	205
6.2.5.1	Tissue Preparation.....	205
6.2.5.2	High Performance Liquid Chromatography (HPLC)-ECD analysis 205	
6.2.6	Immunohistochemistry.....	206
6.2.7	TaqMan analyses.....	206
6.2.8	Data Analysis .....	207
6.3	<i>Protocols</i> .....	208
6.3.1	Study 15: Acute DSP-4 effects on NA (5mg/kg and 50mg/kg).....	208
6.3.2	Study 16: Repeated administration of DSP-4 to TASTPM mice.....	208
6.4	<i>Results</i> .....	209
6.4.1	Study 15: acute DSP-4 effects on NA (5mg/kg and 50mg/kg).....	209
6.4.2	Study 16: Repeated administration of DSP-4 to TASTPM mice.....	211
6.4.2.1	NA depletion following chronic DSP4 treatment.....	211
6.4.2.2	Neuroinflammation following chronic DSP-4 treatment.....	213
A.	Taqman.....	213
B.	Immunohistochemistry (IHC).....	216
6.4.2.3	Amyloid plaque load .....	218
6.4.2.4	Neurodegeneration following chronic DSP-4 treatment.....	221
A.	Noradrenergic depletion in the LC.....	221
B.	Neurodegeneration in hippocampus.....	224
6.5	<i>Discussion</i> .....	227
6.5.1	Acute effect of DSP-4 on NA (5mg/kg and 50mg/kg) .....	227
6.5.2	Repeated administration of DSP-4 to TASTPM mice .....	227
6.5.2.1	Neuroinflammation .....	228
6.5.2.2	Neurodegeneration .....	230
<b>CHAPTER 7: General Discussion &amp; Conclusions.....</b>		<b>232</b>
7.1	<i>Discussion</i> .....	232

7.1.1	Luminex <sup>®</sup> - cytokine detection in plasma and brain tissue.....	232
7.1.2	Communication of inflammation between the brain and periphery.....	234
7.1.3	LPS models of neuroinflammation – utility for compound screening.	235
7.1.4	Injection of exogenous A $\beta$ in vivo.....	237
7.1.5	A $\beta$ models of neuroinflammation & neurodegeneration .....	239
7.1.6	APP & APP/PS1 transgenic mouse models.....	242
7.1.7	Conclusion and future studies .....	243
	<i>Publications</i> .....	245
	<i>References</i> .....	243

## *List of figures*

Figure 1.1: Schematic representation of innate immune system.....	28
Figure 1.2: Schematic representation of TLR4 signalling cascade.....	31
Figure 1.3: Overview of the MAP Kinase cascade.....	33
Figure 1.4: Luminex <sup>®</sup> polystyrene microsphere beads .....	41
Figure 1.5: Detection of analyte by Luminex <sup>®</sup> bead suspension array .....	41
Figure 1.6: Detection of analyte-bead complex by Luminex <sup>®</sup> 100 <sup>TM</sup> system .....	42
Figure 1.7: Schematic representation of APP processing .....	47
Figure 1.8: Schematic representation of the postulated mechanisms of A $\beta$ -mediated neurodegeneration .....	50
Figure 2.1: Cytokine protein in the cortex (A) and hippocampus (B) of adult rats (n = 8) by 2 and 6 hours post IP LPS administration .....	76
Figure 2.2: Cytokine protein in the cortex (A) and hippocampus (B) of adult rats (n = 8) by 2 and 6 hours post IP LPS administration .....	77
Figure 2.3A: Cytokine protein in the cortex (A) and hippocampus (B) and striatum (C) of adult rats (n = 8) by 6 hours post IP LPS administration .....	79
Figure 2.3B: Cytokine protein in the hypothalamus (D), cerebellum (E) and plasma (F) of adult rats (n = 8) by 6 hours post IP LPS administration.....	80
Figure 2.4: Effect of dexamethasone treatment on LPS-induced TNF $\alpha$ (A), IL6 (B) and IL1 $\beta$ (C) mRNA expression in the cortex of adult rats by 6 hours post IP LPS administration.....	83
Figure 2.5: Effect of dexamethasone pre-treatment on cytokine protein in the cortex (A) and hippocampus (B) of adult rats (n = 8) by 6 hours post IP LPS administration .....	85
Figure 2.6: Effect of dexamethasone pre-treatment on cytokine protein in the cortex	

(A) and hippocampus (B) of adult rats (n = 8) by 6 hours post IP LPS administration .....	86
Figure 2.7: TNF $\alpha$ (A), IL6 (B) and IL1 $\beta$ (C) mRNA expression in the cortex of adult rats by 2 and 6 hours post IP LPS administration .....	88
Figure 2.8: Phosphorylation of cortical p38, hippocampal I $\kappa$ B $\alpha$ and cortical JNK intracellular protein expression in adult rats by 2 and 6 hours post IP LPS administration.....	90
Figure 2.9: Plasma nitrite levels in adult rats by 2 and 6 hours post IP LPS administration.....	91
Figure 2.10: Effect of dexamethasone pre-treatment on cytokine protein in the cortex (A) and hippocampus (B) of adult rats (n = 8) by 6 hours post IP LPS administration .....	93
Figure 2.11: Effect of fluparoxan pre-treatment on cytokine protein in the cortex (A) and hippocampus (B) of adult rats (n = 8) by 6 hours post IP LPS administration ...	94
Figure 2.12: Effect of GW569293 pre-treatment on cytokine protein in the cortex (A) and hippocampus (B) of adult rats (n = 8) by 6 hours post IP LPS administration ...	95
Figure 2.13: Effect of dexamethasone pre-treatment on cytokine protein in the cortex (A) and hippocampus (B) of adult rats (n = 8) by 6 hours post IP LPS administration .....	97
Figure 2.14: Effect of fluparoxan pre-treatment on cytokine protein in the plasma of adult rats (n = 8) by 6 hours post IP LPS administration.....	98
Figure 2.15: Effect of GW569293 pre-treatment on cytokine protein in the plasma of adult rats (n = 8) by 6 hours post IP LPS administration.....	98
Figure 2.16: Effect of GW569293 or fluparoxan pre-treatment on plasma nitrite levels in adult rats by 6 hours post IP LPS administration .....	99
Figure 3.1: Effect of dexamethasone pre-treatment on cytokine protein in the cortex (A) and hippocampus (B) of adult rats (n = 8-10) by 2 hours post ICV LPS (20 $\mu$ g) administration.....	114
Figure 3.2: Effect of GW569293 pre-treatment on cytokine protein in the cortex (A) and hippocampus (B) of adult rats (n = 8-10) by 2 hours post ICV LPS (20 $\mu$ g)	

administration.....	115
Figure 3.3: Effect of dexamethasone pre-treatment on cytokine protein in plasma of adult rats (n = 8-10) by 2 hours post ICV LPS (20µg) administration .....	116
Figure 3.4: Effect of GW569293 pre-treatment on cytokine protein in plasma of adult rats (n = 8-10) by 2 hours post ICV LPS (20µg) administration .....	116
Figure 3.5: Effect of dexamethasone pre-treatment on cytokine protein in the cortex (A) and hippocampus (B) of adult rats (n = 4-7) by 2 hours post ICV LPS (5µg) administration.....	118
Figure 3.6: Effect of dexamethasone pre-treatment on cytokine protein in plasma of adult rats (n = 4-7) by 2 hours post ICV LPS (5µg) administration .....	119
Figure 3.7: Effect of fluparoxan pre-treatment on cytokine protein in cortex (A) and hippocampus (B) of adult rats (n = 6-8) by 2 hours post ICV LPS (5µg) administration.....	121
Figure 3.8: Effect of GW569293 pre-treatment on cytokine protein in cortex (A) and hippocampus (B) of adult rats (n = 6-8) by 2 hours post ICV LPS (5µg) administration.....	122
Figure 3.9: Effect of fluparoxan pre-treatment on cytokine protein in plasma of adult rats (n = 6-8) by 2 hours post ICV LPS (5µg) administration .....	123
Figure 3.10: Effect of GW569293 pre-treatment on cytokine protein in plasma of adult rats (n = 6-8) by 2 hours post ICV LPS (5µg) administration .....	124
Figure 4.1: Schematic representation of the methods currently available for delivery of Aβ into rodent brain: direct injection (A), repeated administration (B) and chronic infusion (C) .....	131
Figure 4.2: Western blots demonstrating the expulsion of Aβ1-42 forms from Hamilton syringe (A) and polypropylene tubing (B).....	142
Figure 4.3: Western blot demonstrating the expulsion of Aβ1-42 forms from minipump. ....	143
Figure 4.4: Western blots demonstrating the expulsion of Aβ1-42 forms from 10µl Hamilton syringe using protocols described in the literature (A) or standard preaggregated Aβ1-42 (B). ....	144

Figure 4.5: Representative photomicrographs of coronal sections of the CA1 (A) and dentate gyrus (B) stained for amyloid (1E8) in A $\beta$ 1-42 intra-hippocampal injected rats ..... 145

Figure 4.6: Representative photomicrographs of coronal sections of the hippocampus stained with NeuN in vehicle (A, C) and A $\beta$ 1-42 (B, D) intra-hippocampal injected rats ..... 146

Figure 4.7: Quantification of NeuN positive cells in hippocampus of vehicle and A $\beta$ 1-42 intra-hippocampal injected rats..... 147

Figure 4.8: Measurement of mediolateral lesion in vehicle and A $\beta$ 1-42 intra-hippocampal injected rats..... 147

Figure 4.9: Representative photomicrographs of coronal sections of the hippocampus stained for ED1 positive macrophage and microglia in vehicle (A, C) and A $\beta$ 1-42 (B, D) intra-hippocampal injected rats..... 148

Figure 4.11: Measurement of the average amyloid deposit in the hippocampus of A $\beta$ 1-42 bilateral intra-hippocampally injected rats ..... 150

Figure 4.12: Representative photomicrographs of coronal sections of the hippocampus stained for NeuN in vehicle - PBS (A), vehicle - acetonitrile/PBS (B), A $\beta$ 1-42 - PBS (C) and A $\beta$ 1-42 - acetonitrile/PBS (D) in bilateral intra-hippocampally injected rats..... 151

Figure 4.13: Quantification of NeuN positive cells in vehicle and A $\beta$ 1-42 bilateral intra-hippocampally injected rats ..... 152

Figure 4.14: Measurement of mediolateral lesion in vehicle and A $\beta$ 1-42 intra-hippocampal injected rats..... 152

Figure 4.15: Representative photomicrographs of ED1 staining in hippocampus of vehicle - PBS (A) vehicle - acetonitrile/PBS (B), A $\beta$ 1-42 - PBS (C) & A $\beta$ 1-42 - acetonitrile/PBS (D) bilateral intra-hippocampally injected rats ..... 153

Figure 4.16: Quantification of the percentage stained area of ED1 positive cells in vehicle and A $\beta$ 1-42 intra-hippocampal injected rats ..... 154

Figure 4.17: Representative photomicrographs of coronal sections of the CA1 (A) and dentate gyrus (B) stained for amyloid (1E8) in A $\beta$ 1-42 intra-hippocampal injected rats ..... 155

Figure 4.18: Representative photomicrographs of coronal sections of the cortex of a TASTPM mouse (A) and the A $\beta$ 1-42 deposit in intra-hippocampal injected rats .. 155

Figure 4.19: Representative photomicrographs of coronal sections of the hippocampus stained for NeuN following intra-hippocampal (n=12) vehicle (A) A $\beta$ 42-1 (B) and A $\beta$ 1-42 (C) ..... 156

Figure 4.20: Quantification of NeuN positive cells in vehicle and A $\beta$ 1-42 intra-hippocampal injected rats..... 157

Figure 4.21: Measurement of mediolateral lesion in vehicle and A $\beta$ 1-42 intra-hippocampal injected rats..... 157

Figure 4.22: Representative photomicrographs of coronal sections of the hippocampus stained for ED1 positive macrophage and microglia in vehicle (A), A $\beta$ 42-1 (B) and A $\beta$ 1-42 (C) intra-hippocampal injected rats..... 158

Figure 4.23: Quantification of the percentage stained area of ED1 positive cells in vehicle and A $\beta$ 1-42 intra-hippocampal injected rats ..... 159

Figure 5.1: IL6 protein in the cortex (A), hippocampus (B) of a C57BL6/J control or TASTPM transgenic mouse (n=6-9 per group) by 2.5 hours post a single IP LPS administration..... 176

Figure 5.2 IL1 $\beta$  protein in the cortex (A), hippocampus (B) of a C57BL6/J control or TASTPM transgenic mouse (n=6-9 per group) by 2.5 hours post a single IP LPS administration..... 177

Figure 5.3: TNF $\alpha$  protein in the cortex (A), hippocampus (B) of a C57BL6/J control or TASTPM transgenic mouse (n=6-9 per group) by 2.5 hours post a single IP LPS administration..... 178

Figure 5.4: MIP1 $\alpha$  protein in the cortex (A), hippocampus (B) of a C57BL6/J control or TASTPM transgenic mouse (n=6-9 per group) by 2.5 hours post a single IP LPS administration..... 179

Figure 5.5: IL10 protein in the cortex (A), hippocampus (B) of a C57BL6/J control or TASTPM transgenic mouse (n=6-9 per group) by 2.5 hours post a single IP LPS administration..... 180

Figure 5.6: IL1 $\beta$  protein in plasma of a C57BL6/J control or TASTPM transgenic mouse (n=6-9 per group) by 2.5 hours post a single IP LPS administration ..... 182

Figure 5.7: IL6 (A) and TNF $\alpha$  (B) protein in plasma of a C57BL6/J control or TASTPM transgenic mouse (n=6-9 per group) by 2.5 hours post a single IP LPS administration..... 183

Figure 5.8: MIP-1 $\alpha$  (A) and IL-10 (B) protein in plasma of a C57BL6/J control or TASTPM transgenic mouse (n=6-9 per group) by 2.5 hours post a single IP LPS administration..... 184

Figure 5.9: Effect of repeated IP administration of LPS on cytokine protein in the cortex (A), hippocampus (B) of C57BL6/J and TASTPM mice (n=10-12 per group) by 48 hours post the last IP LPS administration ..... 186

Figure 5.10: Effect of repeated IP administration of LPS on plasma IL1 $\beta$ , TNF $\alpha$ , and MIP1 $\alpha$  protein (A) and plasma IL6 protein (B) of C57BL6/J and TASTPM mice(n=10-12 per group) by 2.5 hours post the last IP LPS administration..... 187

Figure 5.11: Effect of repeated IP administration of LPS on plasma IL6, IL1 $\beta$ , TNF $\alpha$ , and MIP1 $\alpha$  protein of C57BL6/J and TASTPM mice (n=10-12 per group) by 48 hours post the last IP LPS administration ..... 188

Figure 5.12: Representative photomicrographs of coronal sections of the hippocampus and cortex stained for GFAP in vehicle TASTPM (A, B) and LPS TASTPM (C, D) mice..... 189

Figure 5.13: Effect of repeated IP administration of LPS on GFAP in the cortex (A) and hippocampus (B) in C47BL6/J or TASTPM mice..... 190

Figure 5.14: Representative photomicrographs of coronal sections of the hippocampus and cortex stained for CD68 in vehicle TASTPM (A) and LPS TASTPM (B) mice..... 191

Figure 5.15: Effect of repeated IP administration of LPS on brain A $\beta$ 1-40 (A) and A $\beta$ 1-42 (B) in TASTPM mice ..... 191

Figure 5.16: Representative photomicrographs of coronal sections of the cortex stained for A $\beta$  deposits in vehicle TASTPM (A, B) and LPS TASTPM (C, D) mice ..... 192

Figure 5.17: Effect of repeated IP administration of LPS on A $\beta$  load in the cortex (A), hippocampus (B) and whole brain (C) of C57BL6J and TASTPM mice ..... 193

Figure 5.18: Representative photomicrographs of coronal sections of the

hippocampus and cortex stained for NeuN positive cells in vehicle C57BL6/J (A, B) and TASTPM (C, D) mice and LPS treated C57BL6/J (E, F) and TASTPM (G, H) TASTPM mice ..... 194

Figure 5.19: Effect of repeated IP administration of LPS on NeuN staining in the cortex (A) and hippocampus (B) of C57BL6/J and TASTPM mice..... 195

Figure 6.1: Comparison of 5mg/kg and 50mg/kg DSP-4 on NA in left cortex (A), right cortex (B), left hippocampus (C), right hippocampus (D) and whole cerebellum (E) in male C57BL6/J mice ..... 210

Figure 6.2: NA depletion in cortex and hippocampus of 8 month and 11 month DSP-4 and vehicle treated C57BL6/J and TASTPM mice..... 212

Figure 6.3: Cortical inflammatory mRNA markers in 8 month and 11 month vehicle and DSP-4 treated C57BL6/J and TASTPM transgenic mice ..... 214

Figure 6.4: Cortical inflammatory mRNA markers in 8 month and 11 month vehicle and DSP-4 treated C57BL6/J and TASTPM transgenic mice ..... 215

Figure 6.5: Representative photomicrographs of sagittal sections of the cortex stained for GFAP from 8 month vehicle and DSP-4 treated C57BL6/J and TASTPM transgenic mice..... 216

Figure 6.6: Representative photomicrographs of sagittal sections of the cortex stained for GFAP from 11 month vehicle and DSP-4 treated C57BL6/J and TASTPM transgenic mice..... 217

Figure 6.7: Representative photomicrographs of sagittal sections of the cortex stained for CD68 from 8 and 11 month vehicle and DSP-4 treated TASTPM transgenic mice ..... 218

Figure 6.8: Representative photomicrographs of sagittal sections of the cortex and hippocampus stained for amyloid from 8 month vehicle and DSP-4 treated C57BL6/J and TASTPM transgenic mice..... 219

Figure 6.9: Representative photomicrographs of sagittal sections of the cortex and hippocampus stained for amyloid from 11 month vehicle and DSP-4 treated C57BL6/J and TASTPM transgenic mice..... 220

Figure 6.10: Percentage of amyloid stained area in cortex and hippocampus of 8 month and 11 month vehicle and DSP-4 treated C57BL6/J and TASTPM transgenic

mice.....	221
Figure 6.11: Representative photomicrographs of sagittal sections of the locus coeruleus stained for tyrosine hydroxylase (TH) from 11 month vehicle and DSP-4 treated C57BL6/J mice.....	222
Figure 6.12: Representative photomicrographs of sagittal sections of the locus coeruleus stained for tyrosine hydroxylase (TH) from 11 month vehicle and DSP-4 treated TASTPM transgenic mice.....	223
Figure 6.13: TH cell count in the locus coeruleus (LC) of 8 month and 11 month vehicle and DSP-4 treated C57BL6/J and TASTPM transgenic mice.....	224
Figure 6.14: Representative photomicrographs of sagittal sections of the hippocampus stained for NeuN from 8 and 11 month vehicle and DSP-4 treated TASTPM transgenic mice.....	225
Figure 6.15: NeuN cell count in the hippocampus of 8 month (A) and 11 month (B) vehicle and DSP-4 treated C57BL6/J and TASTPM transgenic mice.....	226

## *List of Tables*

Table 1.1: Overview of selected cytokine origin and roles.....	30
Table 2.1: TaqMan reagent sequences .....	72
Table 6.1: TaqMan reagent sequences.....	207

## *Abbreviations*

A $\beta$	Beta Amyloid
ABAD	Amyloid $\beta$ -peptide binding protein alcohol dehydrogenase
ACT	Antichymotrypsin
ACTH	Adrenocorticotrophin
AD	Alzheimer's disease
AGE	Advanced Glycation Endproducts
ANOVA	Analysis of Variance
AP	Activator protein
APC	Antigen presenting cell
APO	Apolipoprotein
APP	Amyloid precursor protein
ATF	Activating transcription factor
VP	Vasopressin
BACE1	$\beta$ -site APP cleaving enzyme
BBB	Blood brain barrier
BSA	Bovine serum albumin
cAMP	Cyclic adenosine monophosphate
ChAT	Choline acetyltransferase
ChP	Choroid Plexus
CNS	Central Nervous System
COX	Cyclo-oxygenase
CRF	Corticotrophin-releasing factor
CSF	Cerebrospinal fluid
CVO	Circumventricular organ
D $\beta$ H	Dopamine - $\beta$ - hydroxylase
DEX	Dexamethasone
DMSO	Dimethylsulfoxide
DNA	Deoxynucleic acid
DSP-4	N- (chloroethyl)-N-ethyl-2-bromobenzylamine
DTT	Dithiothreitol

EDTA	Ethylene diamine tetra acetic acid
ELISA	Enzyme-linked immunosorbant assays
ER	Endoplasmic reticulum
ERK	Extracellular signal-regulated kinase
FAD	Familial Alzheimer's disease
FLU	Fluparoxan
GAPDH	Glyceraldehyde – 3 – phosphate dehydrogenase
GC	Glucocorticoid
GCR	Glucocorticoid receptor
GFAP	Glial fibrillary acidic protein
GRE	Glucocorticoid response element
5-HT	5-Hydroxytryptamine
HDL	High density lipoprotein
HFIP	Hexa-fluoro-iso-propanol
HI	Hypoxia-ischaemia
HPA	Hypothalamic-pituitary-adrenal
HPE	High performance ELISA
ICV	Intracerebroventricular
IFN	Interferon
IL	Interleukin
IL-1Ra	Interleukin-1 receptor antagonist
IMS	Industrial methylated spirit
IP	Intraperitoneal
IV	Intravenous
JNK	c-Jun amino-terminal kinase
LBP	LPS-binding protein
LC	Locus coeruleus
LPS	Lipopolysaccharide
LSAB	Labelled streptavidin biotin
MAP	Mitogen-activated protein
MAPKAPK	Mitogens activated protein kinase activated protein kinase
mCD14	Membrane bound CD14
MCP	Monocyte chemoattractant protein
MFI	Median fluorescence intensity

MHC	Major histocompatibility complex
MIP	Macrophage inflammatory protein
MKP	MAP kinase phosphatase
MNK	MAPK interacting kinase
MRNA	Messenger ribonucleic acid
MSK	Mitogen activated protein kinase
MyD88	Myeloid differentiation factor 88
NA	Noradrenaline
NADH	Nicotinamide adenine dinucleotide hydrogen
NBM	Nucleus basalis of Meynert
NET	Noradrenaline transporter
NF- $\kappa$ B	Nuclear factor- $\kappa$ B
NFT	Neurofibrillary tangles
NK	Natural Killer
NO	Nitric oxide
NOS	Nitric oxide synthase
NSAID	Non steroidal anti-inflammatory drug
PAMPs	Pathogen-associated molecular patterns
PBS	Phosphate buffered saline
PCR	Polymerase chain reaction
PD	Parkinson's disease
PGE	Prostaglandin
PMSF	Phenylmethylsulfonyl fluoride
PRR	Pattern recognition receptor
PS	Polysaccharide
PS-1	Presenilin 1
PS-2	Presenilin 2
RAGE	Receptor for Advanced Glycation Endproducts
RANTES	Regulated on Activation, Normal T Expressed and Secreted
ROS	Reactive Oxygen Species
SAD	Sporadic Alzheimer's disease
SAP	Serum response factor accessory protein
sAPP	Soluble APP

SCD14	Soluble CD14
Tc	Cytotoxic T cell
TGF	Transforming growth factor
Th	Helper T cell
TIRAP	MyD88 adaptor-like protein
TLR	Toll-like receptor
TNF	Tumour necrosis factor
TRAM	TRIF related adaptor molecule
TRIF	TIR-containing adaptor molecule
TUNEL	Terminal deoxynucleotidyl transferase-mediated dUTP. nick-end labelling
VDB	Vertical band of Broca
VLDL-R	Very Low Density Lipoprotein Receptor

# ***CHAPTER 1***

## ***General Introduction***

### **1.1 Overview of thesis**

Neuroinflammation and neurodegeneration is evident in the brain tissue of patients with the chronic neurodegenerative disorder Alzheimer's disease (AD). Current symptomatic therapies for AD focus on alleviating impairments in learning and memory but do not alter underlying neuropathology. Hence, there is an unmet need for disease modifying agents that can slow the progression of AD. Putative anti-inflammatory or neuroprotective therapies need to be adequately characterised using mechanistic and disease relevant preclinical in vivo rodent models that provide markers of neuroinflammation and neurodegeneration relevant to AD. This thesis aims to interrogate the development of rodent in vivo models of neuroinflammation and neurodegeneration that can be used in the preclinical assessment of disease modifying therapies for AD.

This introduction will introduce the innate immune system, specifically focusing on the role of cytokines in mediating innate immunity and a description of LPS, a well characterised immunostimulant used to induce inflammation in vivo. This section will finally discuss the detection of cytokine protein by xMAP<sup>®</sup> technology on Luminex<sup>®</sup> systems, an approach not yet reported for the detection of proteins in rodent brain tissue following LPS treatment. Following this, the epidemiology and neuropathology of the progressive neurodegenerative disorder AD will be described. This will include an overview of proposed mechanisms for beta amyloid (A $\beta$ ) peptide induced neuroinflammation and neurotoxicity and evidence for anti-inflammatory treatment as a putative disease modifying therapy for AD. This introduction will finally discuss the current evidence for LPS and A $\beta$ -induced neuroinflammation and neurodegeneration in rodent in vivo models.

### **1.2 Innate immunity**

Present from birth, the innate immune system is important in the recognition and

removal of invading pathogens and is well conserved between invertebrates and vertebrates (reviewed by Kimbrell & Beutler, 2001). It is responsible for mounting an antigen non-specific defence against infectious stimuli, either immediately or within a very short period after infection. The response does not increase in intensity with each subsequent exposure or rely upon previous recognition of the antigen (reviewed by Kimbrell & Beutler, 2001). The innate immune system can recognise a diverse range of pathogens namely by the recognition of well-conserved pathogen-associated molecular patterns (PAMPs) present in many different pathogenic organisms (Janeway, 1989) by pathogen recognition receptors (PRRs) located on the cell surface of immune cells. PRRs include members of the transmembrane signal transducing toll-like receptor (TLR) family (Gordon, 2002), which recognise PAMPs present on specific organisms such as LPS from the cell wall of gram negative bacteria (toll-like receptor 4 (TLR4)) (Miyake, 2004). Surveillance by the innate system continues throughout an organism's lifetime but ageing causes diminished function of immune cells that result in a compromised innate response (Plackett et al, 2004). Elements of innate immunity occur in a number of chronic neurodegenerative disorders including AD (McGeer & McGeer, 2002) and this will be described in more detail in section 1.3.6.

### ***1.2.1 Effector cells of innate immunity***

The innate immune system comprises of a variety of phagocytic cells including macrophage (reviewed by Gordon, 1998), neutrophil (reviewed by Kobayashi et al, 2005), dendritic (reviewed by Foti et al, 2004; Rossi & Young, 2005) and natural killer (NK) cells (reviewed by O'Connor et al, 2006). These cells engulf foreign pathogen and use intracellular vacuoles containing toxic reactive oxidants such as nitric oxide (NO), superoxide and degradative enzymes to destroy the microbe (Lowenstein et al, 1994). Immune cells are also responsible for the release of soluble proteins including those of the complement cascade and cytokine families to enhance uptake of pathogen, recruit further cells to the site of invasion and control initiation of an antigen-specific response via binding of innate and adaptive immune cells (van Rossum & Hanisch, 2004; reviewed by Liew & McInnes, 2002). Immune cells, particularly macrophage and dendritic cells, act in antigen presentation to initiate adaptive immunity by processing engulfed antigen and displaying fragments on the cell surface combined with class I or class II major histocompatibility complex

(MHC). MHC binding, alongside interaction of costimulatory molecules such as CD28 on the T cell and CD80 or CD86 on antigen presenting cells (APCs), activates subpopulations of T cells. CD4 T helper (Th) or CD8 cytotoxic (Tc) cells differentiate into effector subsets depending on the combination of costimulatory molecules and cytokines present during activation. Recruitment of effector cells of the innate immune system and subsequent activation of cells involved in antigen-specific adaptive immunity is controlled and maintained by circulation of cytokines (Hoebe et al, 2004; Blach-Olszewska, 2005) (fig 1.1).

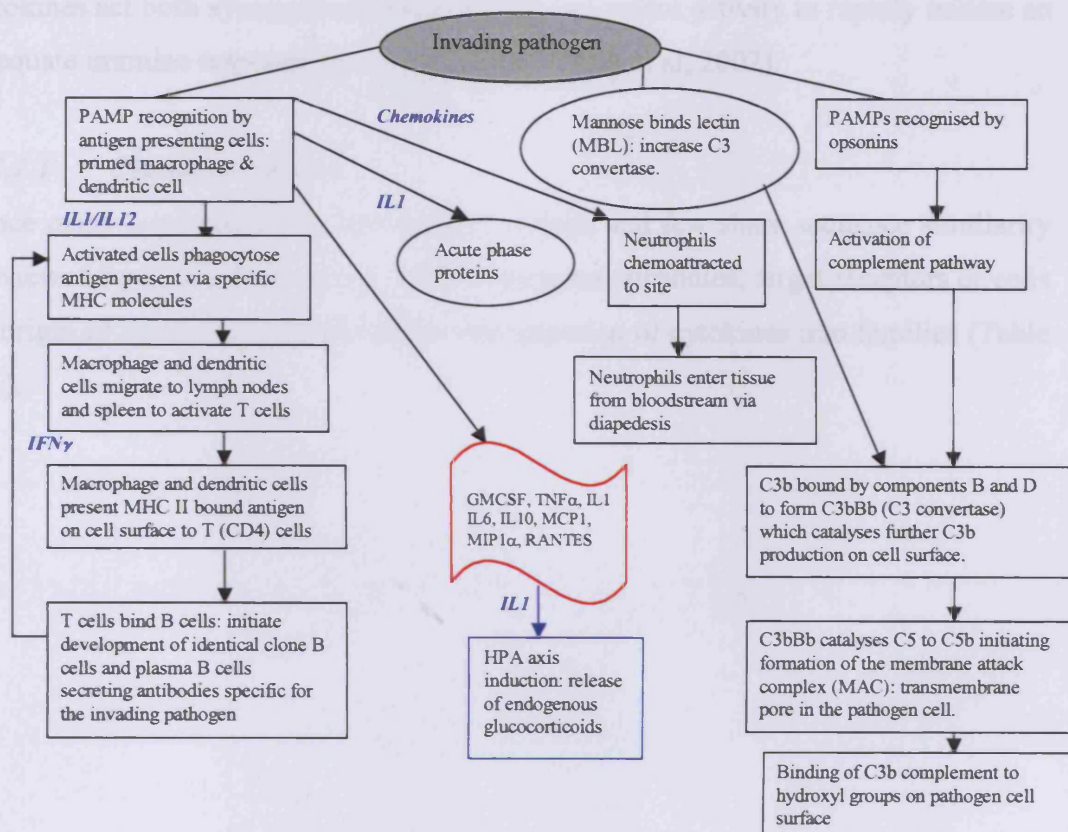


Figure 1.1: Schematic representation of innate immune system

### 1.2.2 Cytokines

Potent short acting protein (15-25kDa) mediators generically termed cytokines mediate the inflammatory response. Cytokines include lymphokines, interleukins, tumour necrosis factors, chemokines (reviewed by Esche et al, 2005; Coelho et al, 2005) and interferons (reviewed by Kunzi & Pitha, 2005) secreted by a wide variety of immune cells (Moller et al, 2005). Cytokines are pleiotropic and function to

regulate the intensity and duration of an inflammatory response by regulating haematopoiesis and mediating cell growth, differentiation and activation (reviewed by Cohen & Cohen, 1996). Due to their role in the maintenance of inflammation, cytokine proteins have a short half-life enabling rapid degradation to control the immune response. Hence, rapid production of these potent proteins remains transient and at low concentration to allow management of inflammation. A single cytokine can initiate a cascade of cytokine production from a multitude of immune cells and may demonstrate autocrine, paracrine and possibly endocrine actions. Furthermore, cytokines act both synergistically and exhibit redundant activity to rapidly initiate an adequate immune response (reviewed by Asadullah et al, 2002).

#### *1.2.2.1 Cytokine Families*

Since many cytokines have over-lapping actions and few share sequence similiarity (reviewed by Turnbull & Rivier, 1999), functional attributes, target receptors or cells of origin of cytokines have allowed a classification of cytokines into families (Table 1.1).

/

Cytokine	Origin	Actions
<b>COLONY STIMULATING FACTOR (CSF)</b>		
Granulocyte Macrophage-CSF	T cells Macrophage Endothelium	Induces growth of granulocytes and macrophage colonies Activates macrophage, neutrophils and eosinophils
<b>INTERFERONS (IFN)</b>		
IFN- $\gamma$	Th1 cells Tc cells NK cells	Primes macrophage & induces MHC I/II Antagonises some IL4 actions Induces B cell antibodies, inhibits viral replication
<b>TUMOUR NECROSIS FACTOR (TNF)</b>		
TNF- $\alpha$	Monocyte Macrophage Neutrophils T & B cells NK cells Astrocytes Mast cells	Activates primed macrophage and NK cells. Anti-tumour activity Promotes neuronal survival Recruitment & activation of neutrophils & monocytes Mediates septic shock, cell proliferation & apoptosis Induction of chemokines, IFN $\gamma$ , TNF $\alpha$ , IL1, GM CSF, IL6 Induces acute phase proteins
<b>INTERLEUKINS (IL)</b>		
IL-1 ( $\alpha$ & $\beta$ )	Monocyte Macrophage Fibroblasts B cells Dendritic cells	Fever induction Induces macrophage PGE2/cytokines Induces neutrophil adhesion molecules B and T cell proliferation Induction of acute phase proteins
IL-2	Th1 cells	Stimulates T & NK cell proliferation
IL-4	B cells Th2 cells Mast cells	Initiates B cell antibody production Stimulates cytokine release & antigen presentation Stimulates T cell growth
IL-6	Th2 cells Macrophages Mast cells Fibroblasts	B & T cell differentiation & T cell growth Induces IL2 & IL2 receptor expression on T cells Initiate and regulate acute phase proteins Involvement in tissue repair
IL-10	Macrophage Th2 cells B cells	Anti-inflammatory, immunosuppressive Down regulates IL1, TNF $\alpha$ and IFN $\gamma$ Alters microglia receptor expression.
IL-12	Macrophage	Induction of T cell and Th1 cytokines
<b>CHEMOKINES</b>		
Monocyte Chemoattractant Protein (MCP) -1	Macrophage, T cells	Chemotactic for T cells
Macrophage Inflammatory Protein (MIP)-1 $\alpha$	Macrophage, T cells	Chemotactic for T cells
Regulated on Activation, Normal T Expressed and Secreted (RANTES)	Macrophage, T cells	Chemotactic for T cells

Table 1.1: Overview of selected cytokine origin and roles (adapted from Kuby, 1997)

### 1.2.3 Cytokine transcription

Specific extracellular cytokine receptors and toll-like receptors (TLRs) mediate cytokine transcription via two distinct MyD88-dependent and MyD88-independent intracellular pathways (reviewed by Gillis, 1991).

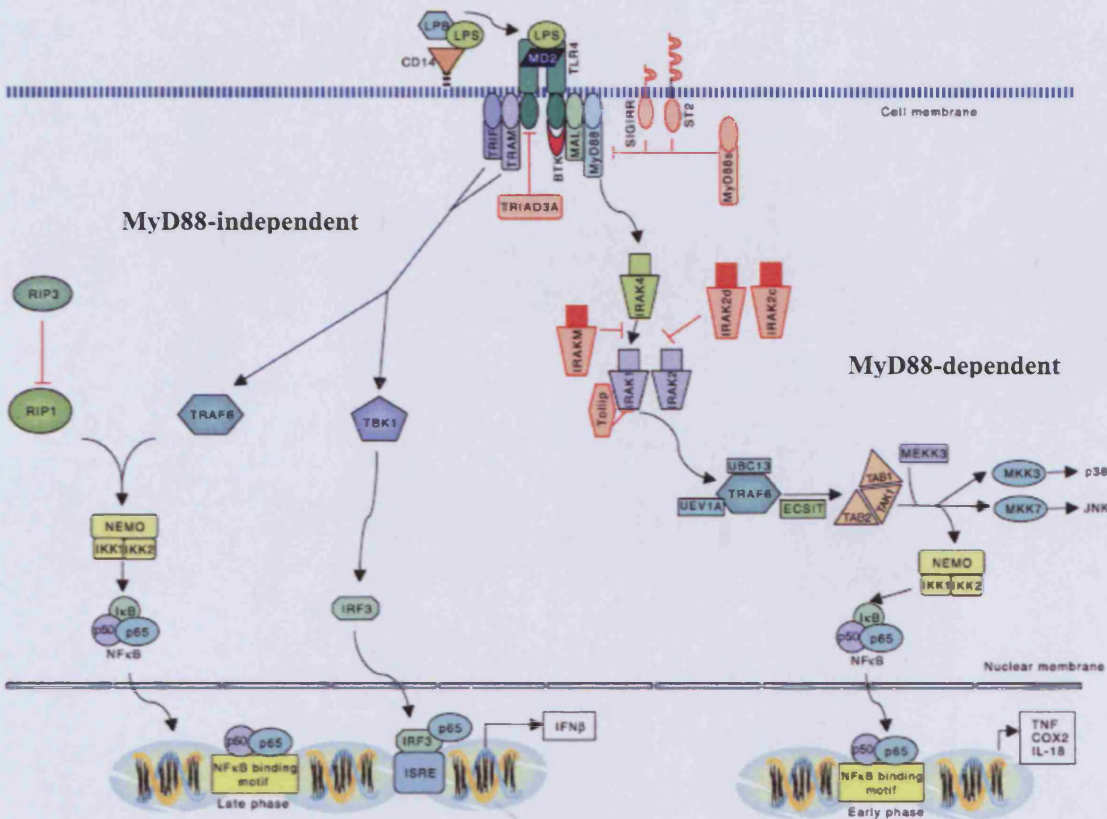


Figure 1.2: Schematic representation of TLR4 signalling cascade (Figure taken from Palsson-McDermott & O'Neill, Immunology, 2004)

Translocation of the transcription factor nuclear factor- $\kappa$ B (NF- $\kappa$ B) (reviewed by Saklatvala et al, 2003; Goodridge & Harnett, 2005) occurs via activation of intracellular adaptor proteins, myeloid differentiation factor 88 (MyD88), MyD88 adaptor-like protein (TIRAP) also known as Mal, TIR-containing adaptor molecule (TRIF) also known as TICAM-1 and TRIF-related adaptor molecule (TRAM) also known as TICAM-2. These communicate signals from transmembrane receptors (fig 1.2). The translocation of NF- $\kappa$ B from the cytoplasm to the nucleus depends on phosphorylation of the inhibitory factors  $\text{I}\kappa\text{B}\alpha$  and/or  $\text{I}\kappa\text{B}\beta$  resulting in the induction of target gene transcription (Krappmann et al, 2004). The MyD88/IRAK/TRAF6

complex can also activate the MAPK cascade. Translocated transcription factors bind to response elements located on the promoter regions of target genes to induce transcription of selected DNA.

#### **1.2.4 *Signal transducing pathways***

The mitogen-activated protein (MAP) kinase cascade (reviewed by Karin, 2004; Woodgett et al, 1996; Dong et al, 2002) mediates and controls target gene transcription as a direct response to the extracellular environment of the cell. The hierarchical organisation of a multitude of specific intermediary kinases allows the control of transcriptional regulatory proteins via amplification and diversification of the initial signal (reviewed by Seger & Krebs, 1995). This is subsequently managed at each kinase level by the action of phosphatases (Zhang et al, 2002).

Evidence supports a role for MAP kinases in a plethora of cellular functions including cell survival (reviewed by Matsuzawa et al, 2005), apoptosis (reviewed by Sumbayev & Yasinska, 2006) and inflammation (Karin, 2005). Signal transducing pathways influence the expression of a number of mediators including proinflammatory cytokines (reviewed by Pocock et al, 2001), nitric oxide synthase (NOS) (reviewed by Guzik et al, 2003), matrix metalloproteinases (Reuben & Cheung, 2006) and cyclo-oxygenase 2 (COX2) (Akundi et al, 2005). The key function of MAP kinases in the immune response has led to intensive research into kinases as potential therapeutic targets for chronic inflammatory diseases (Karin, 2004). The vast number of kinases involved in each pathway suggests targeting individual kinases may not provide a sufficient anti-inflammatory effect owing to compensation by other kinase pathways and manipulating dual or multiple kinases may compromise the vast array of kinase functions (Karin, 2005). There are three well-characterised groups of MAP kinases recently shown to be present in mammalian cells that are activated by dual phosphorylation at a tripeptide motif, Thr-Gly-Tyr, Thr-Pro-Tyr and Thr-Glu-Tyr for p38, c-Jun amino-terminal kinase (JNK) and extracellular signal-regulated kinase (ERK) respectively (Dong et al, 2002) (fig 1.3). The role of these three MAPK cascades in inflammation is outlined below.

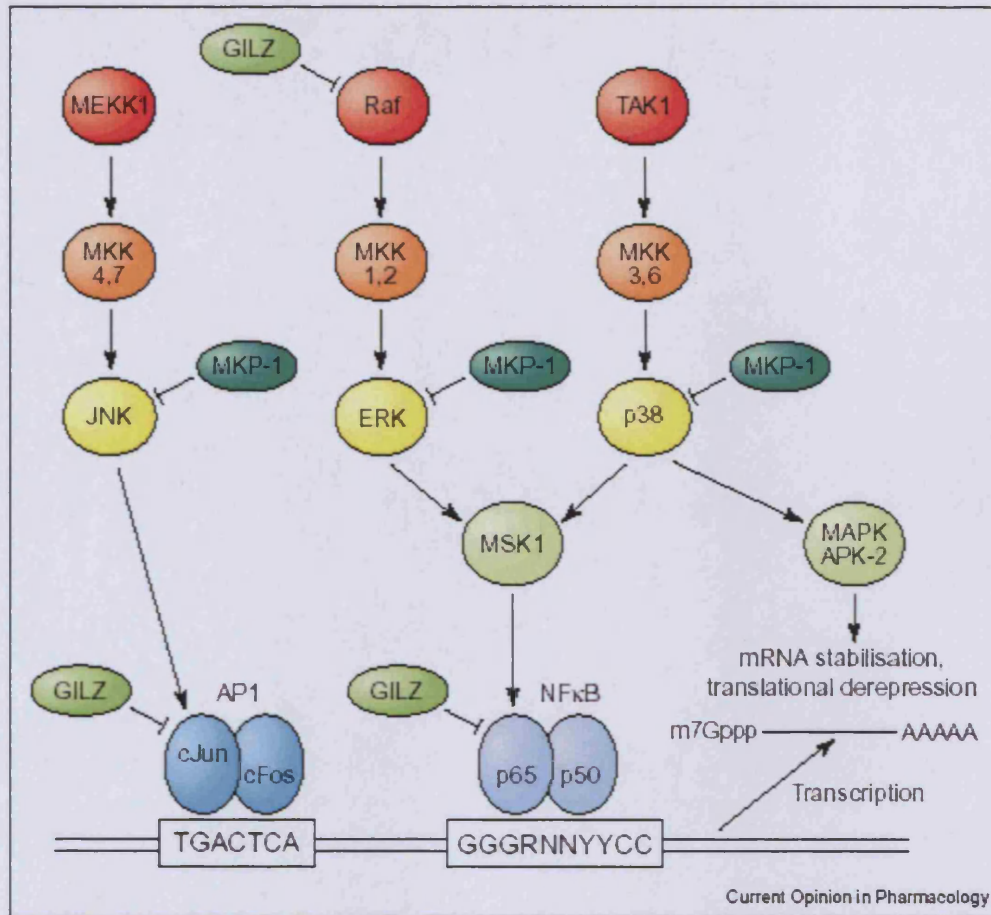


Figure 1.3: Overview of the MAP Kinase cascade (Taken from Clark & Lasa, 2003)

#### 1.2.4.1 Involvement of p38 pathway in inflammation

A wide variety of stimuli can activate p38 kinase including stress, pathogens such as lipopolysaccharide, cytokines, growth factors and some catecholamines (reviewed by Ono & Han, 2000). P38 kinase can phosphorylate or activate both transcriptional and non-transcriptional factors including activating transcription factor 2 (ATF2), sap-1a and GADD153 and alternative targets such as the mitogens activated protein kinase activated protein kinases (MAPKAPKs -2, -3, -5) & MAPK interacting kinase 1(MNK1). Direct phosphorylation of transcription factors or activation of downstream kinases such as mitogen activated protein kinase 1 (MSK1) results in the post-transcriptional regulation of proinflammatory cytokines, iNOS, c-Jun (a component of the transcription factor complex activator protein-1 (AP-1)) and the monocyte chemoattracting protein-1 (MCP-1) via MAPKAPK2 (Ono & Han, 2000). Kotlyarov et al (1999) demonstrated that following intraperitoneal LPS injection, the

attenuation of the proinflammatory cytokine TNF- $\alpha$  was evident in the serum of MAPKAPK2 KO mice supporting the role of MAPKAPK2 in regulating cytokines at the post-transcriptional level (reviewed by Saklatvala, 2004). The anti-inflammatory cytokine IL-10 can also attenuate TNF- $\alpha$  by inhibiting MAPKAPK2 mediated activity on AU-rich elements in TNF- $\alpha$  transcripts. TNF- $\alpha$  possesses AU-rich elements in the 3' untranslated region making the mRNA unstable and short lived (reviewed by Saklatvala, 2004). Inflammation incurs phosphorylation of AU-binding proteins occupying AU-rich elements via a p38-dependant pathway involving MAPKAPK2 (Neininger et al, 2002; Frevel et al, 2003) resulting in release, stabilisation and translation of cytokine mRNA.

#### *1.2.4.2 Involvement of JNK pathway in inflammation*

JNK kinases can bind and phosphorylate transcription factors including ATF2, SMAD3, Elk-1, serum response factor accessory protein 1a (sap-1a) and c-Jun (Tibbles & Woodgett, 1999). The transcription factors, AP-1 and ATF2 increase cytokine mRNA expression that consequently results in JNK mediated TNF- $\alpha$ -induced AP-1 activity and, along with p38 MAPK and NF- $\kappa$ B, TNF- $\alpha$ -induced upregulation of cell adhesion molecules (Herlaar & Brown, 1999). T cell and antigen presenting cell (APC) binding also activate the JNK pathway and, in conjunction with ERK, induce expression of the promoter and enhancer element of IL-2, a cytokine important in T cell proliferation (reviewed by Dong et al, 2001).

#### *1.2.4.3 Involvement of ERK pathway in inflammation*

ERKs are responsible for post-transcriptional control of immune mediators, activation of eosinophils and the positive selection and lineage commitment of thymocytes (Tibbles & Woodgett, 1999). Despite some understanding of the role of the ERK pathway in T cell activation and proliferation, there is relatively little information on the role of ERK in inflammation (Karin, 2004). More recent reports have suggested the role of MAP3K tpl2/cot in ERK-mediated LPS-induced activation of macrophages. Tpl2 knockout mice displayed abrogated LPS-induced ERK activation and TNF- $\alpha$  release (Dumitru et al, 2000). ERK activation appears to modulate translocation of TNF- $\alpha$  mRNA from the nucleus to the cytoplasm rather than affecting transcription or stabilisation of TNF- $\alpha$  mRNA (Dumitru et al, 2000).

### 1.2.5 *The hypothalamic-pituitary-adrenal (HPA) axis*

Cytokine expression in brain tissue can activate the HPA axis (Morand et al, 1999; Beishuizen & Thijs, 2003). The adrenal gland is located above each kidney and comprises two distinct regions, the adrenal cortex and adrenal medulla. The adrenal cortex can release a variety of steroid hormones derived from cholesterol, namely glucocorticoids, mineralocorticoids and androgens. The hormone, adrenocorticotrophin (ACTH), produced by the anterior lobe of the pituitary is responsible for regulating the release of steroid hormones from the adrenal cortex. In turn, the release of corticotrophin-releasing factor (CRF) and vasopressin (AVP) via the median eminence modulates ACTH production (reviewed by Campeau et al, 1998). The most abundant endogenous glucocorticoid (GC) released in humans is cortisol, which has potent anti-inflammatory properties (Sweep et al, 1991).

#### 1.2.5.1 *Cytokine-induced glucocorticoid production*

Studying the role of cytokine-induced glucocorticoid production *in vivo* is difficult and the relative significance and precise mechanism of peripherally and centrally derived cytokines in HPA stimulation remains unclear (Beishuizen & Thijs, 2003, Angeli et al, 1999). However, studies have provided evidence to support a role for IL-1 $\beta$ . There was an early suggestion that central IL-1 $\beta$  can activate noradrenergic neuronal terminals found within the hypothalamus, which modulate the hypothalamic CRF secretion but there remains conflicting evidence both supporting (Gwosdow et al, 1992) and arguing against (Cambronero et al, 1992) the involvement of catecholamines in IL-1 $\beta$ -induced CRF secretion. Subsequent data suggested the involvement of the vagal nerve in communicating the peripheral immune response to the hypothalamus (Hosoi et al, 2000) since CRF and IL-1 $\beta$  mRNA expression was increased in the hypothalamus after vagal stimulation, which increased plasma ACTH and corticosterone levels. More recently, it has been shown that the rapid induction of the HPA axis by IL-1 $\beta$  may be mediated by cyclooxygenase 2 (COX2) since COX inhibitors prevent IL-1 $\beta$  induced HPA activation (Dunn, 2000). The chronic activation of the HPA axis may; however, be mediated by multiple mechanisms as this occurs independently of COX2 expression (Dunn, 2000).

Intravenous (IV) and intracerebroventricular (ICV) injection of IL-1 $\beta$  can dose-

independently increase plasma ACTH and induce hypothalamic CRF secretion (Uehara et al, 1987; Brown et al, 1991). A pre-injection of rabbit antiserum against rat CRF attenuated IL-1 $\beta$ -induced ACTH (Uehara et al, 1987; Payne et al, 1994). IL-1 $\beta$  also upregulates glucocorticoid receptor (GCR) mRNA expression in hypothalamic CRF-secreting cells (Angeli et al, 1999). Attenuation of the IL-1 $\beta$ -induced CRF secretion occurs with treatment of the glucocorticoids, corticosterone and Dexamethasone (DEX), (Cambronero et al, 1992; Betancur et al, 1995). The HPA axis can regulate IL-1 $\beta$  secretion via IL-1 receptor antagonist (IL-1Ra) production (Kovalovsky et al, 2000) and via modulation of IL-1 receptors (Goujon et al, 1997). Post infection, glucocorticoids and IL-1Ra reach a maximum in the plasma simultaneously, preventing chronic IL-1 action (Arzt et al, 1994).

#### *1.2.5.2 Glucocorticoid (GC) modulation of cytokine induction*

GCs act via numerous mechanisms of which the molecular-mediated effects on cytokine release are most widely studied (Refojo et al, 2003: 2001; Ray, 1992: 1990; Bailey, 1991). The actions of GCs can be biphasic; firstly, GCs may reduce cytokine synthesis by macrophage and monocytic cells by preventing transcription and translation of target genes. GCs can, due to their lipophilic nature, diffuse into the cell and bind to receptors that act as specific ligand-induced transcription factors, which are localised throughout most of the body, to form a GC-receptor complex (reviewed by Schleimer, 1993). The complex translocates from the cytoplasm to the nucleus where it undergoes a variety of structural changes to aid its interaction, via zinc fingers (Miesfeld, 1990), with the GC response element (GRE) located in the promoter region of target DNA (Schmidt et al, 1994). The GRE has a conserved palindromic sequence with each half-palindrome binding one subunit of the glucocorticoid receptor. Evidence suggests that GREs and other transcription factor DNA binding sites are in close proximity so that, on binding of the GC-receptor (GCR) complex, other transcription factor binding sites cannot be used, thus preventing the transcription of target genes (Schmidt et al, 1994). GREs can have either positive or negative roles during transcription so that GCs can induce or reduce the transcription of specific target genes on a tissue-specific basis (Kovalovsky et al, 2000).

Post-transcriptionally, GCs may destabilise the resulting mRNA by rapidly reducing

half-life, thus limiting its translation to a protein product. However, this theory remains contested (Brattsand et al, 1996). Whilst limiting the production of cytokines centrally, GCs also act by up-regulating cytokine receptor expression that enhances cytokine effects on target cells and control the further release of proinflammatory cytokines (Wiegers et al, 1998).

The GCR can also repress lipopolysaccharide or cytokine-induced NF- $\kappa$ B activation by protein-protein interaction between NF- $\kappa$ B and the GCR or by inducing I $\kappa$ B $\alpha$ / $\beta$  expression, which acts to further inhibit the actions of NF- $\kappa$ B (Caldenhoven et al, 1995; Van de Saag, 1996; Brostjan et al, 1996; De Bosscher et al, 1997; Vanden Berghe et al, 1999). Inhibiting NF- $\kappa$ B allows GCs to attenuate cytokine production and inhibit T cell proliferation (Ayroldi et al, 2001).

### **1.2.6 Lipopolysaccharide (LPS)**

LPS is derived from the outer membrane of gram-negative bacteria such as *Escherichia coli*. LPS molecules consist of two main components: a well-conserved hydrophobic biphosphorylated lipid (lipid A) and a hydrophilic polysaccharide (PS). The PS has two regions, a non-repeating core oligosaccharide and a polysaccharide chain known as the O-chain (Caroff et al, 2002; Raetz & Whitfield, 2002; Dixon et al, 2005). The O-chain confers serotype specificity on a species or strain of bacteria. The lipid A moiety binds to a variety of receptors including CD14 that can initiate activation of the innate immune system.

#### **1.2.6.1 LPS: Mechanism of action**

LPS-binding protein (LBP), a 65kDa protein, binds LPS circulating in the bloodstream via the lipid A moiety (Ulevitch & Tobias, 1995). LBP behaves as a lipid transfer protein (Gallay et al, 1994) acting to convert aggregates of LPS to monomers to accelerate the binding of LPS to CD14 (Hailman et al, 1994).

Soluble CD14 (sCD14) aids activation of cells that do not express the membrane glycosylphosphatidylinositol-anchored CD14 (Bazil et al, 1989; Fenton et al, 1998). Membrane-bound CD14 (mCD14) lacks a cytoplasmic domain and in order to induce intracellular signals, CD14 forms a complex recognised by TLR4 (Dobrovolskaia et al, 2002; Triantafilou et al, 2002; Heumann & Roger, 2002).

The adaptor protein MD-2, expressed by dendritic cells and monocytes, was

originally identified by Shimazu et al, 1999. Co-expression of MD-2 is essential for the binding of LPS and translocation of the TLR receptor to the cell surface (Fujimoto et al, 2004; Miyake, 2004). Studies using radiolabelled LPS have illustrated a physical interaction between LPS, MD-2 and TLR4 can only occur in the presence of CD14 (da Silva Correia et al, 2002) irrespective of the role of MD-2 in complexes with LPS (Kennedy et al, 2004) or TLR4 (Visintin et al, 2001; Fujimoto et al, 2004). Although the CD14/MD-2/TLR4 complex is well recognised, LPS may also activate CD64, CD16, CD32, CD36, CD55 (Heine et al, 2003) and CD11c/CD18 (Ingalls & Golenbock, 1995) cell surface receptors, depending on cell type and activation state.

#### *1.2.6.2 Communication between periphery and CNS*

Peripheral inflammation may be sensed by the brain via two pathways, namely the neural and humoral mechanisms. Evidence supports a major role for humoral pathways during systemic inflammation (Szelenyi, 2001; Rivest et al, 2000). Blood-borne cytokines can bind to endothelial receptors in brain tissue or cross the blood-brain barrier (BBB) through a saturable carrier-mediated mechanism that is most likely to initiate when very high cytokine concentrations exist in the blood (Pavlov et al, 2003). Much of the communication from periphery to brain occurs via the circumventricular organs (CVOs), areas of minimal BBB, since cytokines in the blood can initiate the synthesis and release of soluble mediators including prostaglandins and nitric oxide at CVO sites. Circulating LPS can bind to TLR4 located on endothelial cells of the circumventricular organs (CVOs), leptomeninges and choroid plexus (ChP) of the brain and on the surface membrane of monocytes, mast cells and neutrophils. TLR4 activation causes transcription of cytokine target genes within immune cells, particularly microglia, firstly at the CVOs, choroid plexus and leptomeninges and then eventually throughout the brain tissue (Nadeau & Rivest, 1999; Ericsson et al, 1995, Herkenham et al, 1998; Vallieres & Rivest, 1997). Expression of mCD14 also increases dramatically in microglia, CVO regions and then throughout the brain following intravenous (IV) or intraperitoneal (IP) LPS (Lacroix et al, 1998). This leads to NF- $\kappa$ B translocation and proinflammatory cytokine production, firstly at areas easily reached by the systemic circulation and then subsequently throughout the brain tissue. IP LPS injection induces rapid IL-6

expression in the CVOs and ChP, however, IV injection of pro-inflammatory cytokines IL-1 $\beta$  and TNF- $\alpha$  fail to stimulate IL-6 transcription (Vallieres & Rivest, 1997). There is also evidence to suggest that intraperitoneal LPS may cause mild breakdown of the microvasculature allowing diffusion of LPS through the barrier (Singh et al, 2004). Entry of molecules into the brain following breakdown of the BBB is molecular weight dependent with molecules of approximately <340Da entering brain tissue (Singh et al, 2004). The molecular weight of LPS is 10kDa so it is possible, but unlikely, that sufficient LPS can enter the brain to elicit a central response.

The neural pathway, consisting of the cytokine-mediated activation of vagus nerve afferent fibres, links the sympathetic nervous system and the hypothalamic-pituitary-adrenal axis (HPA) that ultimately modulates inflammatory processes. Vagal afferents terminate in the dorsal vagal complex located in the medulla oblongata and comprising the nucleus tractus solitarius, the dorsal motor nucleus of the vagus and the circumventricular organ, area postrema. The paraventricular nucleus of the hypothalamus, important in releasing corticotrophin releasing hormone as part of the HPA axis, interacts with the nucleus tractus solitarius. Evidence from vagotomy studies suggests that the neural pathway is more important in mediating mild inflammation since preventing input from the vagus nerve can inhibit activation of the HPA axis (GayKema et al, 1995) whilst failing to attenuate cytokine expression in brain tissue following high doses of LPS (Ishizuka et al, 1997). Humoral mechanisms may have more of a role during a rapid and strong peripheral response to infectious stimuli.

### ***1.2.7 Detection of cytokine expression***

Cytokine mRNA expression can be detected using polymerase chain reaction techniques (reviewed by O'Garra & Vieira, 1992). The detection of mRNA expression provides valuable information on gene activity but does not take into account post transcriptional events that may affect subsequent protein production. Thus, detection of cytokine protein products in addition to the quantification of intermediary mRNA expression may provide a more valuable approach to assessing the magnitude of an inflammatory response (reviewed by Lockhart & Winzeler, 2000). Initial detection of cytokine protein employed molecular hybridisation

techniques or cell-based bioassays (Beckmann & Morrissey, 1991) and the use of radio-labelled or enzyme-linked antibodies directed against the protein of interest allowed the generation of more frequently used, easier and quicker, immuno-based assays (reviewed by Thorpe et al, 1992).

Initially, much standardisation was required between immuno-assay kits to establish specific recognition of antibodies for the target protein to prevent cross-reactivity and false results (reviewed by Mire-Sluis et al, 1995; Whicher & Ingham, 1990; Tsang & Weatherbee, 1996). Further development of highly specific antibodies and appropriate standards has allowed immuno-based assays to become highly successful as a sensitive and reliable method of detecting cytokine protein in samples (reviewed by Mire-Sluis, 1999; Lai et al, 2005; Delarache & Chollet-Martin, 1999). A disadvantage of enzyme-linked immunosorbant assays (ELISAs) is the need to analyse a single protein at one time which makes profiling of a range of cytokines in a single tissue both expensive and low throughput. The advent of multiplexed particle-based flow cytometric assays that use beads as the solid base, akin to a conventional immuno-assay, now allow detection of multiple analytes in a single sample (reviewed by Vignali, 2000; Kellar & Iannone, 2002).

#### *1.2.7.1 Cytokine protein detection using xMAP® technology*

Luminex® suspension bead array systems utilise xMAP® (multi-analyte profiling) technology (Luminex® Corp, Austin, USA) to allow the multiplexing of up to 100 different assays within a single sample. The flow cytometers, FACSCalibur™ or Luminex® 100™, analyse a liquid suspension placed in each well of a standard 96-well plate comprising 5.5 micron polystyrene microspheres internally dyed with different ratios of two spectrally distinct fluorophores (red and infrared) that code the beads into 100 distinct sets (fig 1.4).

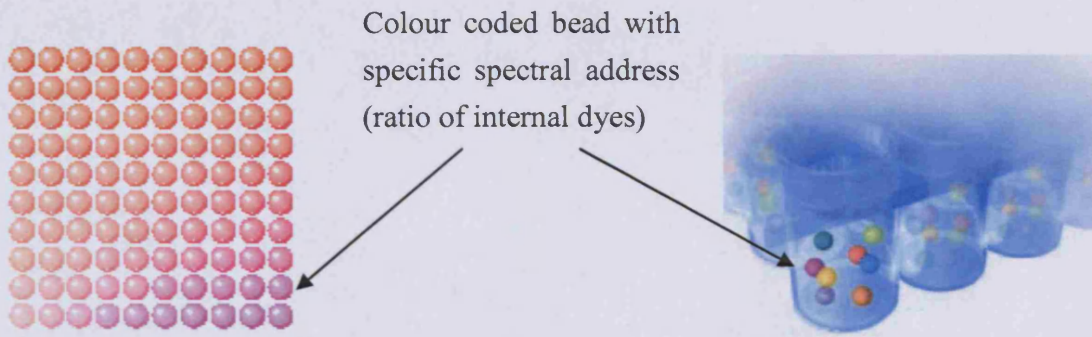


Figure 1.4: Luminex<sup>®</sup> polystyrene microsphere beads (Images derived from [www.Bio-rad.com](http://www.Bio-rad.com))

Each bead set can be coated with a reagent able to capture and bind a specific analyte present in a sample. The microsphere can be coated with a wide variety of reagents including antigens, antibodies, receptors, enzyme substrates or DNA (fig 1.5).

To quantify the captured analyte a biotinylated detection antibody followed by a fluorescently labelled reporter molecule such as Streptavidin-E is added to the suspension and following incubation, each well is read using a Luminex<sup>®</sup> array reader.

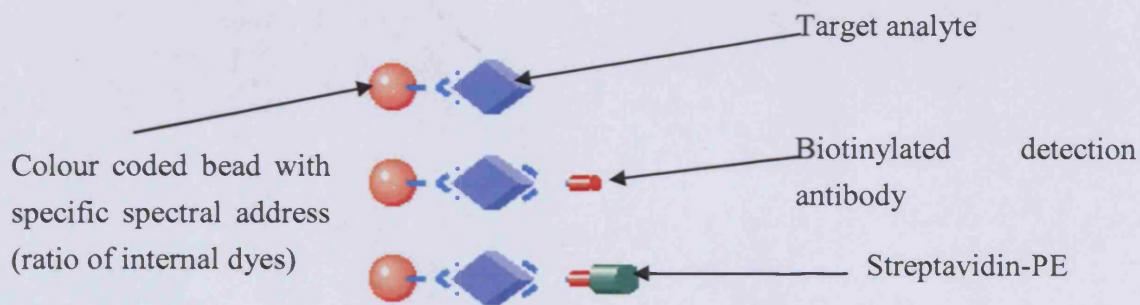


Figure 1.5: Detection of analyte by Luminex<sup>®</sup> bead suspension array (Image derived from [www.Bio-rad.com](http://www.Bio-rad.com))

Precision fluidics within the reader aligns the beads into single file, allowing each bead to move through a flow cell containing two lasers. A red classification laser excites the specific colour coding internal dyes in each microsphere allowing identification of the bead. The green reported laser excites the reporter dye attached to each bead allowing detection and quantification of the captured analyte (fig 1.6).

Digital signal processors and software record the fluorescent signals for each bead translating them into data for each assay.

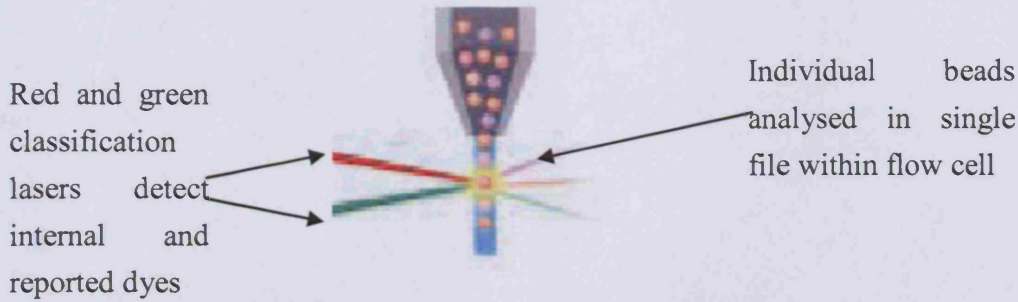


Figure 1.6: Detection of analyte-bead complex by Luminex<sup>®</sup> 100<sup>™</sup> system (Image derived from [www.Bio-rad.com](http://www.Bio-rad.com))

#### 1.2.7.2 Advantages of using xMAP<sup>®</sup> technology

Assessing multiple analytes in a single sample provides greater throughput in data collection and ensures reduced variability within the data set by performing simultaneous readings (up to 1000 events) on each bead set within a sample. A small sample of 12.5  $\mu$ l can be used per multiplex assay allowing the sample to be utilised in further assays and is particularly useful where original sample volumes are small, often a problem with samples obtained from mice. As multiple analytes are assessed within the same sample, a direct correlation can be made between analytes indicating patterns in cytokine profiles more clearly i.e. decreased pro-inflammatory cytokines correlating with increased anti-inflammatory cytokine release.

#### 1.2.7.3 Detection of LPS-induced cytokine protein in brain tissue

LPS can increase the mRNA expression of inflammatory cytokines in plasma and brain compartments, particularly following intracerebroventricular injection (Gayle et al, 1998; Gayle et al, 1999; Turrin et al, 2001; Plata-Salaman et al, 1998; De Simoni et al, 1995). Cytokine mRNA expression also occurs to a lesser degree in brain tissue post IP administration in both mice and rats (Jacobs et al, 1997; Kakizaki et al, 1999; Laye et al, 1994; Pitossi et al, 1997; Satta et al, 1998; Goujon et al, 1997; Castanon et al, 2004). LPS-induced cytokine protein induction in plasma was confirmed via the use of immuno-based assays such as ELISAs and, although central protein changes have been detected in mouse brain (Goujon et al, 1996) this has not

been established in rat. Recent utilisation of xMAP<sup>®</sup> technology on Luminex<sup>®</sup> 100<sup>™</sup> suspension bead array systems has provided further profiling of LPS-induced plasma cytokine protein responses, however, quantification of central cytokine levels post LPS treatment remains more focused on mRNA expression (Bobrowski et al, 2005). Detection of LPS-induced cytokine proteins in the brain using Luminex<sup>®</sup> 100<sup>™</sup> suspension bead array systems has yet to be described in the literature. In the present studies, I chose to apply the Luminex<sup>®</sup> 100<sup>™</sup> suspension bead array system to detecting cytokine protein in rodent brain tissue post intraperitoneal or intracerebroventricular LPS administration.

### **1.3 Alzheimer's disease (AD)**

#### ***1.3.1 Epidemiology***

During 1906, the German doctor, Dr Alois Alzheimer, noted the presence of abnormal tissue and tangled fibre bundles in post mortem brain tissue of a woman who had suffered dementia. The associated disease was named Alzheimer's disease (AD) (Alzheimer A, 1907). AD is a chronic neurodegenerative disorder characterised by the presence of A $\beta$  plaques, neurofibrillary tangles (NFTs), cell loss and associated activated microglia and astrocytes (Blennow et al, 2006). Clinical manifestations of AD often begin with gradually worsening cognitive impairments, particularly in learning and memory (Blennow et al, 2006). As the disease progresses, memory loss is associated with neuropsychiatric symptoms including anomalous motor behaviour, depression, anxiety, weight loss, irritability and agitation (Weiner et al, 2005). In the western world, neurodegenerative disorders have become more prominent due to an aging population, with increasing age being the greatest risk factor for AD (Barranco-Quintana et al, 2005). 1% of people aged <65 years and 24-33% of people aged >85 years are affected by the disease (Blennow et al, 2006).

A further important risk factor for AD is an individual's genetic background (Blennow et al, 2006) but many believe that the disease in a majority of sufferers is due to a close interaction between genetic and non-genetic factors (Tol et al, 1999). The number of Americans alone who have AD has doubled since 1980 to approximately 4.5 million, costing at least \$100 billion in care giving

([www.alz.org/AboutAD/statistics](http://www.alz.org/AboutAD/statistics)). This is despite at least 70% of patients living at home where a large percentage of the care they receive comes from relatives and friends. This corresponds to an increased cost to businesses to account for lost productivity, absenteeism and worker replacement for working individuals who also care for an AD sufferer ([www.alz.org/AboutAD/statistics](http://www.alz.org/AboutAD/statistics)). In America, this costs business approximately \$61 billion per year ([www.alz.org/AboutAD/statistics](http://www.alz.org/AboutAD/statistics)). A treatment able to delay the onset of the disease by 5 years could potentially reduce the number of patients suffering severe stages of AD by 50% in 50 years ([www.alz.org/AboutAD/statistics](http://www.alz.org/AboutAD/statistics)). It is clear that a treatment able to delay the progression of the disease pathology is crucial to diminishing the impact of this disease on both a social and financial scale. Current drugs act solely as symptomatic treatments and can improve or stabilise symptoms in many patients but management of the underlying degenerative pathology with disease modifying drugs now requires more focus in order to control disease progression more successfully.

### **1.3.2 *Early-onset Familial AD (FAD)***

FAD is an uncommon form of AD accounting for <5% of all AD cases (Rocca et al, 1991; Rocchi et al, 2003). The disease is inherited as an autosomal dominant trait and is linked with fully penetrant (causal) mutations in genes coding for APP, presenilin 1 (PS-1) and presenilin 2 (PS-2) located on chromosomes 21, 14 and 1 respectively (Price & Sisodia, 1998). FAD presents early in life (30-60 years of age) and the age of onset depends on the presented mutations. PS-2 mutations are rare, to date there are only 10 mutations established in PS-2 (Sherrington et al, 1996) whilst 142 mutations have been identified in PS-1 (Cruts & Van Broeckhoven, 1998). Mutations in PS-1 and PS-2 can significantly reduce age of onset. PS1 mutations are associated with more aggressive forms of AD and age of onset can occur as early as 25 years of age (Campion et al, 1999) with disease duration lasting 5 years (Russo et al, 2000). FAD PS mutations influence processing of APP resulting in higher ratios of extracellular A $\beta$ 1-42 deposition (reviewed by Morishima-Kawashima & Ihara, 2002).

### **1.3.3 *Sporadic AD (SAD)***

The clinical and pathological phenotypes of SAD are indistinguishable from those

displayed in FAD cases (Price & Sisodia, 1998) and SAD is the most common form of AD, accounting for approximately 95% of all cases (Panza et al, 2002). SAD pathogenesis is associated with a number of risk factors and the apolipoprotein E (ApoE)  $\epsilon$ 4 allele of the ApoE gene located on chromosome 19 is well documented as a partially penetrant genetic risk factor (Pericak-Vance et al, 1991; reviewed by Roses, 1996). Although presence of ApoE4 is neither required nor sufficient to cause AD it has been strongly associated with reducing the age of onset in SAD cases since homozygous carriers demonstrate a younger onset age than patients carrying a single copy (Blacker et al, 1997; Meyer et al, 1998). The mechanism of action of ApoE4 remains unclear, however, increased A $\beta$  plaques in E4 carriers and changes in A $\beta$  deposition in APP overexpressing mice with presence or absence of human ApoE provides evidence that presence of ApoE4 can influence A $\beta$  accumulation (Poirier et al, 2000).

Additional genes have been considered as risk factors for SAD (Sandbrink et al, 1996) including the alpha 1-antichymotrypsin allele A (ACT-A), the 5-repeat allele of the VLDL-receptor (VLDL-R) gene, the A2 allele of the HLA-A locus and the oestrogen receptor alpha gene (Urakami et al, 2001). Genes studied in case-control studies of sporadic AD patients range from those involved in A $\beta$  metabolism, oxidative stress and inflammation and are extensively reviewed by Combarros et al, (2002).

Although there is strong support for the amyloid hypothesis of AD due to close association between APP, PS1 and PS2 mutations, the contribution of environmental risk factors to onset and progression of SAD have been considered (reviewed by Brown et al, 2005). Studies investigating the correlation of aluminium, lead or mercury exposure (Gauthier et al, 2000; Cornett et al, 1998; Mutter et al, 2004), diet (Luchsinger & Mayeux, 2004) and pesticide exposure (Baldi et al, 2003) with incidence of AD have provided controversial data. It remains likely that sporadic AD is a culmination of genetic vulnerability and environmental exposures (Jansson, 2005).

### **1.3.4 Beta Amyloid (A $\beta$ )**

A $\beta$  is defined as a fibrillar protein comprising extracellular fibrils forming parallel  $\beta$  sheets. A $\beta$  has an affinity with Congo red and its presence can be determined by staining with Congo red, which under polarised light produces a green birefringence dependent upon positioning of the Congo red molecules along the fibrils (Nilsson, 2004). Amino acid sequencing of cerebrovascular amyloid took place in 1984 (Glenner & Wong, 1984). The subsequent characterisation of cerebral plaque A $\beta$  revealed that it was similar to cerebrovascular A $\beta$  and to A $\beta$  present in the brains of Down's syndrome patients (Masters et al, 1985). Plaques consist of extracellular deposits of A $\beta$  comprising aggregated A $\beta$  peptides up to 43 amino acids in length. Plaques can form a dense core of aggregated A $\beta$  protein that appear as a beta-pleated sheet when stained with Congo red and viewed under polarised light. Plaques of a diffuse nature lacking a dense core are present in greater abundance than core plaques and require staining with antibodies raised against A $\beta$ . The most common forms of amyloid protein usually present in human cerebrospinal fluid are A $\beta$ 1-40 (50-70%) and A $\beta$ 1-42 (5-20%) (Murphy et al, 1999). A $\beta$ 1-42 possesses two hydrophobic residues, isoleucine and alanine, that encourage aggregation into plaques (Selkoe, 1998) and is the most abundant soluble A $\beta$  fragment evident in AD brain tissue (Tambaton & Gamgetti, 2006).

#### **1.3.4.1 Amyloid precursor protein (APP)**

Isolation of A $\beta$  led to the cloning and localisation of the APP gene on chromosome 21 (Tanzi et al, 1987; St.George-Hyslop et al, 1987). Down's syndrome patients, known to produce cerebral A $\beta$  deposits and develop Alzheimer's disease (AD), possess three copies of chromosome 21 (Trisomy 21) suggesting that increased production of APP and A $\beta$  may underlie the neuropathology (Folin et al, 2003). This remains controversial, however, since recent studies have challenged the theory that amyloid plaque pathology in Down's syndrome patients is due to the presence of trisomy 21 (Argellati et al, 2006). APP comprises a family of glycosylated transmembrane proteins that are ubiquitous and present throughout the body (Hardy, 1997). Alternative splicing of the APP gene codes up to 770 amino acid residues (Kosik, 1994) including APP751, APP770 and APP695, the isoform most commonly expressed by neurons (Goedert, 1987). The derivation of A $\beta$  from APP can occur via

a non-amyloidogenic ( $\alpha$ -secretase) pathway or an amyloidogenic ( $\beta$ -secretase) pathway (Kowalska et al, 2004) (fig 1.7). Cleavage by  $\alpha$ -secretase precludes formation of the amyloid domain and releases the N-terminal portion of APP as soluble APP $\alpha$  (sAPP $\alpha$ ) and a C-terminal membrane bound fragment of 83 amino acids (c83). APP cleavage via the  $\beta$ -secretase pathway forms an N-terminal secreted APP $\beta$  (sAPP $\beta$ ) and a C-terminal peptide comprising 99 amino acids (c99) that contains the A $\beta$  fragment. C83 or c99 cleavage by  $\gamma$  secretase results in the formation of a 3kDa fragment (p3) or A $\beta$ . A $\beta$  is a normal product of neuronal cells released in low concentrations and usually found in the CSF and plasma (Selkoe, 1993).

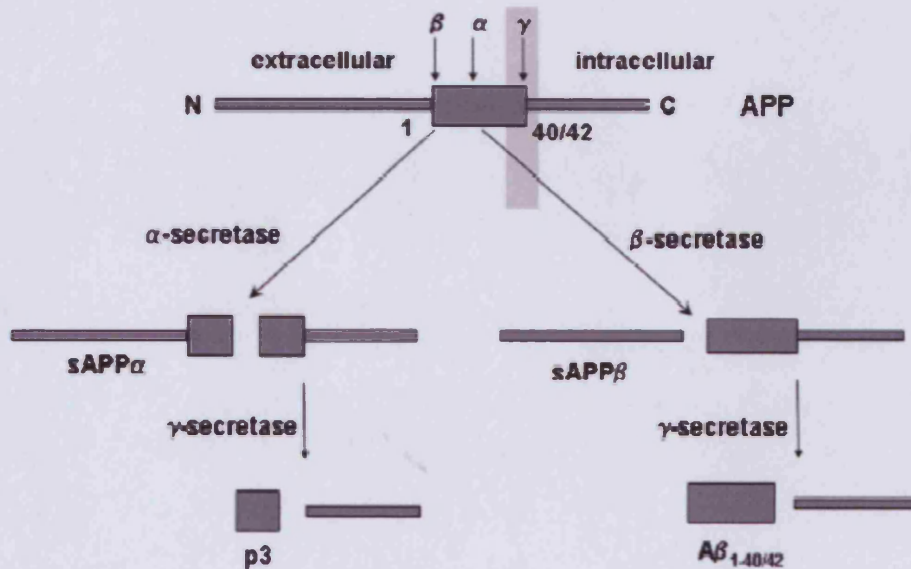


Figure 1.7: Schematic representation of APP processing (Figure taken from Canevari et al, 2004)

#### 1.3.4.2 A $\beta$ : mechanism of action

The mechanism by which A $\beta$  induces inflammation and cell death is unclear but may involve a complex cascade of biochemical events resulting in the imbalance of intracellular ions, production of inflammatory mediators and free radicals, and finally, apoptotic cell death that culminates in massive atrophy of susceptible areas (reviewed by Holscher, 2005) (fig 1.8).

The discovery that A $\beta$  can activate formyl chemotactic receptors (Lorton et al, 2000) or the Receptor for Advanced Glycation Endproducts (RAGE) provided insight into

a potential mechanism for A $\beta$ -induced neurotoxicity (Lue et al, 2001; Sasaki et al, 2001; Du Yan et al, 1997; Yan et al, 1996). Glycooxidation of free amino groups located on the surface of proteins can produce Advanced Glycation Endproducts (AGE) and increased expression of RAGE is evident in microglia and neurons of AD patients (Yan et al, 1996). RAGE has properties of a signal transduction receptor with sites for the transcription factor NF- $\kappa$ B at its promoter. Persistent translocation of NF- $\kappa$ B may occur from binding of A $\beta$  to RAGE resulting in alteration of gene expression in neurons and microglia (Huttunen et al, 1999).

*In vitro* studies have demonstrated that A $\beta$  stimulates glial cells (Kopeck & Carroll, 1998; Akama et al, 1998; Barger et al, 1997; Hu et al, 1999) to release potent inflammatory proteins (Meda et al, 1999; Yates et al, 2000; Del Bo et al, 1995; Apelt & Schliebs, 2001). A $\beta$  can stimulate the production of the proinflammatory cytokines IL-1 $\beta$ , TNF- $\alpha$  and IL-6 from neuronal cultures, microglial cultures (Szczepek et al, 2001; Gitter et al, 1995) and astrocyte cultures (Hu et al, 1998). In addition, the chemokines monocyte chemoattractant protein-1 (MCP-1) and macrophage inflammatory protein-1 $\alpha$  and -1 $\beta$  (MIP-1 $\alpha$  and -1 $\beta$ ) can be stimulated in human monocytes. Cell surface binding of microglia with core plaques may either cause or exacerbate neurotoxicity (reviewed by Bamberger & Landreth, 2001) by increasing the release of cytokines and reactive oxygen species (ROS). Release of such molecules can recruit more immune cells to the area and initiate uptake and degradation of deposited A $\beta$  (reviewed by Tabet et al, 2000; Varadarajan et al, 2000; van Rossum & Hanisch, 2004). Excessive activation of microglia can initiate a vicious cycle in which immune cells recruited to the site release toxic agents that harm surrounding neurons, which further release factors attracting further microglial migration (Ralay Ranaivo et al, 2006).

A $\beta$  induces the production of ROS directly via oxidative stress mechanisms (reviewed by Mattson, 1997; Hensley et al, 1994) and proto-fibrillar and fibrillar A $\beta$  cause ROS toxicity by disturbing the membrane environment of metabolic pathway enzymes and by causing leakage from redox chains (Goodman & Mattson, 1994; Behl & Holsboer, 1998). Antioxidants such as oestrogen (Dykens et al, 2005) and vitamin E (Munoz et al, 2005) have been reported to exert neuroprotection against amyloid-induced oxidative stress suggesting involvement of oxidative stress in the neurodegeneration evident in AD brain tissue. A $\beta$ 1-42 or A $\beta$ 25-35 treatment of

mixed hippocampal cultures reduced intracellular astrocytic and neuronal levels of glutathione, a reducing agent that forms part of an antioxidant system in the CNS, indicating a role for oxidative stress in A $\beta$ -induced neurotoxicity (Abramov et al, 2003). Evidence from in vitro studies suggests A $\beta$  can alter intracellular calcium levels via the modification of voltage-gated ion channels (Green & Peers, 2001; Kasparova et al, 2001; Rovira et al, 2002) or through induction of membrane leakiness and oxidative stress (Huang et al, 2000). A $\beta$ -induced free radical generation may also occur via its binding and reducing of reactive metals such as copper (Bush et al, 2003) and iron to provoke hydroxyl radical production.

Neurons in post mortem tissue from AD patients display signs of apoptosis (Su et al, 1994, Mattson et al, 1998). A $\beta$  may induce apoptosis in surrounding neurons via the p53-Bax cell death pathway (Zhang et al, 2002) although the exact mechanism is unknown. Fibrillar A $\beta$  may also form large voltage-independent non-selective ion channels (reviewed by Kagan et al, 2002) or bind to a mitochondrial endoplasmic reticulum (ER)-associated protein called amyloid  $\beta$ -peptide binding protein alcohol dehydrogenase (ABAD) (Yan et al, 1997). Increased expression of ABAD is evident in aged and AD brain and may potentiate A $\beta$ -induced apoptosis and free radical generation in neurons (Lustbader et al, 2004). In vitro and immunohistochemical studies have revealed that neurons undergoing A $\beta$  mediated cell death exhibit classic characteristics of apoptosis (Cotman & Anderson, 1995; Kusiak et al, 1996) which, correlates with the presence of aggregated A $\beta$  forms (reviewed by Iversen et al, 1995).

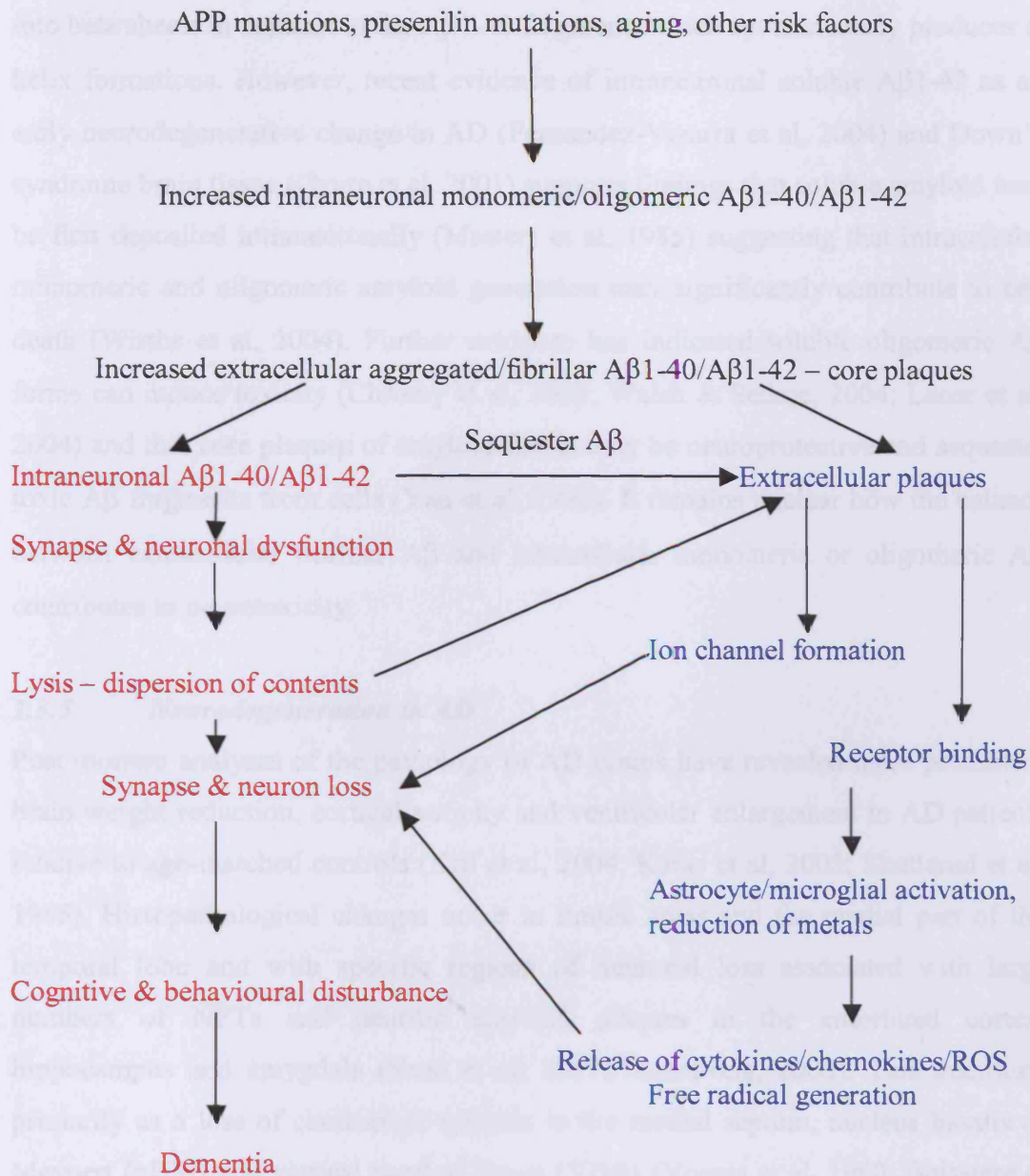


Figure 1.8: Schematic representation of the postulated mechanisms of A $\beta$ -mediated neurodegeneration

#### 1.3.4.3 Role of different A $\beta$ forms in neurotoxicity

The original ‘amyloid hypothesis’ assumed that extracellular deposition of A $\beta$  is necessary for cell death (Hardy & Allsop, 1991) and evidence for A $\beta$  as a causative agent in AD was derived from genetic mutations of APP (Selkoe, 2000). Early literature suggested the extracellular fibrillar form of A $\beta$  to be the most neurotoxic (Simmons et al, 1994; Howlett et al, 1995; Jarrett et al, 1993) and that the neurotoxicity induced by the A $\beta$ 1-42 fragment relates to its readiness to aggregate

into beta sheets in contrast to the A $\beta$ 1-40 fragment, which spontaneously produces  $\alpha$  helix formations. However, recent evidence of intraneuronal soluble A $\beta$ 1-42 as an early neurodegenerative change in AD (Fernandez-Vizarra et al, 2004) and Down's syndrome brain tissue (Gyure et al, 2001) supports findings that soluble amyloid may be first deposited intraneuronally (Masters et al, 1985) suggesting that intracellular monomeric and oligomeric amyloid generation may significantly contribute to cell death (Wirhth et al, 2004). Further evidence has indicated soluble oligomeric A $\beta$  forms can induce toxicity (Chromy et al, 2003; Walsh & Selkoe, 2004; Lacor et al, 2004) and that core plaques of amyloid fibrils may be neuroprotective and sequester toxic A $\beta$  fragments from cells (Yan et al, 1996). It remains unclear how the balance between extracellular fibrillar A $\beta$  and intracellular monomeric or oligomeric A $\beta$  contributes to neurotoxicity.

### ***1.3.5 Neurodegeneration in AD***

Post mortem analyses of the pathology of AD brains have revealed more prominent brain weight reduction, cortical atrophy and ventricular enlargement in AD patients relative to age-matched controls (Kril et al, 2004; Karas et al, 2003; Skullerud et al, 1985). Histopathological changes occur in limbic areas and the medial part of the temporal lobe and with specific regions of neuronal loss associated with large numbers of NFTs and neuritic amyloid plaques in the entorhinal cortex, hippocampus and amygdala (Scott et al, 1991; Armstrong, 2006). This manifests primarily as a loss of cholinergic neurons in the medial septum, nucleus basalis of Meynert (nBM) and vertical band of Broca (VDB) (Vogels et al, 1990; Boissiere et al, 1996). Extensive neurodegeneration is also evident in central noradrenergic neurons projecting from the locus coeruleus (LC) (Lyness et al, 2003; Engelborgh & De Deyn, 1997), the main site of NA synthesis innervating terminal regions including the cortex and hippocampus (Mann et al, 1982; Mann & Yates, 1983). LC degeneration correlates with duration of illness (Zarow et al, 2003) and duration and severity of dementia (Bondareff et al, 1987). Loss of noradrenergic specific neurons or NA is also associated with the incidence of depression in patients suffering from AD or PD (Chan-Palay & Asan, 1989). Remaining LC neurons may compensate for degeneration via neuronal sprouting (Szot et al, 2006; Hoogendijk et al, 1999) however; alpha 2C adrenoceptors remained significantly reduced in the hippocampus

of AD patients (Szot et al, 2006).

### **1.3.6 Neuroinflammation in AD**

#### **1.3.6.1 Cell-mediated inflammation**

Although neuroinflammation is evident in a number of CNS disorders such as stroke, Parkinson's disease and multiple sclerosis, it is uncertain whether the inflammatory response predisposes to or subsequently exacerbates the neuropathology.

Neuroinflammatory changes observed in AD sufferers, of both sporadic and familial cases of AD, occur early on in disease progression (Sasaki et al, 1997). The inflammatory state is characterised by the presence of activated microglia and reactive astrocytes within degenerating brain regions (McGeer et al, 1988; Meda et al, 1995; Akiyama et al, 2000). Microglia, resident macrophage cells in the brain, appear to localise around senile plaques in AD tissue (McGeer et al, 1994; Itagaki et al, 1989; Uchihara et al, 1997; Kalaria et al, 1999) and produce toxic agents that damage neurons (Siman et al, 1989). The activated state of the glial cells can be determined immunohistochemically with antibodies directed against specific proteins expressed on the cell surface such as major histocompatibility complex (MHC) II glycoproteins and integrins such as the CD11b receptor.

Additional resident CNS glial cells, astrocytes (Tanaka et al, 1999), can also become reactive and have a defensive role in the neuropathology of AD (Aschner, 1998, DeWitt et al, 1998). Reactive astrocytes are characterised by their hypertrophic morphology and localised by immunohistochemical staining for the astrocytic marker, glial fibrillary acidic protein (GFAP). Astrocytes are located around senile plaques and appear to create a barrier between plaque and healthy tissue. Astrocytes also have a key role in maintaining the integrity of the blood-brain barrier (BBB) since the astrocytic foot sits alongside the endothelial wall of blood vessels that comprise the microvasculature separating brain tissue and circulating blood (Kim et al, 2006). Discrete BBB breakdown in AD patients, as exemplified by reduced cerebral blood flow and endothelial cell degeneration (Kalaria et al, 1995), suggests compromised cerebrovasculature in the brain may contribute to intense astrocytic activation.

It is difficult to determine whether the localisation of microglia with senile plaques is to enhance clearance of the insoluble plaque or to mediate aggregation of soluble

amyloid. Although aggregated amyloid can induce inflammatory processes and cellular toxicity, it is unclear whether senile plaque production may be a protective mechanism to prevent the neurotoxic effects of precursor amyloid forms. In AD tissue, microglia can assist the conversion of diffuse soluble amyloid to aggregated plaques (Cotman et al, 1996; Griffin et al, 1995, Mackenzie et al, 1995; Sasaki et al, 1997) but also, as phagocytes, internalise plaques (Shaffer et al, 1995; DeWitt et al, 1998).

#### 1.3.6.2 Cytokines

Astrocytes and microglia respond to injury or tissue damage by releasing an array of cytokines capable of recruiting further macrophage and neutrophils (reviewed by Mrazek et al, 1995). Proinflammatory cytokines such as IL-1 $\beta$  (Griffin et al, 1989; Griffin et al, 1995; Shaw et al, 2001), TNF- $\alpha$  (Dickson et al, 1993; Grammas et al, 2001; Tarkowski et al, 1999; Tarkowski et al, 2000) and IL-6 (Luterman et al, 2000) have been detected in post-mortem AD brain tissue. These cytokines are localised in plaque-associated microglia suggesting their involvement in either promoting clearance or modulating formation of aggregated amyloid deposits. IL-1 $\beta$  modulates plaque formation (Sheng et al, 1995; Grilli et al, 1996; Rogers et al, 1999) and APP production (Forloni et al, 1992; Rogers et al, 1999; Goldgaber et al, 1989) implicating amyloid-induced IL-1 $\beta$  in further increasing amyloid levels. IL-1 $\beta$  and TNF- $\alpha$  also appear essential for amyloid induced neurotoxicity (Viel et al, 2001) further exacerbating disease pathology.

Polymorphisms located in promoter and non-coding regions of cytokine genes appear to increase the risk of developing AD (Ravaglia et al, 2006). Their presence is, however, unlikely to initiate the disease alone (reviewed by Griffin, 2006; Cacquevel et al, 2004). Polymorphisms for several cytokines including the IL-6 gene promoter (Licastro et al, 2003), TNF- $\alpha$  (Alvarez et al, 2002), IL-1 $\alpha$  (Combarros et al, 2002), IL-1 $\beta$  (Sciacca et al, 2003) and the anti-inflammatory cytokine IL-10 (Lio et al, 2003) have been associated with AD. Polymorphism for a specific IL-1 $\alpha$  gene can increase the risk of developing AD by three fold and this risk increases if combined with an IL-1 $\beta$  polymorphism (Mrazek & Griffin, 2001). Genetic polymorphisms occur more frequently in AD patients compared with age-matched

controls resulting in increased expression of inflammatory mediators, potentially affecting the progression of AD pathology (McGeer & McGeer, 2001).

#### *1.3.6.3 Chemokines*

Chemokines are a structurally and functionally related family of proteins expressed by astrocytes, microglia and endothelial cells. Chemokines act on receptors located on neurons, microglia and leukocytes to recruit inflammatory cells to the site of injury (Biber et al, 2006). The family includes IL-8, macrophage inflammatory protein (MIP)-1, monocyte chemoattractant protein (MCP)-1 and RANTES (regulated upon activation, normal T-cells, expressed and secreted). Chemokines have been localised throughout the AD brain (Xia et al, 1999).

#### *1.3.6.4 Other markers of neuroinflammation*

Prostaglandin 2 (PGE<sub>2</sub>), a proinflammatory mediator, is elevated in cerebral spinal fluid (CSF) from AD patients relative to controls (Ho et al, 2000; Montine et al, 1999). Post mortem, analysis of AD brain has also established the presence of markers of oxidative stress (Aslan & Ozben, 2004; Luth et al, 2005) and evidence of NOS (Luth et al, 2002; Fernandez-Vizarra et al, 2004). Markers of nitric oxide production, 3-nitrotyrosine (Tohgi et al, 1999) and nitrate (Navarro et al, 1996; Kuiper et al, 1994) were also altered in the CSF of AD patients.

#### *1.3.7 Anti-inflammatory agents as disease modifying therapy for AD*

The incidence of AD in populations with inflammation-associated diseases such as rheumatoid arthritis has provided greater understanding of the potential role of anti-inflammatory therapies for AD (Naccari, 2003). Epidemiological studies suggest patients on non steroidal anti-inflammatory drug (NSAID) therapy have a decreased risk of AD and delayed disease onset (Breitner, 1996; McGeer et al, 1996; McDowell, 2001). The Baltimore Longitudinal Study of Aging confirmed that NSAID use, particularly ibuprofen, was beneficial in preventing AD (Stewart, 1997) and effects were dependent on duration of treatment. Stewart et al, 1997 found that for individuals using NSAIDs for less than 2 years there was a risk reduction of one third. Patients using NSAIDs for > 2 years reduced their risk by 60% whilst in a larger cohort of individuals this length of treatment demonstrated an 80% reduction

in AD incidence (In't Veld et al, 1998). NSAID treatment appears to be more successful if administered before disease onset or early on in disease progression. Hence, patients would need to take treatment before onset of any overt AD-associated symptoms. Additionally, treatment duration will also increase the incidence of gastrointestinal toxicity due to the unwanted peripheral effects of NSAIDS (Rogers et al, 1993; Tabet et al, 2002). Despite epidemiological evidence suggesting NSAIDS may be beneficial in AD, the results obtained from controlled clinical trials in AD patients have not demonstrated any beneficial effect of NSAID treatment (Firuzi & Pratico, 2006). The method by which NSAIDS may halt disease progression remains unclear but it is postulated that NSAIDS may influence the metabolism of APP or alter disease progress by activating peroxisome proliferator-activated receptors (Aisen et al, 2002).

#### **1.4 Neuroinflammation and neurodegeneration in animal models**

The mechanisms by which LPS and A $\beta$  may cause neuroinflammation and neurodegeneration have been described previously in this introduction. In this section, I will outline current reported evidence for neuroinflammation and neurodegeneration following the administration of LPS or A $\beta$  in vivo or in APP and APP/PS1 transgenic A $\beta$  models.

##### **1.4.1 LPS – *in vivo* models**

###### **1.4.1.1 LPS-induced neuroinflammation**

Administration of LPS either centrally (Gayle et al, 1998; Gayle et al, 1999; Plata-Salaman et al, 1998; De Simoni et al, 1995; Gottschall et al, 1992; Muramami et al, 1993; Szczepanik & Ringheim, 2003; Kelehua et al, 2000; Song et al, 1999; Finck et al, 1997; Sanna et al, 1995; Di Santo et al, 1995; Nicholson & Renton, 2001; Chen et al, 2000) or peripherally (Ghezzi et al, 2000; Sironi et al, 1992; Turrin et al, 2001; Castanon et al, 2004) to rodents can induce both pro- and anti-inflammatory cytokine production.

Intracerebroventricular (ICV) injection of LPS induces pro-inflammatory cytokine mRNA expression in the brain (Gayle et al, 1998; Gayle et al, 1999; Plata-Salaman et al, 1998; De Simoni et al, 1995) via direct action on brain tissue. Peripheral

administration of LPS can also induce proinflammatory cytokine mRNA expression in the brain albeit to a lesser magnitude (Jacobs et al, 1997; Kakizaki et al, 1999; Laye et al, 1994; Pitossi et al, 1997; Satta et al, 1998; Goujon et al, 1997; Castanon et al, 2004).

Despite previous reports describing LPS-induced cytokine mRNA expression in rodent brain tissue in vivo, reports of LPS-induced cytokine protein, particularly following peripheral administration of LPS, are limited (Goujon et al, 1996; 1997). Reports focus primarily on intraperitoneal (IP) LPS-induced cytokine protein changes in blood or plasma (Sironi et al, 1992; Purswani et al, 2002; Bobrowski et al, 2005) and the literature does not comprehensively describe the detection of a multitude of central cytokine proteins in brain tissue within the same animal following LPS administration.

#### *1.4.1.2 LPS-induced neurodegeneration*

Some studies have revealed an increase in the number of terminal deoxynucleotidyl transferase-mediated dUTP nick-end labelling (TUNEL) stained cells in various brain regions post IP LPS injection of rats (Nolan et al, 2000; Semmler et al, 2005). This suggests that peripheral administration of LPS may result in limited apoptosis in brain tissue. ICV injection of LPS may cause oxidative damage to the brain, despite the absence of overt neuronal loss. ICV LPS administration to C57BL6/J mice resulted in an acute transient increase in F4-isoprostanes (prostaglandin-like products of free radical-catalysed docosahexaenoic acid peroxidation) (Milatovic et al, 2003). Significant neurodegeneration can also be obtained by the direct injection of LPS into brain regions including the hippocampus (Ambrosini et al, 2005) and the substantia nigra (Li et al, 2004). Neurodegeneration was evident as a substantial loss in NeuN positive neuronal cell bodies or tyrosine hydroxylase-immunoreactive (TH-ir) neurons respectively.

Administration of an additional insult to LPS-treated animals appears to enhance the probability of inducing neuronal death. For example, mice receiving the glucocorticoid receptor inhibitor, RU486, alongside intracerebral LPS, detectable brain damage was evident after 3 days (Soulet & Rivest, 2003). Additionally, BALB/cJ mice administered with an IP dose of LPS before the induction of hypoxia-ischaemia (HI) suffered axonal and neuronal loss in the corpus callosum not evident in control HI mice (Lehnardt et al, 2003).

## 1.4.2 *A $\beta$ – Exogenous in vivo models*

### 1.4.2.1 *Exogenous A $\beta$ -induced neuroinflammation*

Injection or infusion of A $\beta$  peptide into brain tissue causes neuroinflammation. Injection of fibrillar A $\beta$ , but not soluble A $\beta$ , resulted in astrocytic and microglial activation in rat striatum (Weldon et al, 1998) with astrocytes surrounding the fibrillar deposits and providing a ‘wall’ to protect adjacent tissue whilst activated microglia phagocytosed the deposit. Further data support the presence of this pathology in rodent in vivo models (Frautschy et al, 1991; O’Hare et al, 1999; Scali et al, 1999; Stephan et al, 2001; Jantaratnotoi et al, 2003; Ryu et al, 2004; Frautschy et al, 2001).

The activation of microglia and astrocytes and the associated release of inflammatory cytokines, iNOS and COX2 can be potentiated by further insult to the animal. N - (2-chloroethyl)-N-ethyl-2-bromobenzylamine (DSP-4) induced noradrenergic depletion rendered rat brain tissue more susceptible to A $\beta$ -induced neuroinflammation (Heneka et al, 2002). Weldon et al, 1998 suggested that the separation of an A $\beta$  deposit from surrounding neuropil by astrocytes means it is unlikely that neurotoxicity occurs as a result of direct contact between A $\beta$  and neurons. The toxic mediators released by microglia, particularly NO molecules, may act as intermediary factors to induce neurodegeneration in surrounding neuronal populations, a hypothesis supported by in vitro evidence (Giulian et al, 1996); but it may also be the case that microglia phagocytose the A $\beta$  deposit. A recent study described the clearance of A $\beta$ 1-42 following A $\beta$  injection into the hippocampus of Wistar rats suggesting phagocytosis of the deposit by surrounding microglia (Takata et al, 2004).

### 1.4.2.2 *Exogenous A $\beta$ -induced neurodegeneration*

Early studies have focused on the influence of the ICV administration of A $\beta$  on pathology associated with a cognitive impairment (Nakamura et al, 2001; Yamada et al, 1999). ICV infusion of A $\beta$  in vivo causes a reduction in the enzyme choline acetyltransferase (ChAT) usually responsible for degrading acetylcholine, a key neurotransmitter involved in learning and memory systems (Nabeshima & Nitta, 1994). Reduced ChAT may indicate a compensatory mechanism to enhance the level

of acetylcholine in the brain and hence, administration of A $\beta$  into CNS tissue may impair the activity of important neurotransmitter systems and associated neuronal circuits (Verhoeff, 2005). Reduced ChAT activity may underlie the cognitive deficits demonstrated in A $\beta$  treated animals. ICV injection of A $\beta$  results in learning and memory impairments in rodents when assessed in spontaneous alternation, passive avoidance and Morris water maze assays (Yamada, 1999). Animals infused with A $\beta$  plaques derived from AD patients displayed impairments in the watermaze and ChAT loss in the hippocampus and frontal cortex (Nitta et al, 1994). At 2 weeks post amyloid infusion, a reduction in ChAT activity in frontal cortex and hippocampus was associated with memory deficit in watermaze and passive avoidance tests (Nabeshima, 1994).

There are published reports of ICV A $\beta$ -induced cell loss (Nakamura, 2001) and diffuse amyloid deposition in rodent brain tissue, particularly in the presence of transforming growth factor (TGF) - $\beta$  (Frautschy et al, 1996). It remains difficult, however, to consistently achieve A $\beta$  deposition and resulting neurodegeneration using this method of administration. Much work by Frautschy et al (2001) has demonstrated that injection of A $\beta$  into rodent brain tissue results in diffuse A $\beta$  deposition in brain regions pertinent to AD, especially in rats. However, the co-administration of TGF- $\beta$  or high-density lipoprotein (HDL) with A $\beta$  significantly improves A $\beta$  deposition (Frautschy et al, 2001; Harris-white et al, 2004) and results in a reduction in synaptophysin (a protein present in synaptic vesicle membranes) (Craft et al, 2004). In addition to the inconsistent A $\beta$  deposition following injection of exogenous A $\beta$  into brain tissue, recent work has also revealed that A $\beta$  injected ICV may remain in the ventricular systems and be removed by phagocytic cells, thus A $\beta$  peptide may not diffuse into brain tissue sufficiently to cause overt neurodegeneration (Nakagawa, 2004).

Direct injection into discrete brain areas, particularly those usually susceptible to degeneration in AD, may afford an alternative method of eliciting A $\beta$ -induced cell death in vivo. Some authors have not demonstrated A $\beta$ -induced neurodegeneration in vivo using this method (Games et al, 1992; Cleary et al, 1995) and suggest that microglia can phagocytose A $\beta$  deposits (Shin et al, 1997; Bishop et al, 2003). Others demonstrate cell loss that is adjacent to the injection site only (Frautschy et al, 1991;

Emre et al, 1992; Giordano et al, 1994; Wang et al, 1994; Miguel-Hidalgo et al, 1998; Stephan et al, 2001; Nakamura et al, 2001; Jantaratnotai et al, 2003; Ryu et al, 2004) or is evident in specific neuronal populations (Weldon et al, 1998). A $\beta$  deposits may remain in the tissue even up to 6 months post surgery (Giovannelli et al, 1998; Weldon et al, 1998).

Early studies demonstrated that A $\beta$ -induced toxicity may depend upon the solvent used to dissolve A $\beta$ . Particular attention focused on acetonitrile, an organic solvent used as a vehicle for exogenous amyloid application (Kowall et al, 1991). It is clear that acetonitrile alone is toxic to neurons, either via its conversion to cyanide through the actions of cytochrome P450 (Freeman et al, 1998) or via its toxic effect on cell membranes, allowing calcium-mediated neurotoxicity (Mattson et al, 1992). A $\beta$  may enhance toxicity induced by the acetonitrile solvent by potentiating calcium-mediated neurotoxicity. The intra-hippocampal injection of human A $\beta$ 1-40 or rat A $\beta$ 1-40 enhanced the toxicity of 35% acetonitrile whilst A $\beta$  in water or phosphate buffered saline (PBS) demonstrated little effect (Waite et al, 1992). In contrast, A $\beta$ 1-40 dissolved in 35% acetonitrile and injected into the neocortex of rhesus monkeys did not potentiate neurotoxicity relative to acetonitrile alone (Podlisny et al, 1992).

### ***1.4.3 A $\beta$ – Endogenous in vivo models – Transgenic mice***

#### ***1.4.3.1 Endogenous amyloid-induced neuroinflammation***

APP or APP/PS1 overexpressing transgenic mice exhibit neuroinflammation, exemplified by age-dependent activated microglia and astrocytes. APP (V717I) transgenic mice display activated glia in hippocampal and cortical regions at 3 months, which became pronounced by 16 months of age (Heneka et al, 2005). Similarly, the PSAPP model comprising APP and PS1 mutations shows a robust age-dependant increase in amyloid plaques surrounded by activated microglia and associated with reactive astrocytes, which increased with age and amyloid burden (Matsuoka et al, 2001). A small number of activated microglia was observed in the absence of amyloid plaques, most appeared to associate mainly with diffuse and fibrillar deposits. Analysis of the microglial phenotype in Tg2576 APP overexpressing mice indicated microglia may sustain plaque development whilst astrocytic degradation of A $\beta$  and separation of A $\beta$  from surrounding neurons

suggests astrocytes aid neuroprotection (Wegiel et al, 2001). Alteration of the expression of pro- and anti-inflammatory cytokines is also evident in APP and APP/PS1 transgenic mice. Abbas et al, 2002, reported elevated cortical IFN $\gamma$  and IL12 mRNA and protein expression that peaked by 17-19 months and was associated with reactive microglia and astrocytes surrounding plaque deposits in Tg2576 mice. Anti-inflammatory treatment of APP or APP/PS1 transgenic mice using NSAIDs (Yan et al, 2003; Weggen et al, 2001; Lim et al, 2001), curcumin (the active ingredient in the curry spice turmeric) (Lim et al, 2001) or pravastatin (a hypolipidemic agent used for lowering cholesterol) (Chauhan et al, 2004) has demonstrated reduction of either soluble A $\beta$ 1-42 or plaque burden. These findings demonstrate the key role inflammatory mediators possess in modulating amyloid production.

#### *1.4.3.2 Endogenous amyloid-induced neurodegeneration*

Many of the initial APP and APP/PS1 overexpressing transgenic mouse lines that were constructed did not exhibit overt neurodegeneration despite extensive plaque deposition in the hippocampus, cortex and amygdala (Stein & Johnson, 2002; Higgins & Jacobsen, 2003). Evidence suggests that, particularly in models of slow amyloid deposition such as Tg2576, amyloid may be sequestered via increased transthyretin, a sequestering protein upregulated by sAPP $\alpha$  (Stein & Johnson, 2002) as part of a neural mechanism to cope with widespread accumulation of aggregated amyloid. Chronic infusion of an antibody against transthyretin leads to increased amyloid and tau phosphorylation with apoptosis and neuronal loss in the CA1 hippocampal field in Tg2576 mice. This further suggests sAPP $\alpha$  driven neuroprotective gene expression may protect APP transgenic mice from neurodegeneration (Stein et al, 2004). APP23 mice demonstrate hippocampal and cortical neurodegeneration, which can be exacerbated by the noradrenergic neurotoxin, DSP-4 (Heneka et al, 2006). The APP (SL) PS1KI model appears to be the best documented transgenic model presenting extensive neuronal loss (>50%) in the CA1/2 pyramidal hippocampal layer associated with intracellular A $\beta$  and astrogliosis that develops in correlation with the neuronal loss (Casas et al, 2004). Recent data described a reduction of about 30% in pyramidal hippocampal neurons in APP751/PS1 transgenic mice that did not correlate with extracellular A $\beta$  plaque

load, suggesting multiple mechanisms of A $\beta$  neurotoxicity (Shmitz et al, 2004). Rockenstein et al, 2005 compared high levels of human beta-secretase (BACE) -1, with and without hAPP. hBACE1/hAPP double transgenic and hBACE1 transgenic mice exhibited neurodegeneration in the neocortex and hippocampus despite reduced A $\beta$  levels. These recent reports provide evidence that neurodegeneration may correlate with the accumulation of intraneuronal A $\beta$  as the neurodegeneration observed in APP (SL) PS1KI and APP751/PS1 mice correlates with increased intraneuronal A $\beta$  immunoreactivity (Games et al, 2006).

## **1.5 Thesis Objectives**

Presently, therapeutic agents for AD primarily provide symptomatic relief and do not modify the progression of disease pathology. The limitations of current in vivo rodent models of neuroinflammation and neurodegeneration make preclinical screening of putative anti-inflammatory and neuroprotective agents for AD difficult. Quantification of markers of neuroinflammation following LPS, as a commonly used immunostimulant, or A $\beta$ , the peptide associated with AD, administration relies on the detection of cytokine mRNA expression, which may not translate to the final protein product. Current models of exogenous or endogenous A $\beta$  induced neurodegeneration do not demonstrate reproducible and quantifiable neuronal cell death. This thesis explores the development of rodent in vivo models using exogenous LPS and A $\beta$  injection approaches and endogenous A $\beta$  transgenic models and discusses their suitability for screening novel agents.

## **CHAPTER 2**

### ***Peripheral administration of LPS – an in vivo model of neuroinflammation?***

#### **2.1 Introduction**

Despite a number of reports describing the expression of proinflammatory cytokine mRNA in rodent brain (Jacobs et al, 1997; Castanon et al, 2004) there are currently only limited reports of cytokine protein detection in rodent brain tissue (Goujon et al, 1996; 1997) following IP administration of LPS. Previous literature has reported the use of Luminex<sup>®</sup> for detecting a wide range of cytokine proteins within a single rodent plasma sample (Bobrowski et al, 2005). I describe the application of this technology to the detection of LPS-induced cytokine protein in rodent brain tissue. It is important to also establish that the expression of cytokines in brain tissue is a centrally derived response and not due to infiltration of blood borne cytokines. The detection of other proteins by Luminex<sup>®</sup> has not yet been documented but kits have been developed to detect phosphorylated proteins. Phosphorylated proteins are involved in LPS-mediated intracellular signalling and their detection by Luminex<sup>®</sup> may confirm the presence of a brain response to peripheral LPS administration. I describe the application of Luminex<sup>®</sup> for assessing phosphorylated proteins including I $\kappa$ B $\alpha$ , JNK, ERK and p38 in rodent brain tissue. The induction of cytokine mRNA expression in brain tissue is also assessed using Taqman PCR techniques. Finally, to illustrate pharmacological modulation of LPS induced cytokines in the rodent brain, the changes in LPS induced central and peripheral cytokine expression following administration of the glucocorticoid dexamethasone and the  $\alpha$ 2 adrenoceptor antagonist, fluparoxan, will be examined.

##### **2.1.1 Glucocorticoid (GC) modulation and inflammation**

Circulating cytokines can induce endogenous glucocorticoid production via activation of the HPA axis (Buckingham et al, 1994). Levels of serum corticosterone rise rapidly in LPS challenged mice, initially rising in a profile similar to that of

serum TNF- $\alpha$  but remaining elevated for up to 24 hours after LPS administration, well after TNF- $\alpha$  levels have returned to baseline (Eskay et al, 1990). Adrenalectomised animals demonstrate increased expression and production of inflammatory mediators in models of inflammatory disease (Perretti et al, 1989; Calignano et al, 1985; Bertini et al, 1989; Smith et al, 2002) that can be reversed by administration of glucocorticoids. The glucocorticoid receptor inhibitor, RU486, can also increase the inflammatory reaction observed in animals injected intracerebrally with LPS, demonstrating glucocorticoids may protect the brain from inflammatory insult (Nadeau & Rivest, 2003). Systemic glucocorticoids including prednisolone and dexamethasone are strong immunosuppressants that can alleviate symptoms in inflammatory based disorders including asthma and arthritis but their use is limited to a short duration of therapy due to severe adverse effects (Roumestan et al, 2004). Although the attenuation of IP LPS-induced plasma cytokine production by glucocorticoid treatment has been previously described in rodent (Sironi et al, 1992, Mengozzi et al, 1994), the effect of dexamethasone treatment on IP LPS-induced plasma and brain cytokines has not yet been reported. Studies 3 through to 5 of this thesis investigate the effect of the strong anti-inflammatory agent dexamethasone on IP LPS-induced cytokine protein in rodent brain tissue and plasma detected by Luminex<sup>®</sup> suspension bead array system.

### **2.1.2 *P38 $\alpha$ inhibition and inflammation***

P38 $\alpha$ , an isoform of the p38 MAP kinase, has a well defined role in inflammation and its involvement in the expression of cytokines such as IL1- $\beta$  and TNF- $\alpha$  is well documented (reviewed by Adams et al, 2001).

P38 $\alpha$  inhibitors potently inhibit cytokine production in vitro (Lee et al, 1994; Dean et al, 1999) and in vivo (Barone et al, 2001) and demonstrate anti-inflammatory properties in models of chronic inflammatory based neurodegenerative and peripheral disorders, infection, cancer and autoimmune disease (reviewed by Kaminska, 2005). A number of companies began to develop potent, orally bioavailable p38 $\alpha$  inhibitors after the publication of pyridinyl imidazole compounds (Lee et al, 1994) as inhibitors of cytokine production. Currently, the assessment of a number of molecules is taking place in the clinic (reviewed by Lee & Dominguez, 2005; reviewed by Dominguez et al, 2005), particularly for treatment of rheumatoid

arthritis (reviewed by Schieven, 2005).

P38MAPK inhibitors are able to reduce cytokine production by controlling gene transcription and translation and by destabilising cytokine mRNA (Lee et al, 1994). These agents are suitable compounds to assess attenuation of LPS-induced cytokine protein in vivo. There is evidence of central p38 phosphorylation post IP LPS (Kelly et al, 2003) but there is no published literature describing the effect of p38MAPK inhibitors in an IP LPS in vivo model of central and peripheral cytokine protein. Study 5 examines the effect of the p38 $\alpha$  inhibitor, GW569293, on IP LPS-induced cytokine protein in rat brain tissue and plasma detected via Luminex<sup>®</sup> suspension bead array system.

### **2.1.3 *$\alpha$ 2-adrenoceptor antagonism and inflammation***

Early evidence supported the involvement of monoamines such as serotonin (5-HT) and noradrenaline (NA) in the regulation of inflammation. In a model of carrageenan-induced paw oedema, whole brain and hypothalamic concentrations of NA were augmented during acute peripheral inflammation (Bhattacharya et al, 1988). Intraperitoneally (IP) administered LPS significantly increased hippocampal and preoptic NA levels in rat (Linthorst & Reul, 1998). Denervation of NA fibres in a model of arthritis resulted in earlier onset and increased severity of inflammation and arthritic pathology (Felton et al, 1992) whilst carrageenan-induced inflammation in rabbit demonstrated an increase in  $\alpha$ 2 receptor affinity or numbers in articular blood vessels (Gray & Ferrell, 1992). Cytokine modulation through control of intracellular cAMP levels appears to occur via  $\alpha$ 2 adrenoceptor mediated inhibition and beta-adrenoceptor activation of adenylate cyclase demonstrating the role of  $\alpha$ 2 receptors in cytokine production.

NA acts via G-protein linked alpha ( $\alpha$ ) or beta ( $\beta$ ) adrenoceptors. There are two subtypes of  $\alpha$  receptor,  $\alpha$ 1 and  $\alpha$ 2 which, when activated, can either stimulate release of intracellular calcium ( $\alpha$ 1) or decrease adenylate cyclase activity ( $\alpha$ 2). The three subtypes of  $\beta$  receptor ( $\beta$ 1, 2 and 3) can increase adenylate cyclase activity resulting in induction of intracellular cAMP.  $\alpha$ 2 adrenoceptors are further subdivided into three isoforms,  $\alpha$ 2A,  $\alpha$ 2B and  $\alpha$ 2C localised primarily at synaptic junctions where their role is to control neurotransmitter release.  $\alpha$ 2 receptors act as inhibitory

autoreceptors by inhibiting the release of NA. NA or synthetic agents such as the agonists clenbuterol or clonidine (Boyd, 2001) or the antagonists yohimbine or fluparoxan act at  $\alpha_2$  receptors (Maes et al, 2000; Halliday et al, 1991). Antagonists of  $\alpha_2$  adrenoceptors antagonise the inhibitory effect of the receptor on NA release resulting in an increase in synaptic NA.  $\alpha_2$  adrenoceptors are widely distributed throughout the rat brain (Scheinin et al, 1994) and are localised at synapses (Aoki et al, 1994) and on the cell surface of macrophage and monocytes (Spengler et al, 1990).

The anti-inflammatory effect of NA (reviewed by Galea et al, 2003) is mediated by down-regulating the expression and release of pro-inflammatory cytokines (Kaneko et al, 2005; Hu et al, 1991; Willis & Nisen, 1995) and inhibiting microglial activation (Lee et al, 1992; Loughlin et al, 1993; Chang & Liu, 2000) evident in AD. Recent reports describing the role of NA in CNS pathology are controversial. Wenk et al, 2003 demonstrated a lack of DSP-4 mediated potentiation of neuroinflammation or cholinergic neurodegeneration; however, noradrenergic depletion in APP overexpressing mice exacerbated neuroinflammation and neurodegeneration (Heneka et al, 2006) and potentiated A $\beta$ -induced cortical cytokine and iNOS expression in rat in vivo (Heneka et al, 2002). Increasing NA levels via the antagonism of  $\alpha_2$  adrenoceptors may inhibit the expression of IP LPS-induced cytokine protein in brain tissue or plasma and attenuate LPS-induced iNOS expression in plasma. Study 5 investigates the effect of the  $\alpha_2$  adrenoceptor antagonist, fluparoxan, on IP LPS-induced cytokine protein in rat brain tissue and plasma detected by Luminex<sup>®</sup> suspension bead array system and plasma nitrite, a marker of iNOS production.

#### **2.1.4 Chapter Aims**

This series of studies sought to establish a high-throughput model of neuroinflammation by evaluating:

1. The detection of IP LPS-induced plasma and brain-derived cytokine protein using the Luminex<sup>®</sup> suspension bead array system.
2. The involvement of a brain-derived response to IP LPS by assessing cytokine mRNA and phosphoprotein expression in brain tissue.
3. The suitability of the peripheral LPS model for screening putative anti-

inflammatory therapies by investigating the effects of dexamethasone as a standard anti-inflammatory treatment and via p38 inhibition or alpha2 adrenoceptor antagonism.

## **2.2 Materials & Methods**

### **2.2.1 Materials**

The p38 inhibitor GW569293 and the  $\alpha$ 2- adrenoceptor antagonist fluparoxan were synthesised at GSK, Harlow. Methylcellulose was prepared at GSK, Harlow. Phosphate buffered saline (PBS) was prepared using PBS tablets obtained from Sigma, UK. Lipopolysaccharide (0111:B4, L2630) and the glucocorticoid dexamethasone were purchased from Sigma, UK.

Bio-Plex™ cytokine, phosphoprotein and total target assay kits containing standards, primary bead and secondary detection antibody solutions were obtained from Bio-Rad Laboratories, USA. Bio-plex™ phosphoprotein testing reagent kits, total protein assay solutions and Bio-plex™ calibration beads were purchased from Bio-Rad Laboratories, USA. Streptavidin-PE was obtained from VWR, UK. The Luminex®-100™ system was purchased from Luminex® Corporation, USA. 96-well filter plates and vacuum manifold apparatus were obtained from Millipore®, USA.

### **2.2.2 Animals**

Specific, pathogen free male CD (caesarean derived from original Charles River Laboratories Sprague Dawley colonies) rats (250g, approximately 10 weeks of age) were purchased from Charles River, UK housed (4-5 per cage) in an animal facility at GlaxoSmithKline Pharmaceuticals, Harlow, Essex, UK. All rats were maintained under a controlled temperature of 21-24°C and a 12-hour phase light/dark cycle (lights on at 7am) and fed a pellet diet and water *ad libitum*. All experimental procedures were conducted in accordance with the GlaxoSmithKline local ethics committee and conformed to the UK Animals (Scientific Procedures) Act 1986.

### **2.2.3 Drug administration**

Dexamethasone, fluparoxan and GW569293 were sonicated in 0.5% methylcellulose until completely dissolved and administered orally (gavage) at a

dose volume of 2ml/kg. Dosing took place according to a timed schedule of 2 rats every 15 minutes to account for the time required to sample each rat. LPS (100µg/kg, 1ml/kg) was allowed to dissolve in PBS in a falcon tube (VWR International, UK) for at least 30 minutes before administration. This dose of LPS was chosen from previous studies (Turrin et al, 2001; Pezeshki et al, 1996). LPS was injected (i.p) at 30 minutes, 1 hour and 2 hours after oral dosing of fluparoxan, (1, 3 & 10mg/kg), dexamethasone (1mg/kg) or GW569293 (25mg/kg). An in vivo pharmacodynamic assay previously run at GSK, Harlow, revealed that oral treatment of 1, 3 and 10mg/kg fluparoxan caused reversal of agonist (UK, 14304) induced hypothermia. Subsequent PK analysis revealed brain concentrations of 0.592, 1.796 and 3.657µM respectively. Dexamethasone (1mg/kg, oral) and GW569293 (25mg/kg, oral) caused a reduction in neuroinflammation and cell death following intra-nigral injection of LPS into rat brain tissue (Sunter et al, in prep).

#### **2.2.4 *Sample collection***

Rats were deeply anaesthetised with sodium pentobarbitone (Euthatal® 100mg kg<sup>-1</sup> i.p, Rhône Mérieux, Harlow, UK). The right atrium was cut and trunk blood collected into a 1.3ml EDTA micro-tube (VWR International, UK). All rats, unless otherwise stated, were subsequently transcardially perfused with 120ml ice-cold 0.9% sterile saline to wash the brain of circulating blood. During this procedure, the descending artery was clamped to improve upper-body perfusion. Brain regions were microdissected and stored in preweighed labelled eppendorfs (VWR International, UK) at -80°C. The blood was spun in a microcentrifuge (Centrifuge 5415 D, Eppendorf UK Ltd, Cambridge, UK) at 16,110g for 5 minutes and the straw-coloured plasma fraction collected into fresh eppendorfs and stored at -80°C.

#### **2.2.5 *Cytokine protein determination***

##### **2.2.5.1 *Sample preparation***

Microdissected brain tissue samples were diluted (5ul/mg tissue) with high performance ELISA (HPE) buffer (Sanquin Reagents, Amsterdam) and homogenised using a hand-held Ultra-Turrax T8 homogeniser (VWR International, UK). Samples

were spun (16,110g for 2 minutes) in a microcentrifuge (Centrifuge 5415 D, Eppendorf UK Ltd, Cambridge, UK). Supernatant was removed and stored in a fresh eppendorf at -80°C. Brain supernatant and plasma were defrosted and 50µl aliquots of each sample placed into a corresponding well on a standard 96-well plate (Nunc, UK) according to a predetermined plate layout. Each 50µl aliquot was diluted with 150µl assay buffer (1% bovine serum albumin (BSA)-Fraction V, PBS).

#### 2.2.5.2 *Luminex<sup>®</sup> suspension bead array – cytokine analysis*

100µl of each pre-diluted sample was transferred to a pre-wet (100µl of assay buffer added to each well and the plate vacuum filtered) 96-well filter plate. A 50,000pg 9-plex standard was diluted to a 32,000pg solution and then serially diluted 1:2 using assay buffer to provide a 16-point (including zero) standard curve. Each sample was incubated in the dark overnight at 4°C with 50µl of a premixed 9-plex anti-cytokine conjugated bead solution diluted with assay buffer to 1x concentration (250µl stock bead solution diluted with 5,750µl assay buffer). The plate was washed three times with 200µl of assay buffer and filtered using a vacuum manifold apparatus to eliminate unbound protein and prevent cross-contamination. Samples were further incubated with 100µl detection antibody (stock 120µl solution diluted with 11,940µl assay buffer) for 1 hour in the dark at room temperature and then washed three times with 200µl assay buffer. 12µl of Streptavidin-PE (stock solution was diluted with 11,988µl assay buffer) and 100µl added to each well. The plate was left to shake (700rpm) for 30 minutes at room temperature in the dark. The contents of each well were analysed by the Luminex<sup>®</sup>-100<sup>TM</sup> system to achieve median fluorescence intensity (MFI) readings for standard curves and samples. Samples for studies 1 and 2 were analysed using FACScalibur<sup>TM</sup>, since the Luminex<sup>®</sup>-100<sup>TM</sup> system was not available at GSK during these early studies.

The Luminex<sup>®</sup>-100<sup>TM</sup> system was previously calibrated using Bio-plex<sup>TM</sup> calibration beads at a low RP1 value of 3832. Double discriminator gates were positioned from approximately 8,000 to 15,000 to separate singlet and doublet beads. Intensity was identified at bead regions 18, 20, 21, 32, 34, 35, 37, 55 and 72 for IL-2, IL-10, IL-1α, IL-4, IFN-γ, IL-1β, GM-CSF, IL-6 and TNF-α, respectively.

## 2.2.6 *Phosphoprotein determination*

### 2.2.6.1 *Sample preparation*

Brain samples were placed into preweighed eppendorfs and their weight (mg) measured. 500mM phenylmethylsulfonyl fluoride (PMSF) (Sigma, UK) was prepared by dissolving 0.436g PMSF in 5ml DMSO and 0.5ml aliquots stored at -20°C. 10 ml (40µl of factor 1 and 20µl of factor 2 to 9.9ml of cell lysis buffer) of lysing solution was vortexed gently, 40µl of 500mM PMSF added and the solution left to cool on ice. 5µl/mg tissue of lysing solution was added to each sample, which was briefly homogenised until in solution. The samples were stored at -70°C subsequently thawed, vortexed and then centrifuged at 3328g for 4 minutes. The supernatant was collected and the protein concentration determined. Supernatant was further diluted with lysing solution to achieve a protein range of 200-900µg/ml.

### 2.2.6.2 *Total protein assay*

BSA (25mg) was dissolved in 2.5ml of lysing solution and protein standards prepared from a 1mg/ml stock BSA solution. Each stock supernatant sample was diluted 1 in 20 with lysing solution. 25µl of standards and samples were placed into clean dry eppendorfs and 125µl of Reagent I added. All eppendorfs were incubated for one minute and a further 125µl of Reagent II added. Following vortexing, all tubes were centrifuged at 13,200rpm for 3-5mins. The supernatant was discarded by inverting tubes on clean absorbent tissue. 127µl of Reagent A' (reagent S + reagent A) was added to each pellet and the eppendorfs incubated at room temperature for 5 minutes. Eppendorfs were vortexed and 1ml of Reagent B added to each tube. Eppendorfs were incubated at room temperature for 15 minutes. 200µl of each sample was placed into a 96-well plate in duplicate and read at 750nm.

### 2.2.6.3 *Luminex<sup>®</sup> suspension bead array – phosphoprotein analysis*

50µl of sample, in duplicate, were placed onto a standard 96-well plate according to a predetermined plate layout. An equal volume of assay buffer obtained from a Bio-Rad phosphoprotein testing reagent kit was added to each sample. The bead solution for each phosphoprotein (180µl) was vortexed and aliquoted into a single vial before dilution with 8280µl wash buffer. 50µl of beads were added to each well of a pre-

washed filter plate and the plate immediately vacuumed and washed (100µl wash buffer) twice. Sample and control lysates were allowed to thaw and vortexed and 50µl of each sample or control placed in a predetermined well. Each plate was left to incubate in the dark at room temperature for 15-18 hours. Following incubation, the plate was vacuum filtered and washed (100µl wash buffer) three times. Each detection antibody (180µl) was added to a single vial and diluted with 3780µl of detection antibody diluent and 25µl of the final solution added to each well. The plate was left to incubate in the dark at room temperature for 30 minutes and then vacuum filtered and washed (100µl wash buffer) a further three times. 50µl of Streptavidin-PE (180µl stock diluted with 17820µl wash buffer) was placed in each well and left to incubate for 10 minutes in the dark at room temperature. The plate was vacuum filtered and rinsed three times using 100µl of resuspension buffer. Resuspension buffer (125µl) was added to each well and left to incubate for 30 seconds before obtaining MFI readings for phospho- and total protein detected in brain homogenate using the Luminex<sup>®</sup>-100<sup>™</sup> system.

The Luminex<sup>®</sup>-100<sup>™</sup> system was previously calibrated using Bio-plex<sup>™</sup> calibration beads at a high RP1 value of 17435. Double discriminator gates were positioned from approximately 8,000 to 15,000 to separate singlet and doublet beads. Intensity was identified at regions 34, 36, 38 and 58 for JNK, p38MAPK, ERK2 and IκBα, respectively. Total and phospho protein levels were standardised using total protein concentrations for each sample. All samples were corrected to 1mg/ml total protein concentration. The ratio of phosphorylation was calculated by dividing phosphoprotein concentrations by total protein concentrations (i.e. p-JNK/total JNK).

### **2.2.7 Nitric Oxide Assay**

Administration of DSP-4 can increase iNOS expression in vivo (Heneka et al, 2002) suggesting that modulating NA may result in changes in nitrite, a marker of iNOS production. Nitric oxide levels were assessed by quantifying the total nitrite in each sample using a Nitric Oxide Colorimetric Assay Kit (Biomol Research Laboratories, USA), Standards were prepared and 50µl of each standard added to predetermined wells. Sample (25µl) diluted with deionised water (25µl) was plated in duplicate. Reconstituted NADH solution (25µl) was added to every well followed by reconstituted nitrate reductase (25µl). The plate was gently shaken and then left to

incubate at 37°C for 30 minutes. Greiss reagent I and Greiss reagent II (50µl each) in each well was incubated at room temperature for 10 minutes. Optical absorbency was read at 540nm. After adjusting readings for blank wells, a standard curve was constructed and sample concentrations determined.

### **2.2.8 *Quantification of cortical mRNA expression - TaqMan***

The left frontal cortex was dissected and placed into a sterile biopur<sup>®</sup> (RNase-free) safe-lock eppendorfs (VWR International, UK) and stored at -80°C for RNA quantification. Frontal cortex provided sufficient tissue for TaqMan analysis and allowed remaining cortical tissue to be used for Luminex detection of cytokine or phosphoprotein detection. Total RNA was isolated using TRIZOL<sup>®</sup> reagent according to the manufacturer's instructions (Invitrogen, USA). The RNA was resuspended in ultraPURE distilled water (Invitrogen, life technologies, UK), and RNA purity was confirmed by gel electrophoresis, ensuring that A260: A280nm ratio was >1.8. Equal quantities of RNA from each tissue sample were used in reverse transcription reactions to generate cDNAs (Ginham et al, 2001). First strand cDNA was synthesized from 1 µg of each RNA sample in a reaction mixture (0.01 M dithiothreitol (DTT), 0.5 mM each dNTP, 0.5 µg oligo (dT) primer, 40 U RNaseOUT ribonuclease inhibitor (Life Technologies Inc.), and 200 U SuperscriptII reverse transcriptase (Life Technologies Inc.)). Triplicate reverse transcription reactions were performed and resulting cDNA products were divided into aliquots using a Hydra 96 robot (Robbins Scientific, Sunnyvale, CA, USA). Primer (F and R) and probe (P) sets were designed from sequences in the Genbank database using Primer Express software (Perkin-Elmer, UK) (Table 1.1). All Taqman probes contained 6-Carboxyfluorescein at 5' end and the quencher dye, 6-carboxy-tetramethyl-rhodamine at the 3' end. Taqman PCR was carried out using an ABI prism 7700 sequence detector (Perkin-Elmer Applied Biosystems, Foster City, CA, USA) on the cDNA sample mixture (2.5 mM MgCl<sub>2</sub>, 0.2 mM dATP, dCTP, dGTP and dUTP, 0.1 µM each primer, 0.05 µM Taqman probe, 0.01 U AmpErase uracil-N-glycosylase, 0.0125 U Amplitaq Gold DNA polymerase (Perkin-Elmer, UK)). Samples were incubated at 50°C for 2 min, 95°C for 10 min followed by 40 cycles of 95°C for 15 s, 60°C for 1 min. Additional reactions were performed on each 96 well plate using rat genomic DNA (Clontech Laboratories Inc., Palo Alto, CA, USA) to

produce a standard curve (Harrison et al, 2000). Taqman was kindly completed by Ainsley Culbert and Florence Guillot, GSK, Harlow, UK.

Gene	Reagent Sequences
<b>GAPDH</b>	F; GAACATCATCCCTGCATCCA R; CCAGTGAGCTTCCCGTTCA P; CTTGCC CACAGCCTTGGCAGC
<b>TNF<math>\alpha</math></b>	F; GGCATGGATCTCAAAGACAAC R; GGTGTGGGTGAGGAGCAC P; TCTACTCCCAGGTTCTCTTCAAGGGACAAGGC
<b>IL-1<math>\beta</math></b>	F; CCCAACTGGTACATCAGCACC R; ACACGGGTTCATGGTGAAGTC P; TCCCGACCATTGCTGTTTCCTAGGAAG
<b>IL-6</b>	F; CCCAACTCCAATGCTCTCCTA R; GCTTTCAAGATGAGTTGGATG P; TGGTCCTTAGCCACTCCTTCTGTGACTCTAACTT

Table 2.1: TaqMan reagent sequences

### 2.2.9 *Data Analysis*

**Study 1 and 2:** Non-linear regression curves of the cytokine standard values were calculated using the GraphPad Prism one site hyperbola model. The concentrations of unknown samples were determined in GraphPad Prism relative to calculated standard curves.

**Study 3 and 5:** 4/5-parameter logistic regression curves (Hulse et al, 2004) of the cytokine standard values were calculated using STarStation Version 2.0 software (Applied Cytometry Systems, Sheffield, UK) and the concentrations of unknown samples were determined relative to calculated standard curves.

A general linear mixed model approach using the Proc Mixed procedure in SAS<sup>®</sup> Version 8 (SAS<sup>®</sup> Institute, UK) assessed each separate cytokine protein, cytokine mRNA and phosphoprotein response using brain region as a repeated measure. Univariate tests of significance using Statistica<sup>™</sup> Version 6.1 (Statsoft, USA) calculated the overall effect of LPS treatment on each separate response in plasma. In study 5, due to the unexpected variance across treatment groups and presence of zero values within the vehicle and dexamethasone groups for plasma IFN- $\gamma$  and plasma TNF- $\alpha$ , a univariate test of significance was applied in the absence of the vehicle and dexamethasone groups which were treated as a mean of zero. Planned comparisons

on the predicted means from the model assessed individual treatment effects within plasma and brain compartments. Results are represented as means  $\pm$  SEM and significance was set at  $P \leq 0.05$ . Percentage reduction describes attenuation relative to the LPS-induced cytokine response above vehicle levels.

## **2.3 Protocols**

### **2.3.1 *Study 1: Timecourse of cytokine protein induction***

Male CD rats (n=8 per group) were administered with either 100 $\mu$ g/kg LPS dissolved in filtered PBS or filtered PBS alone and euthanased at 2 or 6 hours (based on a protocol described by Quan et al, 1994) post LPS administration for plasma and brain samples. Whole hippocampus and frontal cortex, brain regions that demonstrate significant degeneration in AD (Gomez-Isla et al, 1996), were microdissected for cytokine analysis.

### **2.3.2 *Study 2: Cytokine protein detection throughout brain tissue***

Study 2 validates the detection of LPS induced cytokine protein throughout different brain regions. Male CD rats (n=8 per group) were administered with either 100 $\mu$ g/kg LPS dissolved in filtered PBS or filtered PBS alone. Animals were euthanased at 6 hours post LPS administration and blood and brain samples removed. The brain was microdissected into whole hippocampus, frontal cortex, cerebellum, striatum and hypothalamus.

### **2.3.3 *Study 3: Effect of Dexamethasone on cytokine expression***

Male CD rats (n=8 per group) pre-treated with either 0.5% methylcellulose or the glucocorticoid dexamethasone (1mg/kg) were administered 1 hour later with 100 $\mu$ g/kg LPS dissolved in filtered PBS or filtered PBS alone. Animals were euthanased at 6 hours post LPS administration; blood and brain were quickly removed. Animals were not perfused to prevent potential degradation of mRNA integrity caused by the duration time of the procedure. Whole hippocampus was microdissected for cytokine analysis by Luminex<sup>®</sup>. Frontal cortex was hemidissected providing left frontal cortex for Luminex<sup>®</sup> analysis and right frontal cortex of five animals for the determination of cytokine mRNA expression by taqman.

### **2.3.4 Study 4: Cytokine mRNA and intracellular protein expression**

Study 4 further investigates the induction of a centrally derived inflammatory response following IP LPS injection. IL-1 $\beta$ , TNF- $\alpha$  and IL-6 mRNA expression was assessed in brain tissue at 2 and 6 hours post LPS, the timepoints at which cytokine protein was detected in brain tissue. Further to this, phosphorylated I $\kappa$ B $\alpha$ , p38, JNK and ERK was detected in cortex and hippocampus using Luminex<sup>®</sup>. Phosphoprotein analysis using Luminex<sup>®</sup> was based on personal communication with the manufacturer since available kits had not previously been used for analysis of animal tissue. Male CD rats (n=8 per group) were administered with 100 $\mu$ g/kg LPS dissolved in filtered PBS or filtered PBS alone. Animals were euthanased at 2 or 6 hours post LPS administration. Blood and brain were removed, the perfused brain was microdissected for whole hippocampus and hemidissected left frontal cortex for phosphoprotein analysis and hemidissected right frontal cortex for taqman analysis. Additional male CD rats (n=4 per group) were terminally anaesthetised with an IP overdose of pentobarbitone at 2 and 6 hours post LPS. These animals were not perfused but frontal cortex was microdissected for taqman analysis for comparison of mRNA integrity and mRNA expression levels with perfused cortical samples.

### **2.3.5 Study 5: Effect of p38 inhibition and $\alpha$ 2 adrenoceptor antagonism on cytokine expression**

Male CD rats (n=8 per group) pre-treated with 0.5% methylcellulose or the glucocorticoid dexamethasone (1mg/kg, 1 hour), the p38 inhibitor GW569293 (25mg/kg, 2 hour) or the alpha-2 adrenoceptor blocker fluparoxan (1, 3 or 10mg/kg, 30 mins) before IP administration with LPS (100 $\mu$ g/kg) dissolved in filtered PBS. Animals were euthanased at 6 hours post LPS. The brain was microdissected for whole hippocampus and frontal cortex.

## **2.4 Results**

### **2.4.1 Study 1: Timecourse of cytokine protein in brain and plasma**

#### **2.4.1.1 Cytokine protein in brain**

Separate repeated measures ANOVA of each individual cytokine indicated that LPS

treatment specifically increased the pro-inflammatory cytokines IL-1 $\alpha$ ,  $F_{(1, 27)} = 8.18$ ,  $p < 0.01$ , and IL-1 $\beta$ ,  $F_{(1, 27)} = 16.96$ ,  $p < 0.001$ , in brain tissue (fig 2.1). There were additional significant effects of timepoint,  $F_{(1, 27)} = 5.88$ ,  $p < 0.05$ , and a treatment\*timepoint interaction,  $F_{(1, 27)} = 11.98$ ,  $p < 0.01$ , on IL-1 $\alpha$  in brain tissue.

Post hoc planned comparisons revealed a significant increase of IL-1 $\beta$  was evident by 6 hours in the hippocampus ( $p < 0.01$ ) with a trend to increase by 2 hours that failed to reach significance at the 0.05 level ( $p = 0.06$ ) (fig 2.1B). LPS significantly elevated cortical IL-1 $\beta$  by 2 ( $p < 0.05$ ) and 6 ( $p = 0.05$ ) hours (fig 2.1A).

IL-1 $\alpha$  was significantly elevated at 6 hours in hippocampal ( $p < 0.01$ ) and cortical ( $p < 0.05$ ) tissue relative to vehicle treatment.

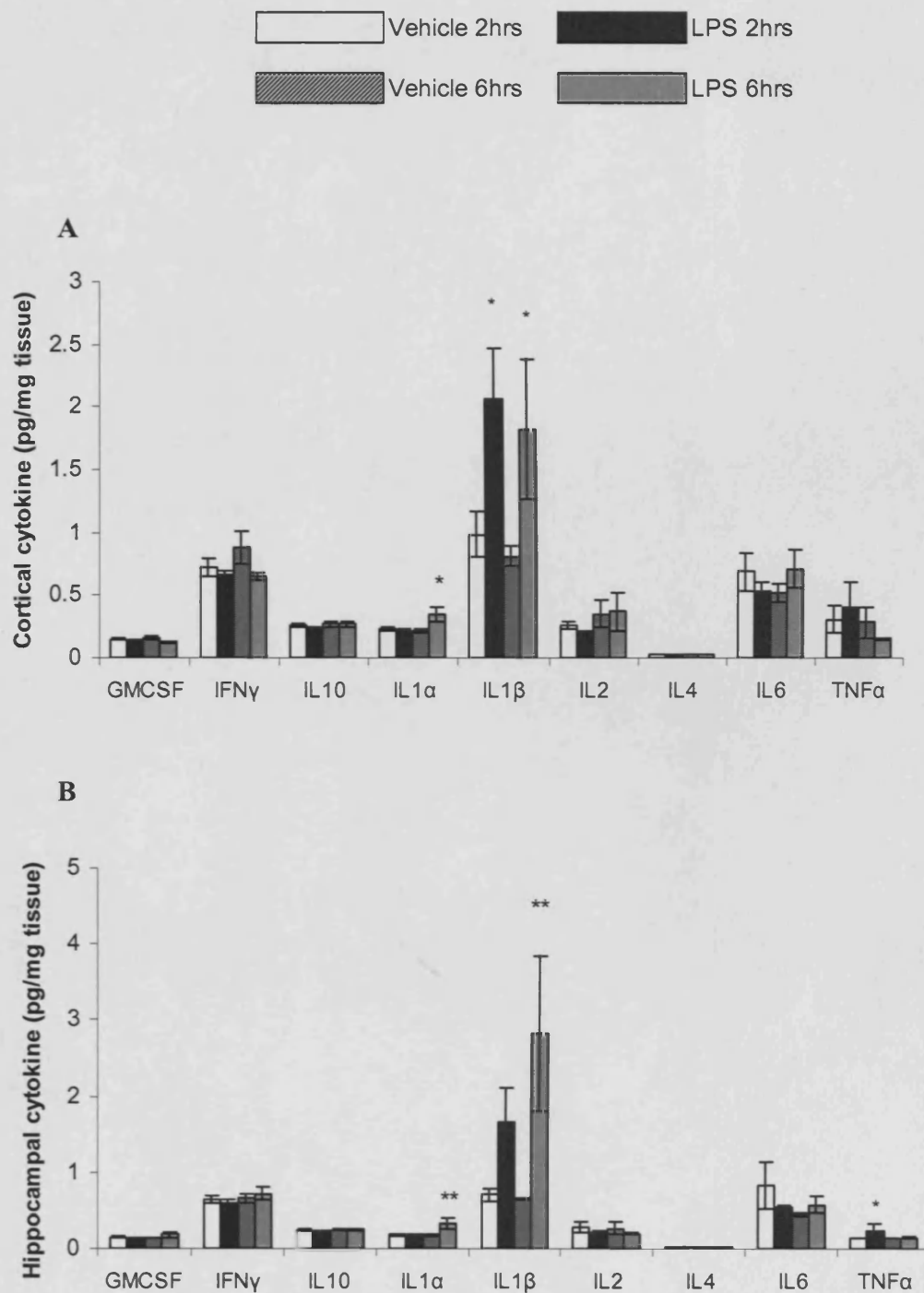


Figure 2.1: Cytokine protein in the cortex (A) and hippocampus (B) of adult rats (n = 8) by 2 and 6 hours post IP LPS administration, data represented as cytokine protein (pg) per milligram of tissue and shows mean  $\pm$  SEM. \*  $p \leq 0.05$ , \*\*  $p \leq 0.01$  significantly different vs. respective timepoint vehicle (repeated measures ANOVA followed by planned comparisons)

### 2.4.1.2 Cytokine protein in plasma

Proinflammatory cytokines were detected in plasma at 2 and 6 hours post intraperitoneal LPS administration (fig 2.2). Separate univariate ANOVAs revealed a significant overall effect of treatment on TNF- $\alpha$ ,  $F_{(1, 24)} = 6.43$ ,  $p < 0.05$ , IL-6,  $F_{(1, 24)} = 15.86$ ,  $p < 0.001$ , IL-1 $\alpha$ ,  $F_{(1, 27)} = 10.41$ ,  $p < 0.01$ , IL-1 $\beta$ ,  $F_{(1, 27)} = 19.74$ ,  $p < 0.001$ , IL-2,  $F_{(1, 25)} = 9.42$ ,  $p < 0.01$  and IL-10,  $F_{(1, 26)} = 10.48$ ,  $p < 0.01$ . There was also a significant effect of timepoint on IL-6,  $F_{(1, 24)} = 8.25$ ,  $p < 0.01$ , IFN $\gamma$ ,  $F_{(1, 27)} = 4.31$ ,  $p < 0.05$  and IL-2,  $F_{(1, 25)} = 4.82$ ,  $p < 0.05$ .

Post hoc planned comparisons revealed plasma TNF- $\alpha$  ( $p < 0.01$ ), IL-6 ( $p < 0.001$ ) and IFN- $\gamma$  ( $p < 0.05$ ) concentrations increased by the greatest magnitude by 6 hours. Elevated IL-1 $\alpha$  and IL-1 $\beta$  were evident at both 2 ( $p < 0.05$ , both cytokines) and 6 ( $p < 0.05$  for IL-1 $\alpha$ ,  $p < 0.001$  for IL-1 $\beta$ ) hours post LPS administration. IL-10 ( $p < 0.01$ ) and IL-2 ( $p < 0.01$ ) were significantly elevated above vehicle levels by 6 hours post LPS (fig 2.2).

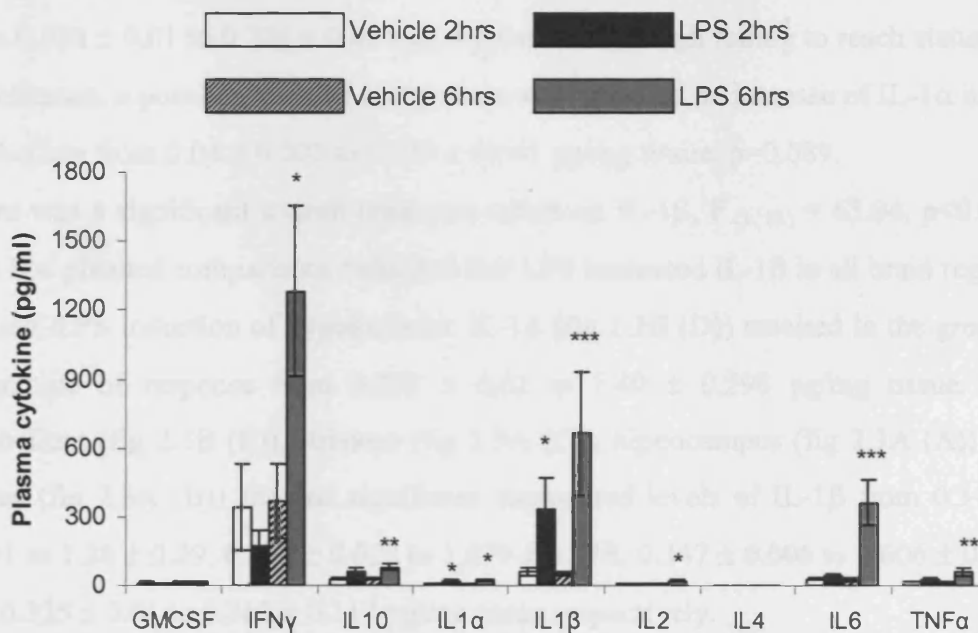


Figure 2.2: Cytokine protein in the cortex (A) and hippocampus (B) of adult rats ( $n = 8$ ) by 2 and 6 hours post IP LPS administration, data represented as cytokine protein (pg) per millilitre of sample and shows mean  $\pm$  SEM. (\*  $p \leq 0.05$ , \*\*  $p \leq 0.01$ , \*\*\*  $p \leq 0.001$  significantly different vs. respective timepoint vehicle (univariate ANOVA followed by planned comparisons))

## 2.4.2 Study 2: Cytokine protein throughout brain tissue

### 2.4.2.1 Cytokine protein in brain

LPS induced cytokine protein in a number of discrete brain regions and demonstrated a specific cytokine profile within brain tissue (fig 2.3A & 2.3B).

Repeated measures ANOVA indicated an overall effect of treatment,  $F_{(1, 34)} = 15.12$ ,  $p < 0.001$  and brain region,  $F_{(4, 31)} = 6.34$ ,  $p < 0.001$  on the pro-inflammatory cytokine TNF- $\alpha$ . Production of TNF- $\alpha$  was significantly increased in the hypothalamus from  $0.039 \pm 0.004$  to  $0.083 \pm 0.015$  pg/mg tissue. There was also an overall effect of treatment on IFN- $\gamma$ ,  $F_{(1, 60)} = 5.42$ ,  $p < 0.05$ , with a significant increase in the hypothalamus from  $0.052 \pm 0.005$  to  $0.069 \pm 0.005$  pg/mg tissue (fig 2.3B (D)).

There was an overall effect of treatment,  $F_{(1, 59)} = 38.3$ ,  $p < 0.001$ , and brain region,  $F_{(4, 32)} = 3.66$ ,  $p < 0.05$ , on IL-1 $\alpha$ . IL-1 $\alpha$  was significantly elevated in the cortex from  $0.069 \pm 0.007$  to  $0.201 \pm 0.04$  pg/mg tissue (fig 2.3A (B)), striatum from  $0.052 \pm 0.003$  to  $0.244 \pm 0.073$  pg/mg tissue (fig 2.3A (C)), and hypothalamus (fig 2.3B (D)) from  $0.084 \pm 0.01$  to  $0.256 \pm 0.054$  pg/mg tissue. Although failing to reach statistical significance, a post hoc planned comparison also revealed an increase of IL-1 $\alpha$  in the cerebellum from  $0.04 \pm 0.003$  to  $0.139 \pm 0.041$  pg/mg tissue,  $p = 0.089$ .

There was a significant overall treatment effect on IL-1 $\beta$ ,  $F_{(1, 51)} = 63.04$ ,  $p < 0.001$ . Post hoc planned comparisons indicated that LPS increased IL-1 $\beta$  in all brain regions studied. LPS induction of hypothalamic IL-1 $\beta$  (fig 2.3B (D)) resulted in the greatest magnitude of response from  $0.355 \pm 0.02$  to  $1.40 \pm 0.298$  pg/mg tissue. The cerebellum (fig 2.3B (E)), striatum (fig 2.3A (C)), hippocampus (fig 2.3A (A)) and cortex (fig 2.3A (B)) showed significant augmented levels of IL-1 $\beta$  from  $0.345 \pm 0.031$  to  $1.26 \pm 0.29$ ,  $0.338 \pm 0.022$  to  $1.079 \pm 0.218$ ,  $0.347 \pm 0.006$  to  $0.606 \pm 0.106$  and  $0.325 \pm 0.01$  to  $0.861 \pm 0.117$  pg/mg tissue respectively.

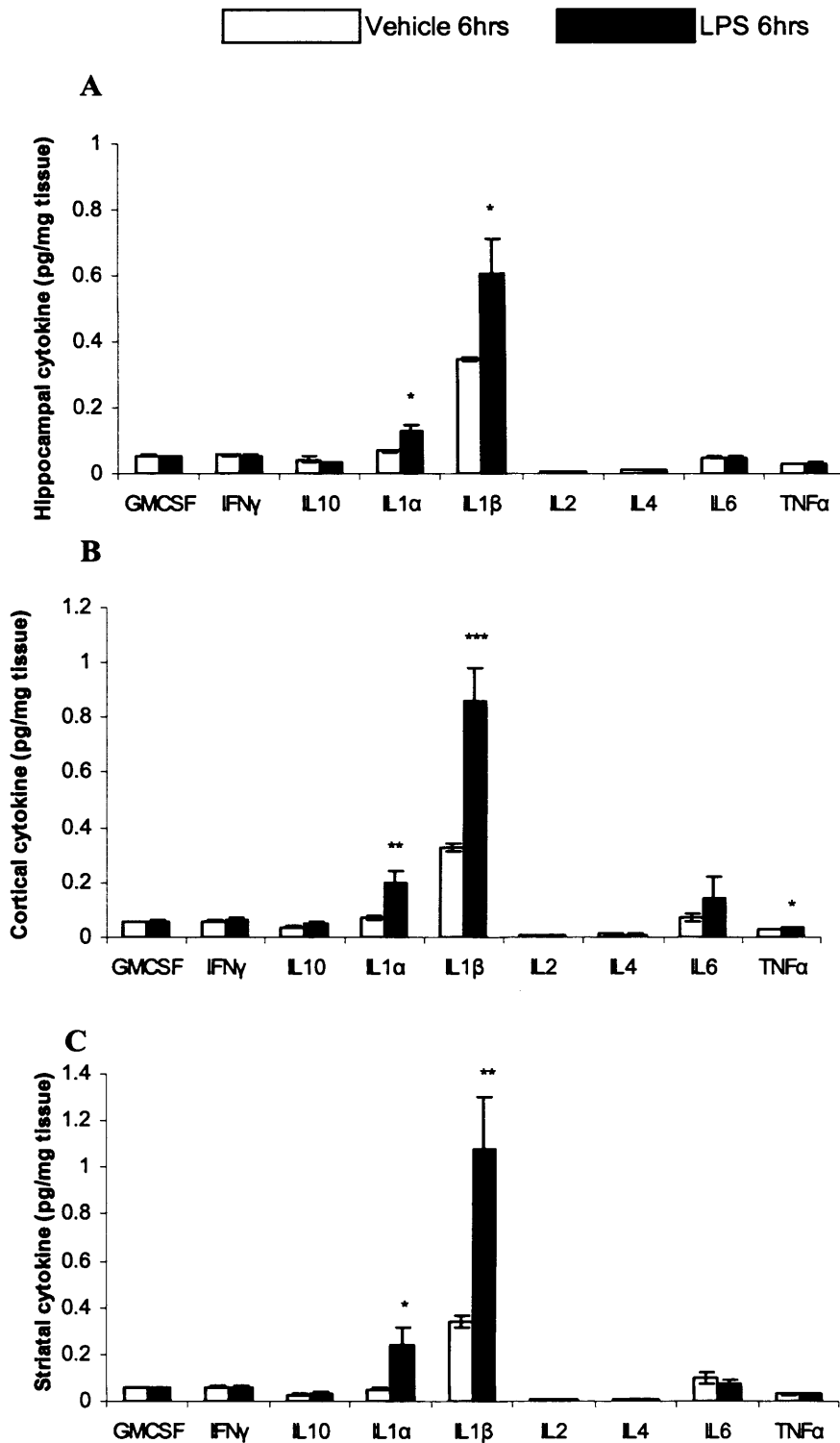


Figure 2.3A: Cytokine protein in the cortex (A) and hippocampus (B) and striatum (C) of adult rats (n = 8) by 6 hours post IP LPS administration, data represented as cytokine protein (pg) per milligram of tissue and shows mean  $\pm$  SEM. \* p  $\leq$  0.05, \*\* p  $\leq$  0.01, \*\*\* p  $\leq$  0.001 significantly different vs. vehicle (repeated measures ANOVA followed by planned comparisons)

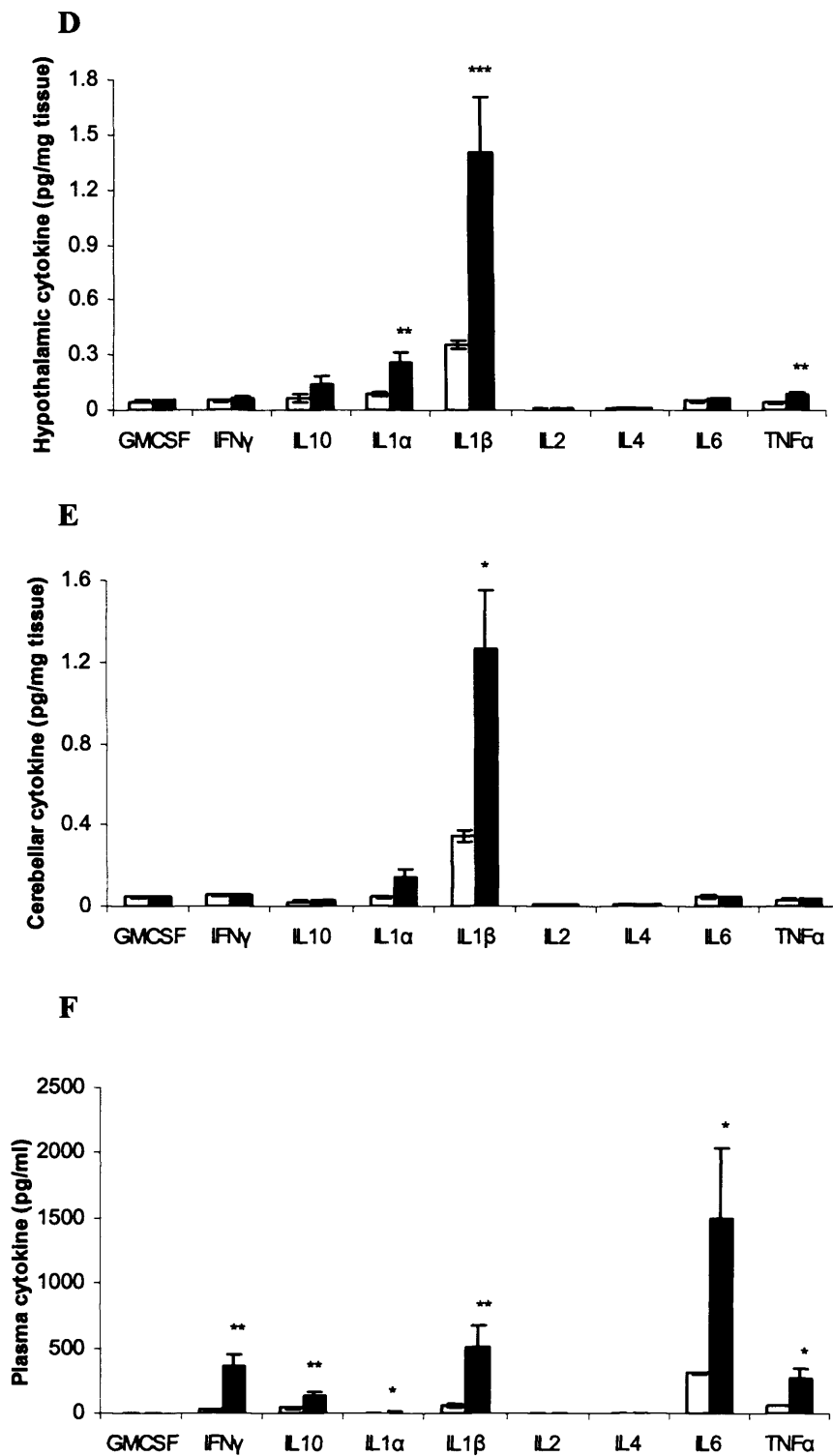


Figure 2.3B: Cytokine protein in the hypothalamus (D), cerebellum (E) and plasma (F) of adult rats ( $n = 8$ ) by 6 hours post IP LPS administration, data represented as cytokine protein (pg) per milligram of tissue (D-E) or cytokine protein (pg) per millilitre of sample (F) and shows mean  $\pm$  SEM. \*  $p \leq 0.05$ , \*\*  $p \leq 0.01$ , \*\*\*  $p \leq 0.001$  significantly different vs. respective timepoint vehicle (ANOVA followed by planned comparisons)

#### 2.4.2.2 Cytokine protein in plasma

IP LPS administration resulted in an increase in a multitude of plasma cytokines (fig 2.3B (F)); only IL-2 demonstrated a reduction relative to vehicle levels from  $4.02 \pm 2.7$  to  $1.63 \pm 0.28$  pg/ml.

Separate univariate ANOVAs indicated an overall effect of treatment on plasma IFN- $\gamma$ ,  $F_{(1,13)} = 38.7$ ,  $p < 0.001$ , IL-1 $\beta$ ,  $F_{(1,14)} = 11.24$ ,  $p < 0.01$ , IL-6,  $F_{(1,14)} = 9.11$ ,  $p < 0.01$ , IL-1 $\alpha$ ,  $F_{(1,13)} = 11.52$ ,  $p < 0.01$ , TNF- $\alpha$ ,  $F_{(1,14)} = 12.01$ ,  $p < 0.01$  and IL-10,  $F_{(1,14)} = 19.75$ ,  $p < 0.001$ .

Post hoc planned comparisons revealed IFN- $\gamma$  was increased from  $26.54 \pm 9.81$  to  $360.4 \pm 96.1$  pg/ml ( $p < 0.01$ ) and IL-1 $\beta$  from  $58.47 \pm 12.53$  to  $503.83 \pm 167.66$  pg/ml ( $p < 0.01$ ). LPS also significantly increased plasma IL-6 from  $307.02 \pm 6.71$  to  $1504 \pm 533.7$  pg/ml ( $p < 0.05$ ), IL-1 $\alpha$  from  $2.35 \pm 0.55$  to  $6.26 \pm 1.64$  pg/ml ( $p < 0.05$ ) and TNF- $\alpha$  from  $53.43 \pm 0.83$  to  $265 \pm 81.7$  pg/ml ( $p < 0.05$ ). LPS administration elevated levels of the anti-inflammatory cytokine IL-10 from  $39.2 \pm 3.09$  to  $133.6 \pm 25.7$  pg/ml ( $p < 0.01$ ).

### 2.4.3 *Study 3: Effect of Dexamethasone on cytokine expression*

#### 2.4.3.1 *Cytokine mRNA changes in frontal cortex*

There were no significant effects of treatment in unperfused brain tissue on expression of the endogenous housekeeper gene, GAPDH. This indicates that treatment with LPS, vehicle or dexamethasone had no significant effect on RNA integrity. In order to control for variations in RNA quality the results were expressed as a percentage of the level of GAPDH expression as described previously (Medhurst et al, 2000).

Repeated measures ANOVA revealed an overall effect of treatment on TNF- $\alpha$ ,  $F_{(3, 14)} = 10.03$ ,  $p < 0.001$ , IL-1 $\beta$ ,  $F_{(3, 15)} = 4.75$ ,  $p < 0.05$ , and IL-6,  $F_{(3, 14)} = 10.13$ ,  $p < 0.001$ , in cortical tissue. Post hoc planned comparisons revealed that LPS significantly increased expression of TNF- $\alpha$  from  $0.64 \pm 0.09$  to  $2.96 \pm 0.2\%$  ( $p < 0.01$ ) (fig 2.4A), IL-1 $\beta$  from  $57 \pm 0.71$  to  $3.6 \pm 1.10\%$  ( $p = 0.01$ ) (fig 2.4C) and IL-6 from  $0.07 \pm 0.08$  to  $1.25 \pm 0.17\%$  ( $p < 0.001$ ) (fig 2.4B). Administration of dexamethasone fully attenuated the LPS induction of TNF- $\alpha$  to  $0.57 \pm 0.18\%$  ( $p < 0.001$ ) and IL-1 $\beta$  to  $0.6 \pm 0.15\%$  ( $p = 0.01$ ). Dexamethasone treatment failed to diminish LPS-induced IL-6 mRNA expression.

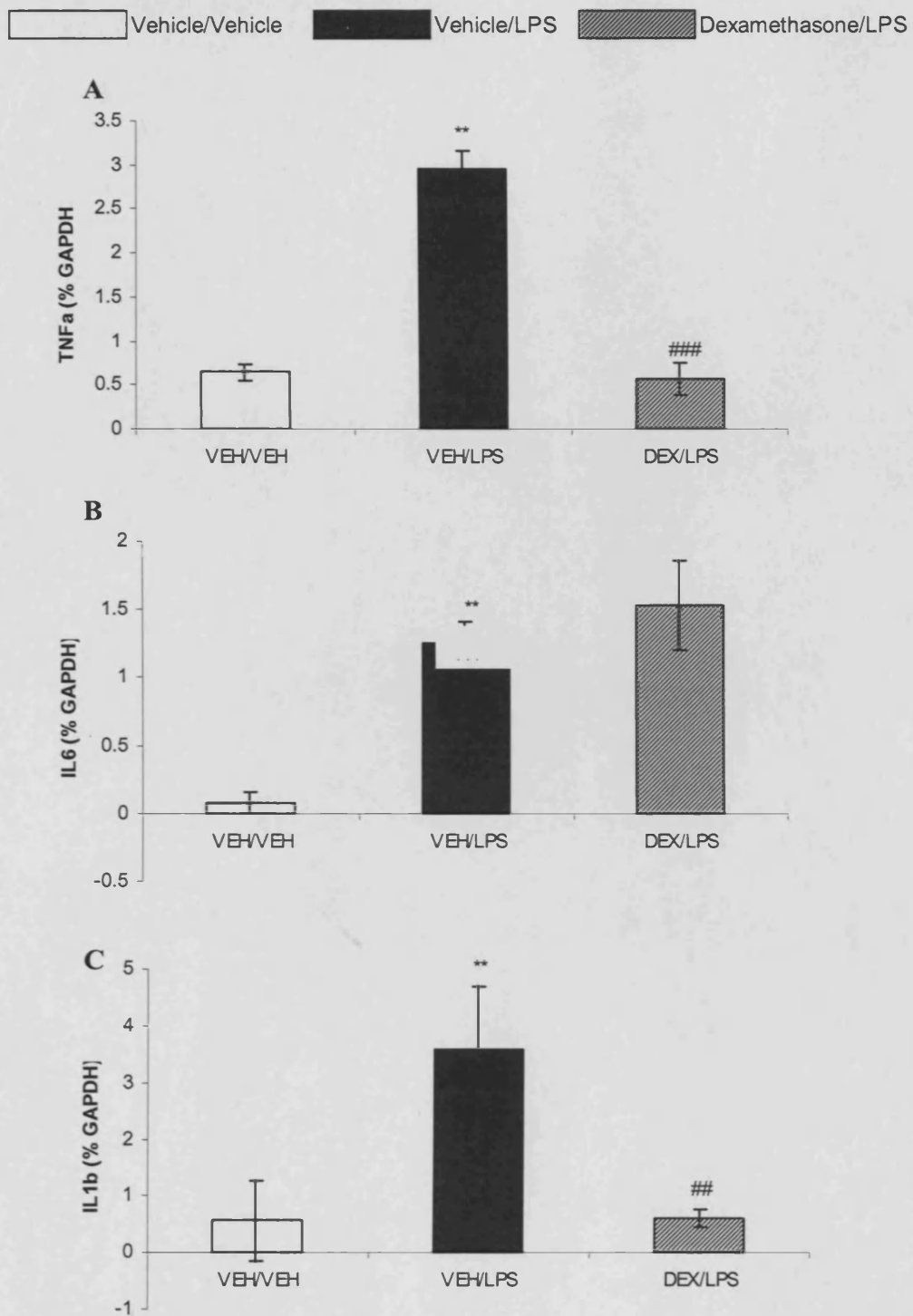


Figure 2.4: Effect of dexamethasone treatment on LPS-induced TNF $\alpha$  (A), IL6 (B) and IL1 $\beta$  (C) mRNA expression in the cortex of adult rats by 6 hours post IP LPS administration, data represented as cytokine mRNA as a percentage of GAPDH expression and shows mean  $\pm$  SEM. \*\*  $p \leq 0.01$ , \*\*\*  $p \leq 0.001$  significantly different vs. vehicle; #  $p \leq 0.05$ , ###  $p \leq 0.001$  significantly different vs. LPS (univariate ANOVA followed by planned comparisons)

#### 2.4.3.2 *Cytokine protein in brain*

Cytokine levels in brain regions of vehicle treated animals were of a similar magnitude to each other and to that demonstrated in study 1.

Repeated measures ANOVA revealed an overall effect of treatment on IL-1 $\beta$ ,  $F_{(2, 27)} = 19.55$ ,  $p < 0.001$ . Post hoc planned comparisons revealed LPS significantly increased hippocampal IL-1 $\beta$  from  $0.67 \pm 0.11$  to  $2.39 \pm 0.35$  pg/mg tissue (fig 2.5B) and cortical IL-1 $\beta$  from  $0.58 \pm 0.12$  to  $2.39 \pm 0.37$  pg/mg tissue (fig 2.5A) ( $p < 0.001$ , both regions relative to the vehicle group). Dexamethasone pre-treatment attenuated both cortical IL-1 $\beta$  to  $0.78 \pm 0.07$  pg/mg tissue (89% reduction,  $p < 0.001$ ) and hippocampal IL-1 $\beta$  to  $0.74 \pm 0.08$  pg/mg tissue (96% reduction,  $p < 0.001$ ) relative to the LPS group.

Repeated measures ANOVA revealed an overall treatment effect on central IL-1 $\alpha$ ,  $F_{(2, 27)} = 6.31$ ,  $p < 0.01$ . Post hoc planned comparisons revealed that LPS significantly induced hippocampal ( $p < 0.05$ ) but not cortical IL-1 $\alpha$  from  $0.20 \pm 0.04$  to  $0.67 \pm 0.24$  pg/mg tissue. Dexamethasone pre-treatment fully attenuated hippocampal IL-1 $\alpha$  ( $p < 0.01$ ) to  $0.08 \pm 0.04$  pg/mg tissue and decreased basal (no significant effect of LPS) cortical IL-1 $\alpha$  to  $0.07 \pm 0.03$  pg/mg tissue (214% reduction,  $p = 0.01$ ) respectively.

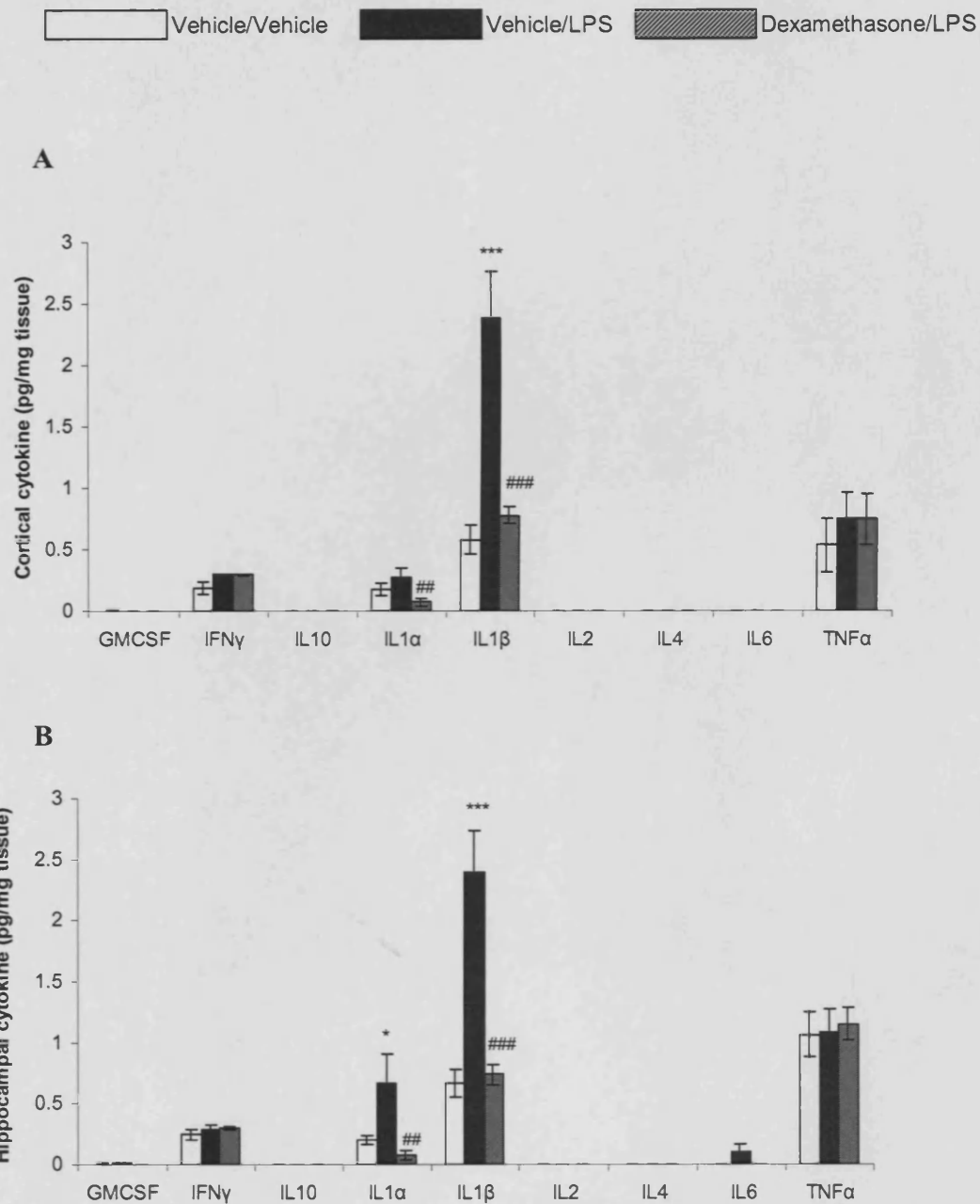


Figure 2.5: Effect of dexamethasone pre-treatment on cytokine protein in the cortex (A) and hippocampus (B) of adult rats (n = 8) by 6 hours post IP LPS administration, data represented as cytokine protein (pg) per milligram of tissue and shows mean  $\pm$  SEM. \*\* p  $\leq$  0.01, \*\*\* p  $\leq$  0.001 significantly different vs. vehicle; # p  $\leq$  0.05, ## p  $\leq$  0.01, ### p  $\leq$  0.001 significantly different vs. LPS (repeated measures ANOVA followed by planned comparisons)

### 2.4.3.3 Cytokine protein in plasma

Cytokine levels for both baseline vehicle treatment and post LPS stimulus were of a similar magnitude to that demonstrated in study 1 (fig 2.6).

Univariate ANOVA revealed a significant overall treatment effect on IFN- $\gamma$ ,  $F_{(2, 26)} = 8.54$ ,  $p=0.001$ , IL-1 $\alpha$ ,  $F_{(2, 27)} = 4.71$ ,  $p<0.05$ , IL-1 $\beta$ ,  $F_{(2, 27)} = 23.55$ ,  $p<0.001$ , IL-6,  $F_{(2, 24)} = 6.37$ ,  $p<0.01$  and TNF- $\alpha$ ,  $F_{(2, 27)} = 16.79$ ,  $p<0.001$ .

Post hoc planned comparisons demonstrated LPS significantly increased IFN- $\gamma$  ( $p<0.001$ ) from  $78.78 \pm 25.88$  to  $631.75 \pm 138.31$  pg/ml, IL-1 $\beta$  from  $15.55 \pm 8.99$  to  $1236.65 \pm 223.47$  pg/ml, IL-1 $\alpha$  from  $0.00 \pm 0.00$  to  $19.49 \pm 8.98$  pg/ml, IL-6 from  $0.00 \pm 0.00$  to  $308.55 \pm 146.22$  pg/ml and TNF- $\alpha$  from  $49.62 \pm 33.15$  to  $765.08 \pm 150.71$  pg/ml,  $p<0.001$ ).

Dexamethasone pre-treatment significantly attenuated the LPS-induced increase of IFN- $\gamma$  by 82% to  $178.25 \pm 94.15$  pg/ml ( $p<0.001$ ) and fully attenuated IL-1 $\alpha$  ( $p=0.01$ ). Dexamethasone also attenuated LPS-induced IL-1 $\beta$  by 81% to  $238.52 \pm 61.83$  pg/ml ( $p<0.001$ ), IL-6 by 97% to  $8.58 \pm 8.58$  pg/ml ( $p<0.01$ ) and TNF- $\alpha$  by 77% to  $211.84 \pm 36.53$  pg/ml ( $p<0.001$ ).

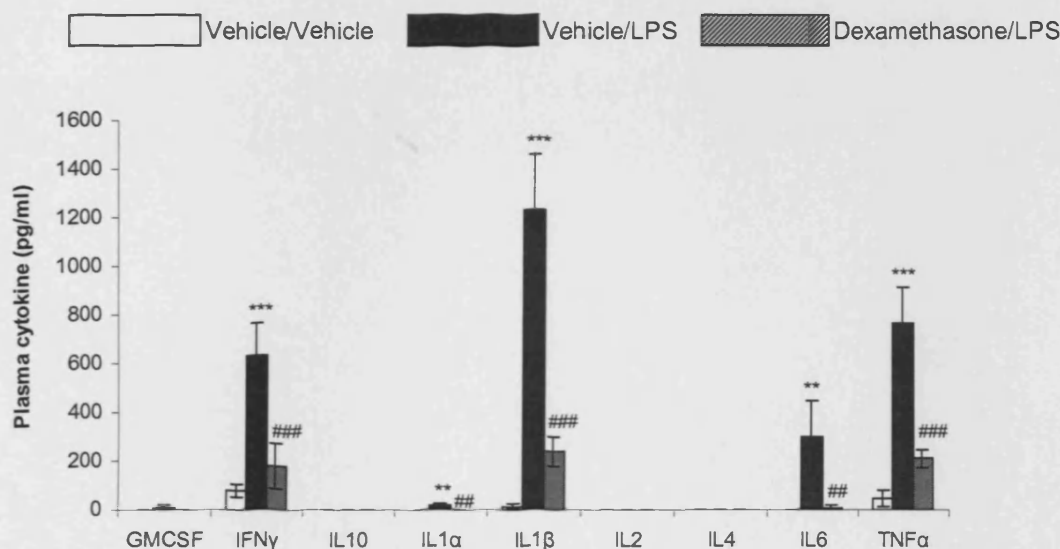


Figure 2.6: Effect of dexamethasone pre-treatment on cytokine protein in the cortex (A) and hippocampus (B) of adult rats ( $n = 8$ ) by 6 hours post IP LPS administration, data represented as cytokine protein (pg) per millilitre of sample and shows mean  $\pm$  SEM. \*  $p \leq 0.05$ , \*\*  $p \leq 0.01$ , \*\*\*  $p \leq 0.001$  significantly different vs. vehicle; #  $p \leq 0.05$ , ###  $p \leq 0.001$  significantly different vs. LPS (univariate ANOVA followed by planned comparisons)

#### 2.4.4 *Study 4: Cytokine mRNA and intracellular protein expression*

##### 2.4.4.1 *LPS-induced mRNA expression in frontal cortex*

There were no significant alterations in GAPDH expression in perfused tissue, however, a two fold significant reduction in GAPDH and cyclophilin expression was evident in unperfused tissue obtained from LPS treated rats relative to unperfused tissue of vehicle treated rats. Further analysis of pro-inflammatory cytokine expression therefore took place using perfused brain tissue since LPS treatment had no significant effect on RNA quantification and integrity or housekeeper gene expression.

Separate univariate ANOVA revealed a significant overall effect of treatment on the mRNA expression of pro-inflammatory cytokines TNF- $\alpha$ ,  $F_{(1, 11)} = 16.77$ ,  $p < 0.01$ , IL-1 $\beta$ ,  $F_{(1, 11)} = 14.06$ ,  $p < 0.01$  and IL-6,  $F_{(1, 11)} = 35.74$ ,  $p < 0.001$ , in cortical tissue. There was also a significant effect of timepoint on TNF- $\alpha$ ,  $F_{(1, 11)} = 18.67$ ,  $p < 0.01$ , and a significant treatment\*timepoint interaction on IL-6,  $F_{(1, 11)} = 11$ ,  $p < 0.01$ .

Post hoc analysis revealed that LPS significantly increased expression of TNF- $\alpha$  from  $1.34 \pm 0.42$  to  $6.40 \pm 1.57\%$  ( $p = 0.001$ ) by 6 hours post administration (fig 2.7A) whilst IL-1 $\beta$  was elevated from  $0.44 \pm 0.01$  to  $11.75 \pm 6.03\%$  by 2 hours post LPS challenge ( $p < 0.01$ ) (fig 2.7C). LPS induced IL-6 from  $-0.08 \pm 0.156$  to  $4.01 \pm 0.95\%$  at 2 hours post administration ( $p < 0.001$ ) (fig 2.7B).

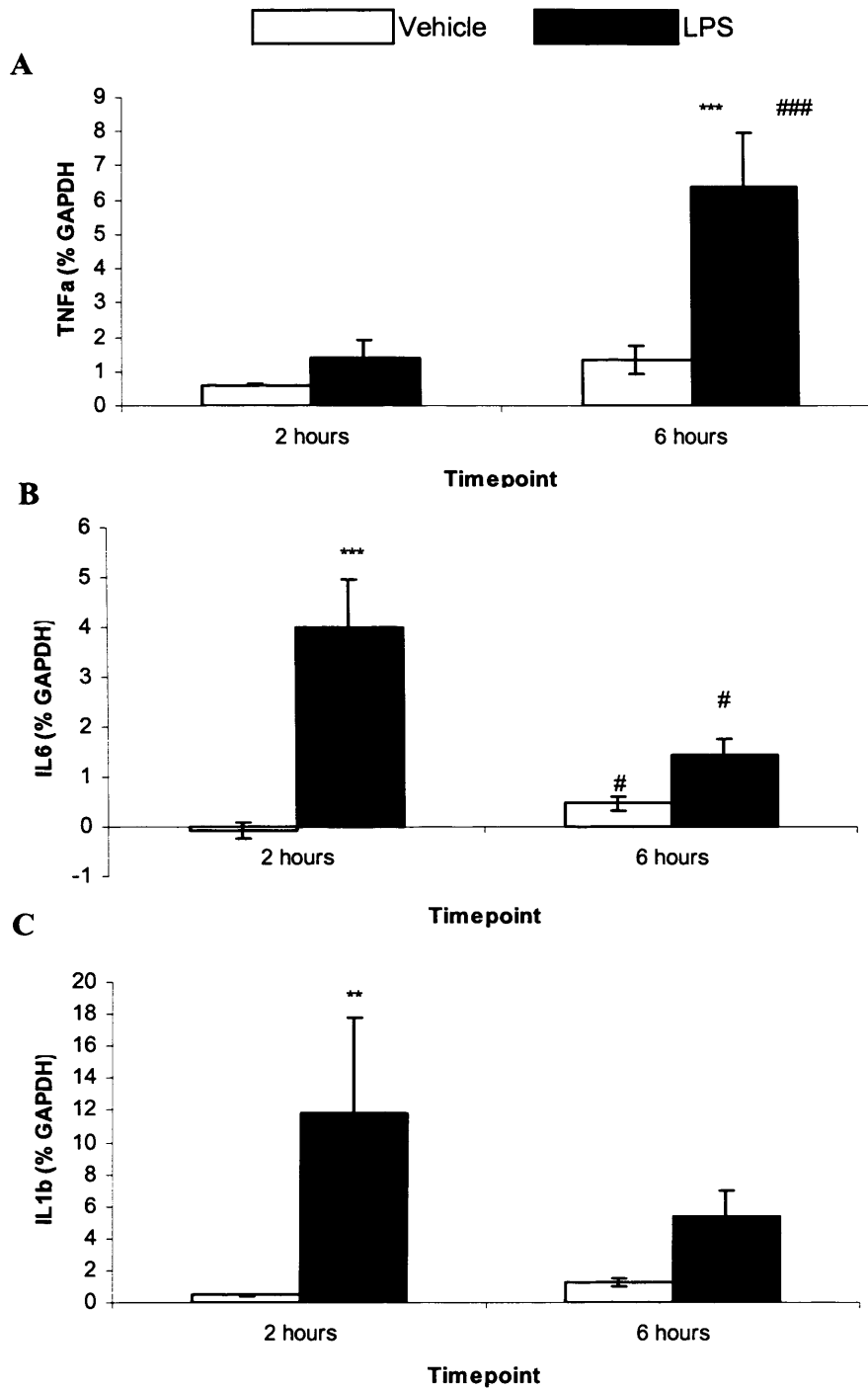


Figure 2.7: TNF $\alpha$  (A), IL6 (B) and IL1 $\beta$  (C) mRNA expression in the cortex of adult rats by 2 and 6 hours post IP LPS administration, data represented as cytokine mRNA as a percentage of GAPDH expression and shows mean  $\pm$  SEM. \*\*  $p \leq 0.01$ , \*\*\*  $p \leq 0.001$  significantly different vs. vehicle; #  $p \leq 0.05$ , ###  $p \leq 0.001$  significantly different vs. LPS (repeated measures ANOVA followed by planned comparisons)

#### 2.4.1.2 *LPS-induced intracellular protein phosphorylation*

Repeated measures ANOVA revealed a significant overall effect of timepoint,  $F_{(1,27)} = 16.00$ ,  $p < 0.001$ , and brain region,  $F_{(1,26)} = 9.16$ ,  $p < 0.01$ , on percentage phosphorylation of p38. Post hoc planned comparisons revealed an increase in p38 phosphorylation by 6 hours post intraperitoneal LPS ( $p < 0.01$ ) relative to vehicle treated animals (fig 2.8A).

Repeated measures ANOVA revealed a significant effect of timepoint,  $F_{(1, 28)} = 15.86$ ,  $p < 0.001$ , brain region,  $F_{(1, 27)} = 54.27$ ,  $p < 0.001$  and a treatment\*region\*timepoint interaction,  $F_{(1, 27)} = 7.11$ ,  $p = 0.01$ , on the percentage phosphorylation of JNK post intraperitoneal LPS treatment. Phosphorylation of JNK was increased in the hippocampus relative to cortex and appeared to be increased, regardless of treatment, by the 6 hour timepoint. JNK phosphorylation was decreased by 2 hours post intraperitoneal LPS ( $p < 0.05$ ) (fig 2.8C).

Repeated measures ANOVA indicated a treatment\*timepoint interaction,  $F_{(1, 21)} = 5.35$ ,  $p < 0.05$ , and a treatment\*region\*timepoint interaction,  $F_{(1, 23)} = 10.49$ ,  $p = 0.01$ , on the percentage of I $\kappa$ B $\alpha$  phosphorylation post IP LPS treatment. Post hoc planned comparisons revealed an increase in I $\kappa$ B $\alpha$  phosphorylation by 2 hours ( $p < 0.05$ ) and a reduction in I $\kappa$ B $\alpha$  phosphorylation by 6 hours ( $p < 0.01$ ) post LPS treatment (fig 2.8B). Phosphorylation of I $\kappa$ B $\alpha$  was higher in hippocampal tissue and by 6 hours in the vehicle group whilst LPS treatment caused higher levels of I $\kappa$ B $\alpha$  phosphorylation in cortical tissue and at 2 hours.

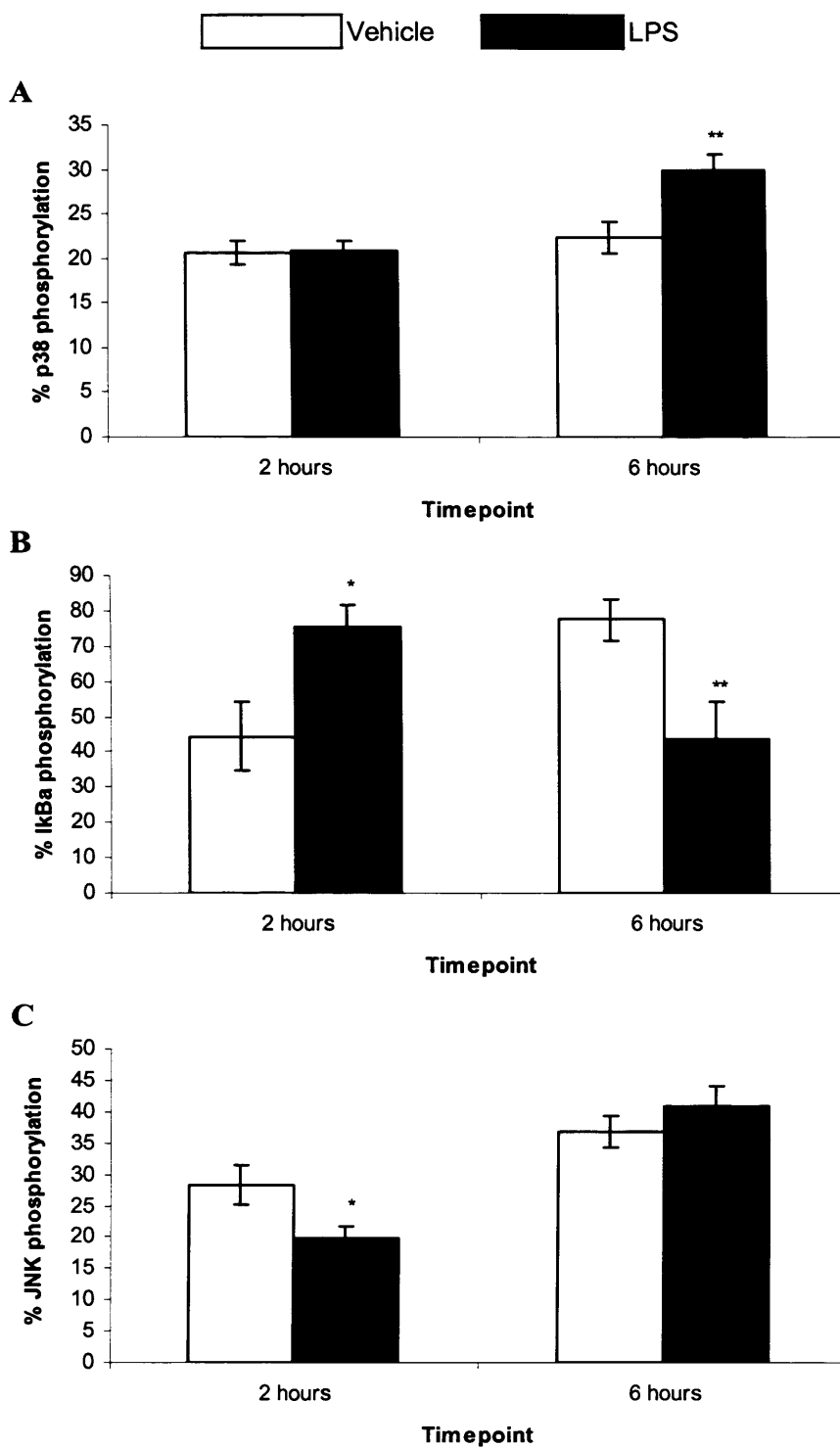


Figure 2.8: Phosphorylation of cortical p38, hippocampal IkBa and cortical JNK intracellular protein expression in adult rats by 2 and 6 hours post IP LPS administration, data represented as percentage phosphorylation of total protein and shows mean  $\pm$  SEM. \*  $p \leq 0.05$ , \*\*  $p \leq 0.01$  significantly different vs. vehicle group within timepoint (repeated measures ANOVA followed by planned comparisons)

#### 2.4.4.3 LPS-induced plasma nitrite

Univariate ANOVA revealed a significant effect of LPS treatment,  $F_{(1, 24)} = 269.21$ ,  $p < 0.001$ , timepoint,  $F_{(1, 24)} = 180.92$ ,  $p < 0.001$  and a significant treatment\*timepoint interaction,  $F_{(1, 24)} = 11.22$ ,  $p < 0.001$ , on plasma nitrite levels as a measure of plasma nitric oxide production (fig 2.9). Post hoc planned comparisons revealed that LPS significantly induced nitrite from  $17.5 \pm 1.15 \mu\text{Mole/L}$  to  $322 \pm 72.78 \mu\text{Mole/L}$  ( $p < 0.001$ ) by 6 hours post IP LPS administration. Nitric oxide levels were not significantly increased by 2 hours post LPS.

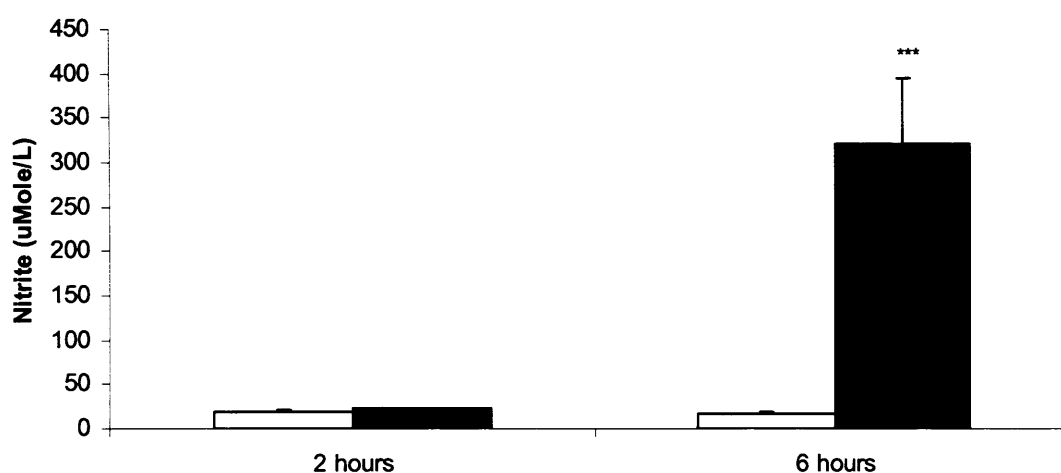


Figure 2.9: Plasma nitrite levels in adult rats by 2 and 6 hours post IP LPS administration, data represented as nitrite ( $\mu\text{Mole/L}$ ) and shows mean  $\pm$  SEM. \*\*\*  $p \leq 0.001$  significantly different vs. vehicle group within timepoint (repeated measures ANOVA followed by planned comparisons)

#### 2.4.5 Study 5: Effect of p38 inhibition and $\alpha 2$ adrenoceptor antagonism on cytokine expression

##### 2.4.5.1 Cytokine protein in brain

Repeated measures ANOVA revealed a significant overall effect of treatment on IL- $1\beta$ ,  $F_{(6, 47)} = 4.40$ ,  $p = 0.001$  in brain tissue. There was also a significant effect of brain region on central IL- $1\beta$ ,  $F_{(1, 46)} = 17.07$ ,  $p < 0.001$  revealed as a significantly higher level of IL- $1\beta$  protein in the hippocampus relative to the cortex.

Post hoc planned comparisons demonstrated that LPS increased cortical IL- $1\beta$  (fig

2.10A) and hippocampal IL-1 $\beta$  (fig 2.10B) from  $0.63 \pm 0.08$  to  $1.60 \pm 0.35$  pg/mg tissue ( $p < 0.001$ ) and from  $1.20 \pm 0.21$  to  $2.74 \pm 0.20$  pg/mg tissue ( $p < 0.001$ ), respectively. Dexamethasone fully abrogated LPS-induced cortical ( $p < 0.001$ ) and hippocampal IL-1 $\beta$  ( $p < 0.001$ ) to  $0.58 \pm 0.05$  and  $1.01 \pm 0.14$  pg/mg tissue respectively (fig 2.10).

Post hoc planned comparisons also revealed a trend for fluparoxan treatment to attenuate the effect of LPS on IL-1 $\beta$  in brain tissue. Fluparoxan reduced hippocampal IL-1 $\beta$  by 79% to  $1.52 \pm 0.39$  pg/mg tissue at 1mg/kg ( $p = 0.01$ ), by 80% to  $1.51 \pm 0.24$  pg/mg tissue at 3mg/kg ( $p < 0.05$ ) and by 88% to  $1.38 \pm 0.27$  pg/mg tissue at 10mg/kg ( $p = 0.08$ ) (fig 2.12B) relative to the LPS group. Fluparoxan did not significantly decrease LPS-induced cortical IL-1 $\beta$  at 1mg/kg (20% to  $1.40 \pm 0.22$  pg/mg tissue ( $p = 0.86$ )), at 3mg/kg (43% to  $1.18 \pm 0.26$  pg/mg tissue ( $p = 0.29$ )) or at 10mg/kg (52% to  $1.10 \pm 0.12$  pg/mg tissue ( $p = 0.37$ )) (fig 2.11). The p38 inhibitor GW569293 had no effect on hippocampal ( $p = 0.23$ ) or cortical IL-1 $\beta$  ( $p = 0.31$ ) (fig 2.12).

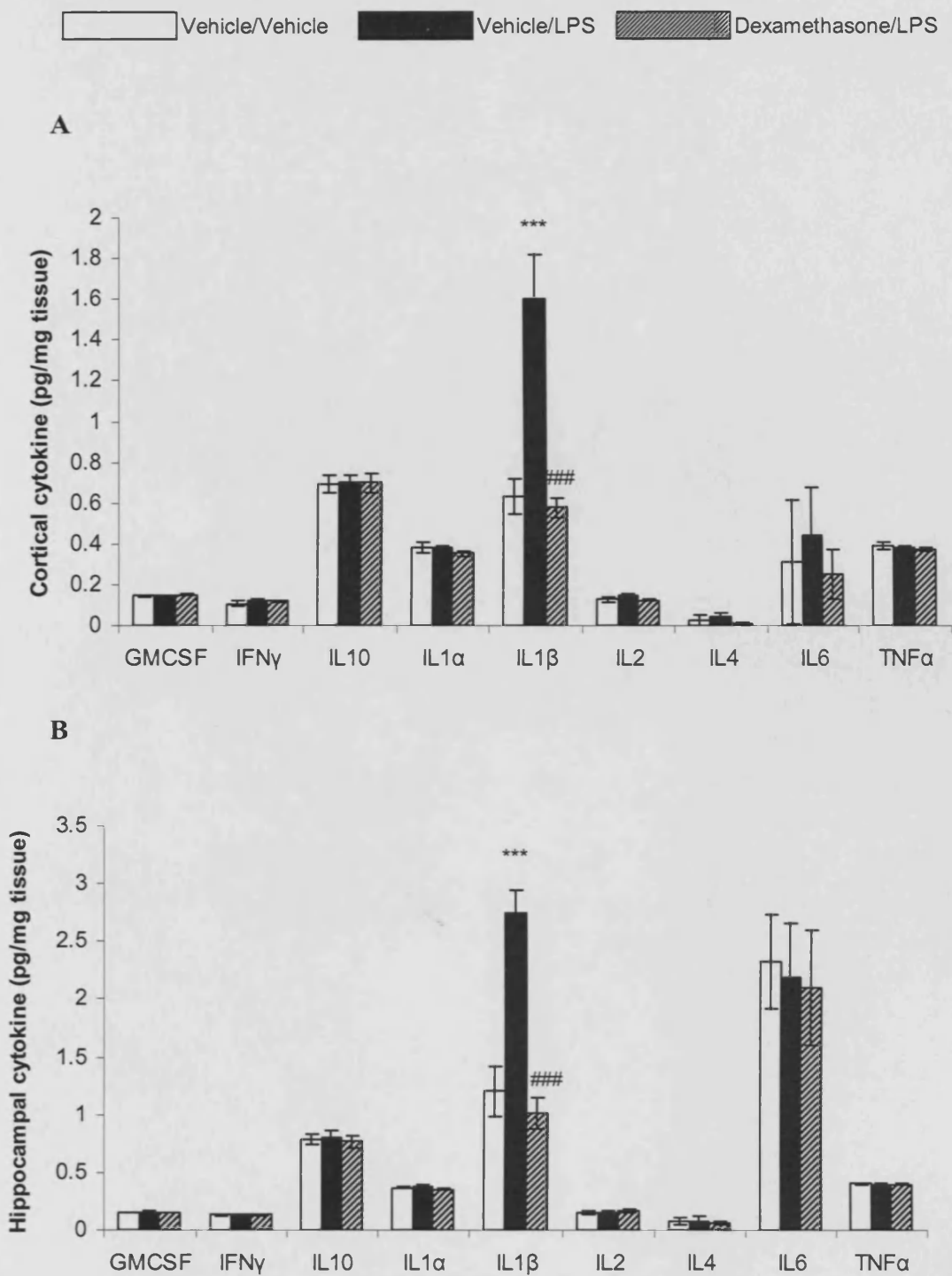


Figure 2.10: Effect of dexamethasone pre-treatment on cytokine protein in the cortex (A) and hippocampus (B) of adult rats (n = 8) by 6 hours post IP LPS administration, data represented as cytokine protein (pg) per milligram of tissue and shows mean  $\pm$  SEM. \*\*\*  $p \leq 0.001$  significantly different vs. vehicle vs. vehicle group; ###  $p \leq 0.001$  significantly different vs. LPS (repeated measures ANOVA followed by planned comparisons)

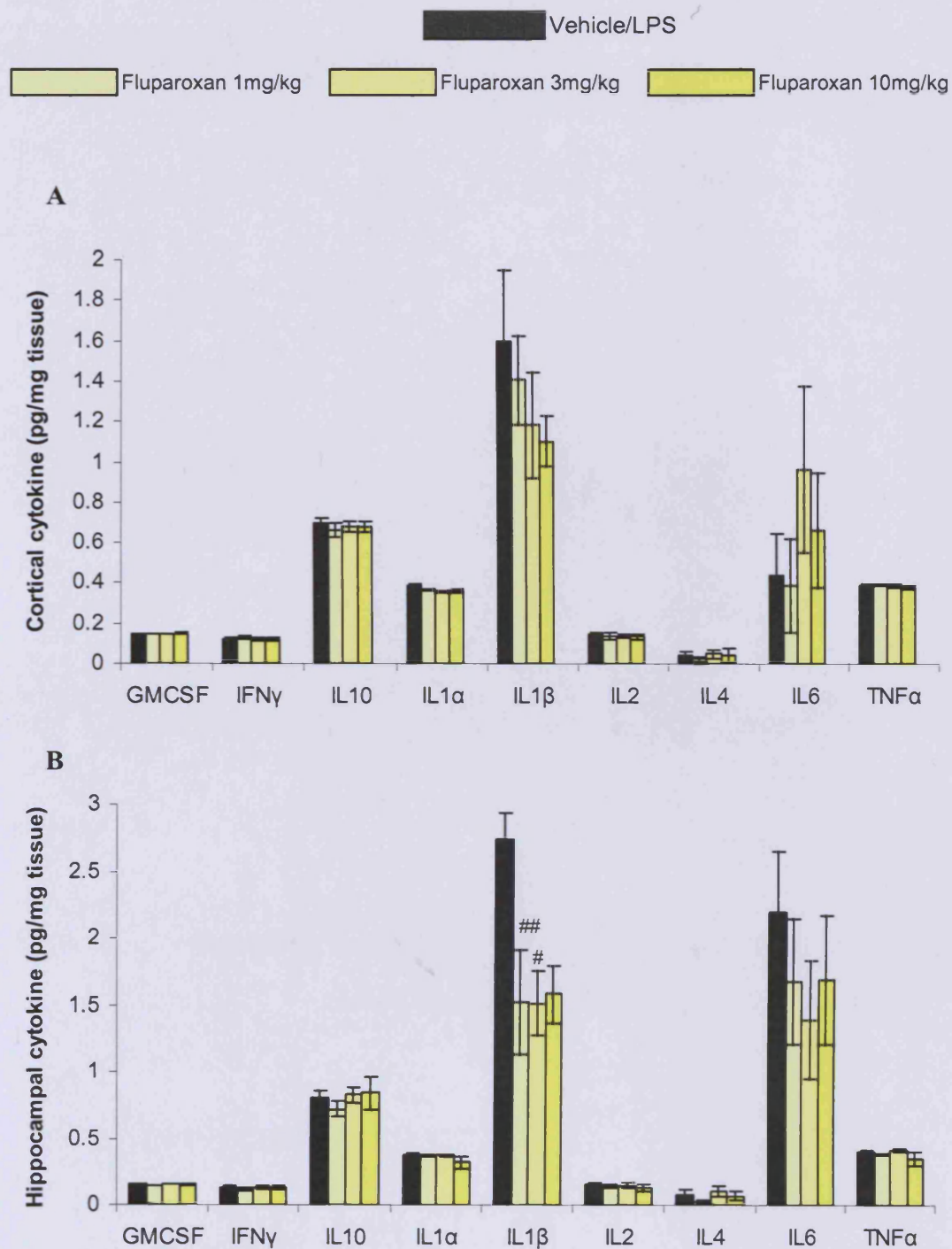


Figure 2.11: Effect of fluparoxan pre-treatment on cytokine protein in the cortex (A) and hippocampus (B) of adult rats (n = 8) by 6 hours post IP LPS administration, data represented as cytokine protein (pg) per milligram of tissue and shows mean  $\pm$  SEM. #  $p \leq 0.05$ , ##  $p \leq 0.01$  significantly different vs. LPS (repeated measures ANOVA followed by planned comparisons)

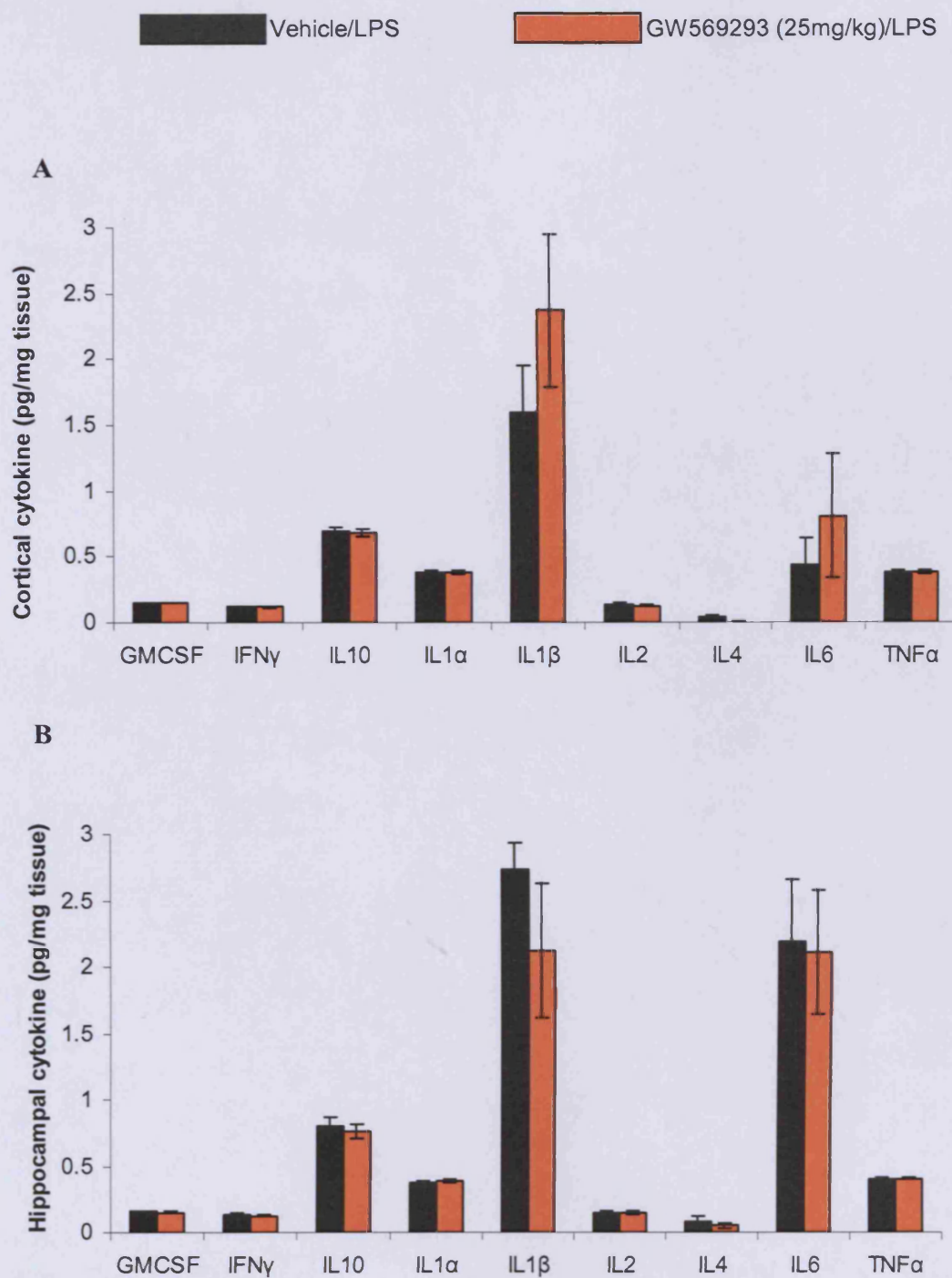


Figure 2.12: Effect of GW569293 pre-treatment on cytokine protein in the cortex (A) and hippocampus (B) of adult rats ( $n = 8$ ) by 6 hours post IP LPS administration, data represented as cytokine protein (pg) per milligram of tissue and shows mean  $\pm$  SEM (repeated measures ANOVA followed by planned comparisons)



#### 2.4.5.2 Cytokine protein in plasma

Univariate ANOVA revealed a significant overall effect of treatment on plasma IFN- $\gamma$ ,  $F_{(4, 25)} = 31.00$ ,  $p < 0.001$ , IL-1 $\beta$ ,  $F_{(6, 43)} = 32.90$ ,  $p < 0.001$ , IL-1 $\alpha$ ,  $F_{(6, 41)} = 8.12$ ,  $p < 0.001$ , TNF- $\alpha$ ,  $F_{(4, 23)} = 7.19$ ,  $p < 0.001$  and IL-10,  $F_{(6, 46)} = 4.09$ ,  $p = 0.01$ .

Post hoc planned comparisons revealed LPS significantly increased plasma IFN- $\gamma$  from 0.00 to  $2359.08 \pm 655.70$  pg/ml ( $p < 0.001$ ) and plasma IL-1 $\beta$  from  $10.36 \pm 9.76$  to  $2844.88 \pm 787.61$  pg/ml ( $p < 0.001$ ). LPS-induced plasma IL-1 $\alpha$  and TNF- $\alpha$  from  $8.89 \pm 3.54$  to  $160.56 \pm 82.93$  pg/ml ( $p < 0.001$ ) and 0.00 to  $3154.44 \pm 408.19$  pg/ml ( $p < 0.001$ ) and increased IL-10 from  $1125.97 \pm 144.35$  to  $2025.73 \pm 434.83$  pg/ml ( $p = 0.05$ ).

Dexamethasone fully attenuated plasma IFN- $\gamma$  to 0.00 pg/ml ( $p < 0.001$ ) and IL1 $\beta$  by 90% to  $305.33 \pm 62.74$  pg/ml ( $p < 0.001$ ) (fig 2.13). Dexamethasone also fully abrogated plasma IL-1 $\alpha$  to  $8.92 \pm 6.89$  pg/ml ( $p < 0.001$ ) and fully attenuated TNF- $\alpha$  to 0.00 pg/ml ( $p < 0.001$ ) (fig 2.13). Dexamethasone did not significantly attenuate LPS-induced IL-10 ( $p = 0.43$ ) similar the profile seen in study 3.

Fluparoxan significantly attenuated LPS-induced plasma IFN- $\gamma$  by 56% to  $1031.58 \pm 433.00$  pg/ml ( $p < 0.05$ ) at 1mg/kg, by 67% to  $768.64 \pm 156.13$  pg/ml ( $p < 0.05$ ) at 3mg/kg and by 73% to  $647.40 \pm 128.03$  pg/ml at 10mg/kg ( $p = 0.01$ ) (fig 2.14). Post hoc planned comparisons revealed that treatment with the p38 inhibitor; GW 569293 potentiated LPS-induced plasma IFN- $\gamma$  by 292% ( $p < 0.001$ ) (fig 2.15).

Fluparoxan did not significantly decrease LPS-induced plasma IL-1 $\beta$  at the  $p < 0.05$  level (at 1mg/kg ( $p = 0.19$ ), at 3mg/kg ( $p = 0.26$ ), at 10mg/kg ( $p = 0.52$ )) (fig 2.14). GW569293 had no significant effect on plasma IL-1 $\beta$  ( $p = 0.43$ ) relative to the LPS group (fig 2.15). Fluparoxan did not significantly attenuate LPS-induced plasma IL-1 $\alpha$  (at 1mg/kg ( $p = 0.64$ ), at 3mg/kg ( $p = 0.53$ ), at 10mg/kg (0.58) (fig 2.14) and GW569293 also had no significant effect on plasma IL-1 $\beta$  ( $p = 0.47$ ) relative to the LPS group (fig 2.15).

Fluparoxan decreased LPS-induced TNF- $\alpha$  by 57% to  $913.12 \pm 203.40$  pg/ml at 1mg/kg ( $p = 0.06$ ), by 65% to  $757.97 \pm 238.52$  pg/ml at 3mg/kg ( $p = 0.01$ ) and by 82% to  $386.25 \pm 118.64$  pg/ml at 10mg/kg ( $p < 0.001$ ) (fig 2.14). GW569293 had no significant effect on LPS-induced TNF- $\alpha$  ( $p = 0.50$ ) (fig 2.15).

There was a trend for fluparoxan at 10mg/kg to potentiate LPS-induced plasma IL-10 by 129% at 1mg/kg ( $p=0.19$ ), by 127% at 3mg/kg ( $p=0.21$ ) and 141% at 10mg/kg ( $p=0.08$ ) (fig 2.14). GW569293 had no effect on LPS-induced IL-10 production ( $p=0.36$ ) (fig 2.15).

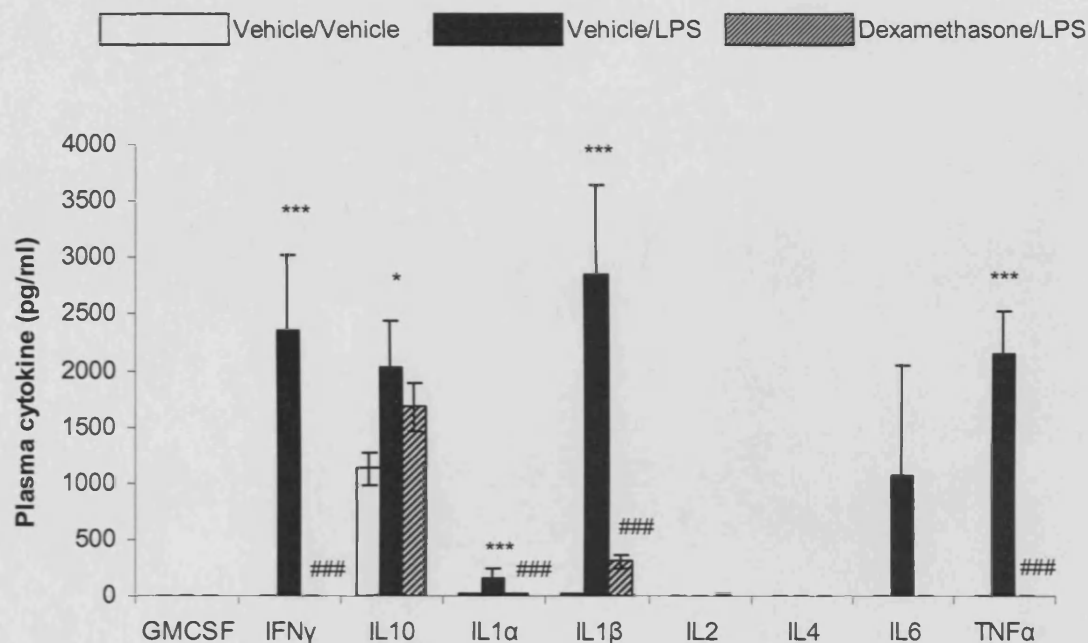


Figure 2.13: Effect of dexamethasone pre-treatment on cytokine protein in the cortex (A) and hippocampus (B) of adult rats ( $n = 8$ ) by 6 hours post IP LPS administration, data represented as cytokine protein (pg) per millilitre of sample and shows mean  $\pm$  SEM. (\*\*\*) $p \leq 0.001$ , (\*\*) $p \leq 0.01$ , (\*) $p \leq 0.05$  significantly different vs. vehicle; (###)  $p \leq 0.001$ , (#)  $p \leq 0.05$  significantly different vs. LPS (univariate ANOVA followed by planned comparisons)

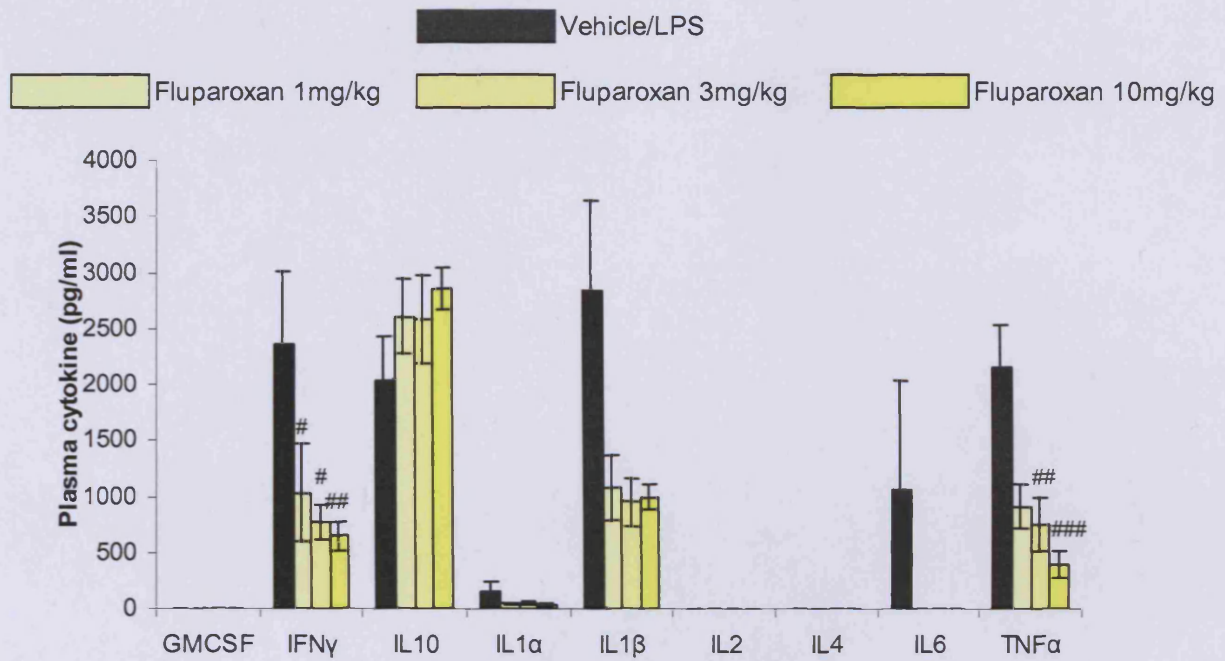


Figure 2.14: Effect of fluparoxan pre-treatment on cytokine protein in the plasma of adult rats (n = 8) by 6 hours post IP LPS administration, data represented as cytokine protein (pg) per millilitre of sample and shows mean  $\pm$  SEM. ### p  $\leq$  0.001, ## p  $\leq$  0.01, # p  $\leq$  0.05 significantly different vs. LPS (univariate ANOVA followed by planned comparisons)

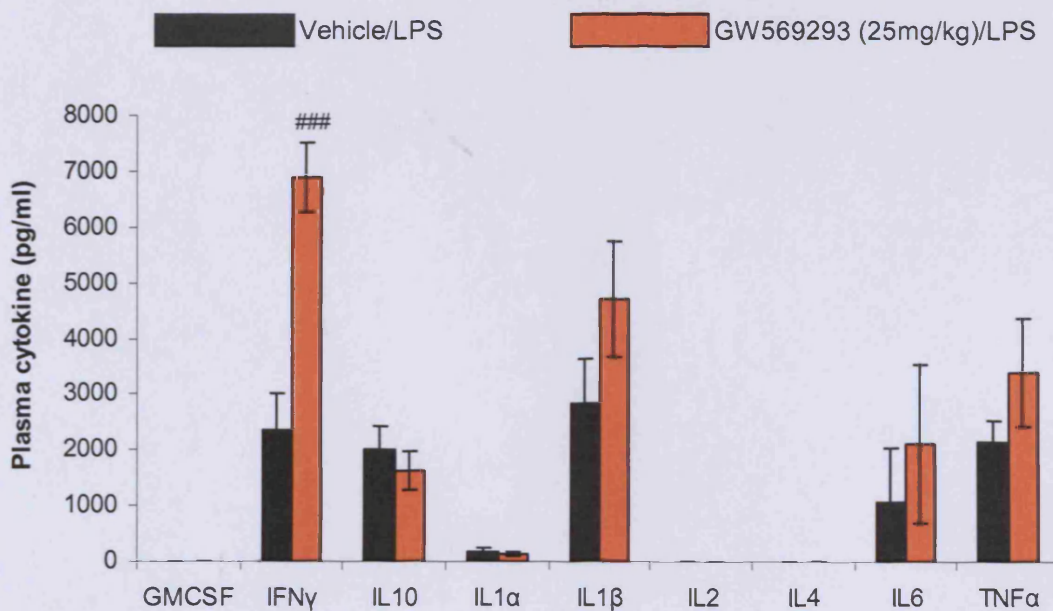


Figure 2.15: Effect of GW569293 pre-treatment on cytokine protein in the plasma of adult rats (n = 8) by 6 hours post IP LPS administration, data represented as cytokine protein (pg) per millilitre of sample and shows mean  $\pm$  SEM. ### p  $\leq$  0.001 significantly different vs. LPS (univariate ANOVA followed by planned comparisons)

#### 2.4.5.3 LPS-induced plasma nitrite

Repeated measures ANOVA indicated a significant effect of treatment,  $F_{(6, 37)} = 49.21$ ,  $p < 0.001$ , on plasma nitrite levels (fig 2.16). Post hoc planned comparisons revealed that LPS significantly induced nitrite from  $12.38 \pm 0.63$  to  $482.55 \pm 74.53$   $\mu\text{Mole/L}$  ( $p < 0.001$ ). This induction was significantly attenuated by dexamethasone treatment (98% reduction,  $p < 0.001$ ) to  $23.3 \pm 3.17$   $\mu\text{Mole/L}$ .

Fluparoxan significantly reduced LPS-induced nitrite by 77% at 1mg/kg ( $p < 0.001$ ) to  $120.54 \pm 24.92$   $\mu\text{Mole/L}$ , 49% at 3mg/kg ( $p < 0.01$ ) to  $251.88 \pm 74.73$   $\mu\text{Mole/L}$  and to  $163.27 \pm 31.83$   $\mu\text{Mole/L}$  (68%) at 10mg/kg ( $p < 0.001$ ). The p38 inhibitor, GW569293, also significantly attenuated plasma nitrite by 67% ( $p < 0.001$ ) to  $166.51 \pm 28.16$   $\mu\text{Mole/L}$ .

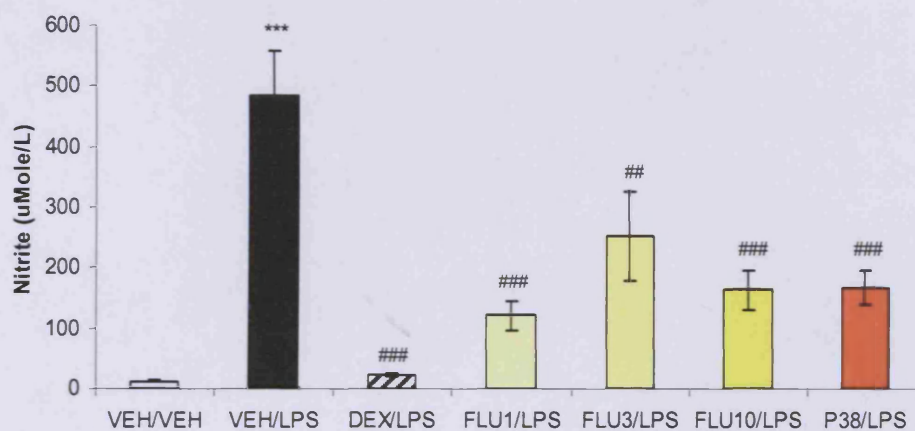


Figure 2.16: Effect of GW569293 or fluparoxan pre-treatment on plasma nitrite levels in adult rats by 6 hours post IP LPS administration, data represented as nitrite ( $\mu\text{Mole/L}$ ) and shows mean  $\pm$  SEM. \*\*\*  $p \leq 0.001$  significantly different vs. vehicle group; ###  $p \leq 0.001$ , ##  $p \leq 0.01$  significantly different vs. LPS group (univariate ANOVA followed by planned comparisons)

## 2.5 Discussion

### 2.5.1 *Detection of cytokine protein in brain and plasma*

Although published literature details the induction of central cytokine mRNA expression post IP LPS (Jacobs et al, 1997; Satta et al, 1998), reports of the detection of cytokine protein in brain tissue have been limited (Goujon et al, 1996; 1997). In this chapter, I have described the first application of the Luminex<sup>®</sup> system for the detection of cytokine protein in brain and plasma following IP LPS to rats. A significant increase of IL-1 $\alpha$  and IL-1 $\beta$  protein throughout discrete regions of the brain by 2 and 6 hours following LPS treatment was associated with inconsistent increases in IL-1 $\alpha$  and TNF- $\alpha$ . Throughout the duration of this thesis, alteration in IL-1 $\beta$  in brain tissue following peripheral injection of LPS has usually been reported as an increase in mRNA expression (Tonelli et al, 2003; Turrin et al, 2001). Although the current studies describe the first reported evidence of the application of Luminex<sup>®</sup> to the detection of cytokine protein changes in brain tissue following peripheral LPA administration, very recently, the detection of IP LPS-induced IL-1 $\beta$  and TNF- $\alpha$  in rat brain tissue by ELISA has been reported (Roche et al, 2006). This evidence supports the current data that an IP injection of LPS can elicit pro-inflammatory cytokine production in rodent brain. The substantial increases of TNF- $\alpha$  in brain tissue reported by Roche et al (2006) may be as a result of the timepoint investigated by the authors since, by 4 hours, TNF- $\alpha$  protein was not detectable in brain tissue. This may explain why, by 6 hours post IP LPS injection, no increase in TNF- $\alpha$  has been detected by Luminex<sup>®</sup> in the current studies. The significant increase in a wide range of cytokines in plasma including IFN- $\gamma$ , IL-1 $\beta$ , TNF- $\alpha$  and IL-6 indicates the primary induction of cytokine protein in blood before the CNS. It is important to determine that cytokine proteins detected in the brain tissue by Luminex<sup>®</sup> are centrally derived and not plasma borne cytokines that travelled through the BBB.

### 2.5.2 *Communication of peripheral inflammation to the brain*

Although a wide range of cytokine proteins were evident in plasma following peripheral LPS treatment, only IL-1 $\beta$  protein and small increases in IL-1 $\alpha$  protein were detectable in brain tissue. There is much literature describing the possible

mechanisms behind the communication of a peripheral inflammatory response to the brain. For example, Singh et al, 2004 suggest that peripheral administration of LPS caused a slight loss of integrity in the BBB that was molecular weight dependent. A protein of approximately 342Da may enter the brain, however [14C] dextran at 50-90kDa was unable to travel through the BBB. LPS has a molecular weight of approximately 10kDa ([www.textbookofbacteriology.net](http://www.textbookofbacteriology.net)). Hence, until further analysis using dextran molecules between 1 and 50kDa establishes more clearly the range of BBB penetration possible following IP LPS, it is difficult to determine whether LPS itself may enter the brain to cause a cytokine response although previous reports have suggested that it is unlikely (Quan et al, 1994). Others argue that LPS and cytokines circulating within the bloodstream activate specific receptors including TLR4, located on the surface of immune cells and endothelial cells of the CVOs, as described in section 1.5.1.2 of chapter 1; however, entry of LPS into the brain via the BBB would also activate TLR4 receptors on immune cells within brain tissue. Regardless of the mechanism by which an LPS-mediated inflammatory response in the blood is communicated to the brain, a neuroinflammatory response will be evident by the presence of cytokine mRNA expression and the activation of NF $\kappa$ B and MAP kinases.

IP LPS injection significantly increased cortical mRNA expression by 2 hours (IL-1 $\beta$  and IL-6) and 6 hours (TNF- $\alpha$ ) post injection in perfused samples (fig 2.7). Prior investigation of cytokine mRNA expression in unperfused brain samples revealed significant increases in IL-1 $\beta$ , IL-6 and TNF- $\alpha$  by 6 hours that were similar in magnitude to expression in perfused samples (fig 2.4). This supports previous literature and indicates that the brain can present an endogenous central cytokine response to peripheral infection (Turrin et al, 2001; Goujon et al, 1995; 1996; Laye et al, 2000; Jacobs et al, 1997, Kakizaki et al, 1999; Laye et al, 1994). The magnitude of IL-1 $\beta$  mRNA expression at 2 hours was greater than TNF- $\alpha$  or IL-6 at either 2 or 6 hours (fig 2.7). A greater magnitude of mRNA expression may translate into a larger amount of protein product, which may explain why IL-1 $\beta$  protein, in the absence of TNF- $\alpha$  or IL-6, can be detected in brain tissue by 6 hours following LPS administration.

In accordance with the literature, I have shown that IP injection of LPS increased cytokine mRNA expression in brain tissue (Turrin et al, 2001; Laye et al, 2000). In addition to this, detection of intracellular protein phosphorylation by Luminex<sup>®</sup> revealed that IP LPS treatment altered phosphorylation of I $\kappa$ B $\alpha$ , JNK and p38 in brain tissue (fig 2.8). This is the first time that the detection of intracellular protein phosphorylation in brain tissue using Luminex<sup>®</sup> has been reported. I $\kappa$ B $\alpha$ , JNK and p38 are intracellular proteins involved in LPS mediated cell signalling pathways important in the induction of target gene transcription. LPS can induce the translocation of the transcription factor NF- $\kappa$ B (Krappmann et al, 2004) subsequently causing the transcription of target cytokine genes, as described in chapter 1. The inhibitory factors I $\kappa$ B $\alpha$  and/or I $\kappa$ B $\beta$  prevent the translocation and DNA binding of NF- $\kappa$ B. Stimulus-dependent phosphorylation of I $\kappa$ B $\alpha$ / $\beta$  releases NF- $\kappa$ B into the nucleus to induce transcription of target genes including that of pro- and anti-inflammatory cytokines (Krappmann et al, 2004). IP LPS caused a significant increase in I $\kappa$ B $\alpha$  phosphorylation in the hippocampus by 2 hours post LPS administration (fig 2.8). There was also a non-significant trend for an increase in I $\kappa$ B $\alpha$  phosphorylation in cortical tissue. Interestingly, analysis of JNK phosphorylation by Luminex<sup>®</sup> also revealed a reduction in JNK phosphorylation by 2 hours after IP LPS administration (fig 2.8). Previous literature suggests that activated NF- $\kappa$ B can exert anti-apoptotic activity by the suppression of JNK phosphorylation (Bubici et al, 2006). Together, these data suggest that the translocation of NF- $\kappa$ B may be responsible for the increased expression of cytokine mRNA and protein in brain tissue, supporting the evidence that peripheral inflammation is communicated to the brain to induce centrally derived cytokine production.

LPS can also activate p38, a MAP kinase important in mediating inflammation (Nolan et al, 2003). IP LPS induced p38 kinase phosphorylation in the cortex by 6 hours post treatment (fig 2.8). LPS did not increase p38 phosphorylation in the hippocampus at 2 or 6 hours following injection. This suggests that p38 in hippocampal tissue is either unaffected by peripheral infection or that the temporal profiles of p38 phosphorylation differ between the cortex and hippocampus. Pharmacological inhibition of p38 kinase in models of chronic inflammation has demonstrated a role for this kinase in modulating cytokine gene transcription. The increase in p38 phosphorylation in brain tissue by 6 hours after peripheral

administration of LPS suggests that p38 has more of a role in later stages of inflammation in this in vivo model.

### **2.5.3 *Pharmacological manipulation of cytokine protein in brain tissue***

#### **2.5.3.1 *Glucocorticoid treatment - dexamethasone***

In accordance with published literature, taqman analysis of central cytokine mRNA expression revealed a large increase in cortical IL-1 $\beta$  mRNA at 2 hours that declined by 6 hours following IP LPS injection (fig 2.7). Quan et al (1998) described the detection, by in situ hybridisation techniques, of IL-1 $\beta$  at the CVOs and BBB by 2 hours following LPS administration. Sustained (8-12hrs post LPS) IL-1 $\beta$  expression was evident in glial cells throughout brain parenchyma that returned to basal levels at 24 hours. In the current studies, pre-treatment with dexamethasone (DEX) significantly attenuated LPS-induced IL-1 $\beta$  mRNA (fig 2.4) and protein expression in brain tissue (fig 2.5) and pro-inflammatory cytokine protein in plasma (fig 2.6). Previous reports have described the exacerbation of central IL-1 $\beta$  mRNA expression in adrenalectomised (inhibiting glucocorticoid release) rats following peripheral LPS injection (Quan et al, 2000). Glucocorticoids such as DEX may enter the brain tissue to increase I $\kappa$ B $\alpha$  expression in microglia, firstly at the CVOs and BBB and then throughout the brain tissue (Quan et al, 2000). The increased expression of the inhibitory factor I $\kappa$ B $\alpha$  prevents the LPS-mediated translocation of NF- $\kappa$ B and subsequently inhibits the endogenous transcription and translation of cytokines including IL-1 $\beta$  in the brain.

Until now, most evidence for the role of glucocorticoids in modulating LPS-induced cytokine expression has stemmed from reports of the potentiation of cytokine production following a reduction in endogenous glucocorticoids. For example, adrenalectomy or administration of the GC type II receptor antagonist RU38486 resulted in a potentiation in cytokine mRNA and protein expression after peripheral LPS challenge (Goujon et al, 1997 & 1996). The lethal effects of LPS or cytokines administered to adrenalectomised rats can be prevented by glucocorticoid replacement (Kapcala et al, 1995). The effect of the GC methylprednisolone on LPS-induced cytokine production in the brain was assessed in rat brain tissue but, in contrast to the current studies, analysis was limited to the detection of TNF- $\alpha$  by

ELISA (Buttini et al, 1997). Hence, there are presently no data published describing the effect of IP LPS injection on the expression of a range of cytokine proteins in rat brain tissue and plasma or detailing the effect of dexamethasone treatment on detectable cytokine protein. In the current study, using Luminex<sup>®</sup> has provided a novel insight into the effect of dexamethasone treatment on central and peripheral cytokine protein release in rat brain following IP LPS injection which is yet to be comprehensively reported in the literature.

#### 2.5.3.2 $\alpha$ 2-adrenoceptor antagonism - fluparoxan

The  $\alpha$ 2-adrenoceptor antagonist, fluparoxan, exhibited a strong anti-inflammatory effect by significantly decreasing cortical IL-1 $\alpha$ , hippocampal IL-1 $\beta$  and a non-significant dose-dependent trend to decrease cortical IL-1 $\beta$  (fig 2.11). Fluparoxan also significantly attenuated plasma TNF- $\alpha$  and IL-1 $\beta$  and potentiated plasma IL-10 (fig 2.14). Antagonism of  $\alpha$ 2 adrenoceptors has previously been shown to inhibit plasma TNF- $\alpha$  (Hasko et al, 1995; Fessler et al, 1996; Szelenyi et al, 2000), either inhibit (Finck et al, 1997) or increase (Hasko et al, 1995) IL-6 and potentiate IL-10 (Szelenyi et al, 2000). The data described in this chapter support reported literature and confirm that antagonism of presynaptic  $\alpha$ 2 adrenoceptors using fluparoxan can exert an anti-inflammatory effect on LPS-induced cytokine production. Fluparoxan and other selective  $\alpha$ 2 antagonists increase central noradrenaline release (Millan et al, 1994) that results in the prolonged activation of  $\beta$  adrenoceptors.  $\beta$  adrenoceptors may exert an anti-inflammatory effect by preventing I $\kappa$ B $\alpha$  degradation and subsequent NF- $\kappa$ B translocation and activation of target cytokine genes (Farmer & Pugin, 2000; Ye, 2000).

The  $\alpha$ 2 antagonist, idazoxan can reduce nitrite production by macrophages in vitro (Shen et al, 1994). There is currently little data describing the effects of  $\alpha$ 2 antagonists on nitrite production in vivo. Here, fluparoxan pretreatment attenuated LPS-induced plasma nitrite at all doses providing the first in vivo evidence of  $\alpha$ 2 modulation of iNOS activity during inflammation (fig 2.16).

#### 2.5.3.3 P38 inhibition – GW569293

The p38 inhibitor, GW569293, failed to reduce central or peripheral cytokine

production (fig 2.12 & 2.15) and significantly enhanced plasma IFN- $\gamma$  with a non-significant trend to increase plasma TNF- $\alpha$  and IL-1 $\beta$  (fig 2.15). The p38 MAP Kinase isoforms have a well-established role as mediators of cytokine release and p38 inhibitors demonstrate potent inhibition of cytokine production, particularly in vitro (Lee et al, 1994; Cuenda et al, 1995; Dean et al, 1999) but also to a lesser degree in vivo (Barone et al, 2001; Legos et al, 2001). Other literature has described p38 inhibitors cause elevation of cytokine production (T ten Hove et al, 2002) or demonstrate a lack of efficacy for cytokine inhibition (Campbell et al, 2004; Zhang et al, 1997; Lu et al, 1999; van den Blink et al, 2001). Previous literature suggests p38 activity may be cell-specific resulting in potentiation of cytokine release in macrophages whilst inhibiting release in other cell types (Van den Blink et al, 2001; Zhang et al, 1997). In addition, the p38 kinase may not modulate TNF- $\alpha$  production to the degree originally supposed or alternative intracellular pathways may compensate for p38-mediated changes in TNF- $\alpha$  levels. In vitro studies also indicate that p38 inhibition may have positive or negative effects on cytokine production depending upon the stimuli, cell populations and levels of cytokines produced (Rao et al, 2002; Salmon et al, 2001; Kim et al, 2004).

Although it is clear LPS can induce phosphorylation of the p38 kinase, TLR4 receptor signalling also directly activates NF- $\kappa$ B particularly in the early stages of the immune response to peripheral LPS injection (Krappmann et al, 2004). Study 4 described in this chapter indicated increased central p38 phosphorylation by 6 hours post LPS, however, phosphorylation of I $\kappa$ B $\alpha$ , an inhibitory factor for NF $\kappa$ B, increased by 2 hours (fig 2.8). This demonstrates a strong role for the NF- $\kappa$ B pathway early in LPS-induced cytokine production. These data also suggest the early phase of cytokine protein induction may be directed more through direct NF- $\kappa$ B activation in the absence of activation of a p38 kinase pathway, possibly explaining the lack of an acute effect of GW569293 in the IP LPS cytokine model.

LPS or cytokines can cause iNOS activation (Liew et al, 1994; Lazarov et al, 2000) and a continuous LPS infusion in rat caused a small elevation in plasma nitrate/nitrite by 4 hours that increased considerably by 6 hours (Soszynski, 2002; Hamilton & Warner, 1998). An iNOS selective inhibitor, 1400W, prevented LPS-induced increase in nitrate/nitrite suggesting nitric oxide production is consistent with

inducible nitric oxide synthase (iNOS) induction (Hamilton & Warner, 1998). Although p38 inhibition exhibited little effect on the cytokines investigated in the current study, the release of nitrite by circulating plasma macrophages and monocytes was significantly reduced by GW569293 (fig 2.16). These data support some *in vitro* evidence (Guan et al, 1997); however, other studies have indicated p38 inhibition may enhance NO production (Lahti et al, 2006). It is possible that iNOS activity occurs independently of cytokine production and may support a cell-specific role for p38 kinase. Variation in the inflammatory stimulus and timepoints investigated between studies may also influence the effect of p38 inhibition on iNOS activity.

This chapter describes the first report of the application of a Luminex<sup>®</sup> suspension bead array system to the detection of cytokine protein and phosphoproteins involved in LPS-mediated intracellular signalling in brain tissue post IP LPS. Importantly, the identification of intracellular protein phosphorylation and cytokine mRNA expression in brain tissue confirmed an endogenous neuroinflammatory response to IP LPS injection. It is evident that IP LPS can induce central inflammatory markers, specifically IL-1 $\beta$  and IL-1 $\alpha$  and that an IP LPS-induced cytokine protein model can successfully act as a first-pass screen for putative anti-inflammatory agents. One caveat of this model is that the peripheral anti-inflammatory actions of an agent may prevent subsequent communication of the presence of inflammation to the brain, making it difficult to clearly assess the anti-inflammatory activity of compounds on brain tissue. Some agents may also modulate cytokines other than IL-1 $\beta$  or IL-1 $\alpha$  released endogenously within the brain. A model providing a broader central cytokine profile is required to provide more in-depth analysis of the effect of a compound on neuroinflammation. mRNA expression of inflammatory cytokines in plasma and brain tissue is increased to a greater extent following administration of LPS directly into the brain in contrast to peripheral LPS injection (Gayle et al, 1998; Gayle et al, 1999; Turrin et al, 2001; Plata-Salaman et al, 1998; De Simoni et al, 1995). The following chapter will describe the measurement of central and peripheral cytokine following ICV injection of LPS using Luminex<sup>®</sup>

## **CHAPTER 3**

### ***Central administration of LPS – confirming anti-inflammatory activity in brain tissue***

#### **3.1 Introduction**

Chapter 2 detailed the validation of a high throughput in vivo model of IP LPS induced central and peripheral cytokine protein in rodent brain. Neuroinflammation was present as evidenced by alterations in pro-inflammatory mRNA expression, IL-1 $\beta$  protein and intracellular proteins in brain tissue indicating the communication of a peripheral immune response to the brain. The glucocorticoid dexamethasone and the  $\alpha$ 2-adrenoceptor antagonist fluparoxan attenuated pro-inflammatory cytokine protein expression in brain tissue and plasma. The peripheral LPS model, however, does not clearly establish anti-inflammatory activity of these agents in brain tissue as reduction of LPS-induced cytokines in the blood affect the communication of an inflammatory response from blood to brain. An in vivo model in which the inflammatory response is initiated in brain tissue first will allow further assessment of the efficacy of agents on centrally derived inflammation. I chose to induce a neuroinflammatory response to LPS via ICV injection into rat brain and to use the Luminex<sup>®</sup> suspension bead array system, previously validated for cytokine detection in chapter 2, to assess the induction of central and peripheral cytokine protein. The model will be used to further investigate the anti-inflammatory properties of dexamethasone and fluparoxan in brain tissue. Glucocorticoid treatment attenuates LPS-induced cytokine production (Sironi et al, 1992, Mengozzi et al, 1994) and dexamethasone demonstrated potent anti-inflammatory properties in chapter 2. Antagonists of  $\alpha$ 2 receptors increase synaptic NA, a catecholamine that inhibits the release of pro-inflammatory cytokines (Kaneko et al, 2005; Hu et al, 1991) and inhibits microglial activation (Lee et al, 1992; Loughlin et al, 1993; Chang & Liu, 2000).

### **3.1.1 *Intracerebroventricular (ICV) injection***

LPS, at a molecular weight of 10kDa is unlikely to cross the blood brain barrier. In order to induce neuroinflammation, LPS must be directly injected into the brain tissue. LPS infusion into the ventricular system, via direct injection or implantation of a permanent indwelling cannula, initiates a strong time-dependant inflammatory response in the brain, ipsilateral to the site of injection (Muramami et al, 1993). Following ICV LPS injection, intraventricular macrophages and microglia increase the expression of cell-surface proteins including both MHC class I and II (Ling et al, 1998). Microglia are subsequently activated in hippocampal and thalamic areas (Nicholson & Renton, 2001) prompting rapid induction of pro-inflammatory cytokines including TNF- $\alpha$  (Zujovic et al, 2001). Evidence suggests that ICV administered LPS induces peripheral cytokine production via its dissipation into the blood from the brain since bioactive LPS can be detected in the blood as early as 5 minutes post injection (Chen et al, 2000). The magnitude and range of cytokine response evident in the periphery following central LPS administration is, however, less than that induced by peripheral LPS challenge.

### **3.1.2 *Evidence of central cytokine induction by ICV LPS***

Acute ICV LPS administration results in the expression of pro-inflammatory cytokine mRNA in the brain (Gayle et al, 1998; 1999; Plata-Salaman et al, 1998; De Simoni et al, 1998; Muramami et al, 1993; Song et al, 1999). ICV administration of LPS may also induce cytokine protein in plasma (Hallenbeck et al, 1991; Gottschall et al, 1992; Song et al, 1999; Ghezzi et al, 2000; Chen et al, 2000; Nicholson & Renton, 2001; Finck et al, 1997). ELISAs have previously been used to detect a small range of cytokine proteins in brain tissue (Szczepanik & Ringheim, 2003; Kalehua et al, 2000; Zujovic et al, 2001).

### 3.1.3 *Chapter Aims*

The goals of this chapter are to:

1. Evaluate the anti-inflammatory effect of dexamethasone pre-treatment on ICV LPS induced cytokine protein in rat brain tissue and plasma.
2. Assess the anti-inflammatory effect of fluparoxan and GW569293 pre-treatment on ICV LPS induced cytokine protein in rat brain tissue and plasma.

## 3.2 **Materials & Methods**

### 3.2.1 *Materials*

The p38 inhibitor GW569293 and the  $\alpha$ 2- adrenoceptor antagonist fluparoxan were synthesised at GSK, Harlow. PBS (Sigma, UK) and methylcellulose were prepared in-house. Lipopolysaccharide (0111:B4, L2630) and the glucocorticoid dexamethasone were purchased from Sigma, UK.

### 3.2.2 *ICV cannulation*

Specific, pathogen free male CD rats (250g, approximately 10 weeks of age) (Charles River, UK) were anaesthetised by inhalation of 3% isoflurane in oxygen (Merial animal Health Ltd, Essex, UK). The head of each rat was shaved and the skin sterilised using a hibitane/alcohol solution. Lacrilube (Allergan, Buckinghamshire, UK) was applied to the eyes to prevent them from drying out during surgery. Animals were secured in a stereotaxic frame (David Kopf Instruments, USA) (incisor bar set -3.2mm below the intra-aural plane) and a midline incision along the sagittal suture made in the skin overlying the skull. 0.1ml intra-epicaine (Arnolds, Surrey, UK) was injected into the subdermal skin layers to provide post-operative local analgesia. Four burr holes were drilled and screws and cannula (Plastics One, Roanoke, Virginia, USA) implanted into the skull, secured in place by cyanoacrylate gel and gel activator (RS components, Corby, UK). The skin either side of the gel was sutured with vicryl rapide 4/0 (Johnson & Johnson, UK) and the animal housed in an incubator set at 37°C until the rat had regained consciousness. All animals were returned to the home cage with warm bedding and soft mash/baby food. The body weights and general health of the rats were monitored daily until pre-operative body

weight had been reached. Rats were individually housed in an animal facility at GlaxoSmithKline Pharmaceuticals, Harlow, Essex UK under controlled conditions (temperature: 21-24°C, 12-h light/dark cycle (7am lights on) and fed a pellet diet and water *ad libitum*.

Post ICV cannulation, all animals were tested for cannulae patency by ICV injection of human angiotensin II (100ng/rat) (Sigma, UK) (Johnson & Epstein, 1975). Animals that failed to display an acute dipsogenic response were culled by an approved schedule one method. All experimental procedures were conducted in accordance with the GlaxoSmithKline local ethics committee and conform to the UK Animals (Scientific Procedures) Act 1986.

### **3.2.3 Drug administration**

Dexamethasone, GW569293 and fluparoxan were sonicated in 0.5% methylcellulose until completely dissolved and administered orally at a dosing volume of 2ml/kg. Dosing took place according to a timed schedule of two rats every 15 minutes to account for the time required to sample each rat. ICV cannulated rats were administered with either 20µg or 5µg LPS (0111:B4 *E. coli*, L2630, Sigma, UK) dissolved in 5µl of filtered PBS. LPS (4mg/1ml or 1mg/1ml) was allowed to dissolve in PBS in a falcon tube (VWR International, UK) for at least 30 minutes before administration. Initial studies completed at GSK, Harlow, assessed cytokine protein induction in plasma following 20µg LPS ICV therefore, I used this dose for the preliminary study. LPS (5µg) was reported to increase hippocampal TNF-α protein; hence, this dose is also reported in this chapter (Zujovic et al, 2001). LPS was injected ICV at 30 minutes, 1 hour or 2 hours following oral (gavage) treatment with fluparoxan (3mg/kg), dexamethasone (1mg/kg) or GW569293 respectively.

### **3.2.4 ICV administration and cytokine determination**

An infusion pump (Harvard PHD 4400 Hpsi, Harvard Apparatus, Kent, UK) was loaded with a 100ul Hamilton syringe (Hamilton, Birmingham, UK) attached to PVC tubing and tipped with a stainless steel injector (Plastics One, Roanoke, Virginia, USA). The tubing and syringe were filled with 0.9% saline and a 10µl air bubble drawn up at the distal end to enable separation of the test compound and the saline.

LPS was injected over the duration of two minutes with a further 30 seconds before injector removal to ensure complete diffusion of LPS into the ventricle. Dosing took place according to a timed schedule of two rats every fifteen minutes to account for the time required to sample each rat. Rats were deeply anaesthetised with sodium pentobarbitone (Euthatal<sup>®</sup> 100mg kg<sup>-1</sup> i.p, Rhône Mérieux, Harlow, UK) 2 hours post ICV LPS administration. This sampling timepoint was based on evidence in the literature (Kalehua et al, 2000; Zujovic et al, 2001) and previous in-house studies (GSK, Harlow) demonstrating peak IL-1 $\alpha$ , IL-1 $\beta$  and TNF- $\alpha$  induction in brain tissue by 2 hours post ICV LPS. Plasma and ipsilateral brain samples were obtained using the method described in 2.2.4. All samples were prepared for cytokine determination as described in 2.2.5.1 and subsequently analysed using the Luminex<sup>®</sup> suspension array system using the method described in 2.2.5.2.

### **3.2.5 Data Analysis**

4/5-parameter logistic regression curves (Hulse et al, 2004) of the cytokine standard values were calculated using StarStation software and the concentrations of unknown samples were determined relative to calculated standard curves.

A general linear mixed model approach using the Proc Mixed procedure in SAS<sup>®</sup> Version 8 (SAS<sup>®</sup> Institute, UK) assessed each separate cytokine response using brain region as a repeated measure. Univariate tests of significance using Statistica<sup>™</sup> Version 6.1 (Statsoft, USA) calculated the overall effect of LPS treatment on plasma cytokine responses. Planned comparisons on the predicted means from the model assessed individual LPS effects on cytokine levels within plasma and brain compartments. Results are represented as means  $\pm$  SEM and significance was set at  $P \leq 0.05$ . Percentage reduction describes attenuation relative to the LPS-induced cytokine response.

## **3.3 Protocols**

### **3.3.1 Study 6: Pre-treatment of dexamethasone or GW569293: 20 $\mu$ g ICV LPS**

Male CD rats (n=8-10 per group) were pre-treated with 0.5% methylcellulose, dexamethasone (1mg/kg, 1 hour) or GW569293 (25mg/kg, 2 hours) before ICV LPS

(20µg/rat) dissolved in filtered PBS. All animals were euthanased 2 hours post LPS administration and plasma, ipsilateral hippocampus and frontal cortex were taken for cytokine analysis

### **3.3.2 Study 7: Pretreatment of dexamethasone: 5µg ICV LPS**

Male CD rats (n=4-7 per group) pre-treated with either 0.5% methylcellulose or the glucocorticoid dexamethasone (1mg/kg) were administered 1 hour later with 5µg/rat LPS dissolved in filtered PBS or filtered PBS alone. All animals were euthanased 2 hours post LPS administration and plasma, ipsilateral hippocampus and frontal cortex were taken for cytokine analysis.

### **3.3.3 Study 8: Pretreatment of fluparoxan or GW569293: 5µg ICV LPS**

Male CD rats (n=6-8 per group) pre-treated with 0.5% methylcellulose, fluparoxan (3mg/kg, 30 mins) or GW569293 (25mg/kg, 2 hours) before ICV LPS (5µg/rat) dissolved in filtered PBS. All animals were euthanased 2 hours post LPS administration and plasma, ipsilateral hippocampus and frontal cortex were taken for cytokine analysis.

## **3.4 Results**

### **3.4.1 Study 6: Pre-treatment of dexamethasone or GW569293: 20µg ICV LPS**

#### **3.4.1.1 Cytokine protein in brain**

CD rats (n=8) were pre-treated with the glucocorticoid dexamethasone followed by ICV 20µg LPS (fig 3.1A & 3.1B). Separate repeated measure ANOVAs on each cytokine indicated an overall effect of treatment,  $F_{(3, 29)} = 8.04$ ,  $p < 0.001$ , region,  $F_{(1, 29)} = 58.38$ ,  $p < 0.001$  and a treatment\*brain region interaction,  $F_{(3, 29)} = 5.47$ ,  $p < 0.01$  on LPS-induced IL-1 $\alpha$ . There was a significant effect of treatment [ $F_{(3, 30)} = 7.78$ ,  $p < 0.001$ ], region [ $F_{(1, 29)} = 61.38$ ,  $p < 0.001$ ] and a treatment\*brain region interaction [ $F_{(3, 29)} = 5.49$ ,  $p < 0.01$ ] on LPS-induced IL-1 $\beta$ . Repeated measures revealed an overall effect of treatment,  $F_{(3, 30)} = 7.22$ ,  $p < 0.001$  region,  $F_{(1, 30)} = 24.16$ ,  $p < 0.001$  and a treatment\*brain region interaction,  $F_{(3, 30)} = 6.64$ ,  $p = 0.001$  on the

proinflammatory cytokine TNF- $\alpha$ . There was also a significant treatment effect on IFN- $\gamma$ ,  $F_{(3, 27)} = 4.01$ ,  $p < 0.05$ .

Post hoc planned comparisons revealed LPS increased cortical IFN- $\gamma$  from  $1.13 \pm 0.06$  to  $1.27 \pm 0.07$  pg/mg tissue, however, this failed to reach significance at the  $p < 0.05$  level ( $p = 0.08$ ). (fig 3.1A & 3.1B).

Post hoc planned comparisons also revealed LPS increased hippocampal IL-1 $\alpha$  from  $0.76 \pm 0.09$  to  $4.3 \pm 1.07$  pg/mg tissue ( $p < 0.01$ ) and from  $0.77 \pm 0.14$  to  $8.33 \pm 1.24$  pg/mg tissue in the cortex ( $p < 0.001$ ). Dexamethasone significantly attenuated hippocampal IL-1 $\alpha$  to  $2.12 \pm 0.49$  pg/mg tissue (61% reduction of LPS response ( $p < 0.05$ )). ICV LPS also significantly increased hippocampal IL-1 $\beta$  from  $2.42 \pm 0.03$  to  $11.48 \pm 2.50$  pg/mg ( $p < 0.001$ ) and cortical IL-1 $\beta$  from  $2.59 \pm 0.69$  to  $21.45 \pm 2.99$  pg/mg tissue. Dexamethasone reduced hippocampal IL-1 $\beta$  by 48% to  $7.14 \pm 1.40$  pg/mg tissue ( $p < 0.05$ ). LPS augmented hippocampal TNF- $\alpha$  from  $2.28 \pm 0.08$  to  $3.51 \pm 0.36$  pg/mg ( $p < 0.05$ ) and cortical TNF- $\alpha$  from  $2.19 \pm 0.14$  to  $5.28 \pm 0.39$  pg/mg ( $p < 0.001$ ). Dexamethasone attenuated hippocampal TNF- $\alpha$  by 83% to  $2.48 \pm 0.30$  pg/mg ( $p < 0.05$ ) and cortical TNF- $\alpha$  by 53% to  $3.65 \pm 0.52$  pg/mg tissue ( $p < 0.01$ ).

The p38 inhibitor, GW569293 did not significantly attenuate any LPS-induced cytokine protein measure within brain tissue (fig 3.2A & B).

#### 3.4.1.2 Cytokine protein in plasma

Separate univariate ANOVAs revealed overall treatment effect on plasma IL-1 $\alpha$ ,  $F_{(3, 28)} = 4.20$ ,  $p = 0.01$ , and TNF- $\alpha$ ,  $F_{(3, 30)} = 19.21$ ,  $p < 0.001$  (fig 3.3). LPS reduced plasma IL-1 $\alpha$  from  $372.43 \pm 134.91$  to  $71.88 \pm 14.53$  pg/ml ( $p = 0.01$ ) and increased plasma TNF- $\alpha$  from  $648.83 \pm 172.97$  to  $47460.7 \pm 10013.24$  pg/ml ( $p < 0.001$ ). Dexamethasone attenuated TNF- $\alpha$  by 93% decreasing LPS induced plasma TNF- $\alpha$  to  $4114.79 \pm 1146.03$  pg/ml ( $p < 0.0001$ ). GW569293 significantly decreased plasma TNF- $\alpha$  by 87% to  $6414.03 \pm 1552.53$  pg/ml ( $p = 0.001$ ) (fig 3.4).

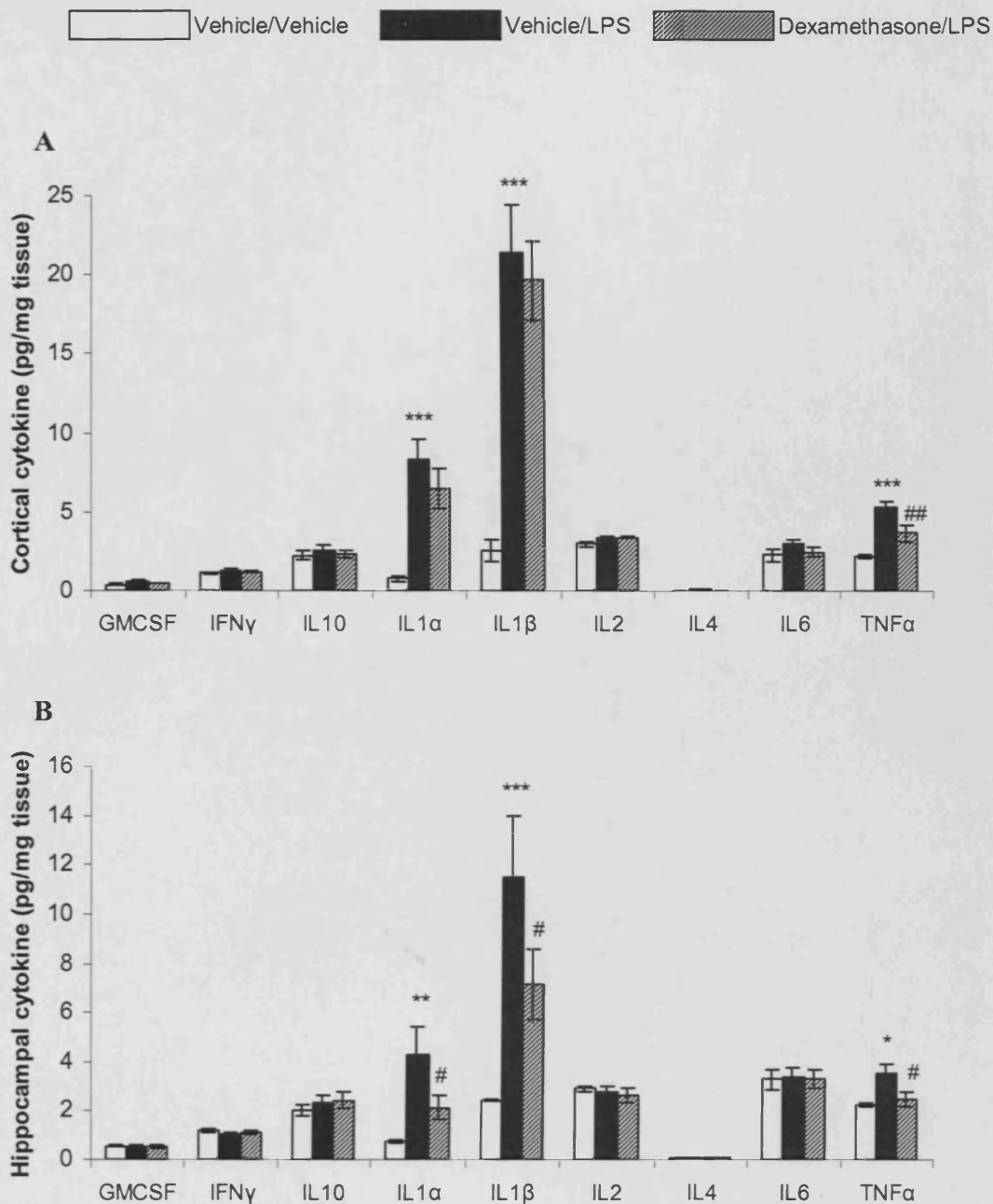


Figure 3.1: Effect of dexamethasone pre-treatment on cytokine protein in the cortex (A) and hippocampus (B) of adult rats ( $n = 8-10$ ) by 2 hours post ICV LPS ( $20\mu\text{g}$ ) administration, data represented as cytokine protein (pg) per milligram of tissue and shows mean  $\pm$  SEM. \*\*\* $p \leq 0.001$ , \*\* $p \leq 0.01$ , \*  $p \leq 0.05$  significantly different vs. vehicle; ##  $p \leq 0.01$ , #  $p \leq 0.05$  significantly different vs. LPS (repeated measures ANOVA followed by planned comparisons)

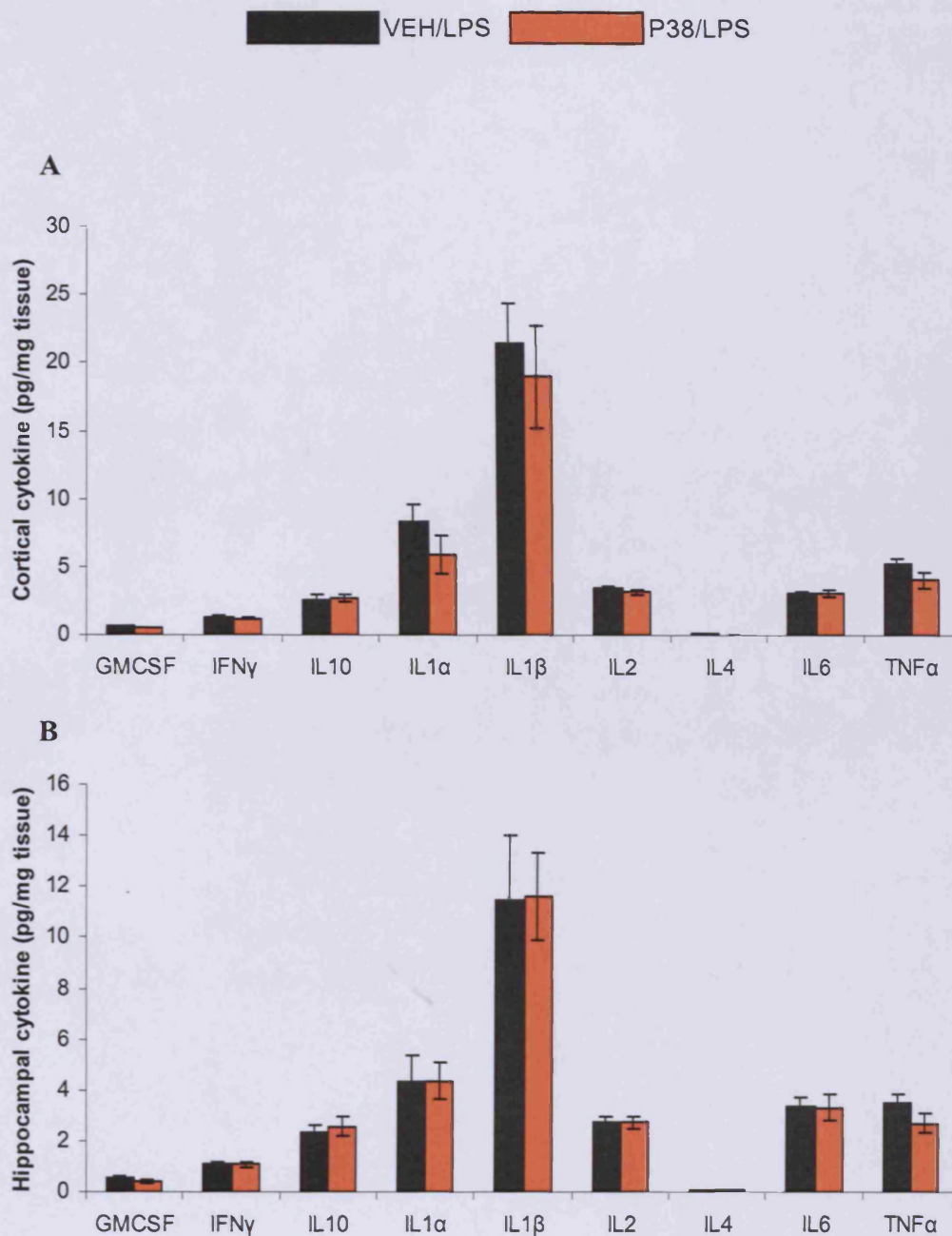


Figure 3.2: Effect of GW569293 pre-treatment on cytokine protein in the cortex (A) and hippocampus (B) of adult rats ( $n = 8-10$ ) by 2 hours post ICV LPS ( $20\mu\text{g}$ ) administration, data represented as cytokine protein (pg) per milligram of tissue and shows mean  $\pm$  SEM (repeated measures ANOVA followed by planned comparisons)

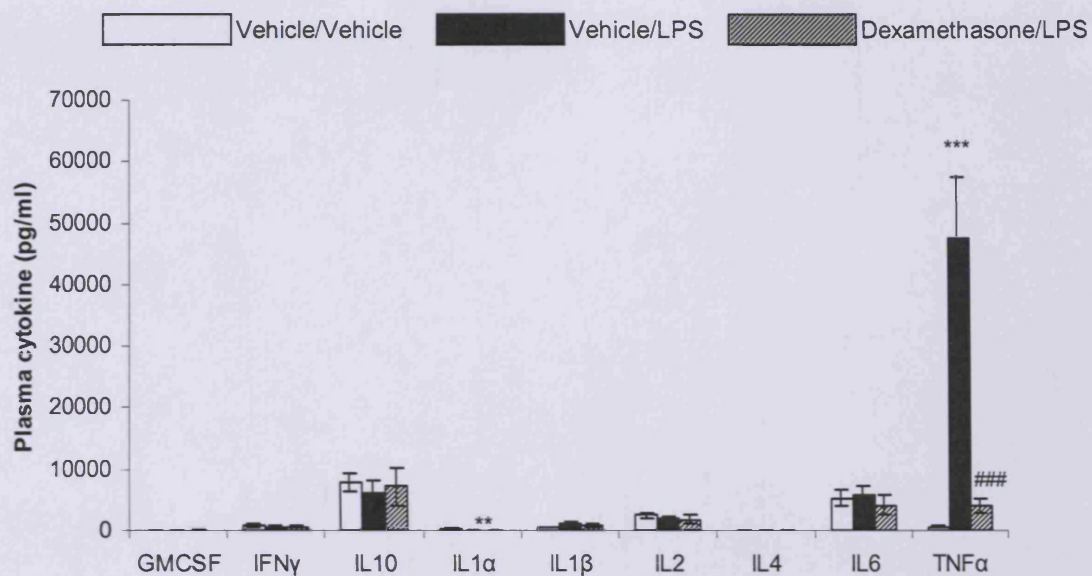


Figure 3.3: Effect of dexamethasone pre-treatment on cytokine protein in plasma of adult rats (n = 8-10) by 2 hours post ICV LPS (20 $\mu$ g) administration, data represented as cytokine protein (pg) per millilitre of sample and shows mean  $\pm$  SEM. \*\*\*p  $\leq$  0.001, \*\*p  $\leq$  0.01 significantly different vs. vehicle; ### p  $\leq$  0.001 significantly different vs. LPS (univariate ANOVA followed by planned comparisons)

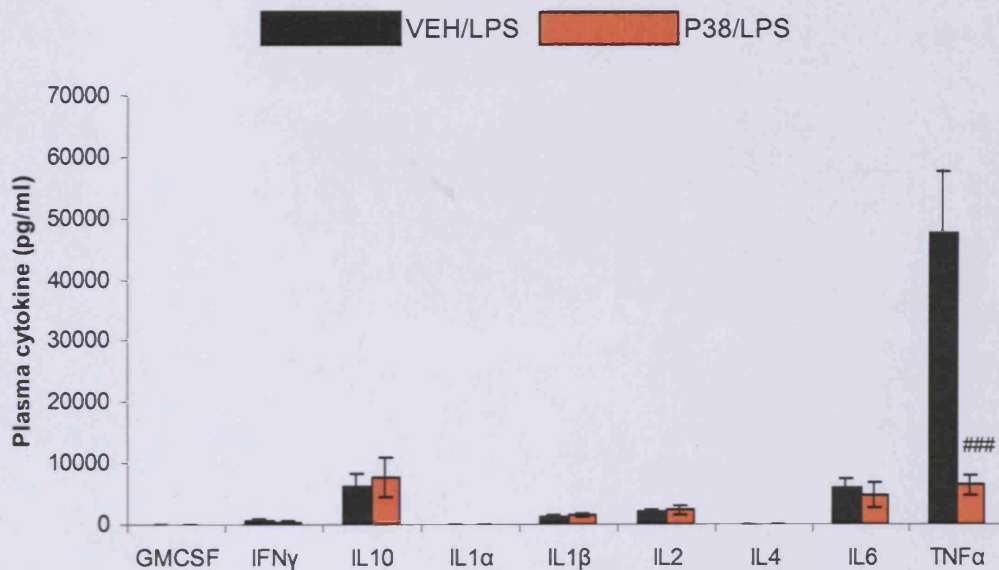


Figure 3.4: Effect of GW569293 pre-treatment on cytokine protein in plasma of adult rats (n = 8-10) by 2 hours post ICV LPS (20 $\mu$ g) administration, data represented as cytokine protein (pg) per millilitre of sample and shows mean  $\pm$  SEM. ### p  $\leq$  0.001 significantly different vs. LPS (univariate ANOVA followed by planned comparisons)

### 3.4.2 **Study 7: Pretreatment of dexamethasone: 5µg ICV LPS**

#### 3.4.2.1 *Cytokine protein in brain*

Repeated measures ANOVA on each cytokine indicated an overall treatment effect on IL-1 $\alpha$ ,  $F_{(2, 14)} = 14.88$ ,  $p < 0.001$ , IL-1 $\beta$ ,  $F_{(2, 9)} = 11.21$ ,  $p < 0.01$  and TNF- $\alpha$   $F_{(2, 14)} = 7.33$ ,  $p < 0.01$  in brain tissue (fig 3.5A & 3.5B). There was also a significant effect of brain region on TNF- $\alpha$ ,  $F_{(1, 14)} = 5.47$ ,  $p < 0.05$ .

Post hoc planned comparisons revealed LPS significantly increased cortical ( $p < 0.001$ ) and hippocampal ( $p = 0.001$ ) IL-1 $\alpha$  from  $0.31 \pm 0.06$  to  $1.19 \pm 0.11$  pg/mg tissue and from  $0.45 \pm 0.13$  to  $2.4 \pm 0.65$  pg/mg tissue respectively. Dexamethasone significantly attenuated LPS-induced cortical IL-1 $\alpha$  ( $p < 0.01$ ) by 75% to  $0.53 \pm 0.14$  pg/mg tissue and fully attenuated hippocampal IL-1 $\alpha$  ( $p < 0.001$ ) to  $0.42 \pm 0.11$  pg/mg tissue. LPS significantly increased cortical ( $p < 0.01$ ) and hippocampal ( $p < 0.01$ ) IL-1 $\beta$  from  $0.72 \pm 0.23$  to  $33.30 \pm 4.01$  pg/mg tissue and from  $1.49 \pm 0.84$  to  $46.85 \pm 11.88$  pg/mg tissue respectively. Dexamethasone significantly decreased LPS-induced hippocampal IL-1 $\beta$  by 68% ( $p < 0.05$ ) to  $15.61 \pm 7.49$  pg/mg tissue and attenuated LPS-induced cortical IL-1 $\beta$  by 43% ( $p = 0.09$ ) to  $19.42 \pm 9.05$  pg/mg tissue. ICV LPS administration increased cortical TNF- $\alpha$  ( $p < 0.01$ ) from  $0.69 \pm 0.37$  to  $2.35 \pm 0.23$  pg/mg tissue and hippocampal TNF- $\alpha$  ( $p < 0.01$ ) from  $1.07 \pm 0.43$  to  $3.48 \pm 0.81$  pg/mg tissue. Dexamethasone treatment reduced the LPS induction of cortical and hippocampal TNF- $\alpha$  by 85% ( $p < 0.01$ ) to  $1.17 \pm 0.33$  pg/mg tissue and 89% ( $p < 0.01$ ) to  $1.42 \pm 0.30$  pg/mg tissue respectively.

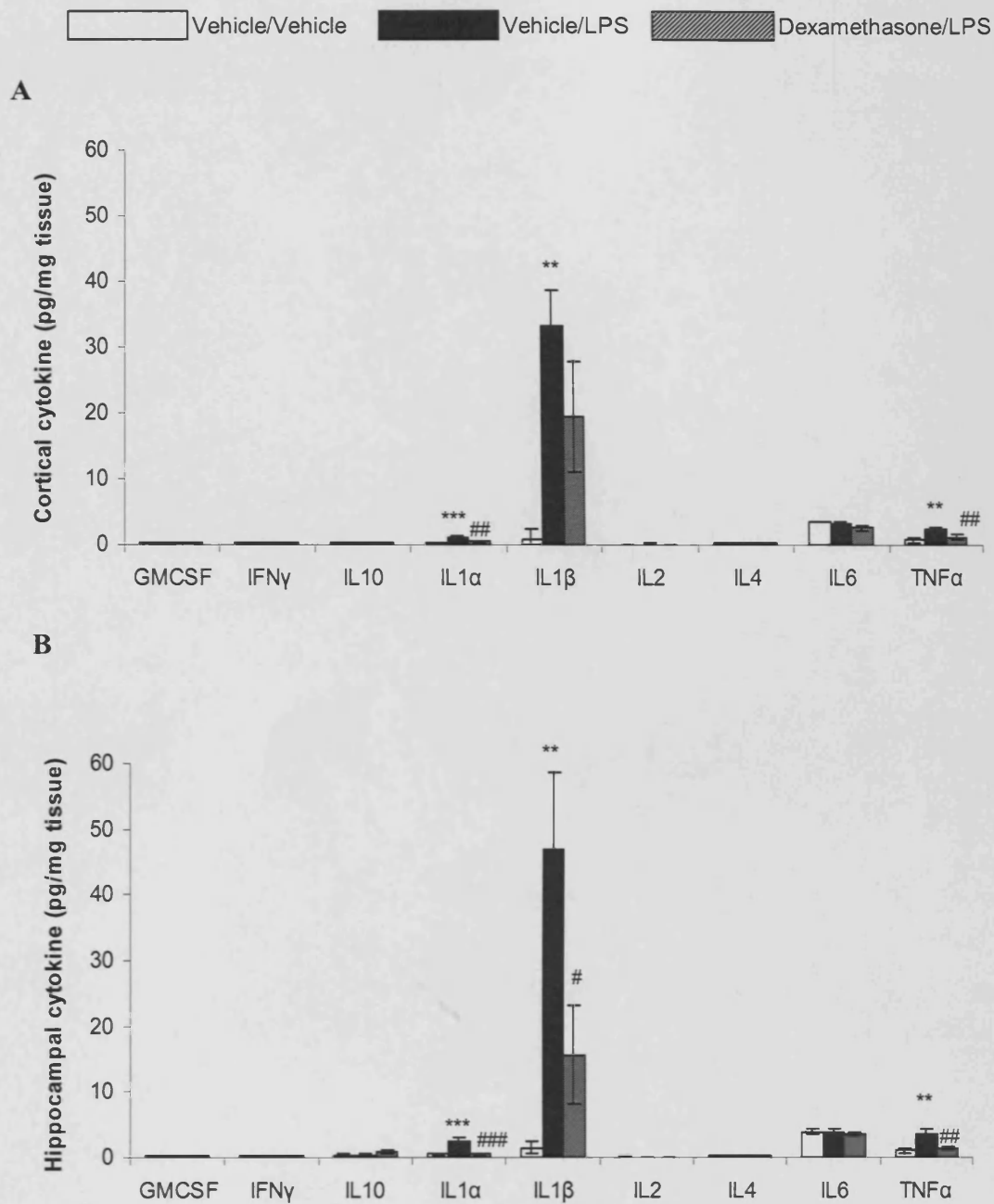


Figure 3.5: Effect of dexamethasone pre-treatment on cytokine protein in the cortex (A) and hippocampus (B) of adult rats (n = 4-7) by 2 hours post ICV LPS (5 $\mu$ g) administration, data represented as cytokine protein (pg) per milligram of tissue and shows mean  $\pm$  SEM. \*\*\*p  $\leq$ 0.001, \*\*p  $\leq$ 0.01 significantly different vs. vehicle; ### p  $\leq$ 0.001, ## p  $\leq$ 0.01 significantly different vs. LPS (repeated measures ANOVA followed by planned comparisons)

### 3.4.2.2 Cytokine protein in plasma

Plasma IL-1 $\beta$  was increased ( $p < 0.01$ ) from  $0.20 \pm 0.20$  to  $779.67 \pm 605.86$  pg/ml and IL-6 and TNF- $\alpha$  was augmented from  $128.00 \pm 0.00$  to  $693.61 \pm 162.23$  pg/ml ( $p < 0.05$ ) and from  $0.00 \pm 0.00$  to  $4132.36 \pm 1866.86$  pg/ml ( $p < 0.001$ ) respectively. Dexamethasone attenuated the LPS-induced increase in IL-1 $\beta$  by 98% ( $p < 0.06$ ) to  $14.71 \pm 14.71$  pg/ml and fully attenuated IL-6 ( $p < 0.01$ ) and TNF- $\alpha$  ( $p < 0.001$ ) to 0.00 pg/ml (fig 3.6).

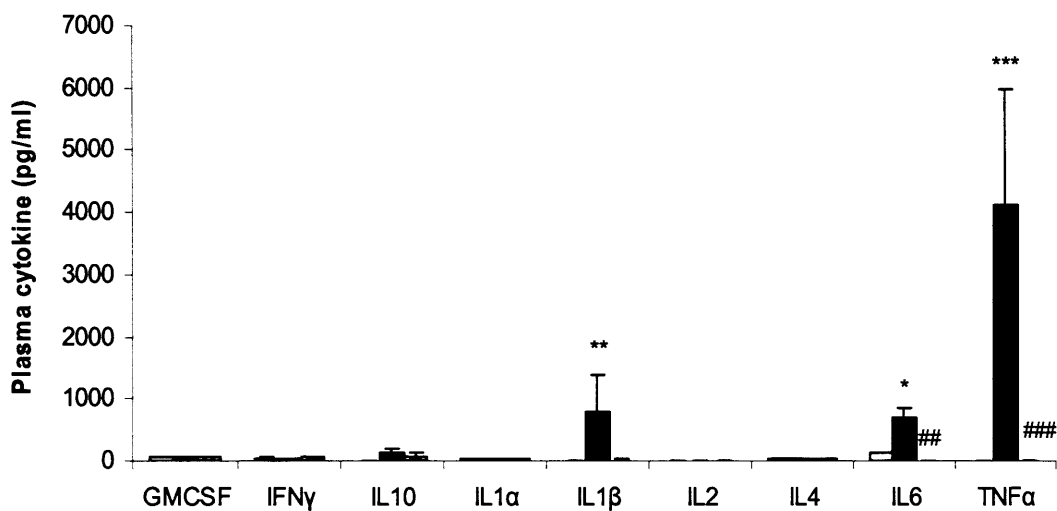


Figure 3.6: Effect of dexamethasone pre-treatment on cytokine protein in plasma of adult rats ( $n = 4-7$ ) by 2 hours post ICV LPS ( $5\mu\text{g}$ ) administration, data represented as cytokine protein (pg) per millilitre of sample and shows mean  $\pm$  SEM. \*\*\* $p \leq 0.001$ , \*\* $p \leq 0.01$ , \*  $p \leq 0.05$  significantly different vs. vehicle; ###  $p \leq 0.001$ , ##  $p \leq 0.01$  significantly different vs.

LPS (univariate ANOVA followed by planned comparisons)

### 3.4.3 *Study 8: Pretreatment of fluparoxan or GW569293: 5µg ICV LPS*

#### 3.4.3.1 *Cytokine protein in brain*

Separate repeated measure ANOVAs indicated an overall effect of treatment on IL-1 $\alpha$ ,  $F_{(3, 25)} = 3.53$ ,  $p < 0.05$ , IL-1 $\beta$ ,  $F_{(3, 25)} = 2.85$ ,  $p = 0.06$  and TNF- $\alpha$   $F_{(3, 24)} = 5.34$ ,  $p < 0.01$  in brain tissue (fig 3.7A and 3.7B). There were also significant effects of brain region on GM-CSF,  $F_{(1, 24)} = 13.84$ ,  $p = 0.001$ , IFN- $\gamma$ ,  $F_{(1, 25)} = 9.12$ ,  $p < 0.01$ , IL-4,  $F_{(1, 25)} = 22.06$ ,  $p < 0.001$ , IL-6,  $F_{(1, 25)} = 21.22$ ,  $p < 0.001$  and TNF- $\alpha$ ,  $F_{(1, 24)} = 4.18$ ,  $p = 0.05$ .

Post hoc planned comparisons revealed LPS significantly increased cortical ( $p < 0.05$ ) and hippocampal ( $p < 0.01$ ) IL-1 $\alpha$  from  $0.85 \pm 0.27$  to  $2.86 \pm 1.82$  pg/mg tissue and from  $0.82 \pm 0.19$  to  $2.64 \pm 0.79$  pg/mg tissue respectively. LPS-increased cortical IL-1 $\alpha$  was attenuated by 96% following fluparoxan treatment ( $p < 0.05$ ) to  $0.93 \pm 0.16$  pg/mg tissue. Increased hippocampal IL-1 $\alpha$  in response to ICV LPS was also reduced by 65% to  $1.46 \pm 0.34$  pg/mg tissue following fluparoxan but this failed to reach significance at the  $p = 0.05$  level ( $p = 0.09$ ).

LPS significantly increased IL-1 $\beta$  from  $8.39 \pm 6.21$  to  $33.48 \pm 8.93$  pg/mg tissue and from  $8.72 \pm 3.55$  to  $43.29 \pm 20.37$  pg/mg tissue in cortex ( $p < 0.05$ ) and hippocampus ( $p < 0.05$ ) respectively. Fluparoxan also reduced the production of cortical and hippocampal IL-1 $\beta$  by 79% to  $13.74 \pm 3.64$  pg/mg tissue ( $p = 0.05$ ) and 65% to  $20.96 \pm 5.05$  pg/mg tissue ( $p = 0.08$ ) respectively.

LPS induced a significant elevation of TNF- $\alpha$  in cortex from  $0.63 \pm 0.29$  to  $2.39 \pm 0.81$  pg/mg tissue ( $p < 0.05$ ) and hippocampus from  $1.04 \pm 0.26$  to  $2.54 \pm 0.32$  pg/mg tissue ( $p < 0.01$ ). This was attenuated by fluparoxan treatment to  $0.87 \pm 0.17$  pg/mg tissue in cortex (86% reduction,  $p < 0.05$ ) and by 42% to  $1.91 \pm 0.42$  pg/mg tissue in hippocampus, however this failed to reach significance at  $p < 0.05$  ( $p = 0.19$ ).

The p38 inhibitor, GW569293 did not significantly attenuate any LPS-induced cytokine protein measure within brain tissue (IL-1 $\beta$ : cortex –  $p = 0.11$  vs. LPS; hippocampus –  $p = 0.42$  vs. LPS) (fig 3.8A & B).

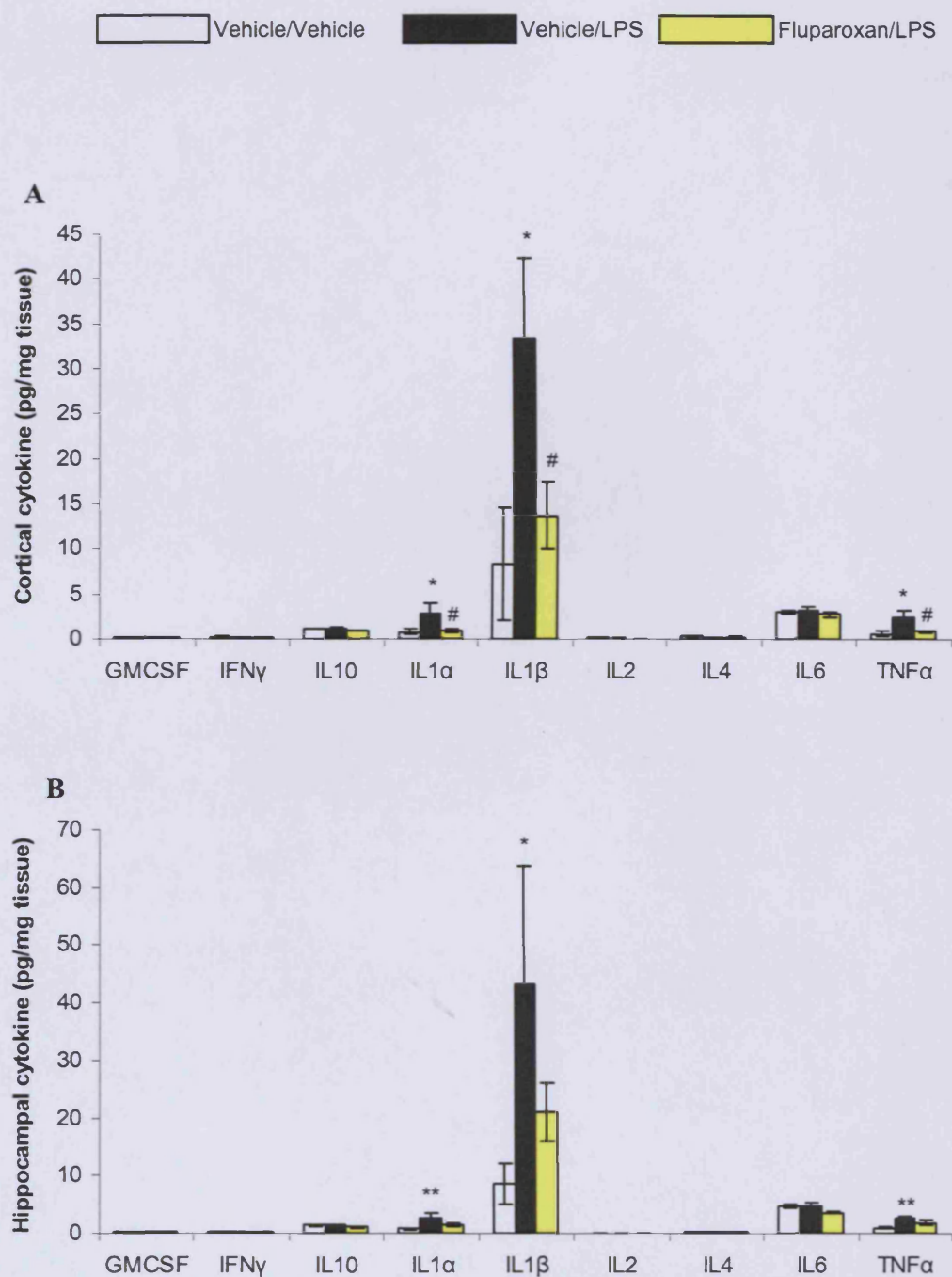


Figure 3.7: Effect of fluparoxan pre-treatment on cytokine protein in cortex (A) and hippocampus (B) of adult rats ( $n = 6-8$ ) by 2 hours post ICV LPS ( $5\mu\text{g}$ ) administration, data represented as cytokine protein (pg) per milligram of tissue and shows mean  $\pm$  SEM. \*\* $p \leq 0.01$ , \*  $p \leq 0.05$  significantly different vs. vehicle; #  $p \leq 0.05$  significantly different vs. LPS (repeated measures ANOVA followed by planned comparisons)

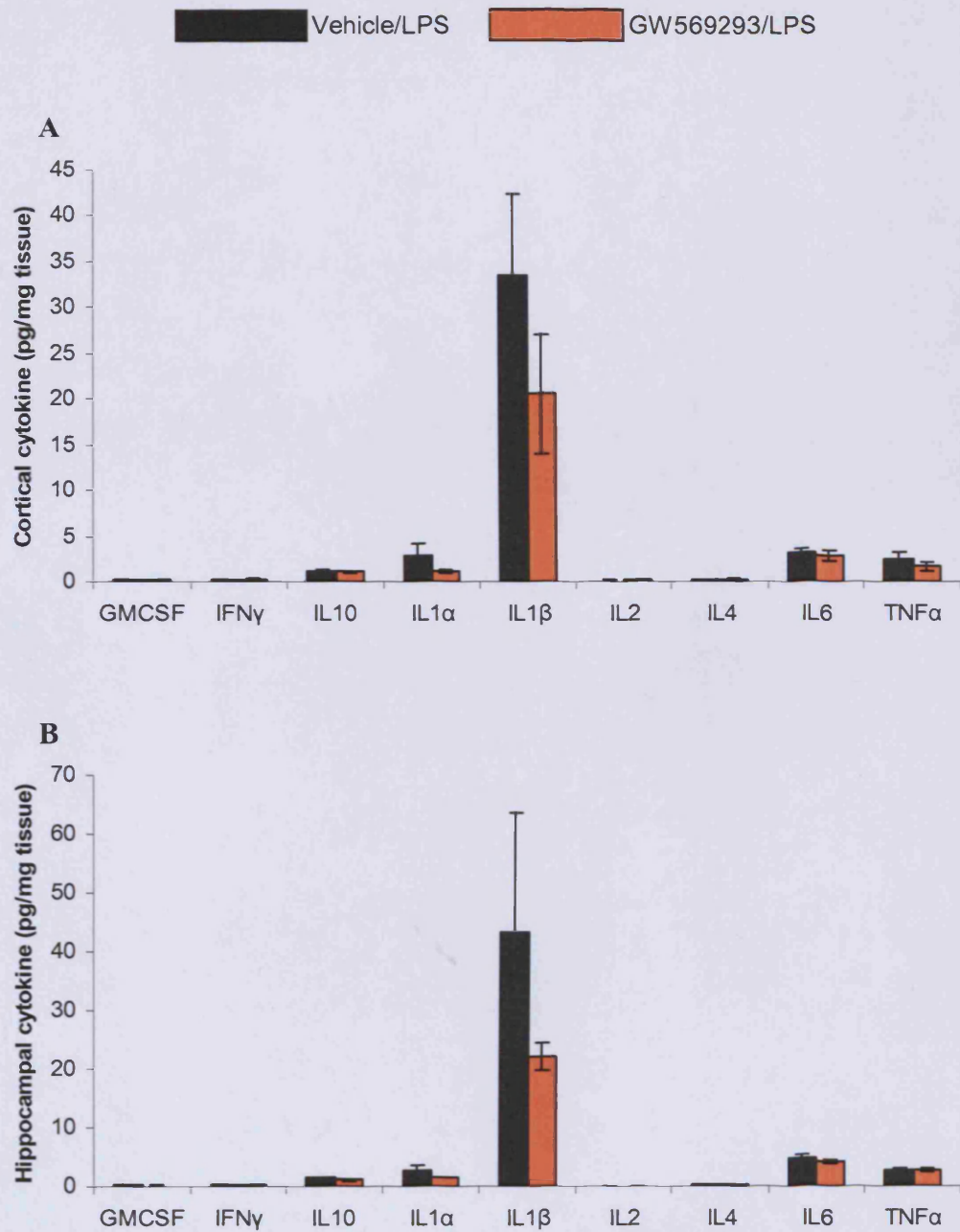


Figure 3.8: Effect of GW569293 pre-treatment on cytokine protein in cortex (A) and hippocampus (B) of adult rats (n = 6-8) by 2 hours post ICV LPS (5 $\mu$ g) administration, data represented as cytokine protein (pg) per milligram of tissue and shows mean  $\pm$  SEM (repeated measures ANOVA followed by planned comparisons)

### 3.4.3.2 Cytokine protein in plasma

A univariate ANOVA revealed an overall effect of treatment on plasma IL-10,  $F_{(3, 25)} = 3.36$ ,  $p < 0.05$ , IL-1 $\beta$ ,  $F_{(3, 25)} = 5.47$ ,  $p < 0.01$ , IL-6,  $F_{(3, 17)} = 6.93$ ,  $p < 0.01$  and TNF- $\alpha$ ,  $F_{(3, 19)} = 8.86$ ,  $p < 0.001$  (fig 3.9 & 3.10).

Post hoc comparisons revealed that ICV administered LPS increased plasma IL-1 $\beta$  ( $p = 0.08$ ) and TNF- $\alpha$  ( $p = 0.07$ ) from  $81.24 \pm 27.76$  to  $412.12 \pm 120.03$  pg/ml and from  $482.62 \pm 105.34$  to  $2513.32 \pm 1008.41$  pg/ml respectively. Fluparoxan treatment fully attenuated plasma IL-10 to  $95.28 \pm 40.60$  pg/ml ( $p < 0.01$ ) and attenuated plasma IL-1 $\beta$  by 85% to  $132.19 \pm 60.20$  pg/ml ( $p < 0.01$ ) (fig 3.9). Fluparoxan also significantly decreased plasma IL-6 relative to LPS treatment ( $p < 0.001$ ) although LPS did not significantly increase plasma IL-6 above vehicle levels ( $p = 0.10$ ). Plasma TNF- $\alpha$  was significantly attenuated by 93% to  $623.60 \pm 298.25$  pg/ml ( $p = 0.01$ ) (fig 3.9). GW569293 significantly increased plasma TNF- $\alpha$  by 371% to  $9343.88 \pm 2632.91$  pg/ml ( $p < 0.05$ ) (fig 3.10).

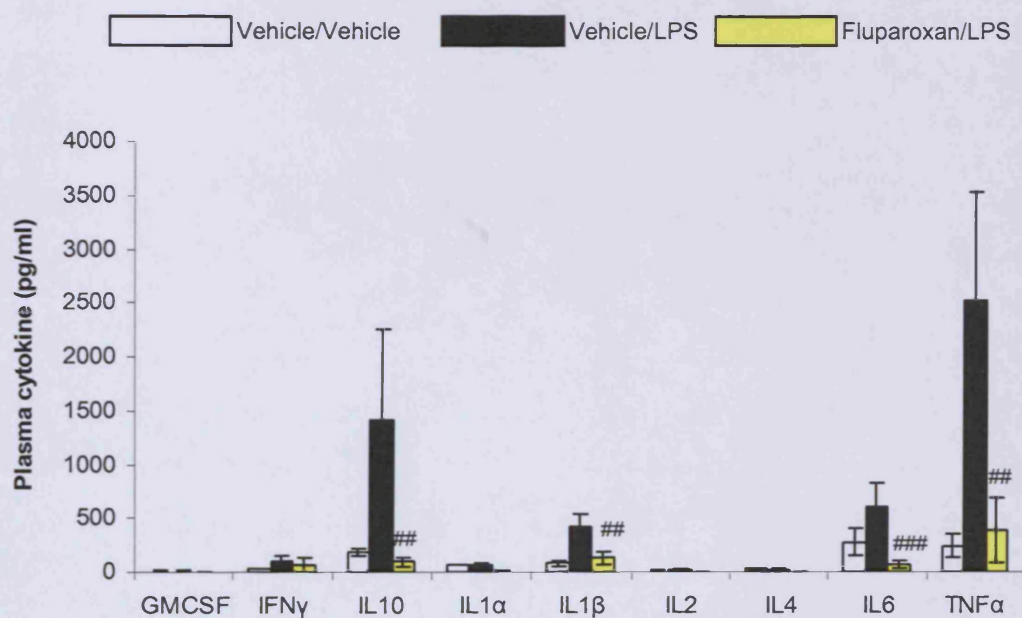


Figure 3.9: Effect of fluparoxan pre-treatment on cytokine protein in plasma of adult rats ( $n = 6-8$ ) by 2 hours post ICV LPS ( $5\mu\text{g}$ ) administration, data represented as cytokine protein (pg) per millilitre of sample and shows mean  $\pm$  SEM. ###  $p \leq 0.001$  #  $p \leq 0.01$  significantly different vs. LPS (univariate ANOVA followed by planned comparisons)

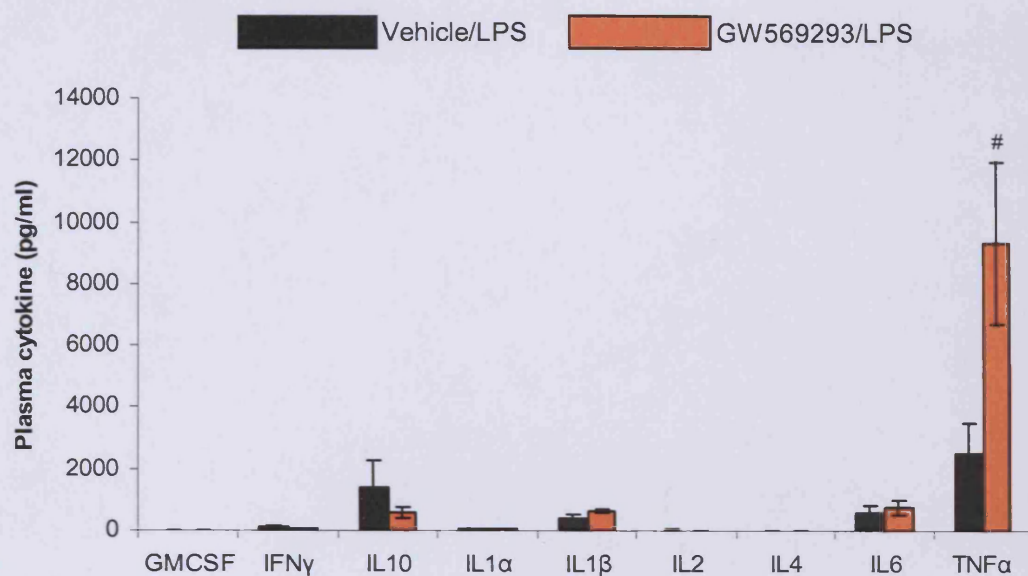


Figure 3.10: Effect of GW569293 pre-treatment on cytokine protein in plasma of adult rats (n = 6-8) by 2 hours post ICV LPS (5 $\mu$ g) administration, data represented as cytokine protein (pg) per millilitre of sample and shows mean  $\pm$  SEM. #  $p \leq 0.05$  significantly different vs. LPS (univariate ANOVA followed by planned comparisons)

### 3.5 Discussion

#### 3.5.1 Central vs. peripheral cytokine response

The activation of microglia in the endothelial wall of ventricles and hippocampal and thalamic areas causes a rapid increase in mRNA expression (Gayle et al, 1998; 1999; Plata-Salaman et al, 1998; De Simoni et al, 1998; Muramami et al, 1993) and protein (Zujovic et al, 2001) of pro-inflammatory cytokines, particularly TNF- $\alpha$ , in rat brain. Using the Luminex<sup>®</sup> system, modulation of ICV LPS-induced cytokine protein in plasma and brain tissue by dexamethasone and fluparoxan was assessed. An initial study using 20 $\mu$ g LPS, a dose previously used at GSK Harlow, to assess the anti-inflammatory activity of compounds, revealed that, in addition to a robust increase in central TNF- $\alpha$  protein there was a significant induction of cortical and hippocampal IL-1 $\alpha$  and IL-1 $\beta$  (fig 3.1). This demonstrates a similar effect of LPS in brain tissue to that described in chapter 2 in which IP LPS caused a significant induction in cortical IL-1 $\beta$  and TNF- $\alpha$  mRNA expression (fig 2.4) and a detectable increase in cortical and hippocampal IL-1 $\beta$  protein (fig 2.5). In general, the hippocampal response to

ICV administered LPS was greater than that evident in cortical tissue. This is likely due to the timecourse of events that occur following administration, since initial activation of microglia occurs within the ventricles and hippocampal regions (Nicholson & Renton, 2001). Central IL-1 $\alpha$ , IL-1 $\beta$  and TNF- $\alpha$  protein induction was also evident following 5 $\mu$ g ICV LPS but the magnitude of cytokine protein production was increased, particularly in the hippocampus, relative to 20 $\mu$ g LPS (fig 3.5). Interestingly, Zujovic et al, 2001 reported that following completion of a dose response curve of LPS, maximal TNF- $\alpha$  production was achieved using 10 $\mu$ g ICV LPS, however, in order to observe modulation of cytokine protein by anti-inflammatory agents, 5 $\mu$ g LPS was used to obtain a sub-maximal TNF- $\alpha$  response in brain tissue. This suggests LPS-mediated cytokine production is dose-dependent, achieving maximal levels at 10 $\mu$ g and decreasing in magnitude at higher doses of LPS (20 $\mu$ g).

The peripheral response to ICV administered LPS did not directly relate to the central profile. There was a massive increase in plasma TNF- $\alpha$  protein production in the absence of IL-1 $\alpha$  and a small associated increase in IL-1 $\beta$  protein (fig 3.4 & 3.6). LPS can be detected in the blood approximately five minutes after ICV LPS injection (Chen et al, 2000). Hence, plasma cytokine induction may possibly be caused by the direct interaction of LPS with immune cells circulating in the blood. However, it cannot be discounted that centrally derived cytokines may travel through the damaged (due to the surgically implanted cannulae) blood-brain barrier.

### **3.5.2 Central efficacy of peripherally administered anti-inflammatory agents**

#### **3.5.2.1 Glucocorticoid treatment - Dexamethasone**

Chapter 2 described the complete attenuation of IP LPS-induced central cytokine mRNA (fig 2.4) and protein (fig 2.5) expression by dexamethasone. Assessing the central efficacy of peripherally administered dexamethasone in the model was difficult as a reduction of cytokines in the blood by dexamethasone meant reduced communication to the brain of peripheral inflammation. Hence, reduced cytokine protein production in brain tissue following dexamethasone may be a knock-on effect of the agent on cytokine release in blood. The central efficacy of dexamethasone was assessed following injection of LPS into the ventricular system to initiate

inflammation in brain tissue. Dexamethasone significantly attenuated central TNF- $\alpha$ , hippocampal IL-1 $\alpha$  (61% reduction) and IL-1 $\beta$  (48% reduction) protein increased by a 20 $\mu$ g ICV LPS injection (fig 3.1). Interestingly, dexamethasone exhibited greater anti-inflammatory activity on cytokine protein induced by a 5 $\mu$ g ICV LPS injection. Dexamethasone significantly attenuated hippocampal (100%) and cortical IL-1 $\alpha$  (75%) and hippocampal IL-1 $\beta$  (69%), fully abrogated TNF- $\alpha$  protein and there was a non-significant trend to a decrease in cortical IL-1 $\beta$  (43%) protein following ICV administration of 5 $\mu$ g LPS (fig 3.5). Lower magnitude of cytokine production, particularly IL-1 $\beta$ , after ICV administration of 20 $\mu$ g LPS (hippocampus: 11.48; cortex: 21.49 pg/mg tissue) relative to 5 $\mu$ g LPS (hippocampus: 46.85; cortex: 33.30 pg/mg tissue) may be responsible for the decreased central efficacy of dexamethasone. Further research may elucidate the exact reasons why 20 $\mu$ g dose of LPS elicits a reduced central cytokine protein response relative to 5 $\mu$ g LPS. It is possible that a larger inflammatory stimulus initiates an enhanced endogenous glucocorticoid response in brain tissue relative to that caused by an ICV injection of 5 $\mu$ g LPS. Enhanced glucocorticoid levels in the brain may result in the attenuation of cytokine protein production. Subsequent studies to assess the anti-inflammatory behaviour of the  $\alpha$ 2-adrenoceptor antagonist, fluparoxan describe the administration of 5 $\mu$ g LPS since the anti-inflammatory activity of the strong immunosuppressant agent, dexamethasone was most effective at this dose of LPS.

#### 3.5.2.2 $\alpha$ 2 adrenoceptor antagonism - Fluparoxan

Antagonism of presynaptic  $\alpha$ 2-adrenoceptors can modulate the levels of various cytokines including TNF- $\alpha$ , IL-6 and IL-10 (Hasko et al, 1995; Szelenyi et al, 2000; Song et al, 2001). Assessment of the anti-inflammatory properties of fluparoxan (reported in section 2.4.5) revealed that fluparoxan abrogated the levels of IL-1 $\beta$  in brain tissue (fig 2.11) associated with attenuated levels of IFN- $\gamma$  and TNF- $\alpha$  in plasma and increased plasma IL-10 levels (fig 2.14) following IP injection of LPS. Peripheral administration of fluparoxan (3mg/mg) significantly attenuated the ICV LPS induced central production of the pro-inflammatory cytokines, TNF- $\alpha$ , IL-1 $\alpha$  and IL-1 $\beta$  (fig 3.7), abrogated plasma IL-6 and TNF- $\alpha$  and also attenuated ICV LPS induced plasma IL-10 by 75% (fig 3.9). ICV administered LPS activates endothelial

microglia (Nicholson & Renton, 2001) known to possess  $\alpha_2$ -adrenoceptors (Spengler et al, 1990). Antagonism of presynaptic  $\alpha_2$ -adrenoceptors, as discussed in chapter 2, results in an increase of synaptic NA. NA is known to modulate key aspects of the immune response, controlling the release of pro-inflammatory cytokines via subsequent activation of  $\beta$ -adrenoceptors (Szelenyi et al, 2001). In vitro analysis of the effects of  $\beta$ -adrenoceptor agonists on LPS-induced cytokine production has revealed that agonism of the  $\beta_2$ -adrenoceptor elicits an abrogation of pro-inflammatory cytokine release (Verhoeckx et al, 2005), possibly by preventing NF- $\kappa$ B translocation (Farmer & Pugin, 2000).

Fluparoxan pre-treatment caused an increase in plasma IL-10 (fig 2.14) in the IP LPS model, in contrast to an abrogation of plasma IL-10 (fig 3.9) in the ICV LPS model. In support of published literature, this may suggest a differential role for central and peripherally derived NA on cytokine release. Song et al, 1999 reported that depletion of NA in mouse brain attenuated ICV LPS induced plasma IL-6 in contrast to a significant potentiation of ICV LPS-induced plasma IL-6 following depletion of peripheral NA. It is possible that central and peripheral NA levels differ between the LPS models described in the current studies, resulting in a disparity between the IL-10 response to LPS injected via different administration routes. Overall, the data presented here and in chapter 2 of this thesis lends support to the role of NA in inflammation. Assessment of the anti-inflammatory activity of fluparoxan using both the IP and ICV LPS models has provided the first in vivo evidence that peripheral pre-treatment with the  $\alpha_2$ -adrenoceptor antagonist, fluparoxan, can modulate LPS induced neuroinflammation.

### 3.5.2.3 *P38 inhibition - GW569293*

The p38 inhibitor GW569293 attenuated plasma TNF- $\alpha$  following ICV LPS (20 $\mu$ g) (fig 3.4) but increased plasma TNF- $\alpha$  post ICV administration of 5 $\mu$ g LPS (fig 3.10). As discussed in section 2.5.3.3 of this thesis, the modulatory effects of p38 inhibition on cytokine production has been previously reported as dependent upon the stimuli, cell populations and levels of cytokines produced (Rao et al, 2002; Salmon et al, 2001; Kim et al, 2004). In vitro studies have demonstrated that inhibition of the p38 kinase can elevate TNF- $\alpha$  (T ten Hove et al, 2002; Kim et al, 2004). Interestingly, the current studies demonstrate p38 inhibition can significantly attenuate a large

increase in LPS-induced plasma TNF- $\alpha$  levels (approx 47,000 pg/ml) but augments lower levels of LPS-induced plasma TNF- $\alpha$  (approx 2500 pg/ml). It is possible that there are different cell populations involved in the production of plasma TNF- $\alpha$  at different doses of LPS but it is more likely that the modulation of cytokine protein production following p38 kinase inhibition depends upon the levels of cytokine protein produced during activation of the NF- $\kappa$ B pathway. Further research is merited to investigate the exact response of plasma TNF- $\alpha$  relative to increasing doses of ICV LPS following administration of a p38 inhibitor.

### **3.5.3 *The limitations of in vivo LPS-induced neuroinflammation models***

The use of LPS to elicit robust and reliable markers of neuroinflammation in vivo has been clearly demonstrated in chapters 2 and 3 of this thesis. Detection and quantification of inflammatory markers in plasma and brain tissue by Luminex<sup>®</sup> following IP LPS injection provides a model that can be used for the high throughput screening of putative anti-inflammatory agents. Novel agents that demonstrate clear anti-inflammatory properties using this model can be further screened for central efficacy using an ICV LPS model of neuroinflammation. It remains important, however, to understand the mechanism of action that results in increased cytokine protein release and iNOS activity in these models. Using Luminex<sup>®</sup>, the assessment of intracellular protein phosphorylation following IP LPS indicated the early cellular response (by 2 hours post LPS) is mediated by direct NF- $\kappa$ B activation. The later phase (6 hours post LPS) of LPS-mediated cell signalling appeared to involve p38 phosphorylation. Any target of interest must have a role in the acute innate immune response to LPS to accurately assess anti-inflammatory properties of agents in these models as, demonstrated in this thesis, dexamethasone and fluparoxan can significantly alter NF- $\kappa$ B mediated cytokine production whereas the p38 inhibitor, GW569293 has demonstrated inconsistent changes in plasma TNF- $\alpha$ . Despite the caveat that a reduction in peripheral inflammation by an anti-inflammatory agent will prevent communication of infection to the brain in the IP LPS model, the IP LPS model appears to be predictive of the subsequent effect of agents following ICV LPS.

Screening of novel anti-inflammatory agents for specific neurodegenerative diseases may additionally or alternatively require assessment in more disease relevant models.

Preclinical *in vivo* models specifically designed to assess compounds for AD may involve injection of A $\beta$  peptide into brain tissue to induce neuroinflammatory and neurodegenerative changes (Nabeshima et al, 1995). Subsequent chapters will describe studies intended to determine the successful delivery of A $\beta$  into the rodent brain and the subsequent induction of A $\beta$ -induced neuroinflammation and neurodegeneration *in vivo*.

## **CHAPTER 4**

### ***Injection of A $\beta$ 1-42 into the brain of the adult rat: neurodegeneration & neuroinflammation***

#### **4.1 Introduction**

Previous chapters have discussed the use of LPS to induce neuroinflammation in the rat brain. Using Luminex<sup>®</sup>, the rapid increase in cytokine protein in brain tissue and plasma was detected following either ICV or IP LPS injection. Proinflammatory cytokines have been detected in post-mortem AD brain tissue (Shaw et al, 2001). However, the AD brain is also characterised by activated microglia associated with amyloid plaques within degenerating brain regions such as the hippocampus (McGeer et al, 1988; Armstrong, 2006). Hence, the development of in vivo models with pathology related to AD is important, particularly the use of A $\beta$  fragments to induce neuroinflammation and neurodegeneration in rodent brain tissue. There are conflicting reports of the neuroinflammatory and neurotoxic effects following injection of A $\beta$  into rodent brain. Injection of A $\beta$  into the hippocampus resulted in increased neuroinflammation and cell loss in rats (Miguel-Hidalgo et al, 1998; Ryu et al, 2004); however, the absence of a convincing neurotoxic effect of A $\beta$  in vivo has also been described (Games et al, 1992; Cleary et al, 1995). Much of the reported inconsistency in A $\beta$ -induced neurotoxicity in rodent brain may be explained by variability in A $\beta$  fragments used, A $\beta$  aggregation state, vehicle and the apparatus used for A $\beta$  delivery. For example, many different types of apparatus have been used to administer A $\beta$  into the brain including the minipump (Craft et al, 2004), ICV tubing and injector (Nakagawa, 2004) or Hamilton syringe (Jantaratnotoi et al, 2003; Ryu et al, 2004).

##### **4.1.1 *Delivery of A $\beta$ into the rodent brain***

A $\beta$  can be delivered into the brain via a number of different routes. Direct injection into the ventricular system or a discrete brain region such as the hippocampus using a Hamilton syringe (A) can include a number of injections within one surgical procedure; however, this method usually involves a single administration at each

injection point. Administration of A $\beta$  via an indwelling cannula using Hamilton syringe and tubing (B) allows a controlled number of repeated single injections into ventricles or discrete brain regions. An implanted minipump (C) provides constant delivery of A $\beta$  and, currently is the most convenient method for chronic administration of A $\beta$  into rodent brain.

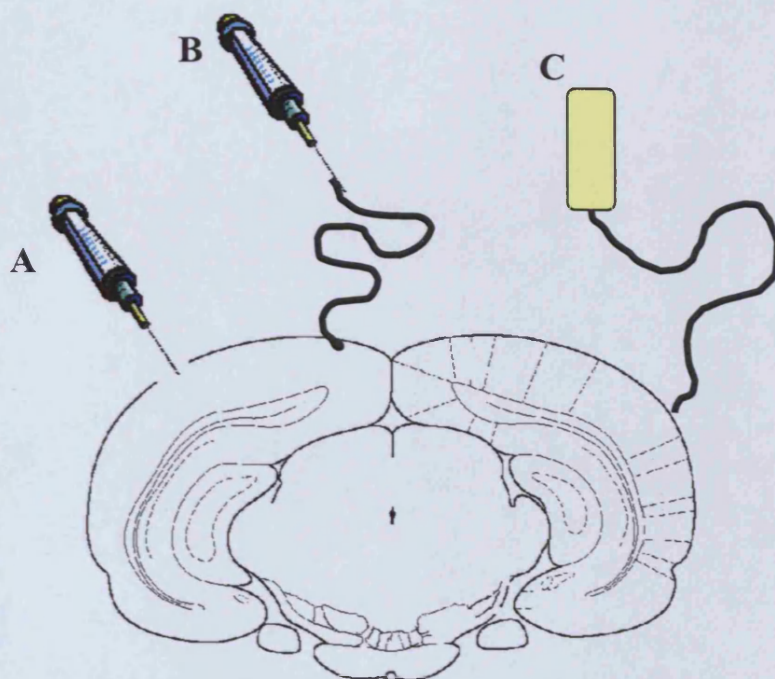


Figure 4.1: Schematic representation of the methods currently available for delivery of A $\beta$  into rodent brain: direct injection (A), repeated administration (B) and chronic infusion (C)

#### 4.1.2 *A $\beta$ aggregation process*

Extracellular A $\beta$  plaques in the AD brain consist of a dense core of insoluble fibrillar A $\beta$  protein mainly comprising the A $\beta$ 1-42 fragment (Rossor, 1993) and A $\beta$ 1-42 is considered the most neurotoxic A $\beta$  fragment in AD brain tissue (Tabaton et al, 1994). Fibrillar A $\beta$ 1-42 consists of parallel  $\beta$  strands that form  $\beta$  pleated sheets (Antzutkin et al, 2002). Under polarised light, A $\beta$ 1-42 stained with Congo red reveals a green birefringence signifying the presence of  $\beta$  pleated sheets. A $\beta$ 1-42 neurotoxicity has been related to both its fibrillar and oligomeric aggregated states (Pike et al, 1993; Tamagno et al, 2006). Soluble A $\beta$ 1-42 aggregates easily in solution; however, the rate of aggregation is dependent on peptide concentration, pH, duration of incubation and the length of the carboxyl terminus (Burdick et al, 1992).

Initially, A $\beta$  exists in a monomeric (random coil) form that can rapidly convert into a partial  $\beta$  structure called an A $\beta$  dimer (Soreghan et al, 1994). As the amount of dimer decreases, the concentration of higher molecular weight aggregates increases, evident as spherical particles with the characteristics of protein micelles (Soreghan et al, 1994). These A $\beta$  oligomers eventually co-aggregate to form strings of micelles named protofibrils (Hartley et al, 1999). These intermediaries undergo a conformational change resulting in the exposure of an initially protected C-terminus to the surrounding solvent and the formation of mature A $\beta$  fibrils (Garzon-Rodriguez et al, 2000).

#### **4.1.3 Western blot analysis of A $\beta$ 1-42 forms**

SDS-polyacrylamide gel electrophoresis enables the detection and assessment of the size of a single protein within a sample relative to a molecular weight marker. As the proteins move through the gel, they are separated by size and charge as small proteins migrate through the gel faster than larger molecules. The protein bands present on the gel can then be driven into a nitrocellulose membrane by using electrophoresis to push negatively charged proteins onto the positively charged membrane. Following incubation with primary and reporter-linked secondary antibodies, protein bands can be visualised by a variety of methods depending upon the type of reporter molecule. Fluorescent detection methods require the fluorescence of a probe when excited by light. The emission of the excitation is detected by a photosensor e.g. Odyssey Infrared Imaging System (LI-COR Biosciences, USA) which takes a digital image of the blot. This technique is a highly sensitive method since infra red detection eliminates variability and gives a high signal to noise ratio allowing accurate quantification. I will use SDS-polyacrylamide gel electrophoresis and the Odyssey Infrared Imaging System (LI-COR Biosciences, USA) to detect A $\beta$  protein forms expelled from apparatus used to inject A $\beta$  into rodent brain tissue.

#### **4.1.4 Chapter Aims**

The series of studies described in this chapter sought to:

1. Assess different A $\beta$ 1-42 delivery systems namely the minipump, Hamilton syringe or ICV tubing and metal cannulae.
2. Evaluate subsequent neurodegenerative and neuroinflammatory effects of

exogenous human A $\beta$ 1-42 protein into rat brain dissolved in PBS or acetonitrile solvent.

3. Establish A $\beta$ 1-42 specific neurotoxicity by comparing neuronal cell death and neuroinflammation following intra-hippocampal injection of A $\beta$ 1-42 and the reverse peptide A $\beta$ 42-1.

## **4.2 Materials & Methods**

### **4.2.1 Materials**

A $\beta$ 1-42 was obtained from California Peptide Research, USA. All gels, gel reagents and buffers used for western blot analysis were obtained from Novex/Invitrogen, UK and bovine serum albumin (BSA), Acetonitrile, Tween 20 and 1M Tris was purchased from Sigma, UK. Sterile saline was purchased from VWR International, UK. Sterile 0.1M PBS and 4% paraformaldehyde were prepared at GSK, Harlow, UK. Immunostaining machines, antibody diluent, PAP pens, peroxidase blocking solution and LSAB 1, LSAB 2 HRP-conjugate and diaminobenzidine substrate kits obtained from DakoCytomation, UK. Optimax buffer was obtained from A. Menarini, UK. Gills haematoxylin stain was purchased from HD Supplies, UK. The sources of additional materials are individually stated.

### **4.2.2 A $\beta$ 1-42 preparation**

Unless otherwise stated, A $\beta$ 1-42 was prepared as described by Ryu et al, 2004. Ryu et al, 2004 reported significant cell loss in rat brain tissue following intra-hippocampal injection of A $\beta$ 1-42.

1mg A $\beta$ 1-42 was reconstituted into 443.4 $\mu$ l of vehicle solution to provide 500 $\mu$ M solution. The solution was thoroughly vortexed for approximately ten minutes and then allowed to incubate at 37°C for 18 hours. Following incubation, the solution was aliquoted into sterile biopur<sup>®</sup> safe-lock eppendorfs (VWR International, UK) and stored at -20°C until immediately before use.

### **4.2.3 Gel analysis of amyloid samples**

Based on an established protocol for the detection of the A $\beta$  peptide using western blotting (GSK, UK):

A $\beta$ 1-42 solution was drawn up into a Hamilton syringe and expelled into eppendorfs containing PBS to produce 0.2 $\mu$ g/ $\mu$ l solution. 5 $\mu$ l was added to 5 $\mu$ l NuPage sample reducing agent 10X, 12.5 $\mu$ l NuPage LDS sample buffer 4X and 27.5 $\mu$ l PBS resulting in a 0.02 $\mu$ g/ $\mu$ l solution. 10 $\mu$ l sample was loaded onto a gel (NuPage 12% Bis-Tris gel – 1mm thick x 12well) secured in a Novex Mini gel system and transfer apparatus. 500 $\mu$ l NuPage Antioxidant was added to 200ml 1X SDS running buffer (50ml 20X NuPage MES running buffer and 950ml deionised water) and used to fill the upper buffer chamber. The lower buffer chamber was filled with 600ml 1X SDS running buffer. The gel was run at 120V for approximately 2 hours until the coomassie dye front had almost reached the bottom of the gel. The cassette was rinsed under running water and the gel removed. The gel, a nitrocellulose membrane and blotting pads were soaked in 700ml of 1X NuPage transfer buffer (50ml 20X NuPage transfer buffer, 100ml methanol, 850ml deionised water, 1ml NuPage antioxidant) and assembled in a Novex module. The module was locked into the lower buffer chamber and filled with transfer buffer. Following transfer at 30V for 1.5 hours, the membrane was shaken gently for 1 hour at room temperature or overnight at 4°C with blocking solution (3% BSA (4.5mg) in 150ml 1X western wash buffer (10x western wash buffer = 20ml 100% Tween 20, 400ml 5M NaCl and 200ml 1M TRIS pH 7.5 and diluted to 2 litres with deionised water). 6E10 anti A $\beta$  antibody at 1:1000 (Senetek via Signet Labs Inc, USA) was added to the membrane and left for 1 hour at room temperature prior to a wash with 1X wash buffer for a duration of 30 minutes, changing the buffer every 5 minutes. The membrane was wrapped in foil and incubated at room temperature with Goat anti-mouse IgG affinity purified IR dye 800 at 1:6000 (Rockland Immunochemicals Inc., USA). After 1 hour, the membrane was kept in the dark and washed with 1X wash buffer for a duration of 30 minutes, changing the buffer every 5 minutes and subsequently analysed using an Odyssey Infrared Imaging System (LI-COR Biosciences, USA).

#### **4.2.4 *Intra-hippocampal (IH) direct injection surgery***

Specific, pathogen free male CD rats (250g) (Charles River, UK) were anaesthetised by inhalation of 3% isoflurane in oxygen (Merial animal Health Ltd, Essex, UK). Rats were shaved around the crown of the head and the skin sterilised using a hibitane/alcohol solution. Lacrilube (Allergan, Buckinghamshire, UK) was applied to

the eyes to prevent them from drying out during surgery. Animals were secured in a stereotaxic frame (David Kopf Instruments, USA) and a midline incision along the sagittal suture made in the skin overlying the skull. 0.1ml intra-epicaine (Arnolds, Surrey, UK) was injected into the subdermal skin layers to provide post-operative local analgesia. A burr hole was drilled in the skull at co-ordinates relative to bregma: anterior-posterior: -3.6; medio-lateral: -1.8 and a 26 gauge 10 $\mu$ l Hamilton syringe (Hamilton, Birmingham, UK) stereotaxically lowered to a dorso-ventral coordinate of -3.8. Vehicle or A $\beta$ 1-42 was injected at a speed of 0.2 $\mu$ l min<sup>-1</sup> to a final volume of 2 $\mu$ l (1nmol) according to the protocol of Ryu et al, 2004. Following injection, the needle was withdrawn and the burr hole sealed with bone wax. The skin incision was sutured using vicryl Rapide 4/0 (Johnson & Johnson, USA) and the animal was placed back in the home cage with warm bedding and soft mash/baby food. The body weights and general health of the rats were monitored daily until pre-operative body weight had been reached. Rats were housed under controlled conditions at 21-24°C and on a 12-hour light/dark cycle (7am lights on) and fed a pellet diet and water *ad libitum* in an animal facility at GlaxoSmithKline Pharmaceuticals, Harlow, Essex, UK. All experimental procedures were conducted in accordance with the GlaxoSmithKline local ethics committee and conformed to the UK Animals (Scientific Procedures) Act 1986.

#### **4.2.5 Sample collection**

At 7 days post intra-hippocampal injection, rats were deeply anaesthetised with sodium pentobarbitone (Euthatal<sup>®</sup> 100mg kg<sup>-1</sup> i.p, Rhône Mérieux, Harlow, UK) prior to transcardial perfusion with 120ml ice-cold 0.9% sterile saline followed by 120ml of ice-cold 4% paraformaldehyde. The descending artery was clamped throughout this procedure to improve upper-body perfusion. Whole brain was removed and stored in 4% paraformaldehyde in a 20ml glass vial for 5 days.

#### **4.2.6 Immunohistochemistry**

A 3mm coronal block was cut from each brain to incorporate the injection site at approximately -2.0 through -5.0 relative to bregma and processed into paraffin wax using a Shandon Citadel 1000 tissue processor. Each block was embedded in paraffin wax using a Shandon Histocentre II embedding centre. Serial sections of 5 $\mu$ M

thickness were taken throughout the injection site using a Microm HM 355S rotary microtome and dried at room temperature for at least 24 hours before staining. 4 sections per stain were examined excluding NeuN staining for which between 4 and 8 sections that spanned the injection site were analysed. Sections were stained for general cell morphology (Haematoxylin & Eosin (H&E)), A $\beta$  (1E8), neurons (NeuN) and macrophage/microglia (ED1) immunohistochemistry. Sections were dewaxed in Histoclear (National Diagnostics, UK) and hydrated through 100% industrial methylated spirit (IMS), 70% IMS and deionised water. All sections were washed in deionised water and a hydrophobic barrier applied above and below the section using a PAP pen to prevent the antibody solutions from running off the slide. Slides were loaded into an autostainer and treated with a primary antibody as described in section 4.2.7.1. Sections were then treated with LSAB 1 biotinylated link for 10 minutes, LSAB 2 HRP-conjugate for 10 minutes and diaminobenzidine substrate kit for 10 minutes. Optimax buffer was applied to each section and between each step and deionised water applied after the diaminobenzidine step. After staining, sections were washed in running tap water for 5 minutes before counter staining in Gills haematoxylin for 3 seconds and placed in running tap water to "blue", dehydrated in graded followed by absolute IMS, cleared in Histoclear and mounted in DPX (VWR, UK). Sections were viewed using a Colourview digital camera attached to an Olympus BX41 microscope. Photomicrographs were captured and analysed using image analysis software (AnalySIS, Soft Imaging Systems). Sections stained for ED1 positive cells were viewed using a Leica DC100 camera attached to a Leitz DMRB microscope. Photomicrographs were captured and analysed using Leica Qwin software (Leica systems. Buckinghamshire, UK).

#### 4.2.6.1 *Primary antibody staining*

##### *Amyloid (1E8) staining*

Sections received DAKO peroxidase block for 5 minutes followed by primary mouse monoclonal antibody 1E8 (raised against 13-27 fragment of beta amyloid) (GSK, UK), diluted 1/1000 with antibody diluent, for 30 minutes.

##### *NeuN staining*

Sections were incubated for 30 minutes with NeuN antibody (Chemicon International, UK) diluted to 1/1000 with antibody diluent.

#### *Macrophage/Microglia (ED1) staining*

Sections were immersed in citrate antigen retrieval buffer (HD Supplies, Buckinghamshire, UK) and microwaved (Sanyo supershower wave (Sanyo, UK)) at 900W (2.5 minutes), 300W (5 minutes) and 300W (5 minutes) for each rack and allowed to cool for 20 minutes. Sections were washed 3 times in dH<sub>2</sub>O for 5 minutes and loaded onto an autostainer. The slides were treated with DAKO peroxidase block for 5 mins followed by mouse anti-rat CD68 (ED1) Ab (Serotec, UK) at a dilution of 1/1000 for 30 minutes.

#### *4.2.6.2 Quantification of immunohistochemical staining*

Photomicrographs of sections under an x4 objective were captured and used to calculate A $\beta$  deposit volume (4 sections), percentage number of ED1 positive stained cells, number of NeuN positive stained cells within a 700 $\mu$ metre distance either side of the central point of mediolateral damage and the width of hippocampal CA1 or dentate gyrus neuronal cell layer missing throughout the injection site. The protocol used for quantification of NeuN positive cells in the hippocampus was adapted from Ryu et al, (2004) and the protocol for measurement of medio-lateral lesion size was taken from Miguel-Hidalgo et al, (1998). The percentage of ED1 positive stained cells was quantified (4 sections) within a 225cm<sup>2</sup> (1.06x10<sup>6</sup> pixels) box placed so that the central point of mediolateral damage was in the centre of the box.

#### *4.2.6.3 Detection of fibrillar A $\beta$*

Sections were viewed under a x40 objective using a Leica DC500 camera attached to a Leica DMR microscope (Leica systems, Buckinghamshire, UK). Photomicrographs were captured under differential interference contrast and a polarised light source using Leica Qwin software (Leica systems, Buckinghamshire, UK).

#### *4.2.7 Data Analysis*

Univariate tests of significance using Statistica<sup>TM</sup> Version 6.1 (Statsoft, USA) calculated the effect of A $\beta$  treatment and solvent on the number of NeuN positive cells, extent of medio-lateral hippocampal damage and percentage ED1 stained area. Planned comparisons on the predicted means from the model assessed individual A $\beta$ 1-42 and A $\beta$ 42-1 effects on these measurements. Results are represented as

means  $\pm$  SEM and significance was set at  $P \leq 0.05$ .

### **4.3 Protocols**

#### **4.3.1 *Study 9: Western blot analysis of the expulsion of the A $\beta$ 1-42 fragment from apparatus***

Prior to the commencement of in vivo studies, Study 9 examined the A $\beta$ 1-42 forms that were expelled from apparatus commonly used for injecting A $\beta$  into rodent brain tissue. This study also sought to identify the apparatus that could consistently expel A $\beta$ 1-42 protein and therefore be used most successfully for in vivo studies.

##### **4.3.1.1 *Lowest concentration of aggregated A $\beta$ 1-42 used in vivo***

In order to establish if the A $\beta$ 1-42 fragment, particularly in its aggregated form, could be expelled from apparatus commonly used for administering substances directly into rodent brain, I initially assessed the lowest A $\beta$ 1-42 concentration previously reported as successfully administered into brain tissue (Hare et al, 1999). A $\beta$ 1-42 was aggregated by continually stirring a 100 $\mu$ M solution (0.45ug/ul) of soluble A $\beta$ 1-42 in PBS at 23°C for 40 hours. Following incubation, the A $\beta$ 1-42 solution was turbid and approximately 80% of the peptide was sedimented by centrifugation leaving approximately 20% as supernatant. The supernatant and pellet were frozen at -20°C until use. Supernatant and pellet were drawn up either polypropylene tubing attached to a metal injector or a 10 $\mu$ l Hamilton syringe.

##### **4.3.1.2 *Oligomeric A $\beta$ 1-42 using minipump***

Previously, the infusion of oligomeric A $\beta$ 1-42 via minipump has resulted in A $\beta$  deposition and neuroinflammation in rodent brain (Frautschy et al, 2001, Frautschy et al, 1996). As an alternative to the injection of aggregated A $\beta$ 1-42 via ICV tubing or Hamilton syringe, I investigated the expulsion of oligomeric forms of A $\beta$ 1-42 from a minipump using a protocol described by Frautschy et al, 2001.

1mg A $\beta$ 1-42 in 221.7 $\mu$ l hexa-fluoro-iso-propanol (HFIP) was left to dissolve for 1 hour at room temperature. The HFIP was allowed to evaporate from 45 $\mu$ g A $\beta$  aliquot transferred to sterile eppendorfs. Eppendorfs were transferred to a speedvac and

centrifuged for 10 minutes at 30°C, sealed with parafilm and stored at -20°C. Each 45µg aliquot was reconstituted in 1µl DMSO and 100µl 4mM HEPES buffer and sonicated for 3 minutes followed by incubation at 4°C for 24 hours. 100µl of a 500µg/ml high density lipoprotein (HDL) solution was added to the Aβ solution before the minipump and associated tubing was filled and incubated in a 37°C water bath for 14 days.

#### *4.3.1.3 Concentrations of Aβ1-42 used in vivo to induce neurotoxicity*

Aβ1-42 peptide (1nmol/2µl) was dissolved in 4.43µl 35% acetonitrile and 438.57µl sterile 0.1M PBS to produce a 500µM solution (2.25µg/µl (1 nmol)) and left to incubate overnight as described in section 4.2.2. Aβ solution (5µl) was loaded into a 10µl Hamilton syringe or a pipette (control sample) and expelled into PBS to produce a 0.2µg/µl solution. Aβ1-42 was also prepared by dissolving 1mg Aβ1-42 in 148µl deionised water (3nmol/2µl) following the protocol described by Miguel-Hidalgo et al, 1998. The solution was stored for 3 hours at room temperature, 4°C overnight and room temperature for three hours. Aliquots were incubated at 4°C further 21-hour incubation before loading into a 10µl Hamilton syringe or pipette.

As a comparison, Aβ1-42 (dissolved in 443µl sterile 0.1M PBS) was incubated at 37°C for four days allowing formation of higher molecular weight aggregates and oligomeric forms of Aβ.

#### *4.3.2 Study 10: Aβ1-42 in 0.35% acetonitrile/0.1M PBS*

A variety of solvents has been used to dissolve Aβ including acetonitrile and PBS (Winkler et al, 1994; Ryu et al, 2004). Acetonitrile is toxic in its own right and its use in vivo must be appropriately validated.

Aβ1-42 peptide was dissolved in 4.43µl 35% acetonitrile and 438.57µl sterile 0.1M PBS and left to incubate overnight as described in section 4.2.2. Male CD rats (250g, approx 10 weeks of age, n=8 per group) were unilaterally injected with 1nmol/2µl Aβ1-42 or sterile PBS alone.

#### *4.3.3 Study 11: Aβ1-42 in 0.035% acetonitrile/0.1M PBS or 0.1M PBS alone*

Aβ1-42 peptide was dissolved in 443µl 0.035% acetonitrile/0.1M PBS solution

(44.3µl 35% acetonitrile and 44.3ml sterile 0.1M PBS) and left to incubate overnight as described in section 4.2.2. Male CD rats (250g, approx 10 weeks of age, n=12 per group) were administered bilaterally with 1nmol/2µl Aβ1-42 in 0.035% acetonitrile and 1nmol/2µl Aβ1-42 in sterile PBS. The hemisphere injected with acetonitrile vehicle was randomised between animals and between surgeons so that n=6 animals received Aβ1-42 in 0.035% acetonitrile in the left hemisphere and n=6 animals received Aβ1-42 in 0.035% acetonitrile in the right hemisphere. The remaining hemisphere was injected with 1nmol/2µl Aβ1-42 in sterile PBS.

#### **4.3.4 Study 12: Aβ1-42 vs. Aβ42-1 in 0.1M PBS alone**

The reverse peptide Aβ42-1 was used as a non-fibrillar Aβ protein control as described by Ryu et al, 2004. Aβ1-42 and Aβ42-1 peptides were dissolved in sterile 0.1M PBS solution and left to incubate overnight as described in section 4.2.2. Male CD rats (n=12 per group) were unilaterally injected with 1nmol/2µl Aβ1-42 or 1nmol/2µl Aβ42-1 or sterile PBS alone.

## **4.4 Results**

### **4.4.1 Study 9: Western blot comparison of Aβ1-42 preparations for direct hippocampal injection**

#### **4.4.1.1 Aβ1-42 expulsion: polypropylene tubing and Hamilton syringe**

Western blot analysis of the Aβ forms expelled from a 10µl Hamilton syringe or plastic tubing attached to a metal injector revealed that Aβ1-42 is expelled from a Hamilton syringe as aggregates (52kDa and above) and as oligomeric (11kDa) and monomeric (3kDa) forms (fig 4.2). In contrast, use of polypropylene tubing and injector only allowed the expulsion of monomeric and oligomeric forms under both pellet and supernatant conditions. The amount of these forms expelled from plastic tubing was also greatly reduced relative to that expelled by the Hamilton syringe.

#### **4.4.1.2 Oligomeric Aβ1-42 using minipump**

Western blot analysis revealed dense bands of oligomeric Aβ (≥11kDa) in the oligomeric control relative to a monomeric control indicating the preparation

protocol successfully produced oligomeric A $\beta$  (fig 4.3). In the absence of the cannula injector positioned on the end of the tubing, diffuse bands of monomeric and oligomeric A $\beta$  were evident, however, in the presence of the cannula injector, no bands of A $\beta$  were apparent. Removing a sample of A $\beta$  solution from the incubating minipump at 14 days indicated a large presence of oligomeric forms although much of the A $\beta$  solution had also aggregated ( $\geq 52$ kDa).

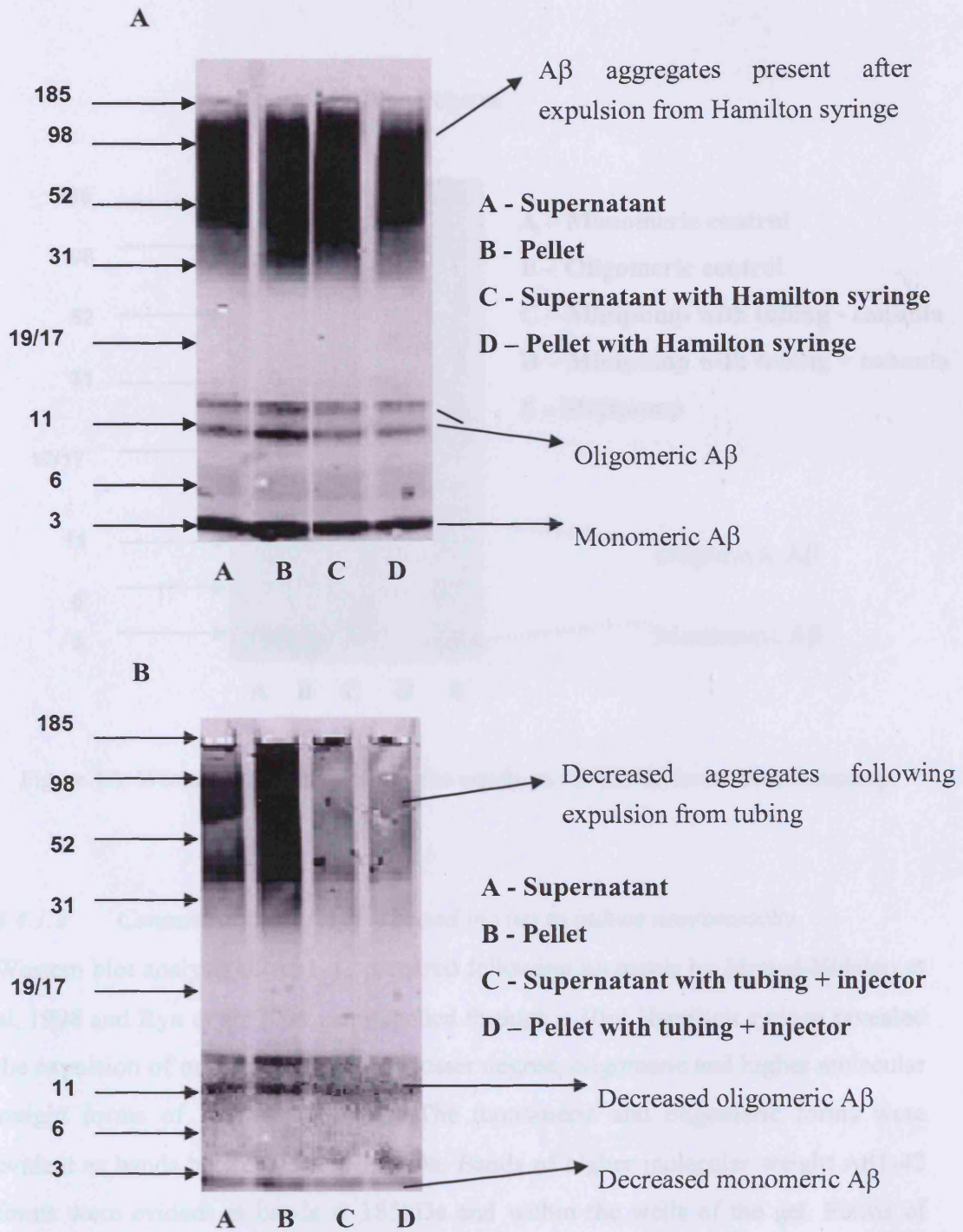


Figure 4.2: Western blots demonstrating the expulsion of Aβ<sub>1-42</sub> forms from Hamilton syringe (A) and polypropylene tubing (B).

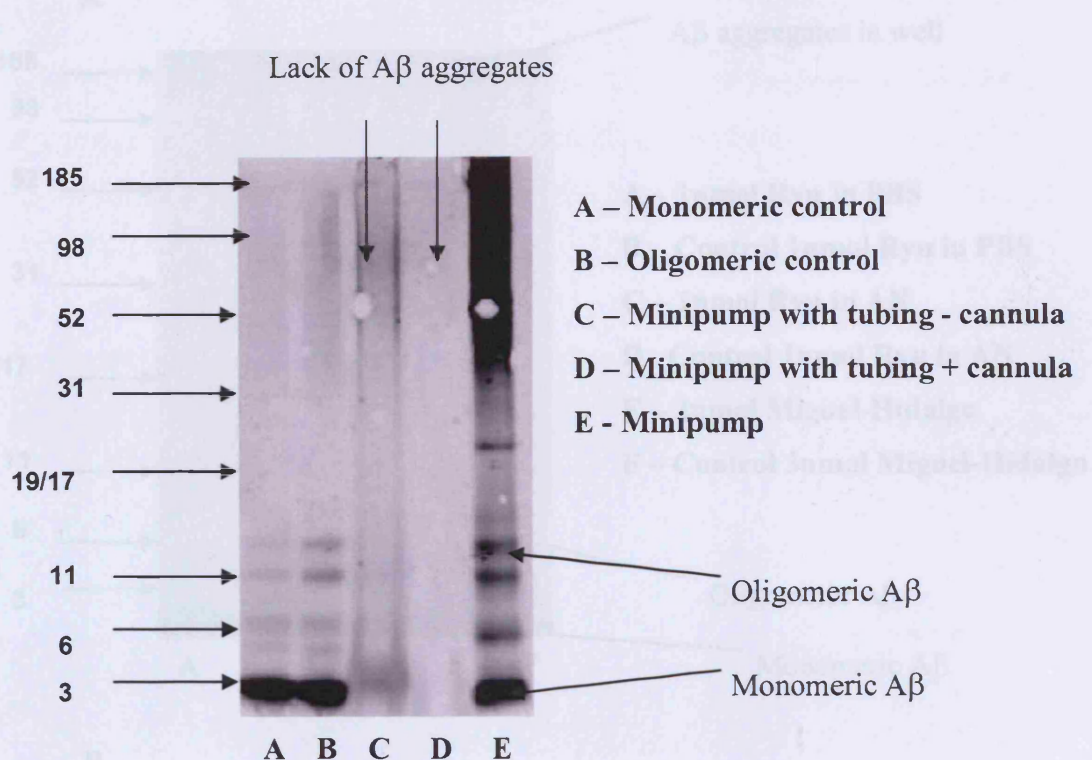


Figure 4.3: Western blot demonstrating the expulsion of A $\beta$ 1-42 forms from minipump.

#### 4.4.1.3 Concentrations of A $\beta$ 1-42 used in vivo to induce neurotoxicity

Western blot analysis of A $\beta$ 1-42 prepared following protocols by Miguel-Hidalgo et al, 1998 and Ryu et al, 2004 and expelled through a 10 $\mu$ l Hamilton syringe revealed the expulsion of monomeric and, to a lesser degree, oligomeric and higher molecular weight forms of A $\beta$ 1-42 (fig 4.4). The monomeric and oligomeric forms were evident as bands between 3 and 19 kDa. Bands of higher molecular weight A $\beta$ 1-42 forms were evident as bands at 185kDa and within the wells of the gel. Forms of A $\beta$ 1-42 expelled from a 10 $\mu$ l Hamilton syringe were not different from control samples obtained via pipette, suggesting the Hamilton syringe did not limit the expulsion of A $\beta$  forms into brain tissue. Monomeric forms of a preaggregated A $\beta$ 1-42 solution were expelled from a 10 $\mu$ l Hamilton syringe, however, oligomeric and higher molecular weight aggregates were less evident with diffuse bands of aggregated A $\beta$  evident in the wells of the gel.

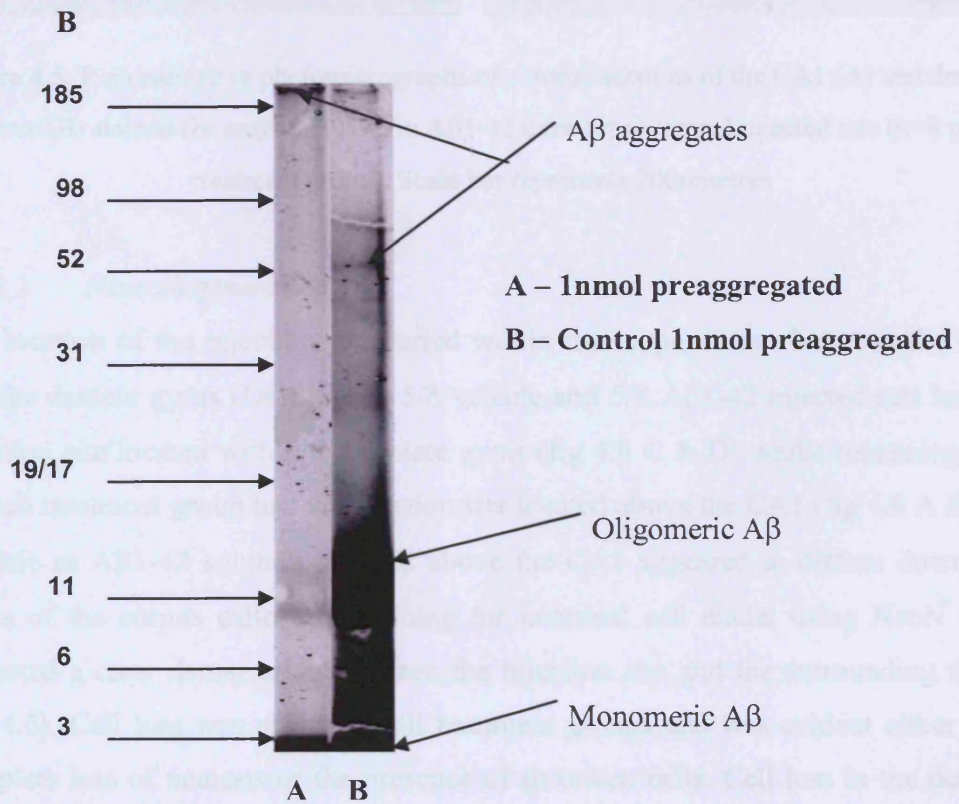
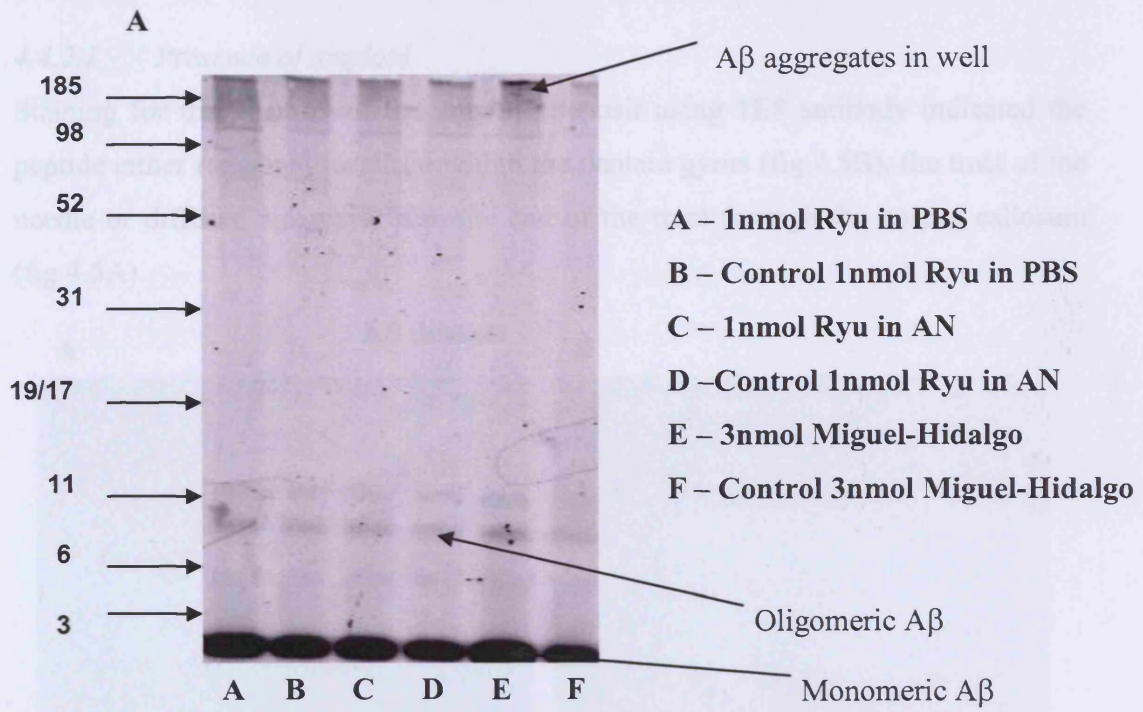


Figure 4.4: Western blots demonstrating the expulsion of Aβ<sub>1-42</sub> forms from 10μl Hamilton syringe using protocols described in the literature (A) or standard preaggregated Aβ<sub>1-42</sub> (B).

#### 4.4.2 Study 10: IH A $\beta$ 1-42 (1nmol) in 0.35% acetonitrile/0.1M PBS

##### 4.4.2.1 Presence of amyloid

Staining for the position of the amyloid deposit using 1E8 antibody indicated the peptide either remained localised within the dentate gyrus (fig 4.5B), the tract of the needle or diffused sideways from the end of the tract through the corpus callosum (fig 4.5A).

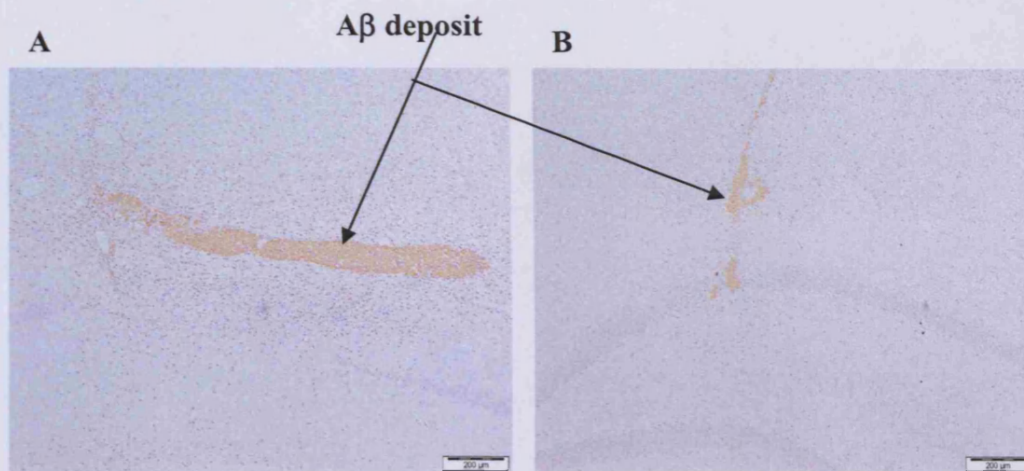


Figure 4.5: Representative photomicrographs of coronal sections of the CA1 (A) and dentate gyrus (B) stained for amyloid (1E8) in A $\beta$ 1-42 intra-hippocampal injected rats (n=8 per treatment group). Scale bar represents 200 $\mu$ metres

##### 4.4.2.2 Neurodegeneration

The location of the injection site varied within the hippocampus between the CA1 and the dentate gyrus (DG) layers. 5/8 vehicle and 5/8 A $\beta$ 1-42 injected rats had an injection site located within the dentate gyrus (fig 4.6 C & D) whilst remaining rats in each treatment group had an injection site located above the CA1 (fig 4.6 A & B). Vehicle or A $\beta$ 1-42 solution injected above the CA1 appeared to diffuse down the fibres of the corpus callosum. Staining for neuronal cell nuclei using NeuN stain indicated a clear demarcation between the injection site and the surrounding tissue (fig 4.6). Cell loss was present in all treatment groups and was evident either as a complete loss of neurons or the presence of shrunken cells. Cell loss in the dentate gyrus (DG) occurred adjacent to the amyloid deposit whilst localisation of the deposit along the corpus callosum significantly affected the CA1 granule layer. There was no significant effect of A $\beta$ 1-42 relative to vehicle treatment on numbers

of NeuN positive cells within 700µmetres of the lesion centre (fig 4.7) or on the extent of mediolateral damage (fig 4.8), regardless of injection site location. Differentiating between sub regions of the hippocampus revealed no significant effect of Aβ1-42 treatment relative to vehicle control on NeuN count in dentate gyrus (DG) or CA1 of the hippocampus (DG: vehicle –  $380.83 \pm 90.11$  cells, Aβ1-42 –  $367 \pm 141.38$  cells; CA1: vehicle –  $141.13 \pm 23.77$  cells, Aβ1-42 –  $114.57 \pm 26.71$  cells). Similarly, there was no treatment effect on the extent of mediolateral damage in DG or CA1 (DG: vehicle –  $1170.26 \pm 183.70$  cells, Aβ1-42 –  $956.05 \pm 372.23$  cells; CA1: vehicle –  $100 \pm 0.00$  cells, Aβ1-42 –  $173.50 \pm 89.41$  cells).

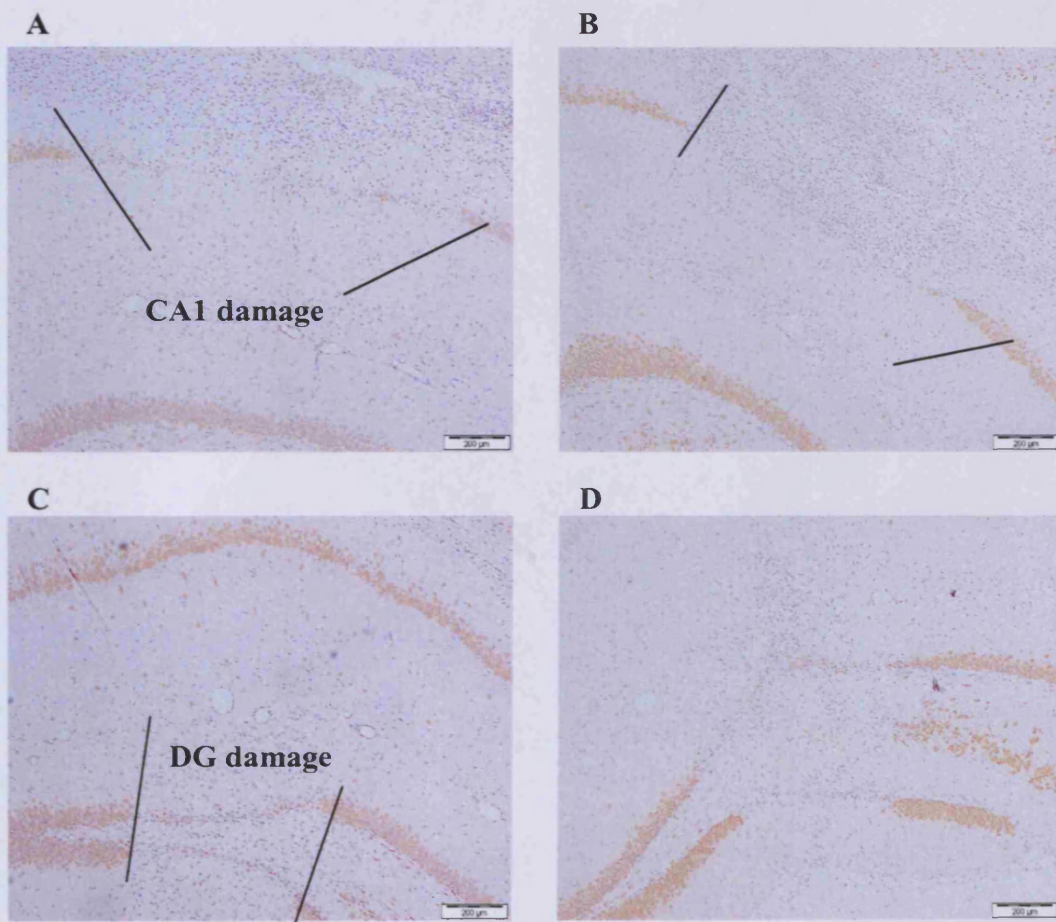


Figure 4.6: Representative photomicrographs of coronal sections of the hippocampus stained with NeuN in vehicle (A, C) and Aβ1-42 (B, D) intra-hippocampal injected rats (n=8 per treatment group). Scale bar represents 200µmetres

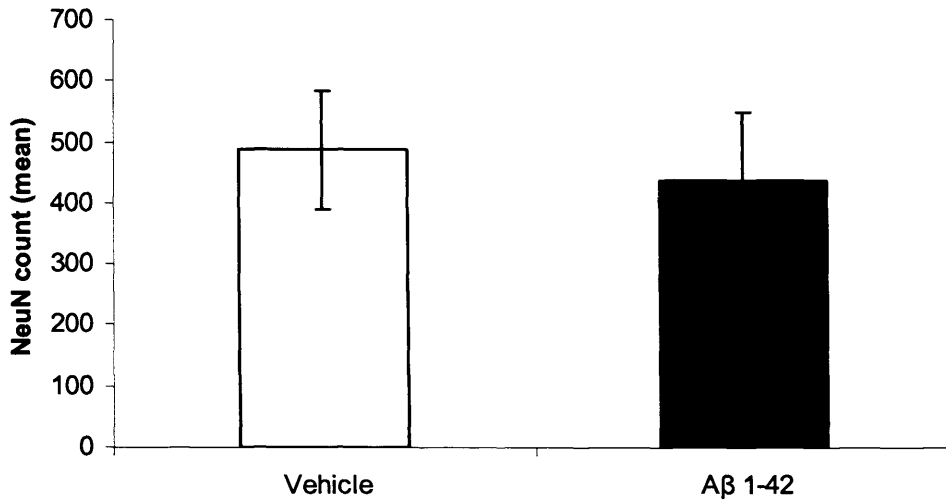


Figure 4.7: Quantification of NeuN positive cells in hippocampus of vehicle and Aβ1-42 intra-hippocampal injected rats (n=8 per treatment group), data represented as the count of NeuN positive stained cells and shows mean ± SEM (planned comparisons following ANOVA)

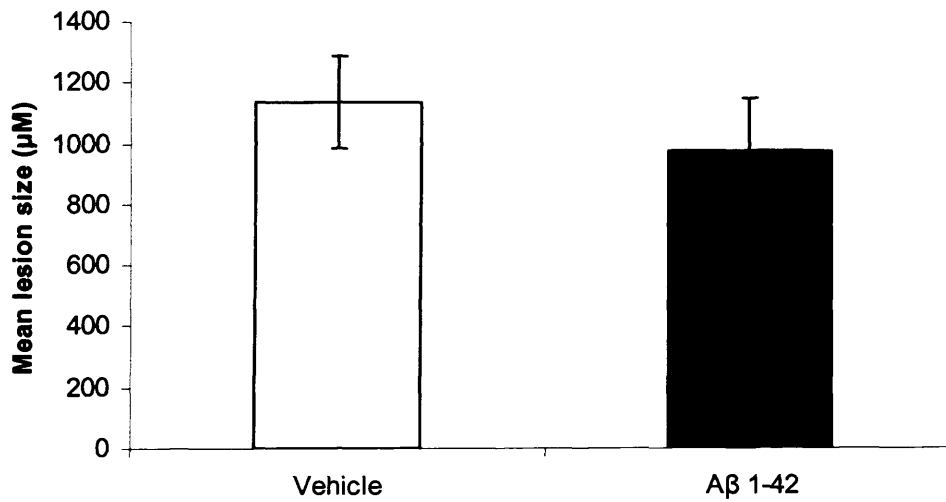


Figure 4.8: Measurement of mediolateral lesion in vehicle and Aβ1-42 intra-hippocampal injected rats (n=8 per treatment group), data represented as the mediolateral lesion size in μM and shows mean ± SEM (univariate ANOVA followed by planned comparisons)

#### 4.4.2.3 Neuroinflammation

Staining for activated macrophage (and microglia) at the injection site was localised around the vehicle and A $\beta$ 1-42 deposit and, to a much lesser extent, within the injection tract (fig 4.9). The inflammatory cells surrounding the deposit were a mix of large amoeboid macrophage cells and activated microglia.

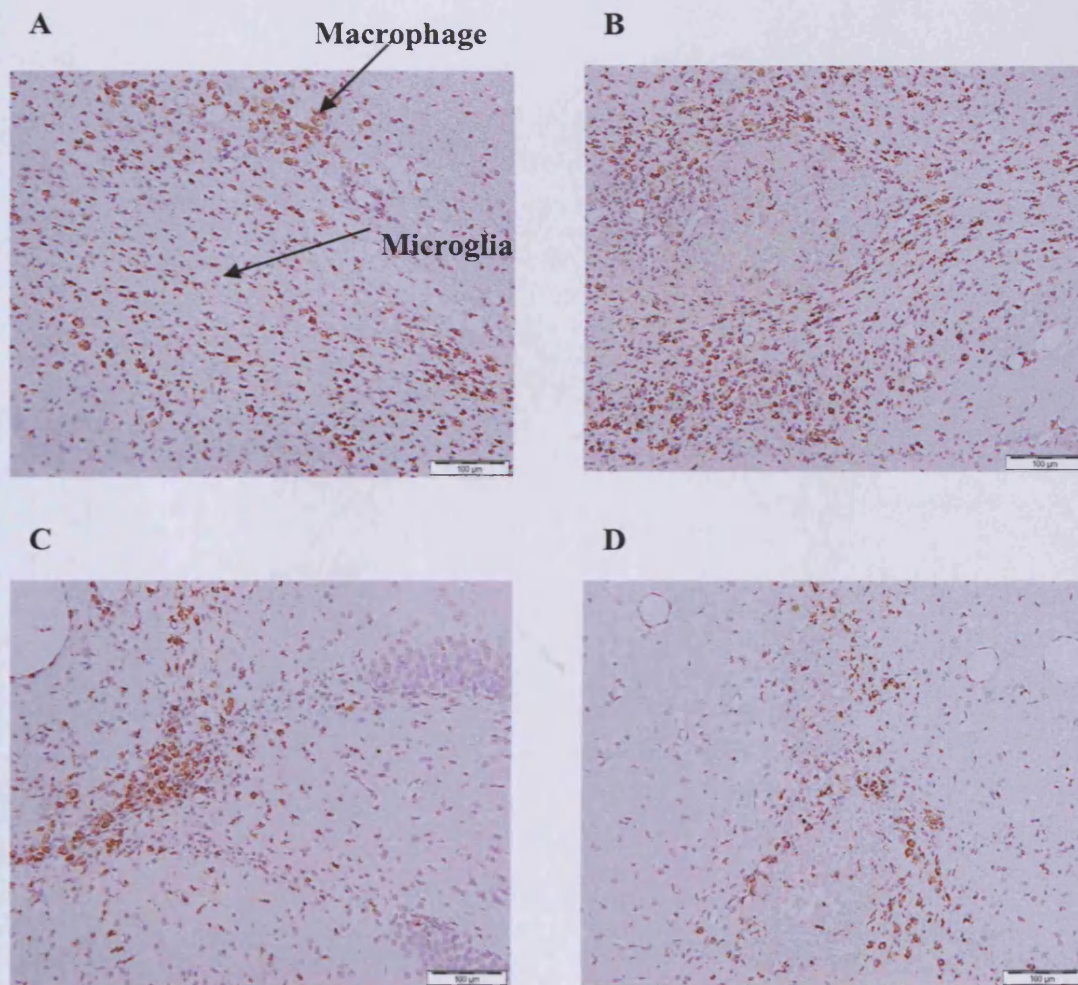


Figure 4.9: Representative photomicrographs of coronal sections of the hippocampus stained for ED1 positive macrophage and microglia in vehicle (A, C) and A $\beta$ 1-42 (B, D) intra-hippocampal injected rats (n=8 per treatment group). Scale bar represents 100µmetres

**4.4.3 Study 11: IH A $\beta$ 1-42 (1nmol) in 0.035% acetonitrile/0.1M PBS or 0.1M PBS alone**

**4.4.3.1 Presence of A $\beta$**

A $\beta$ 1-42 deposits were located within the corpus callosum across the top of the CA1 granular layer, through the dentate gyrus or within the needle tract (fig 4.10). There was no significant difference in deposit volume within the tissue between PBS and acetonitrile based vehicles (fig 4.11). This suggests the maximum amount of A $\beta$  was expelled from the syringe needle or that acetonitrile, at this concentration, does not aid amyloid expulsion.

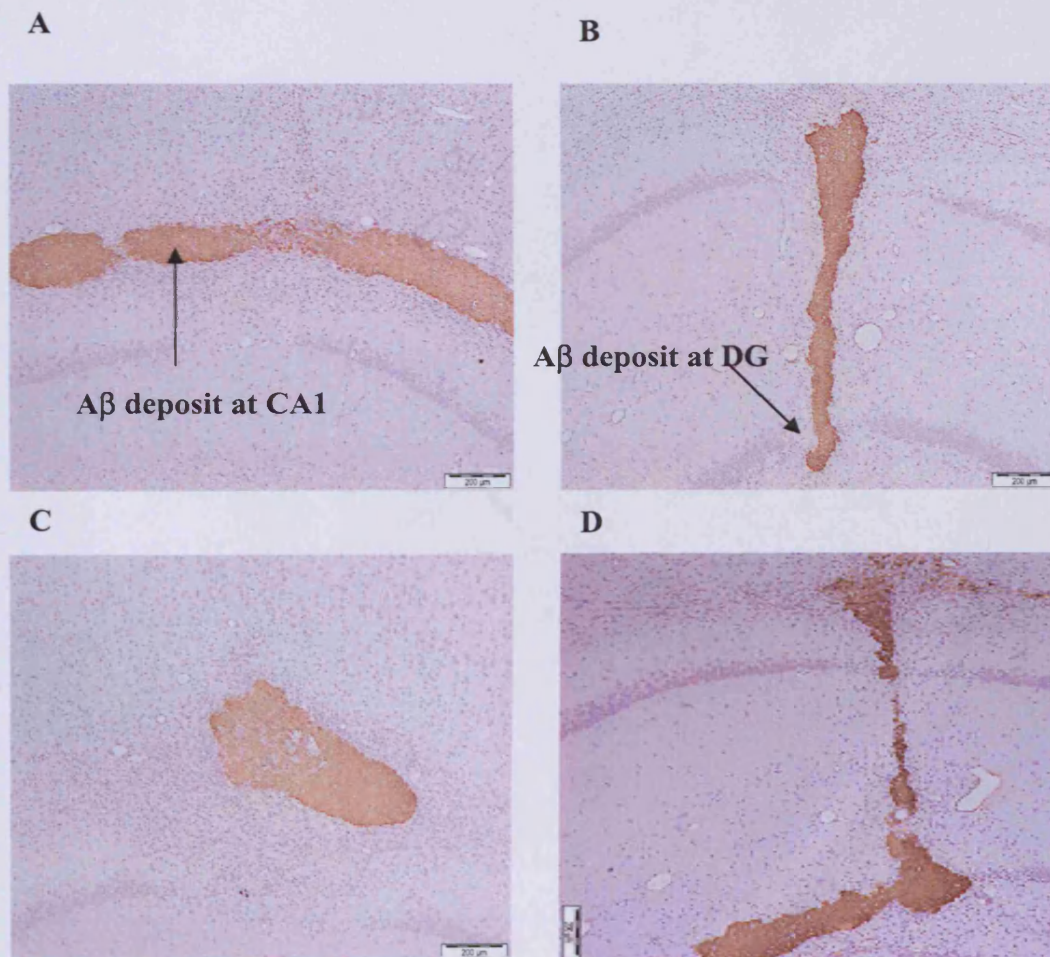


Figure 4.10: Representative photomicrographs of coronal sections of the hippocampus stained for A $\beta$  in 0.1M PBS alone (A, B) or 0.035% acetonitrile (C, D) in bilateral intra-hippocampally injected rats (n=12 per vehicle or A $\beta$  treatment group). Scale bar represents 200 $\mu$ metres

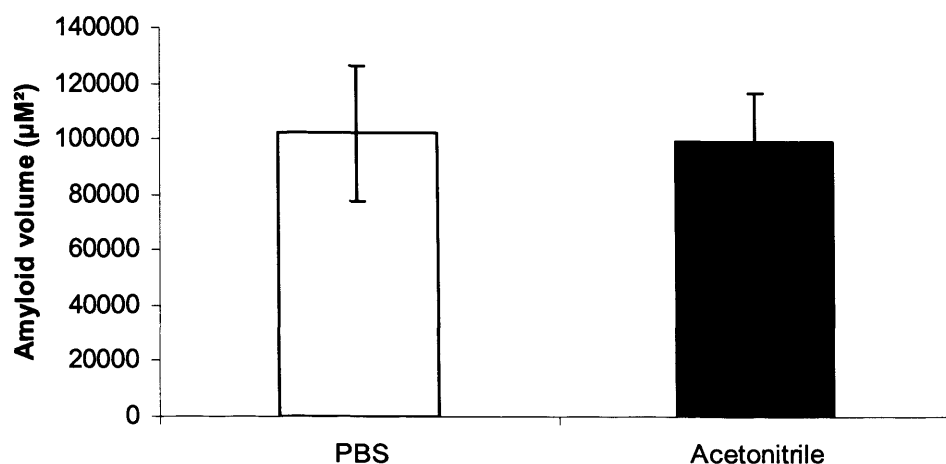


Figure 4.11: Measurement of the average amyloid deposit in the hippocampus of A $\beta$ 1-42 bilateral intra-hippocampally injected rats (n=12 per vehicle or A $\beta$  treatment group), data represented as the volume of A $\beta$  deposit ( $\mu\text{M}^2$ ) and shows mean  $\pm$  SEM (univariate ANOVA followed by planned comparisons)

#### 4.4.3.2 Neurodegeneration

There remained variation in the dorso-ventral location of the injection site as reported previously in study 9; however, there were a greater number of animals in both vehicle and A $\beta$ 1-42 treatment groups that had a deposit located above the CA1 granular layer (fig 4.12). The clear demarcation between healthy surrounding CA1 or dentate gyrus neurons and the neuronal loss within the injection site allowed quantification of healthy cells remaining within 700 $\mu\text{m}$  either side of the centre of the injection site and the lateromedial measurement of cell loss.

Repeated measures ANOVA revealed there was no overall effect of treatment,  $F_{(1, 30)} = 2.47$ ,  $p=0.13$ , a significant effect of solvent,  $F_{(1, 30)} = 4.41$ ,  $p<0.05$  and a non-significant trend for an overall interaction between treatment and solvent,  $F_{(1, 30)} = 3.05$ ,  $p=0.09$ . Post hoc comparisons revealed a significant reduction in NeuN positive cells within the injection site, demonstrated as a 25% loss in cells with A $\beta$ 1-42 treatment in PBS only ( $p<0.05$ ). Acetonitrile at 0.035%, masked A $\beta$ 1-42 induced cell loss since a similar number of NeuN positive cells remained following acetonitrile, A $\beta$ 1-42 in acetonitrile or A $\beta$ 1-42 in PBS (fig 4.13). Acetonitrile vehicle resulted in significantly fewer remaining NeuN positive cells than PBS vehicle ( $p=0.01$ ) demonstrating a toxic effect of acetonitrile in vivo.

There was no overall treatment effect on the extent of mediolateral damage,  $F_{(1, 32)} = 0.57$ ,  $p = 0.46$ . There was a non-significant trend for an overall interaction between treatment and solvent,  $F_{(1, 32)} = 3.27$ ,  $p = 0.08$ . Post hoc planned comparisons revealed that A $\beta$ 1-42 in PBS caused an increase in the extent of mediolateral damage demonstrated as a 69% increase above PBS treatment alone ( $p < 0.05$ ). Utilisation of an acetonitrile vehicle masked this effect as evident by the increase in lesion size with acetonitrile alone relative to PBS treatment ( $p < 0.05$ ) (fig 4.14).

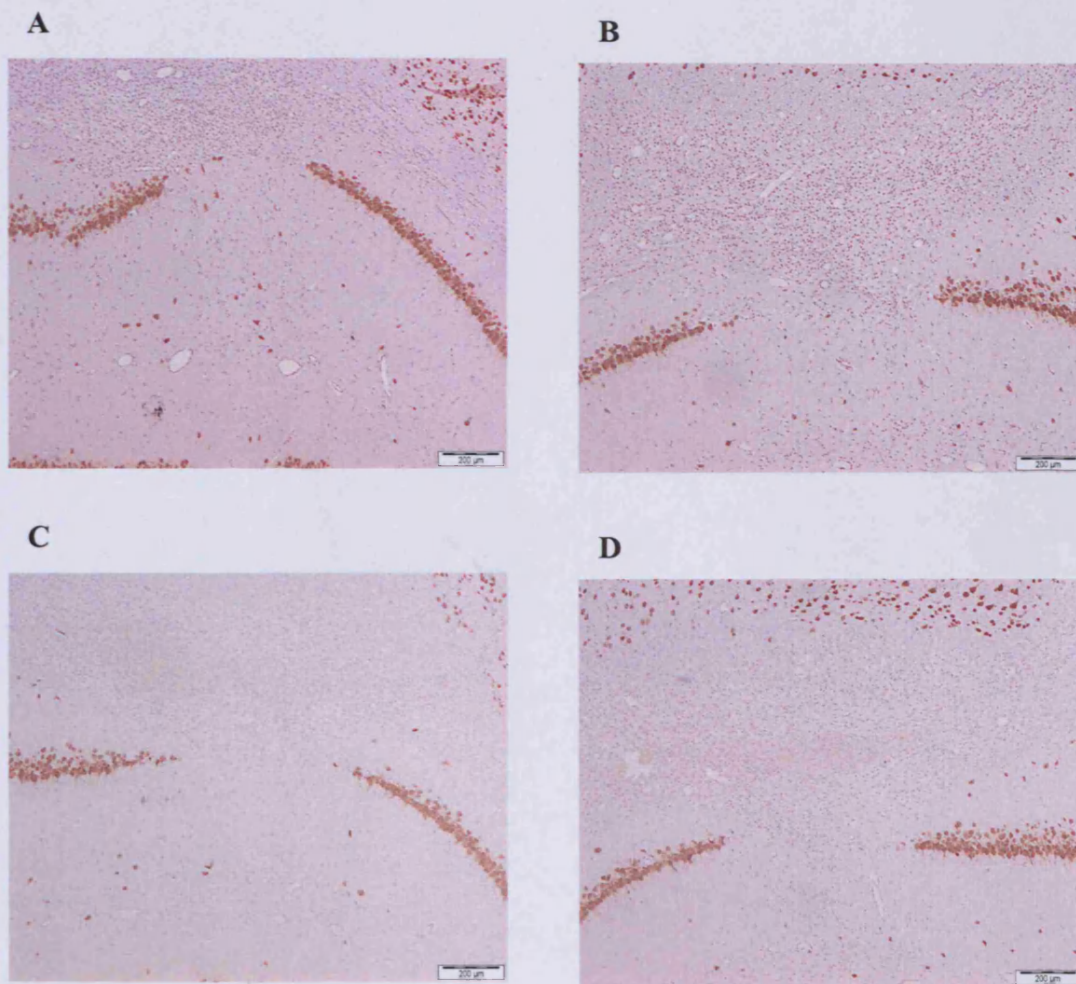


Figure 4.12: Representative photomicrographs of coronal sections of the hippocampus stained for NeuN in vehicle - PBS (A), vehicle - acetonitrile/PBS (B), A $\beta$ 1-42 - PBS (C) and A $\beta$ 1-42 - acetonitrile/PBS (D) in bilateral intra-hippocampally injected rats (n=12 per vehicle or A $\beta$  treatment group). Scale bars represent 200 $\mu$ metres

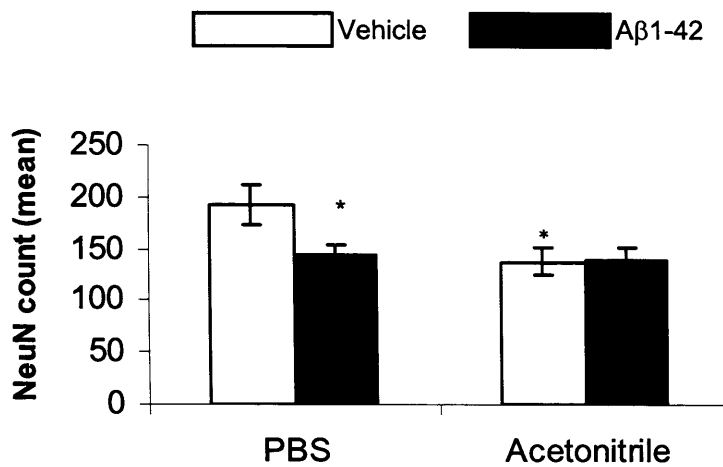


Figure 4.13: Quantification of NeuN positive cells in vehicle and Aβ1-42 bilateral intra-hippocampally injected rats (n=12 per vehicle or Aβ treatment group), data represented as the count of NeuN positive stained cells and shows mean ± SEM. \* p ≤0.05 significantly different vs. PBS vehicle (repeated measures ANOVA followed by planned comparisons)

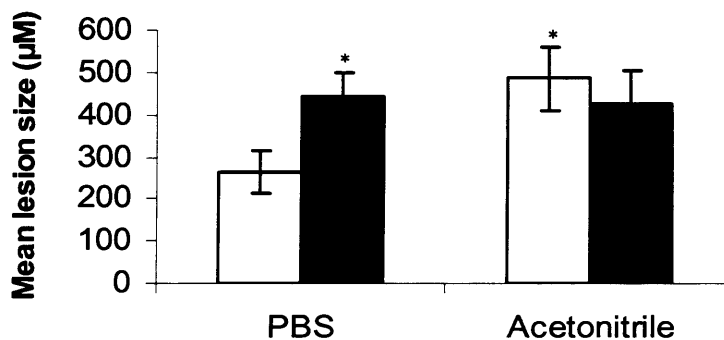


Figure 4.14: Measurement of mediolateral lesion in vehicle and Aβ1-42 intra-hippocampal injected rats (n=12 per vehicle or Aβ treatment group), data represented as the mediolateral lesion size (μM) and shows mean ± SEM. \* p ≤0.05 significantly different vs. PBS vehicle (repeated measures ANOVA followed by planned comparisons)

#### 4.4.3.3 Neuroinflammation

There was an overall treatment effect,  $F_{(3,33)} = 12.73$ ,  $p < 0.001$  on ED1 positive cells present within the injection site (fig 4.15). Post hoc planned comparisons revealed Aβ1-42 induced a significant 88% ( $p=0.01$ ) increase when dissolved in PBS alone and a significant 64% ( $p < 0.05$ ) increase in ED1 positive cells when using a vehicle

containing 0.035% acetonitrile (fig 4.16).

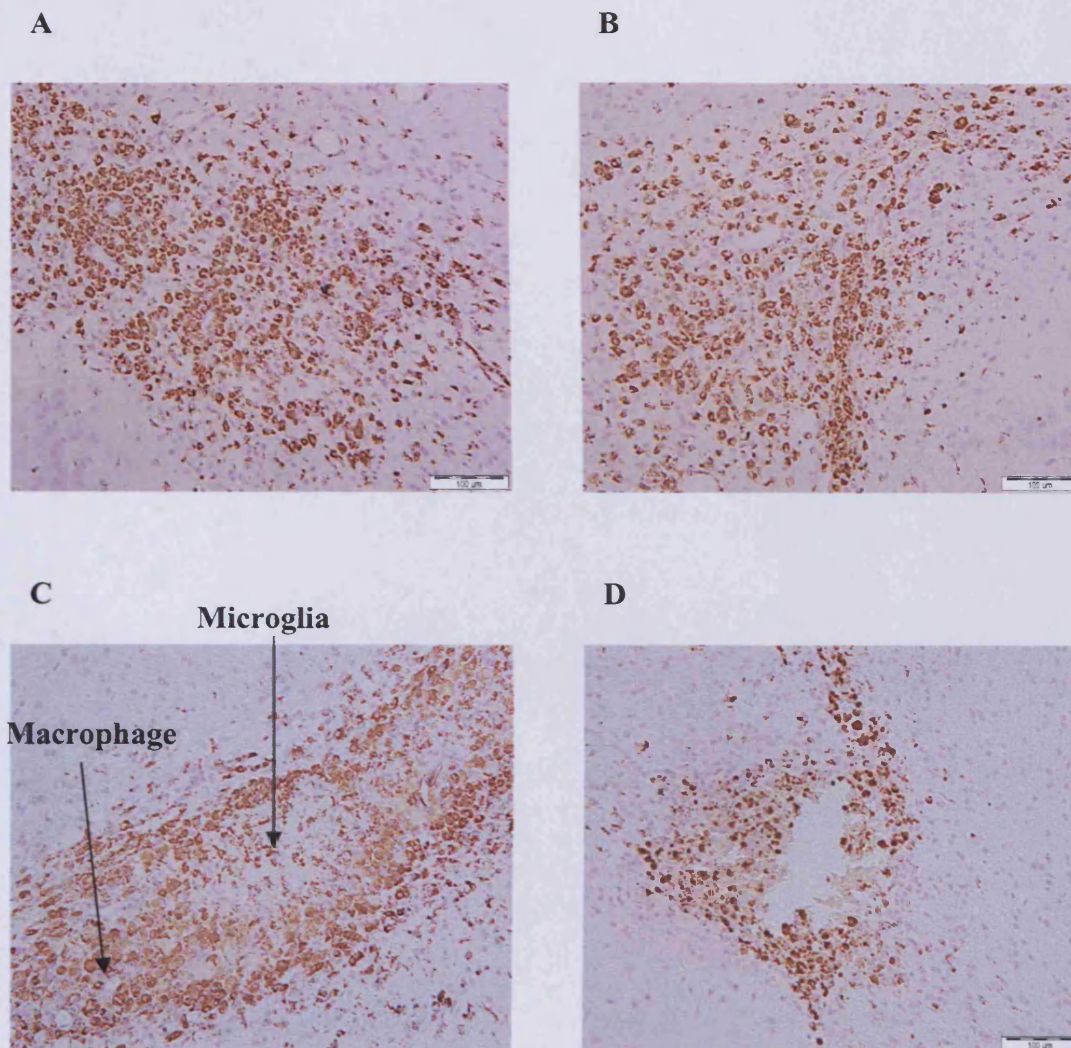


Figure 4.15: Representative photomicrographs of ED1 staining in hippocampus of vehicle - PBS (A) vehicle - acetonitrile/PBS (B), A $\beta$ 1-42 - PBS (C) & A $\beta$ 1-42 - acetonitrile/PBS (D) bilateral intra-hippocampally injected rats (n=12 per vehicle or amyloid treatment group), scale bar represents 100 $\mu$ metres

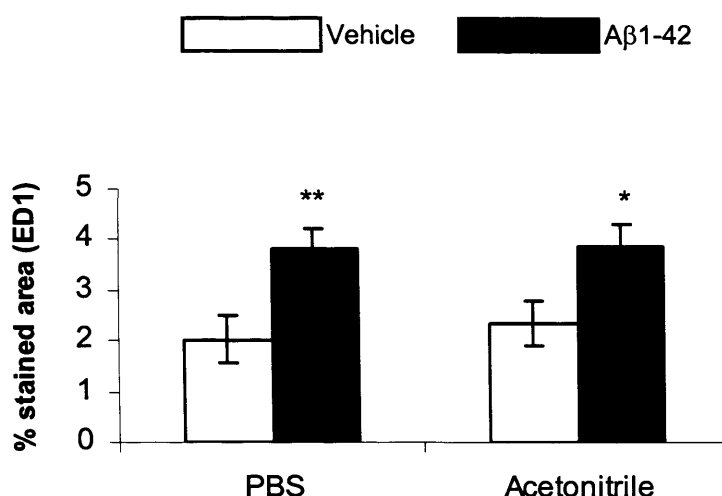


Figure 4.16: Quantification of the percentage stained area of ED1 positive cells in vehicle and Aβ1-42 intra-hippocampal injected rats, data represented as percentage stained area and shows mean ± SEM. \*  $p \leq 0.05$ , \*\*  $p \leq 0.01$  significantly different vs. respective vehicle (repeated measures ANOVA followed by planned comparisons)

#### 4.4.4 Study 12: IH Aβ1-42 (1nmol) vs. Aβ42-1 (1nmol) in 0.1M PBS alone

##### 4.4.4.1 Presence of amyloid

As demonstrated in previous studies, Aβ1-42 deposition was evident within the CA1 and dentate gyrus regions of the hippocampus. 6/12 animals per treatment group had a deposit within the CA1 (fig 4.17). Further investigation revealed that, under polarised light, the Congo red stained deposit did not demonstrate the apple-green birefringence typical of fibrillar Aβ. As a positive control, Congo red stained cortical Aβ plaques of a heterozygous double mutant APP/PS1 transgenic TASTPM mouse (TASTPM developed in GSK, Harlow, UK) revealed apple-green birefringence (fig.4.18).

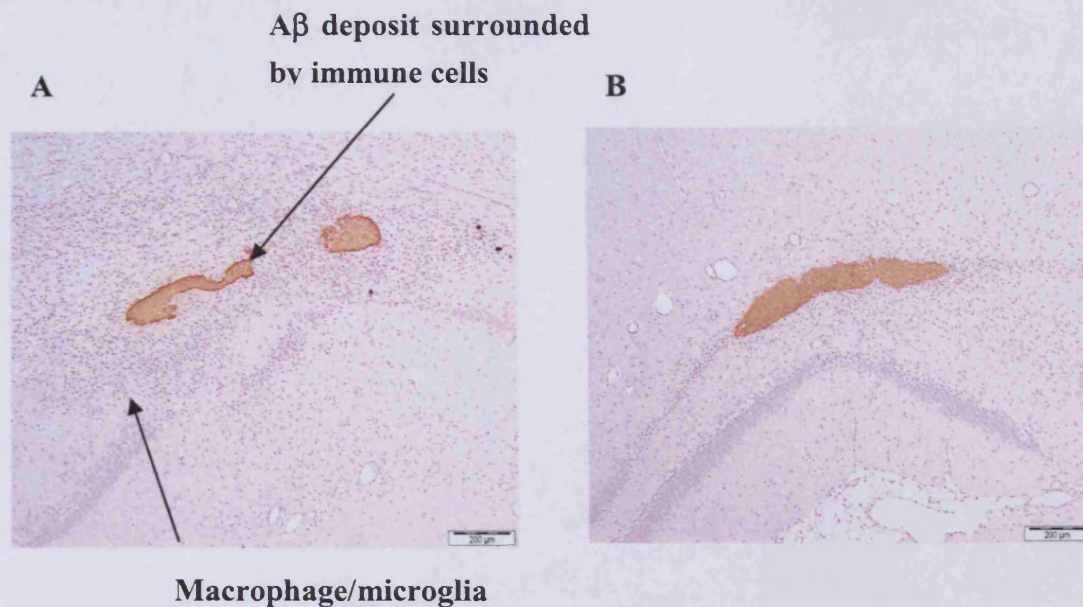


Figure 4.17: Representative photomicrographs of coronal sections of the CA1 (A) and dentate gyrus (B) stained for amyloid (1E8) in A $\beta$ 1-42 intra-hippocampal injected rats (n=12 per treatment group). Scale bar represents 200 $\mu$ metres

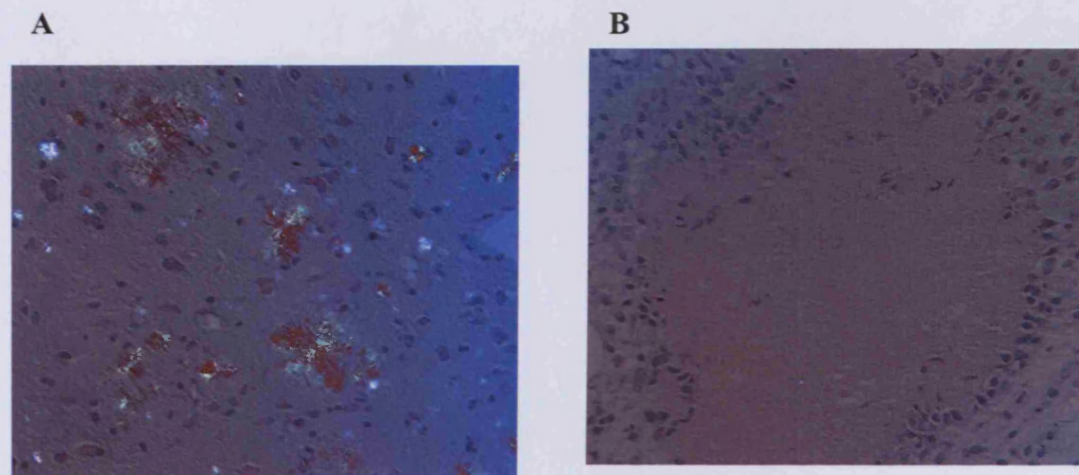


Figure 4.18: Representative photomicrographs of coronal sections of the cortex of a TASTPM mouse (A) and the A $\beta$ 1-42 deposit in intra-hippocampal injected rats(n=12 per treatment group) (B) under polarised light (x40 magnification)

#### 4.4.4.2 Neurodegeneration

There was no overall effect of treatment,  $F_{(2, 22)} = 0.84$ ,  $p = 0.44$ , on hippocampal cell loss (fig 4.19). The greater variability within the A $\beta$ 1-42 treatment group, in contrast to study 11, meant a loss in statistical significance evident as a non-significant decrease in NeuN positive cells relative to vehicle (26% loss,  $p = 0.35$ ) and A $\beta$ 42-1 (29% cell loss,  $p = 0.84$ ) (fig 4.20). There was a significant overall effect of treatment on the extent of mediolateral damage present,  $F_{(2, 26)} = 4.06$ ,  $p < 0.05$ . Post hoc planned comparisons revealed a non-significant increase in lesion size of A $\beta$ 1-42 treated rats relative to vehicle (42% increase,  $p = 0.09$ ) and a significant increase relative to A $\beta$ 42-1 (69% increase,  $p < 0.01$ ) (fig 4.21).

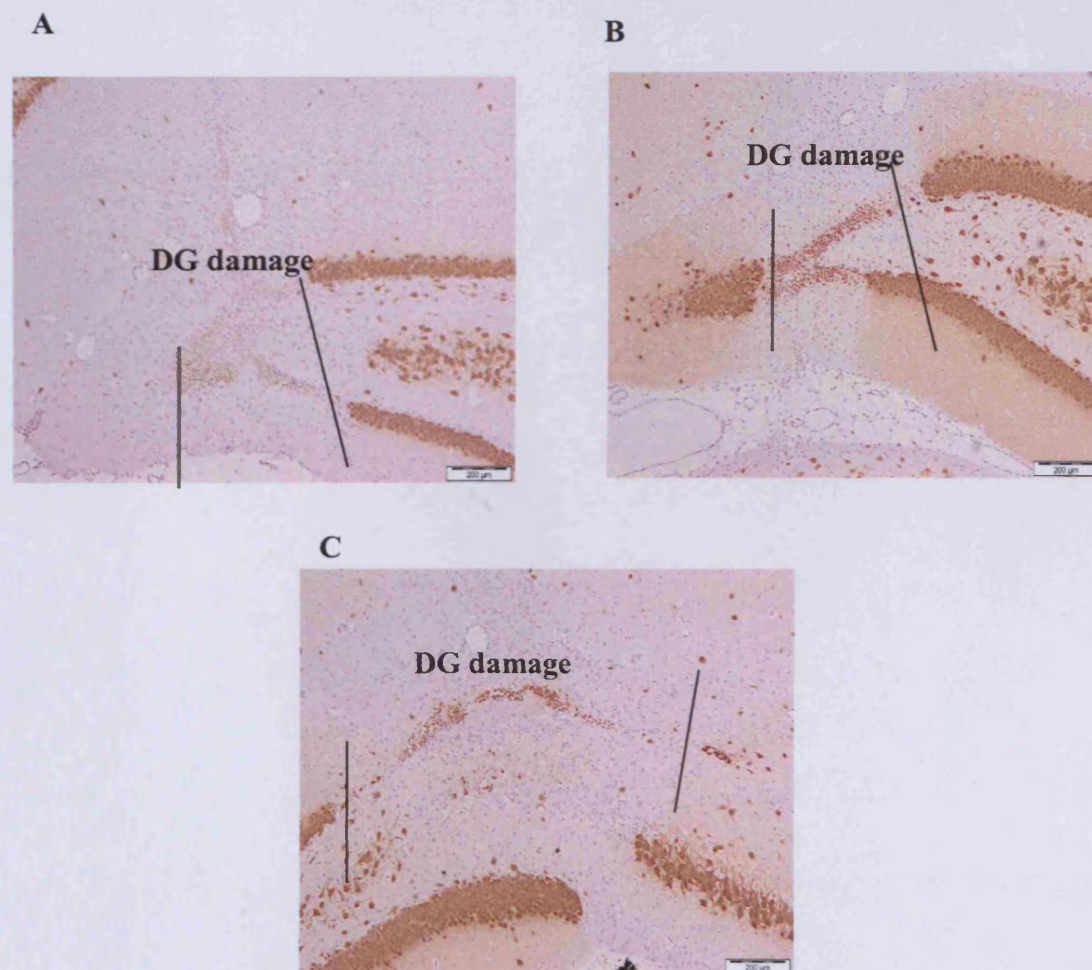


Figure 4.19: Representative photomicrographs of coronal sections of the hippocampus stained for NeuN following intra-hippocampal (n=12) vehicle (A) A $\beta$ 42-1 (B) and A $\beta$ 1-42 (C), Scale bars represent 200μmetres

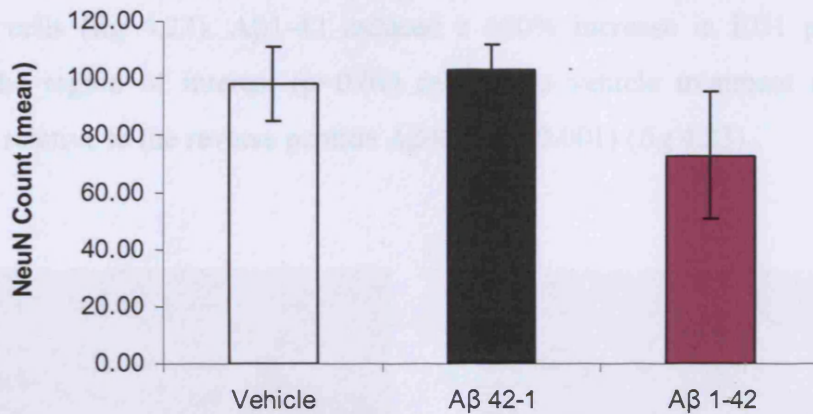


Figure 4.20: Quantification of NeuN positive cells in vehicle and Aβ1-42 intra-hippocampal injected rats (n=12), data represented a count of the NeuN positive stained cells and shows as mean ± SEM (univariate ANOVA followed by planned comparisons)

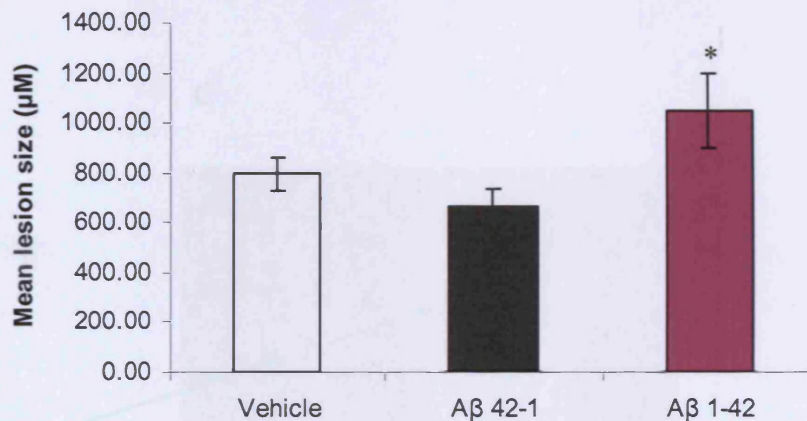


Figure 4.21: Measurement of mediolateral lesion in vehicle and Aβ1-42 intra-hippocampal injected rats, data represented as mediolateral lesion size (μM) and shows mean ± SEM. \* p ≤0.05 significantly different vs. Aβ42-1 (univariate ANOVA followed by planned comparisons)

#### 4.4.4.3 Neuroinflammation

There was an overall effect of treatment,  $F_{(2, 25)} = 9.84$ ,  $p < 0.001$  on presence of ED1 positive cells (fig 4.22). A $\beta$ 1-42 induced a 100% increase in ED1 positive cells within the region of interest ( $p = 0.01$ ) relative to vehicle treatment and a 138% increase relative to the reverse peptide A $\beta$ 42-1 ( $p < 0.001$ ) (fig 4.23).

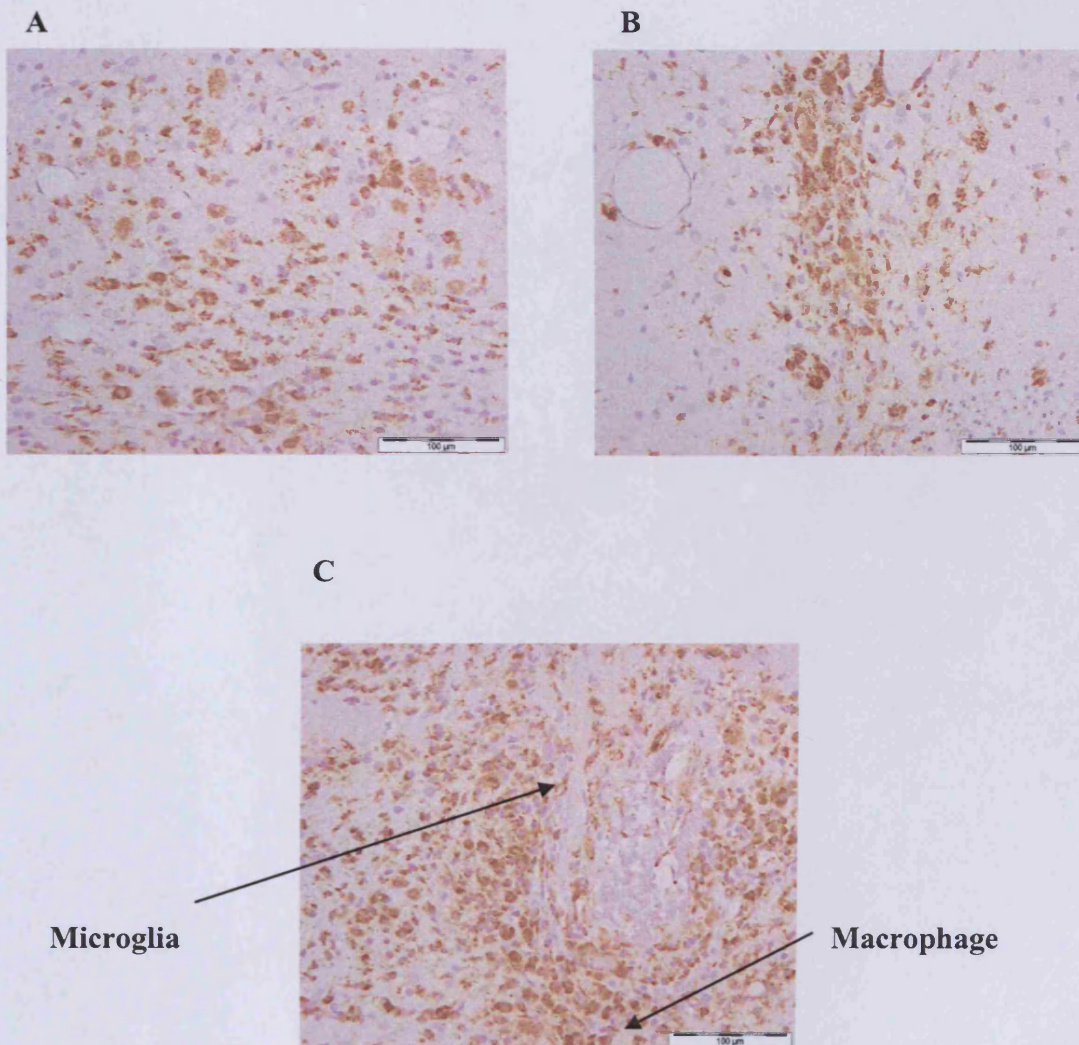


Figure 4.22: Representative photomicrographs of coronal sections of the hippocampus stained for ED1 positive macrophage and microglia in vehicle (A), A $\beta$ 42-1 (B) and A $\beta$ 1-42 (C) intra-hippocampal injected rats ( $n = 12$ ). Scale bar represents 100  $\mu$ m

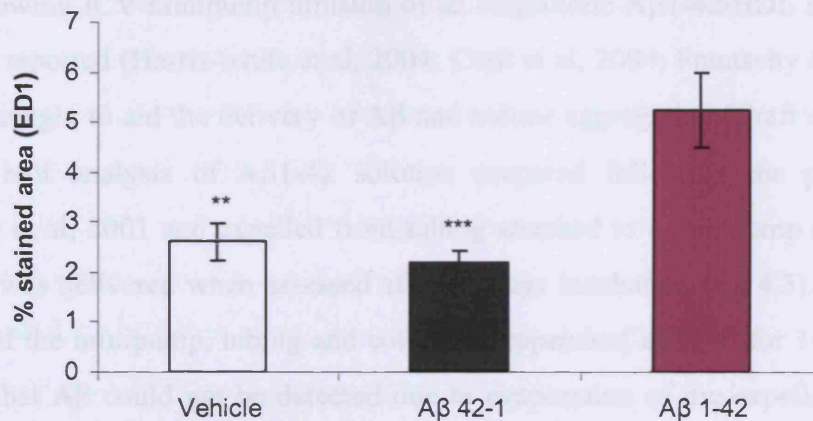


Figure 4.23: Quantification of the percentage stained area of ED1 positive cells in vehicle and Aβ1-42 intra-hippocampal injected rats (n=12 per treatment group), data represented as percentage stained area and shows mean ± SEM. \*\* p ≤ 0.01, \*\*\* p ≤ 0.001 significantly different vs. Aβ1-42 (univariate ANOVA followed by planned comparisons)

## 4.5 Discussion

### 4.5.1 Delivery of Aβ1-42 forms into rodent brain

Using western blot analysis, the expulsion of Aβ from apparatus commonly used to deliver Aβ into rodent brain was assessed. A 100μM Aβ solution prepared following a protocol by O'Hare et al, 1999 and previously described to be successfully injected into rat brain was expelled through a Hamilton syringe or plastic tubing attached to a metal injector. Diffuse bands indicated little aggregated Aβ1-42, shown to be present in pellet and supernatant control samples was released from plastic tubing (fig 4.2). The amount of oligomeric and monomeric Aβ forms expelled was also decreased. This was in contrast to the Aβ forms delivered by using a 10μl Hamilton syringe, in which monomeric, oligomeric and aggregated forms were successfully expelled under both pellet and supernatant conditions (fig 4.2). This confirms that, at 100μM concentration, Aβ1-42 can be successfully delivered into rodent brain via Hamilton syringe, in agreement with data described by O'Hare et al, 1999. This may explain why many authors choose to inject Aβ into discrete brain regions or the ventricular system by using a Hamilton syringe (Song et al, 2001; Ryu et al, 2004; Jantaratnotai

et al, 2003). Alternatively, the A $\beta$  deposition and neuroinflammation in rats and mice following ICV minipump infusion of an oligomeric A $\beta$ 1-42/HDL solution has also been reported (Harris-white et al, 2004; Craft et al, 2004; Frautschy et al, 2001). HDL is thought to aid the delivery of A $\beta$  and reduce aggregation (Craft et al, 2004). Western blot analysis of A $\beta$ 1-42 solution prepared following the protocol by Frautschy et al, 2001 and expelled from tubing attached to a minipump revealed no A $\beta$  form was delivered when assessed after 14 days incubation (fig 4.3). Due to the housing of the minipump, tubing and collecting ependorf at 37°C for 14 days, it is possible that A $\beta$  could not be detected due to evaporation of the expelled solution, hence the possibility that A $\beta$  was expelled cannot be discounted and Frautschy et al, 2001 does describe limited deposition of A $\beta$  in brain tissue with this protocol. Additional assessment of the remaining A $\beta$ 1-42 solution within the minipump after 14 days incubation revealed the presence of A $\beta$  aggregates (fig 4.3). The likelihood that A $\beta$  contained within a minipump may aggregate easily and limit the deposition of A $\beta$  within the brain tissue highlights the difficulty of using this method for delivering significant A $\beta$  into the tissue to induce quantifiable neurodegeneration. Using this A $\beta$  minipump protocol, overt cell death has not yet been described by the Frautschy group, although a reduction of synaptophysin, a synaptic-associated protein, indicates compromised synaptic density (Craft et al, 2004). Much published literature describes the direct injection of A $\beta$  into rodent brain (O'Hare et al, 1999; Weldon et al, 1998; Ryu et al, 2004; 2006; Jantaratnotai et al, 2003; Miguel-Hidalgo et al, 1998; 2002; Song et al, 2001). Further assessment using A $\beta$ 1-42 solutions prepared following protocols by Miguel-Hidalgo et al, 1998 or Ryu et al, 2004 and described as neurotoxic in vivo, revealed mainly monomeric and some oligomeric A $\beta$ 1-42 were present in control samples and expelled from a 10 $\mu$ l Hamilton syringe (fig 4.4). This suggests that, on injection, A $\beta$  is delivered into brain tissue as soluble A $\beta$  forms. Frautschy et al, 1996 suggested that A $\beta$  toxicity in brain tissue is dependent on A $\beta$  remaining in its soluble state, however, A $\beta$ 1-42 aggregates easily and may aggregate once injected into rodent brain.

#### **4.5.2 *Presence of A $\beta$ in brain tissue following intra-hippocampal injection***

Following the protocol by Ryu et al, intra-hippocampal injection of A $\beta$ 1-42 resulted

in a deposit located within the CA1, corpus callosum or dentate gyrus of the hippocampus (fig 4.5). It is likely that much of the variability observed within these studies is due to the inherent variability in injection procedure as, in agreement with previous literature, consistent direct injection to one specific sub-region is difficult (Miguel-Hidalgo et al, 1998). As in the studies described in this chapter, Miguel-Hidalgo et al, 1998 also described that, under polarised light, A $\beta$ 1-42 deposits stained with Congo red did not demonstrate apple-green birefringence (fig 4.18). This indicates that A $\beta$  neurotoxicity evident in this model is caused by soluble A $\beta$  forms rather than fibrillar A $\beta$ . Recently, the possibility that soluble A $\beta$  causes neurotoxicity in brain tissue has been extensively discussed, particularly the role of oligomers in A $\beta$  neurotoxicity (Chromy et al, 2003; Walsh & Selkoe, 2004; Lacor et al, 2004).

#### **4.5.3 *A $\beta$ -induced neurodegeneration***

The purpose of the in vivo studies described in this chapter was to investigate the influence of the solvents acetonitrile diluted in PBS and PBS alone on A $\beta$ -induced neurotoxicity in rat brain. Following this, the neurotoxic effect of A $\beta$ 1-42 was compared to the reverse peptide, A $\beta$ 42-1. Despite earlier conflicting reports regarding the neurotoxic effects of A $\beta$  in vivo (Smyth et al, 1994; Winkler et al, 1994; Games et al, 1992), recent literature has described the neurotoxic effects of the A $\beta$ 1-42 fragment when directly injected into the hippocampus. Quantification of neurodegeneration following protocols previously described by Ryu et al, 2004 and Miguel-Hidalgo et al, 1998 revealed a trend for increased neurodegeneration in rats treated with A $\beta$ 1-42 relative to vehicle and A $\beta$ 42-1 when all treatments were dissolved in PBS alone. This was evident as approximately a 25% NeuN positive cell loss (fig 4.13) and a 69% increase in the extent of mediolateral damage (fig 4.14). The 25% cell loss evident in studies described within this chapter supports previously published literature (Ryu et al, 2004); however, this window of cell loss was relative to vehicle injected rats. Ryu et al, 2004 described a 28% reduction in NeuN count relative to sham rats following intra-hippocampal A $\beta$ 1-42 injection into the hippocampus although the A $\beta$ 1-42 was dissolved in the solvent acetonitrile.

Synthetic A $\beta$  has been dissolved in a number of commonly used solvents including dimethylsulfoxide (DMSO) (Mattson et al, 1993), acetonitrile (Yankner et al, 1994,

Jantaratnotoi et al, 2003; Ryu et al, 2004), water (O'Hare et al, 1999) and saline or PBS (Bishop et al, 2003) and the inherent toxicity should be taken into consideration when injecting directly into rodent brain tissue. In vitro studies revealed that A $\beta$  neurotoxicity was influenced by the solvent employed and the peptide aggregation state (Pike et al, 1993; Busciglio et al, 1992). Further evidence suggests the solvent may alter A $\beta$  aggregation state. For example, Mattson et al, 1992 reported the potentiation of excitotoxicity by A $\beta$  which had been dissolved in DMSO as a stock solution and then further diluted in saline. This resulted in predominantly monomeric forms of A $\beta$  and a 100x greater toxicity than A $\beta$  dissolved in saline, which resulted in A $\beta$  dimer formation. A comparison of the neurotoxicity resulting from the injection of A $\beta$  dissolved in various solvents revealed that acetonitrile can cause a large degree of toxicity, which is significantly enhanced by either A $\beta$ 1-42 or A $\beta$ 1-40 (Waite et al, 1992). There are conflicting reports relating to the influence of acetonitrile solvent on A $\beta$ -induced neurotoxicity in rodent brain (Ryu et al, 2004, Waite et al, 1992, Podlisny et al, 1992). Acetonitrile can be converted to cyanide by cytochrome P450 (Freeman & Hayes, 1988). Cyanide toxicity elicits changes in calcium homeostasis mediating the influx of calcium into the cell resulting in cell death (Waite et al, 1992). Using acetonitrile at either 0.35% (fig 4.7 & 4.8) or 0.035% (fig 4.13 & 4.14) concentration, failed to result in a window of cell death between vehicle and A $\beta$ 1-42 treatment groups which supports a study described by Podlisny et al, 1992 in which injections of A $\beta$ 1-40 dissolved in 35% acetonitrile into primate cerebral cortex did not significantly increase cell loss relative to acetonitrile alone. In contrast, Ryu et al, 2004 reported 28% cell loss following the intra-hippocampal injection of A $\beta$ 1-42 dissolved in an acetonitrile/PBS based solvent although it is unclear what final percentage of acetonitrile remained following dilution of A $\beta$ 1-42 with 0.1M PBS to a 500 $\mu$ M concentration. The comparison of the A $\beta$ 1-42 group with sham animals may also suggest that the neurotoxicity was wholly or partly due to the effect of acetonitrile since comparing studies described here indicated no difference in the magnitude of cell loss between A $\beta$  in acetonitrile and acetonitrile (vehicle) treated rats.

#### **4.5.4 A $\beta$ 1-42 - induced neuroinflammation**

Previous reports suggest the full length A $\beta$  peptide is required to induce

neuroinflammation, since A $\beta$ 1-42 elicits greater inflammation both in vivo (Miguel-Hidalgo et al, 1998) and in vitro (Velazquez et al, 1997) than shorter A $\beta$  fragments. Neuroinflammation has long been considered as a potential mechanism for mediating or exacerbating A $\beta$  neurotoxicity in AD and recent studies have described the induction of an early inflammatory response to oligomeric amyloid in contrast to a less profound but chronic inflammatory state elicited by fibrillar A $\beta$  (White et al, 2005). Intra-hippocampal injection of A $\beta$ 1-42 increased neuroinflammation, evident as the increased presence of microglia and macrophage cells surrounding the A $\beta$  deposit relative to both acetonitrile and PBS vehicle treatment (fig 4.16). Neurodegeneration of hippocampal cells occurred adjacent to the deposit suggesting a combination of contact with A $\beta$  and the phagocytic activity and release of toxic molecules such as cytokines and NO by associated phagocytic cells mediates cell death in this model (Minagar et al, 2002). This theory is supported by in vitro evidence that in mixed neuron-glia cultures, following incubation with low concentrations (1-3 $\mu$ M) of A $\beta$ , significant neurotoxicity was evident in contrast to neuron-enriched cultures (without microglia) in which no neurotoxicity was observed (Qin et al, 2002).

Although A $\beta$  is a key characteristic of AD brain tissue, the role of A $\beta$  load and particularly the relative contribution of different A $\beta$  forms in causing or exacerbating cell death remain uncertain. Both fibrillar and oligomeric A $\beta$  forms have been shown to cause neurotoxicity (Howlett et al, 1995; Chromy et al, 2003). The accumulation of intraneuronal A $\beta$ 1-42 may also significantly contribute to causing overt neurodegeneration, particularly on the scale evident in AD (Fernandez-Vizarra et al, 2004; Masters et al, 1985). In AD brain tissue, microglia can congregate around core plaques as they develop and may convert the extracellular soluble A $\beta$  released from intraneuronal stores to fibrillar A $\beta$  plaques (Nagele et al, 2004). Further research would clarify whether the soluble A $\beta$ 1-42 deposit present by 7 days after intra-hippocampal injection may fibrillise if the study duration was extended. This may also have further implications on the neuroinflammation and neurodegeneration evident by later timepoints since it is unclear which A $\beta$  form is most neurotoxic in vivo. Intraneuronal soluble A $\beta$  has also been identified as an early neurodegenerative change in AD (Fernandez-Vizarra et al, 2004). Intraneuronal soluble A $\beta$  may significantly contribute to cell death (Wirhth et al, 2004) hence the exogenous A $\beta$

induced neurodegeneration evident in this model is limited since it is unlikely to affect intracellular A $\beta$  levels.

Overall, my thesis thus far has reported the development and validation of IP and ICV LPS induced neuroinflammation in rat brain. Assessment of the more AD relevant peptide, A $\beta$ 1-42, revealed successful delivery of A $\beta$ 1-42 concentrations reported to be neurotoxic via injection by Hamilton syringe into rodent brain tissue. Intra-hippocampal injection of A $\beta$ 1-42 resulted in a significant increase in cell-mediated inflammation associated with quantifiable but variable endpoints of neurodegeneration observed at 7 days post injection. Thus, the exogenous application of A $\beta$ 1-42 into rat brain does not provide a robust and reliable in vivo model of A $\beta$ -induced neurodegeneration. An alternative to the exogenous injection of A $\beta$  into rodent brain is to use APP or APP/PS1 overexpressing transgenic mouse models. Transgenic mouse lines overexpressing mutant human APP and PS1 genes, identified as genetic mutations important in familial AD, exhibit age-dependent increases in extracellular senile and diffuse A $\beta$  deposits within specific brain regions including the cerebral cortex and hippocampus. A $\beta$  deposits are associated with activated microglia, reactive astrocytes and increased cytokine expression within brain tissue. Despite the presence of A $\beta$  deposition, a majority of transgenic models overexpressing APP (and PS1) do not exhibit overt neurodegeneration, however, the peripheral administration of inflammatory or neurotoxic challenges such as LPS or DSP4 to APP and APP/PS1 overexpressing mice has been previously reported to modulate A $\beta$  load, exacerbate neuroinflammation and induce neurodegeneration (Sheng et al, 2003; Brugg et al, 1995; Heneka et al, 2006). Hence, subsequent chapters will evaluate the effects of inflammatory or neurotoxic challenges on inflammation and neurodegeneration in an APP/PS1 overexpressing transgenic mouse model, TASTPM.

## **CHAPTER 5**

### ***Single and repeated administration of LPS to TASTPM APP/PS1 overexpressing mice***

#### **5.1 Introduction**

APP and APP/PS1 overexpressing transgenic mouse models have been routinely used to characterise the effects of amyloid neuropathology on neuroinflammation and neurodegeneration (Price et al, 2000). APP and APP/PS1 overexpressing mice demonstrate A $\beta$  induced neuroinflammation evident as activated microglia and reactive astrocytes associated with increased mRNA expression of pro- and anti-inflammatory cytokines in brain tissue (Apelt et al, 2001; Abbas et al; 2002; Benzing et al, 1999). However, a majority of transgenic models do not exhibit the overt neurodegeneration evident in brain tissue of AD patients (Games et al, 2006). More recently, newly constructed APP/PS1 transgenic lines have been reported to exhibit some level of neurodegeneration in brain ranging from approximately 15 – 50% cell loss (Schmitz et al, 2004; Casas et al, 2004; Bondolfi et al, 2002); however, this is low relative to the neurodegeneration evident in specific brain regions, particularly the entorhinal cortex, of AD brain (Gomez-Isla et al, 1996). Recent evidence derived from in vivo animal models (Cunningham et al, 2005; Combrinck et al, 2002; Perry et al, 2003) and patient studies (Holmes et al, 2003) suggests systemic infection may exacerbate the progression of chronic neurodegenerative diseases such as AD by enhancing the production of inflammatory mediators and recruitment of immune cells in compromised brain tissue. There is further evidence that peripheral administration of LPS can modulate A $\beta$  load and neuroinflammation in APP or APP/PS1 overexpressing mice (Sheng et al, 2003; Sly et al, 2001; Qiao et al, 2001). Much of the current literature describes the quantification of cytokine mRNA (Abbas et al, 2002; Lim et al, 2000) in APP overexpressing mice and there is data indicating modulation of cytokine protein in brain tissue following IP LPS administration (Sly et al, 2001). Exacerbating the pathology of APP/PS1 transgenic models using peripheral administration of inflammatory stimuli such as LPS or specific neurotoxic agents may therefore provide a suitable model of neuroinflammation and

neurodegeneration.

### **5.1.1 *Peripheral infection in AD***

Severe systemic infections in elderly patients can induce the development of delirium, a state of cognitive impairment comprising a loss of memory, hallucinations and confusion (Perry et al, 2004). At their time of death, many AD patients are suffering from infections of peripheral organs such as the lungs or bladder. Holmes et al, 2003 reported that for at least two months following the resolution of a systemic infection, patients suffering mild-to-moderate AD exhibited greater cognitive decline relative to uninfected patients. A subset of infected patients also displayed enhanced IL1 $\beta$  at initial mini-mental state examination (MMSE) assessment and subsequent MMSE tests revealed an exacerbated cognitive decline relative to other infected AD patients. The induction of a peripheral infection in a preclinical model demonstrating amyloid deposition in brain tissue, such as APP/PS1 overexpressing mice, may enhance pre-existing neuroinflammation. I was also interested in examining the consequence of peripheral infection on the occurrence of neurodegeneration.

### **5.1.2 *LPS administration to APP (&PS1) overexpressing mice***

There are a limited number of reports detailing the effect of LPS administration to APP or APP/PS1 overexpressing mice. Differences in route of administration, treatment protocols, animal genotype, LPS serotype and sampling timepoint have resulted in variability in the in vivo effects of LPS on APP or APP/PS1 overexpressing mice. Intra-hippocampal LPS, administered after plaque onset, resulted in increased number and size of reactive astrocytes and activated microglia in Tg2576 transgenic mice with (DiCarlo et al, 2001) and without (Herber et al, 2004) the presence of a PS1 transgene. In both reports, there was a corresponding decrease in A $\beta$  load that was due to a reduction in diffuse amyloid plaques, since congophilic deposits remained unaffected (Herber et al, 2004). Additionally, the IP administration of LPS (single bolus of 25mg/kg at 13 and 14 months) post plaque onset in Tg2576 mice caused a reduction in A $\beta$  load (Quinn et al, 2003). Acute peripheral administration of LPS also induced cortical and hippocampal IL1 $\beta$  in aged Tg2576 mice (Sly et al, 2001). This supports evidence that an acute inflammatory

response in the brain can occur after a peripheral inflammatory challenge and that this is exacerbated in animals exhibiting amyloid neuropathology. In contrast, chronic administration of LPS either via repeated ICV or IP injection results in an increase in A $\beta$  load, evident as an increase in A $\beta$  and APP positive neurons, A $\beta$ 1-40 and A $\beta$ 1-42 protein, intracellular A $\beta$  accumulation (Sheng et al, 2003) or thioflavin-S-positive amyloid deposits (Qiao et al, 2001). Interestingly, these authors administered LPS before the onset of robust fibrillar amyloid deposition. This suggests that pre-existing neuroinflammation caused by chronic administration of an inflammatory challenge can exacerbate A $\beta$  neuropathology. LPS treatment after extensive amyloid deposition may induce clearance of plaques since IP administration of LPS after the onset of plaque deposition the brains of Tg2576 mice caused a reduction in amyloid plaque burden (Quinn et al, 2003).

### **5.1.3 *The TASTPM APP/PS1 overexpressing transgenic mouse model***

Heterozygous double mutant mice (TASTPM) previously generated by Dr. Jill Richardson at GSK, Harlow, UK were used in these studies. TAS10 mice (Richardson et al, 2003) carrying the Swedish double familial mutation hAPP695swe (K670N; M671L) and backcrossed onto a pure C57BL/6 background and mice carrying the PS-1 (M146V) mutation were generated at GlaxoSmithKline. Human cDNA for APP695 (K670N; M671L) or PS-1 (M146V) was inserted into a vector and replaced the coding sequence of the murine Thy-1 gene to allow brain-specific expression of either transgene as described by Howlett et al, 2004.

TASTPM mice demonstrate age-dependant amyloid neuropathology and cognitive impairments (extensively characterised at GSK, Harlow and initially described by Howlett et al, 2004). Using immunohistochemical techniques, amyloid deposits were observed in the brain tissue of all TASTPM mice by four months of age. Fibrillar A $\beta$  plaques, when observed under an electron microscope, were not evident until six months of age. Female mice displayed more extensive cerebral plaque pathology by six and ten months of age relative to male mice. Cortical extracellular A $\beta$  plaques were surrounded by dystrophic neurites and in close proximity to astrocytes and microglia, however, overt neuronal loss was not evident.

### **5.1.4 Chapter Aims**

This chapter will describe the effects of peripheral administration of LPS to the APP/PS1 overexpressing mouse, TASTPM. Using Luminex<sup>®</sup>, the effects of a peripheral inflammatory challenge on cytokine expression in brain tissue and plasma will be investigated. The effect of LPS on amyloid neuropathology, neuroinflammation and neurodegeneration will be characterised using immunohistochemical techniques.

## **5.2 Materials & Methods**

### **5.2.1 Animals**

Specific, pathogen free male heterozygous double mutant TASTPM and male C57BL6/J mice at 2, 5 and 10 months of age (for assessing effects of acute LPS administration) and at 4 months of age (for assessing effects of repeated administration of LPS) were purchased from Charles River, UK. All mice were singly housed under controlled conditions (temperature: 21-24°C, 12-h light/dark cycle (7am lights on) and provided with Global Rodent Maintained Diet (Harlan Teklad) and water *ad libitum*. Sheng et al, 2003 described evidence of adverse effects 1-2 hours following LPS administration, which included shivering. Hence, during repeated LPS injection animals were provided with extra bedding. All experimental procedures were conducted in accordance with the GlaxoSmithKline local ethics committee and conformed to the UK Animals (Scientific Procedures) Act 1986.

### **5.2.2 Materials**

Phosphate buffered saline (PBS) was prepared using PBS tablets obtained from Sigma, UK. Lipopolysaccharide (0111:B4, L2630) was purchased from Sigma, UK. Immunostaining machines, PAP pens, the antigen retrieval solution proteinase K, peroxidase blocking solution and diaminobenzidine substrate kit were obtained from DakoCytomation, UK. Optimax buffer was obtained from A. Menarini, UK. Gills haematoxylin stain and citrate buffer was purchased from HD Supplies, UK. The sources of additional materials are individually stated.

### **5.2.3 Treatment**

LPS was allowed to dissolve in filtered PBS in a falcon tube (VWR International, UK) for at least 30 minutes before administration.

For single dosing, LPS was dissolved at 600µg/5ml and administered at 5ml/kg. This dose was based on previous validation studies assessing a dose response and a timecourse of LPS induced cytokine protein in brain and plasma in C57BL6/J mice (GSK, Harlow, UK). For repeated dosing, 5mg LPS was dissolved in 100ml of filtered PBS and was administered at 10µl/g body weight (0.5µg/g body weight) according to a protocol by Sheng et al, 2003. Repeated administration of LPS at 0.5µg/g increased Aβ load and neuroinflammation in APP<sup>swe</sup> transgenic mice (Sheng et al, 2003).

### **5.2.4 Sample collection**

Mice were deeply anaesthetised with sodium pentobarbitone (Euthatal<sup>®</sup> 100mg kg<sup>-1</sup> i.p, Rhône Mérieux, Harlow, UK). Trunk blood was collected into a 1.3ml EDTA micro-tube (VWR International, UK) via a cut in the right atrium. Mice were transcardially perfused with 15ml ice-cooled 0.9% sterile saline. Hemidissected brain and microdissected brain regions were stored in preweighed and labelled eppendorfs at -80°C. The blood was spun in a microcentrifuge at 6000g for 6 minutes (according to a previous protocol, GSK, Harlow) and the straw-coloured plasma fraction collected into fresh eppendorfs and stored at -80°C.

### **5.2.5 Cytokine protein determination**

#### **5.2.5.1 Sample preparation**

Brain tissues were diluted to the appropriate concentration (5ul/mg tissue) with high performance ELISA (HPE) buffer (Sanquin Reagents, Amsterdam) and homogenised using a hand-held Ultra-Turrax T8 homogeniser (VWR International, UK). All samples were spun in a microcentrifuge (Centrifuge 5415 D, Eppendorf UK Ltd, Cambridge, UK) at 16,110g for 2 minutes. The supernatant was removed and stored in a fresh eppendorf at -80°C. Brain supernatant and plasma were subsequently allowed to defrost and 50µl aliquots of each sample placed into a corresponding well on a standard 96-well plate (Nunc, UK) according to a predetermined plate layout.

All samples were diluted with 100µl assay buffer (1% BSA in PBS).

#### 5.2.5.2 *Luminex<sup>®</sup> suspension bead array – cytokine analysis*

100µl of sample was transferred to a pre-wet (100µl of assay buffer added to each well and then vacuum filtered) 96-well filter plate (Millipore<sup>®</sup>, USA). A 5000pg standard (Upstate, Hampshire, UK) was reconstituted in 500µl of assay buffer, added to a 14600pg standard for MIP-1α (Biosource, UK), and serially diluted 1:3 using assay buffer to provide an 8 point standard curve (0 to 5000 pg/ml). Samples were incubated in the dark overnight at 4°C with 50µl of anti-cytokine conjugated beads (60µl of 25x stock solution for each cytokine diluted to 1x in total of 5940µl assay buffer per plate) multiplexed from individual kits for each cytokine (R & D Systems, UK, (MIP-1α (Biosource, UK))). Plates were washed three times with 200µl of assay buffer, filtered using a vacuum manifold apparatus (Millipore<sup>®</sup>, USA) and incubated with 100µl of detection antibody (R & D Systems, UK, (MIP-1α (Biosource, UK))) (60µl stock solution of each cytokine diluted to 1x dilution in a total of 11940µl assay buffer per plate) in the dark at room temperature for 1 hour. Following three washes (200µl assay buffer), each sample was incubated with 100µl streptavidin phycoerythrin - PE (VWR International, UK) (12µl stock solution diluted with 11,988µl assay buffer) and placed in the dark on a plate shaker at 700rpm for 30 minutes at room temperature. Plates were analysed by the Luminex<sup>®</sup>-100<sup>TM</sup> system (Luminex<sup>®</sup> Corporation, USA) to achieve MFI readings for standard curves and cytokines in brain homogenate and plasma. Double discriminator gates were positioned from approximately 8,000 to 15,000 to separate singlet and doublet beads. Intensity was identified at bead regions 50, 06, 32, 79, 26 for IL-10, IL-1β, IL-6, TNF-α and MIP-1α respectively. 4/5-parameter logistic regression curves (Hulse et al, 2004) of the cytokine standards were calculated using StarStation software and the concentrations of unknown samples were determined relative to calculated standard curves.

#### 5.2.6 *Aβ ELISA*

Hemidissected brain samples were prepared by adding 1ml 5M guanidine HCl (Calbiochem, USA) containing Complete TM protease inhibitor tablet (Roche

Diagnosics, UK) resulting in approximately 150mg/ml w/v. Each sample was homogenised using a Torax/hand held pellet pestle (Sigma, UK) and mixed on a shaker for 90 minutes at 4°C. IGEN buffer (50mM Tris HCl, pH7.4, 150mM NaCl, 0.05% Tween-20+ 1% BSA) was added to each sample at a 1/10,000 dilution and an aliquot of the resulting solution removed. The aliquot was vortexed and centrifuged at 20000g for 20 mins at 4°C. The supernatant was removed and transferred to a 2ml deep polypropylene 96 well block and 100µl of each sample pipetted in triplicate into polypropylene 96 well plates (VWR international, UK). Standard curves for human Aβ40 (0 to 40ng/ml) and Aβ42 (0 to 20 mg/ml) dissolved in guanidine containing IGEN buffer were constructed, in triplicate. An antibody/bead mix of 15ml per plate was prepared using 10µl of 0.66µg/ml biotinylated 6E10 (Signet Labs, USA), 4µl ori-tag G210 (Aβ40) or 8µl 5G5 (Aβ42) (IGEN® International, USA), 125µl streptavidin dynabeads® (Invitrogen Ltd, UK) and 15ml assay buffer (50mM Tris HCl, pH7.4, 150mM NaCl, 0.05% Tween-20)+ 1% BSA. 150µl of the mix was added to each well and the plate vigorously mixed overnight at room temperature. The following day, the plate was read on an IGEN M8 analyser (IGEN® International, USA). The Aβ ELISA was kindly completed by Peter Soden, GSK, Harlow, UK.

### **5.2.7 Immunohistochemistry**

Hemi-dissected brains were immersed fixed in 4% paraformaldehyde for 3 days at room temperature and prepared for paraffin wax processing using a Shandon Citadel 1000 tissue processor and embedded in paraffin wax using a Shandon Histocentre II embedding centre. A Microm HM 355S rotary microtome was used to cut at least 40 semi-serial sections of 5µM thickness were prepared from each sample to include the cortex and hippocampus (bregma -1 to -4mm). Slides were dried at room temperature for at least 24 hours before staining. 6 sections per stain were assigned for amyloid (1E8), neuronal cell nuclei (NeuN), astrocytes (GFAP) and microglia (CD68) immunohistochemistry. Sections were dewaxed in HistoClear (National Diagnostics, UK) and hydrated through industrial methylated spirit (IMS), 70% IMS and deionised water. Sections were washed in deionised water and a hydrophobic barrier applied above and below the section using a PAP pen to prevent the antibody solution falling off the slide. Slides were loaded into an autostainer and Optimax

buffer applied. Buffer was added between each step and deionised water applied after the diaminobenzidine step. After staining, sections were washed in running tap water for 5 minutes before counter staining in Gills haematoxylin for 3 seconds. Sections were placed in running tap water to "blue", dehydrated in graded followed by absolute IMS, cleared in Histoclear and mounted in DPX (VWR, UK).

#### 5.2.7.1 *Amyloid (1E8) Staining*

Sections were treated with 85% formic acid (VWR) for 8 minutes then washed thoroughly in deionised water and loaded into the automated immunostaining machine. Sections received peroxidase block for 5 minutes, primary mouse monoclonal antibody 1E8 (raised against 13-27 fragment of beta amyloid) (GSK, UK) diluted 1 in 1000 in antibody diluent for 30 minutes, prediluted labelled streptavidin biotin system (LSAB) 1 for 10 minutes, prediluted LSAB 2 for 10 minutes and diaminobenzidine substrate kit for 10 minutes.

#### 5.2.7.2 *NeuN*

Sections were microwaved in 1 % citrate buffer (pH 6.0) at 900 W for 3½ minute, then twice at 300 W for 5 minutes and left to cool at room temperature for 20 minutes. Sections received peroxidase block for 5 minutes, primary mouse monoclonal antibody NeuN (1/1000, antibody diluent) (Chemicon International, UK) for 30 minutes, prediluted labelled streptavidin biotin system (LSAB) 1 for 10 minutes, prediluted LSAB 2 for 10 minutes and diaminobenzidine substrate kit for 10 minutes.

#### 5.2.7.3 *GFAP Staining*

Sections were treated with proteinase K for 5 minutes followed by peroxidase block for 5 minutes and primary antibody rabbit anti bovine GFAP (1/500, optimax buffer) (DakoCytomation, UK) for 30 minutes. Biotinylated goat anti rabbit (1/200, optimax buffer) (Vector Laboratories, UK) was added for 30 minutes followed by peroxidase ABC kit (Vector Laboratories, UK) for 45 minutes and diaminobenzidine substrate kit for 10 minutes.

#### 5.2.7.4 *Macrophage (CD68) Staining*

Sections were treated with proteinase K for 5 minutes followed by peroxidase block

for 5 minutes, rat anti mouse CD68 (1/50, antibody diluent) (Serotec, UK) for 30 minutes, biotinylated anti rat IgG (1/100, optimax buffer) (Serotec, UK) for 30 minutes followed by peroxidase ABC kit (Vector Laboratories, UK) for 45 minutes and diaminobenzidine substrate kit for 10 minutes.

#### *5.2.7.5 Quantification of A $\beta$ plaque deposition, neuronal cell loss and GFAP*

The effect of repeated LPS challenge on immunohistochemical endpoints was quantified by using a Leica microscope and Qwin software (Leica systems, Buckinghamshire, UK) to calculate percentage area stained for 1E8 positive A $\beta$  plaques, NeuN positive cells and GFAP positive astrocytes in cortex and hippocampus of all mice. CD68 positive macrophage/microglia were not quantified, as the staining was too diffuse to accurately obtain contrast against background.

#### *5.2.8 Data Analysis*

A general linear mixed model approach using the Proc Mixed procedure in SAS<sup>®</sup> Version 8 (SAS<sup>®</sup> Institute, UK) assessed the overall effects and interactions of treatment genotype and age on cytokine responses in brain tissue within subjects. Separate univariate tests of significance using Statistica<sup>™</sup> Version 6.1 (Statsoft, USA) calculated the overall effect of LPS treatment on plasma cytokine responses, A $\beta$  load and A $\beta$ , NeuN and GFAP immunohistochemical quantification. Planned comparisons on the predicted means from the model assessed individual treatment, genotype and age effects on acute LPS challenge in TASTPM mice and individual treatment and genotype effects on immunohistochemical endpoints. Results are represented as means  $\pm$  SEM and significance was set at  $P \leq 0.05$ . Percentage induction refers to the effect of LPS versus vehicle.

### **5.3 Protocols**

#### *5.3.1 Study 13: Acute administration of LPS in TASTPM mice*

Male TASTPM and age-matched C57BL6/J controls were IPly administered with filtered PBS or 600 $\mu$ g/kg LPS (5ml/kg) dissolved in filtered PBS at either 2, 5 or 10 months of age (n=6-9) and euthanased at 2.5 hours post dose as described in section 5.2.4. These ages were chosen in order to span the progression of A $\beta$

neuropathology.

### **5.3.2 Study 14: Inflammation and neurodegeneration following repeated LPS administration in TASTPM mice**

Male TASTPM mice aged 4 months (prior to onset of fibrillar A $\beta$  plaque deposition in brain tissue) and age matched C57BL6/J controls (n=10-12) were IPly administered with filtered PBS or 10 $\mu$ l/g body weight with 5mg/100ml LPS solution weekly for 12 weeks. I chose to begin the administration of LPS to TASTPM mice at 4 months of age, based on published reports that highlight the possibility that initiating a peripheral inflammatory response prior to onset of fibrillar A $\beta$  plaque deposition could increase neuroinflammation and A $\beta$  load (Qiao et al, 2001; Sheng et al, 2003). 48 hours following the last IP dose, brain tissue was hemisected for half brain for immunohistochemical analysis and the remaining half brain was either stored for A $\beta$  ELISA, or cortex and hippocampus microdissected for Luminex<sup>®</sup> cytokine analysis. Blood was removed via tail tip amputation at 2.5 hours post the final IP dose and at 48 hours post the final IP dose as described in section 5.2.4.

## **5.4 Results**

### **5.4.1 Study 13: Acute LPS administration of TASTPM mice**

#### **5.4.1.1 Cytokine protein in brain**

Repeated measures ANOVA indicated an overall effect of treatment,  $F_{(1, 72)} = 309.67$ ,  $p < 0.001$ , age,  $F_{(2, 72)} = 7.18$ ,  $p < 0.01$  and treatment\*age,  $F_{(2, 72)} = 11.47$ ,  $p < 0.001$  and age\*brain region,  $F_{(2, 71)} = 5.73$ ,  $p < 0.01$ , interactions on central IL-6 (fig 5.1). Cortical and hippocampal IL-6 was significantly increased in all LPS treated groups relative to vehicle controls. Additionally, by 5 months of age, there was a significant increase in hippocampal IL-6 from  $0.51 \pm 0.175$  pg/mg tissue in LPS treated C57BL6/J mice to  $2.69 \pm 0.77$  pg/mg tissue in LPS treated TASTPM mice (431% increase,  $p < 0.001$ ). Cortical IL-6 levels also increased in LPS treated TASTPM relative to C57BL6/J mice at 5 months of age from  $1.1 \pm 0.263$  pg/mg tissue to  $1.73 \pm 0.41$  pg/mg tissue, however this was non-significant (58% increase,  $p = 0.188$ ).

Repeated measures ANOVA indicated an overall effect of age,  $F_{(2, 74)} = 74.4$ ,  $p < 0.001$ , and brain region,  $F_{(1, 74)} = 9.94$ ,  $p < 0.01$  on central IL-1 $\beta$  (fig 5.2). Post hoc planned comparisons revealed a significant age-dependent reduction in central IL-1 $\beta$  in C57BL6/J and TASTPM mice (2 vs. 5 & 10 months,  $p < 0.001$ ; 5 vs. 10 months,  $p < 0.01$ , both genotypes) and a significant difference between cortical and hippocampal IL-1 $\beta$  response ( $p < 0.01$ ).

Repeated measures ANOVA indicated an overall effect of age,  $F_{(2, 74)} = 47.63$ ,  $p < 0.001$ , brain region,  $F_{(1, 74)} = 12.88$ ,  $p < 0.001$  on central TNF- $\alpha$  (fig 5.3). Post hoc planned comparisons revealed a significant age-dependent reduction in central TNF- $\alpha$  in C57BL6/J and TASTPM mice (2 vs. 5 & 10 months,  $p < 0.001$ , both genotypes; 5 vs. 10 months,  $p = 0.01$ , C57BL6/J mice) and a significant difference between cortical and hippocampal TNF- $\alpha$  response ( $p < 0.001$ ).

Repeated measures ANOVA indicated an overall effect of age,  $F_{(2, 69)} = 15.07$ ,  $p < 0.001$ , genotype,  $F_{(1, 69)} = 30.26$ ,  $p < 0.001$ , and an age\*genotype interaction,  $F_{(2, 69)} = 10.46$ ,  $p < 0.001$ , on central MIP-1 $\alpha$  (fig 5.4). There was also a significant effect of brain region,  $F_{(1, 65)} = 16.55$ ,  $p < 0.001$ , and significant age\*brain region,  $F_{(2, 55)} = 9.09$ ,  $p < 0.001$ , and genotype\*brain region interactions,  $F_{(1, 55)} = 5.5$ ,  $p < 0.05$ . Post hoc planned comparisons revealed significant age-dependent changes in central MIP-1 $\alpha$  in C57BL6/J (2 vs. 5 months,  $p < 0.001$ ; 2 vs. 10 months,  $p < 0.01$ ; 5 vs. 10 months,  $p < 0.05$ ) and TASTPM mice (2 vs. 10 months,  $p < 0.01$ ; 5 vs. 10 months,  $p < 0.001$ ). There was also a significant overall difference between cortical and hippocampal MIP-1 $\alpha$  response irrespective of group ( $p < 0.001$ ). By 10 months of age, cortical ( $p < 0.01$ ) and hippocampal ( $p < 0.001$ ) MIP-1 $\alpha$  was significantly increased in vehicle treated TASTPM relative to vehicle treated C57BL6/J mice. Cortical and hippocampal MIP-1 $\alpha$  was increased by 5 months (cortical:  $p < 0.01$ , hippocampal:  $p < 0.001$ ) and 10 months ( $p < 0.001$ , both brain regions) in LPS treated TASTPM relative to LPS treated C57BL6/J mice.

Repeated measures ANOVA indicated an overall effect of age,  $F_{(2, 74)} = 62.38$ ,  $p < 0.001$ , brain region,  $F_{(1, 74)} = 28.93$ ,  $p < 0.001$ , and an age\*brain region interaction,  $F_{(2, 74)} = 17.62$ ,  $p < 0.001$  on IL-10 (fig 5.5). Post hoc planned comparisons revealed a significant age-related increase in central IL-10 in C57BL6/J and TASTPM mice (2 vs. 5 & 10 months,  $p < 0.001$ ; 5 vs. 10 months,  $p < 0.01$ , both genotypes) and a significant difference between cortical and hippocampal IL-10 response ( $p < 0.001$ ).

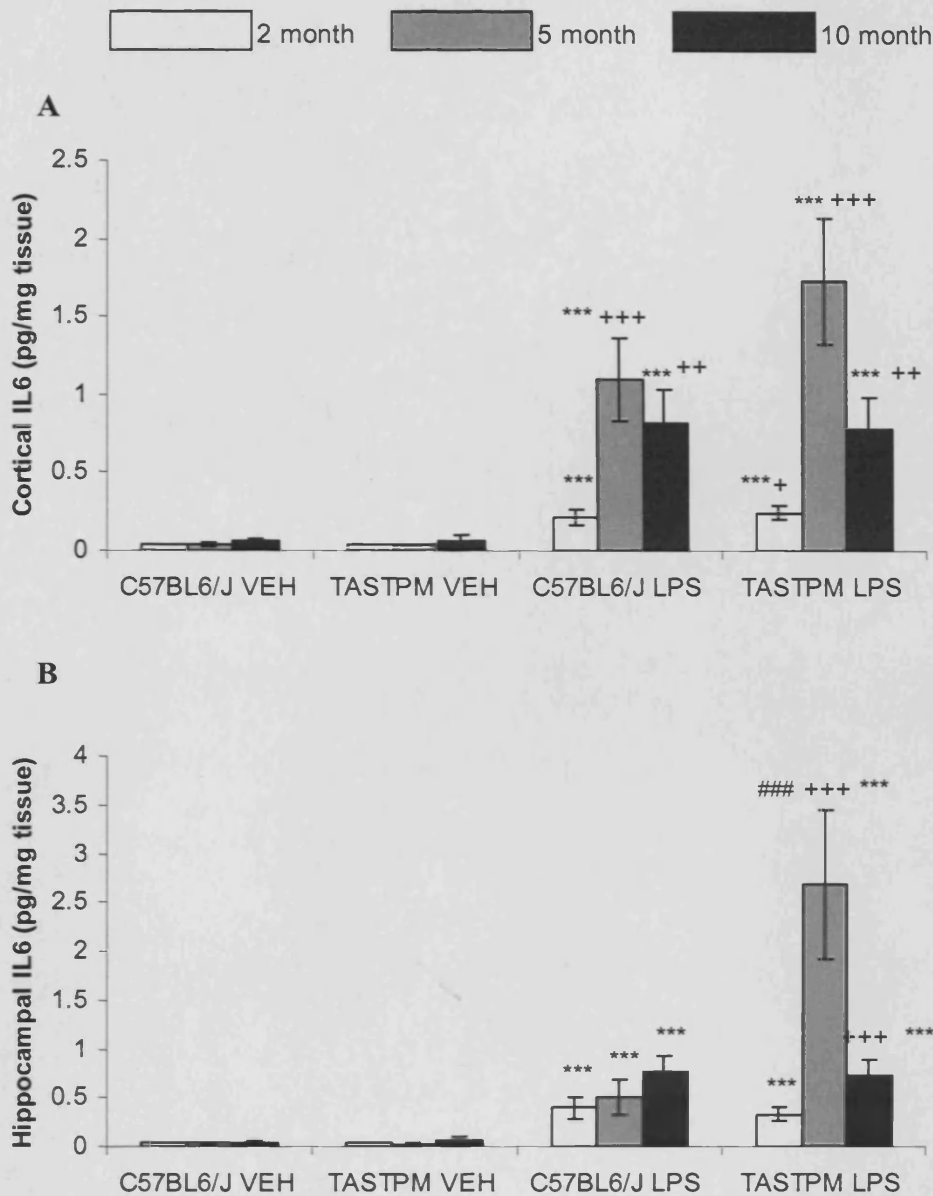


Figure 5.1: IL6 protein in the cortex (A), hippocampus (B) of a C57BL6/J control or TASTPM transgenic mouse (n=6-9 per group) by 2.5 hours post a single IP LPS administration, data represented as cytokine protein (pg) per milligram of tissue and shows mean  $\pm$  SEM (\*\*\*)  $p \leq 0.001$  vs. respective vehicle group, +++  $p \leq 0.001$ , ++  $p \leq 0.01$  vs. 2 month within treatment, +  $p \leq 0.05$  vs. 5 month within group) (repeated measures ANOVA followed by planned comparisons)

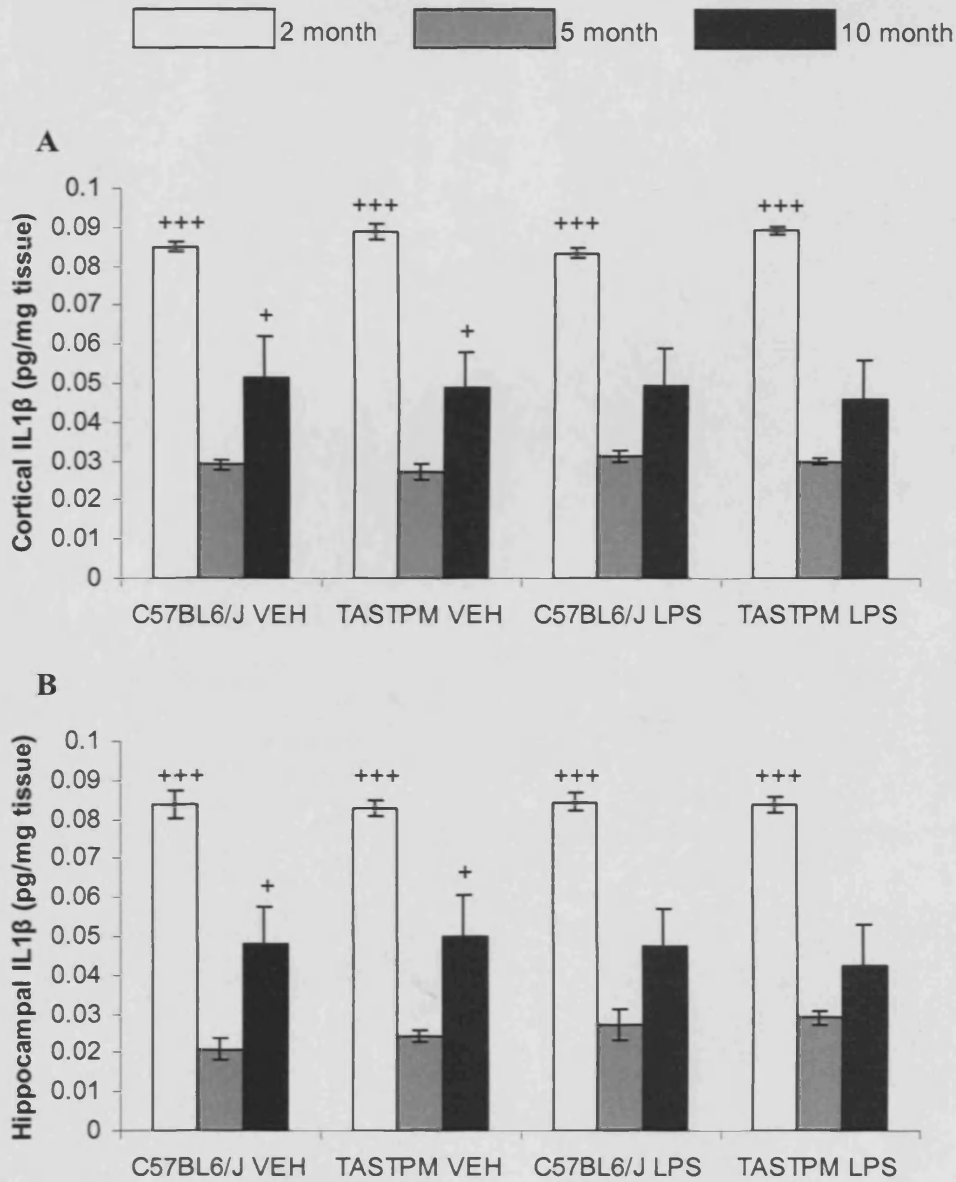


Figure 5.2 IL1 $\beta$  protein in the cortex (A), hippocampus (B) of a C57BL6/J control or TASTPM transgenic mouse (n=6-9 per group) by 2.5 hours post a single IP LPS administration, data represented as cytokine protein (pg) per milligram of tissue and shows mean  $\pm$  SEM. +++  $p \leq 0.00$  vs. 5 & 10 month within group, +  $p \leq 0.05$  vs. 5 month within group (repeated measures ANOVA followed by planned comparisons)

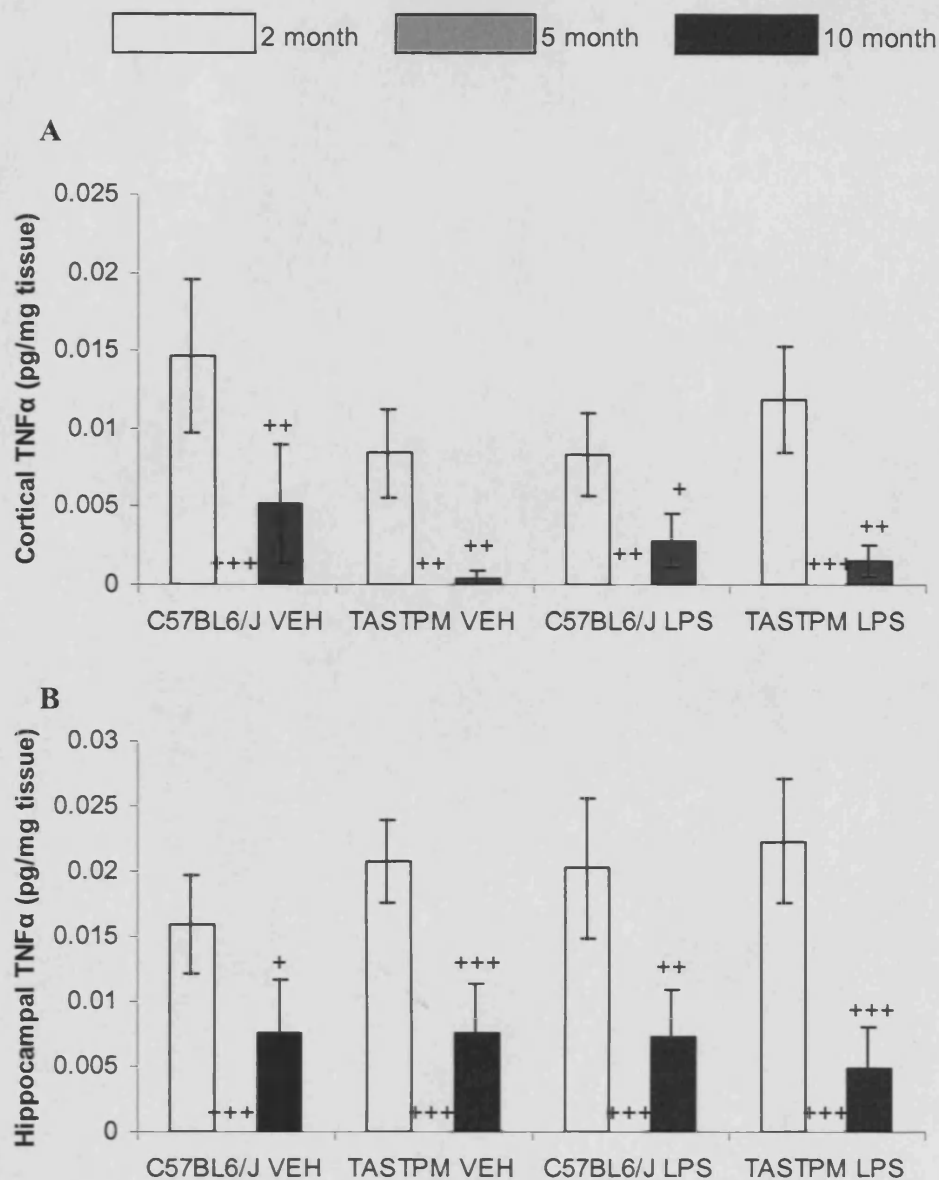


Figure 5.3: TNF $\alpha$  protein in the cortex (A), hippocampus (B) of a C57BL6/J control or TASTPM transgenic mouse (n=6-9 per group) by 2.5 hours post a single IP LPS administration, data represented as cytokine protein (pg) per milligram of tissue and shows mean  $\pm$  SEM. +++ p  $\leq$  0.001, ++ p  $\leq$  0.01, + p  $\leq$  0.05 vs. 2 month within group (repeated measures ANOVA followed by planned comparisons)

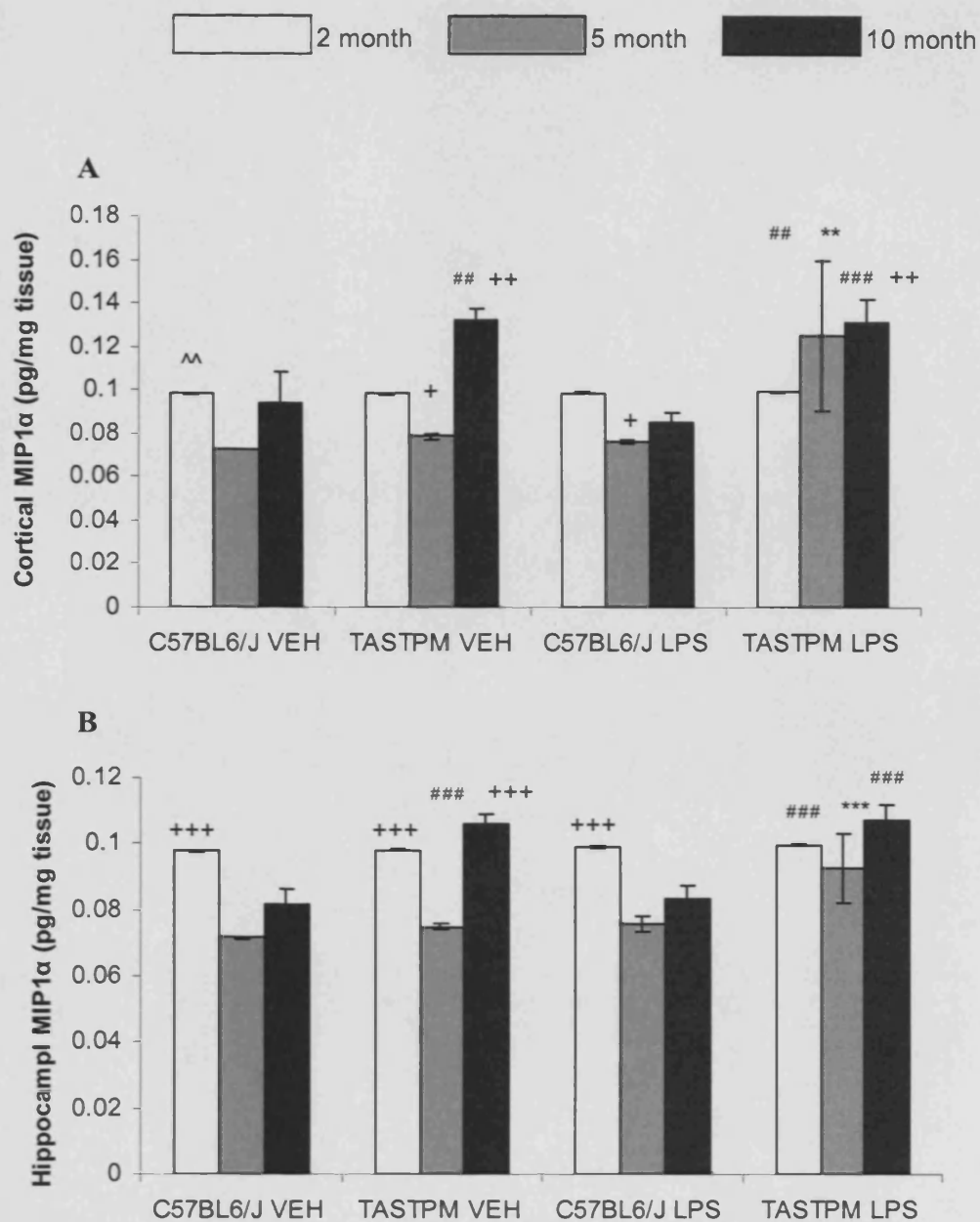


Figure 5.4: MIP1 $\alpha$  protein in the cortex (A), hippocampus (B) of a C57BL6/J control or TASTPM transgenic mouse (n=6-9 per group) by 2.5 hours post a single IP LPS administration, data represented as cytokine protein (pg) per milligram of tissue and shows mean  $\pm$  SEM. \*\*\*  $p \leq 0.001$ , \*\*  $p \leq 0.01$  vs. respective vehicle group, +++  $p \leq 0.001$  vs. 5 months within group, ++  $p \leq 0.01$ , +  $p \leq 0.05$  vs. 2 month within group, ^  $p \leq 0.01$  vs. 5 month within group, ###  $p \leq 0.001$ , ##  $p \leq 0.01$  vs. respective C57BL6/J within age group (repeated measures ANOVA followed by planned comparisons)

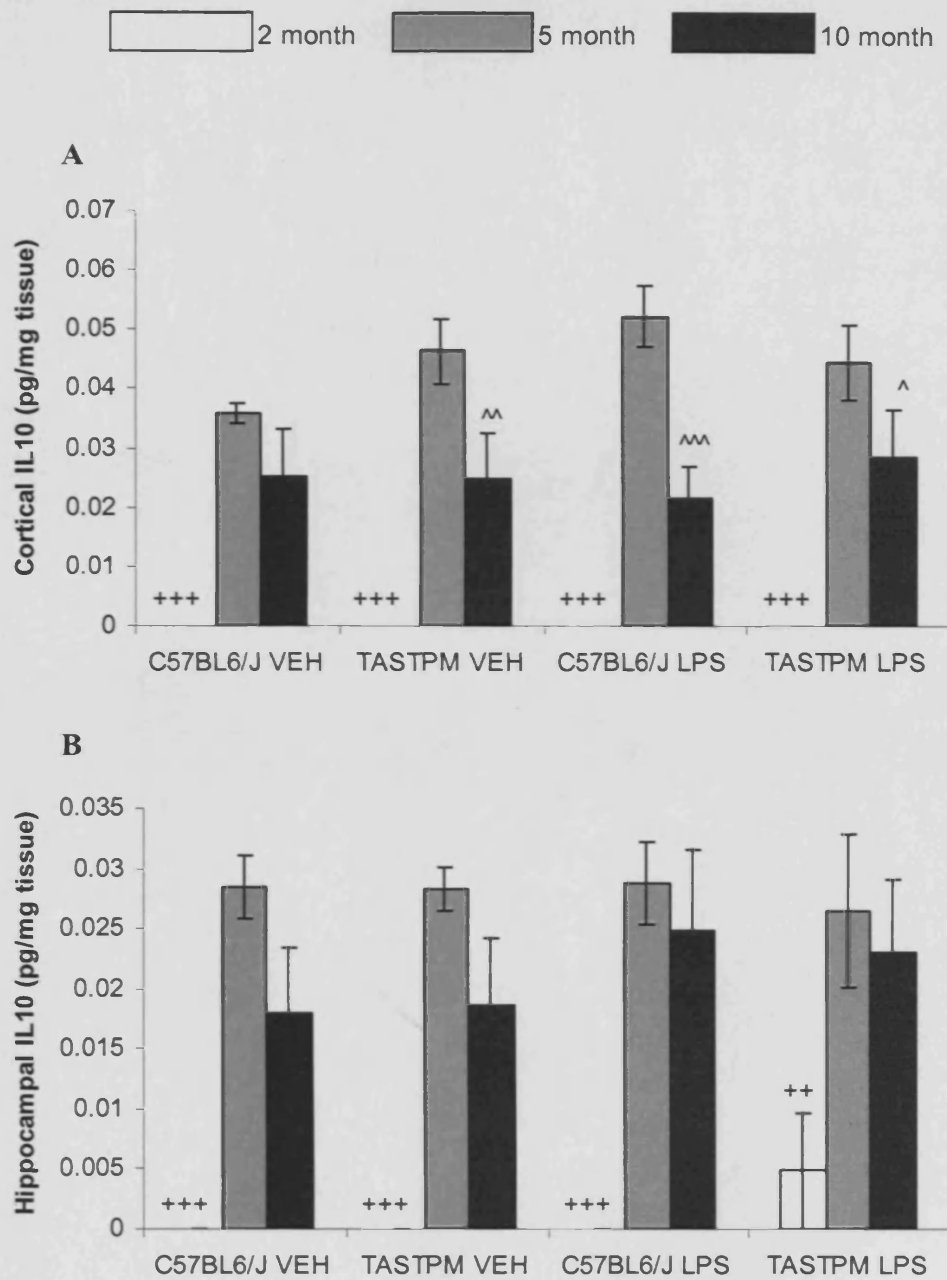


Figure 5.5: IL10 protein in the cortex (A), hippocampus (B) of a C57BL6/J control or TASTPM transgenic mouse (n=6-9 per group) by 2.5 hours post a single IP LPS administration, data represented as cytokine protein (pg) per milligram of tissue and shows mean  $\pm$  SEM. +++ p  $\leq$  0.001, ++ p  $\leq$  0.01 vs. 5 & 10 month within group, ^^ p  $\leq$  0.001, ^^ p  $\leq$  0.01, ^ p  $\leq$  0.05 vs. 5 month within group (repeated measures ANOVA followed by planned comparisons)

#### 5.4.1.2 Cytokine protein in plasma

Univariate ANOVA demonstrated an overall effect of treatment on plasma IL-1 $\beta$  (fig 5.6),  $F_{(1, 72)} = 65.56$ ,  $p < 0.001$ , IL-6 (fig 5.7A),  $F_{(1, 72)} = 303.35$ ,  $p < 0.001$ , TNF- $\alpha$  (fig 5.7B),  $F_{(1, 72)} = 125.11$ ,  $p < 0.001$ , MIP-1 $\alpha$  (fig 5.8A),  $F_{(1, 73)} = 178.05$ ,  $p < 0.001$ , and IL-10 (fig 5.8B),  $F_{(1, 74)} = 76.71$ ,  $p < 0.001$ . There were also significant treatment\*genotype,  $F_{(1, 72)} = 9.19$ ,  $p < 0.01$  and treatment\*age\*genotype,  $F_{(2, 73)} = 3.13$ ,  $p < 0.05$ , interactions on IL-1 $\beta$  and MIP-1 $\alpha$  respectively and an effect of age on IL-10,  $F_{(2, 74)} = 5.78$ ,  $p < 0.01$ . Plasma IL-6, IL-1 $\beta$ , TNF- $\alpha$ , MIP-1 $\alpha$  and IL-10 protein was induced by LPS in C57BL6/J and TASTPM mice, although by 5 and 10 months of age, the increase in plasma IL-1 $\beta$  in LPS treated TASTPM relative to vehicle treated TASTPM mice failed to reach significance at the  $p < 0.05$  level ( $p = 0.09$  and  $p = 0.06$  respectively). LPS treated TASTPM mice also exhibited a significantly stunted IL-1 $\beta$  response relative to LPS treated C57BL6/J controls by 2 months of age from  $30.49 \pm 2.49$  pg/ml to  $18.06 \pm 3.76$  pg/ml (40% reduction,  $p < 0.01$ ). Although plasma IL-1 $\beta$  was also decreased in LPS treated TASTPM relative to LPS treated C57BL6/J mice by 5 and 10 months of age, this failed to reach significance at the  $p < 0.05$  level (5 months:  $p = 0.17$ ; 10 months:  $p = 0.07$ ).

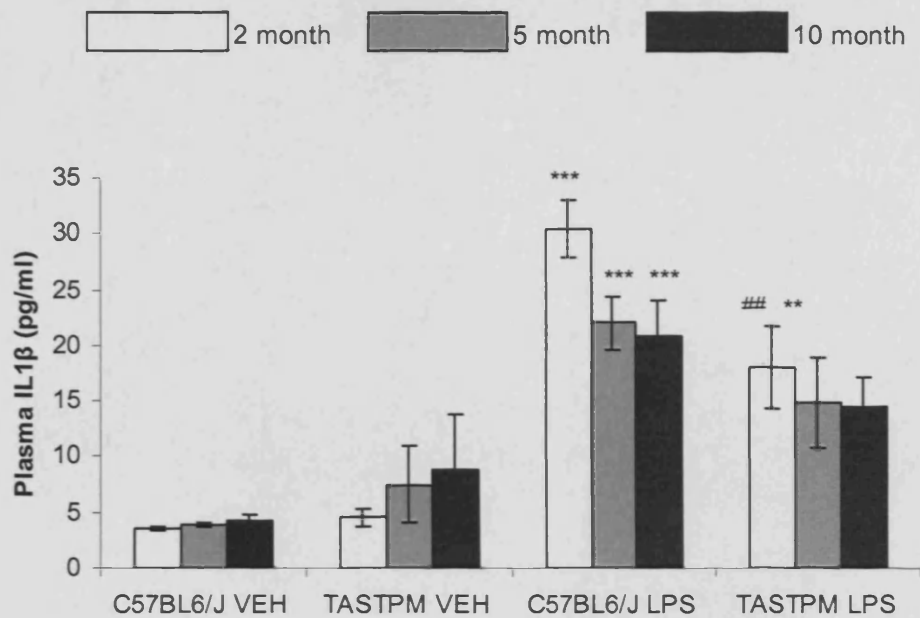


Figure 5.6: IL1 $\beta$  protein in plasma of a C57BL6/J control or TASTPM transgenic mouse (n=6-9 per group) by 2.5 hours post a single IP LPS administration, data represented as cytokine protein (pg) per millilitre of sample and shows mean  $\pm$  SEM. ##  $p \leq 0.01$  vs. 2 month C57BL6/J LPS, \*\*\*  $p \leq 0.001$ , \*\*  $p \leq 0.01$  vs. respective vehicle group (univariate ANOVA followed by planned comparisons)

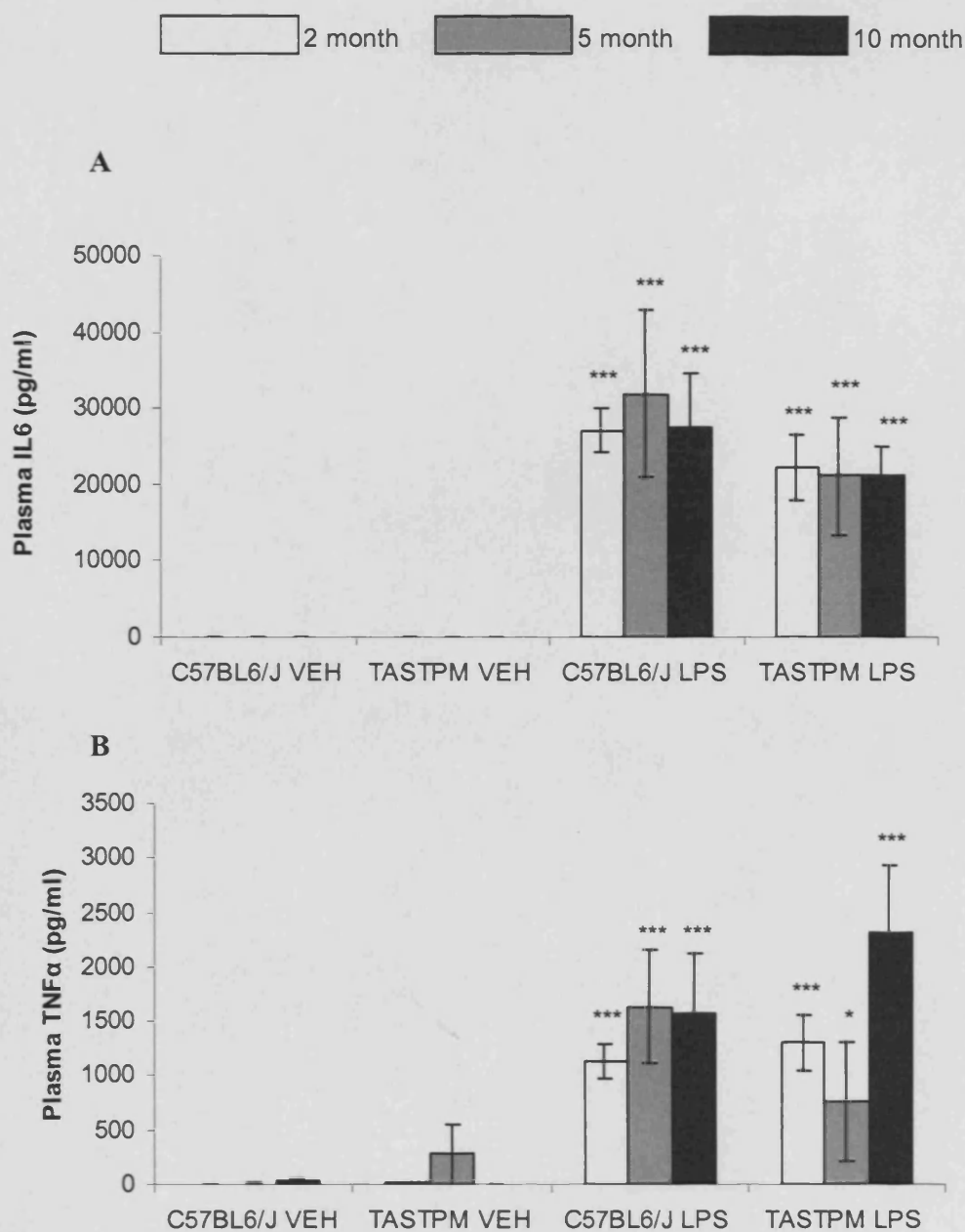


Figure 5.7: IL6 (A) and TNF $\alpha$  (B) protein in plasma of a C57BL6/J control or TASTPM transgenic mouse (n=6-9 per group) by 2.5 hours post a single IP LPS administration, data represented as cytokine protein (pg) per millilitre of sample and shows mean  $\pm$  SEM. \*\*\* p  $\leq$  0.001, \* p  $\leq$  0.05 vs. respective vehicle group (univariate ANOVA followed by planned comparisons)

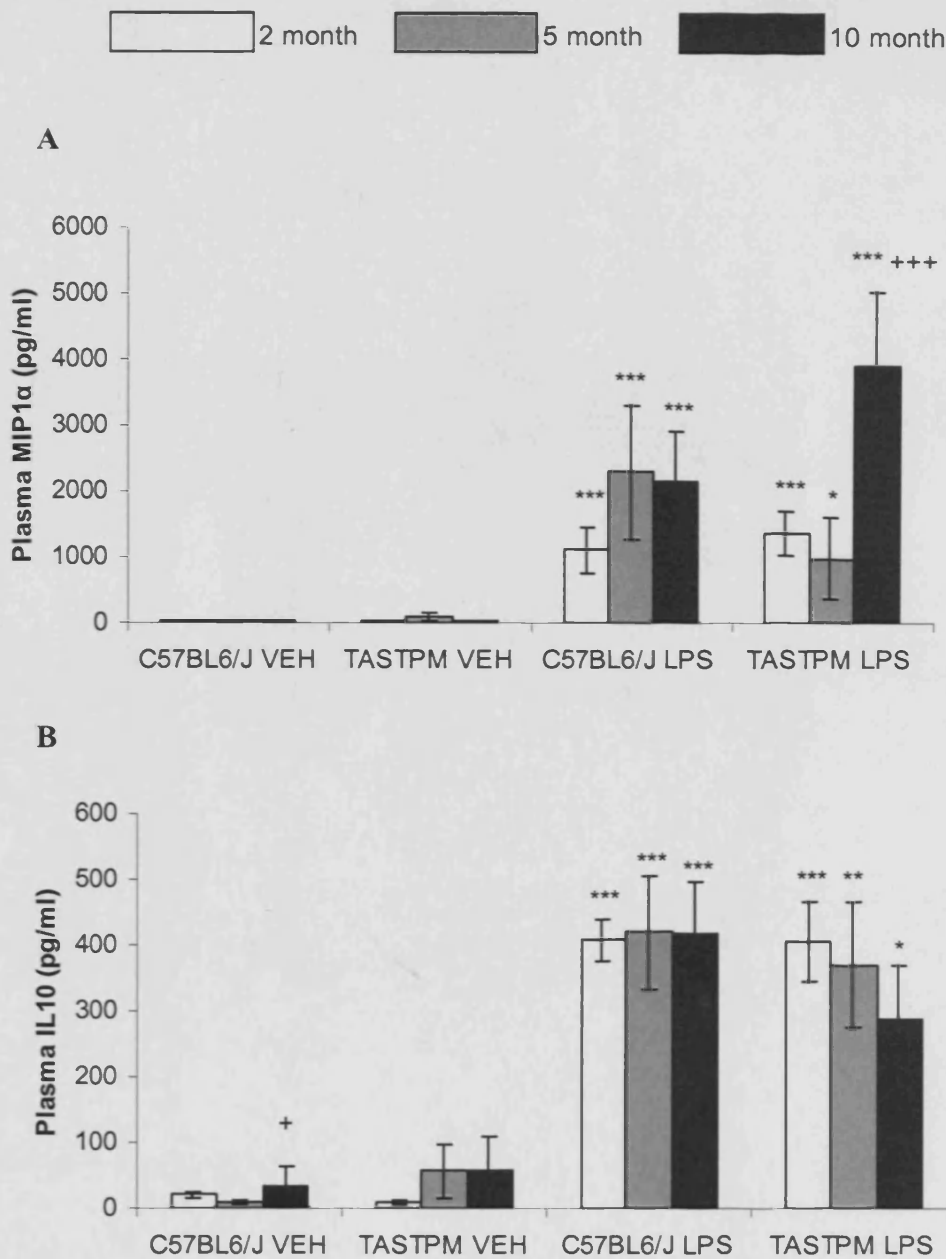


Figure 5.8: MIP-1 $\alpha$  (A) and IL-10 (B) protein in plasma of a C57BL6/J control or TASTPM transgenic mouse (n=6-9 per group) by 2.5 hours post a single IP LPS administration, data represented as cytokine protein (pg) per millilitre of sample and shows mean  $\pm$  SEM. \*\*\*  $p \leq 0.001$ , \*\*  $p \leq 0.01$ , \*  $p \leq 0.05$  vs. respective vehicle group, +++  $p \leq 0.001$  vs. 5 month TASTPM LPS, +  $p \leq 0.05$  vs. 2 month C57BL6/J VEH (univariate ANOVA followed by planned comparisons)

## 5.4.2 *Study 14: Repeated LPS administration of TASTPM mice*

### 5.4.2.1 *Cytokine protein in brain at 48 hours*

Repeated measures ANOVA revealed no overall effect of treatment on IL-6,  $F_{(1, 23)} = 0.00$ ,  $p = 0.97$ , IL-1 $\beta$ ,  $F_{(1, 23)} = 0.07$ ,  $p = 0.80$ , TNF- $\alpha$ ,  $F_{(1, 23)} = 0.50$ ,  $p = 0.49$  or MIP-1 $\alpha$ ,  $F_{(1, 23)} = 0.83$ ,  $p = 0.37$  on cytokine protein in brain tissue 48hrs after the final administration of IP LPS (fig 5.9A & B). There was also no overall effect of genotype on IL-6,  $F_{(1, 23)} = 1.88$ ,  $p = 0.18$ , IL-1 $\beta$ ,  $F_{(1, 23)} = 1.81$ ,  $p = 0.19$ , TNF- $\alpha$ ,  $F_{(1, 23)} = 1.77$ ,  $p = 0.20$  or MIP-1 $\alpha$ ,  $F_{(1, 23)} = 0.79$ ,  $p = 0.38$ . An overall treatment\*genotype interaction was evident in central IL-1 $\beta$ ,  $F_{(1, 23)} = 4.82$ ,  $p < 0.05$ . Planned comparisons revealed vehicle treated TASTPM transgenic mice exhibited significantly higher cortical IL-1 $\beta$  relative to vehicle treated C57BL6/J animals ( $p < 0.01$ , 34% increase). The elevation of cortical IL-1 $\beta$  in this group was not significant relative to either LPS treated C57BL6/J or transgenic animals.

### 5.4.2.2 *Cytokine protein in plasma at 2.5hrs*

Univariate ANOVA analysis of each cytokine revealed an overall effect of treatment on plasma IL-1 $\beta$ ,  $F_{(1, 49)} = 17.05$ ,  $p < 0.001$ , TNF- $\alpha$ ,  $F_{(1, 49)} = 35.22$ ,  $p < 0.001$ , MIP-1 $\alpha$ ,  $F_{(1, 49)} = 22.74$ ,  $p < 0.001$  and IL-6,  $F_{(1, 48)} = 34.37$ ,  $p < 0.001$  (fig 5.10A & B). Levels of plasma IL10 were below the lower limit of detection for all groups. Post hoc planned comparisons revealed that LPS administration induced a 120% ( $p < 0.001$ ) and a 421% ( $p < 0.001$ ) increase in IL-1 $\beta$  and TNF- $\alpha$  in C57BL6/J and a 127% ( $p = 0.08$ ) and 257% ( $p < 0.01$ ) increase in IL-1 $\beta$  and TNF- $\alpha$  in TASTPM mice. Plasma IL-1 $\beta$  was significantly decreased in LPS treated TASTPM relative to LPS treated C57BL6/J mice ( $p < 0.05$ ). IP LPS increased MIP-1 $\alpha$  and IL-6 in both C57BL6/J (620% and 18439%, respectively,  $p < 0.001$  both groups) and TASTPM (455% ( $p < 0.01$ ) and 2083% ( $p < 0.001$ ) respectively) mice.

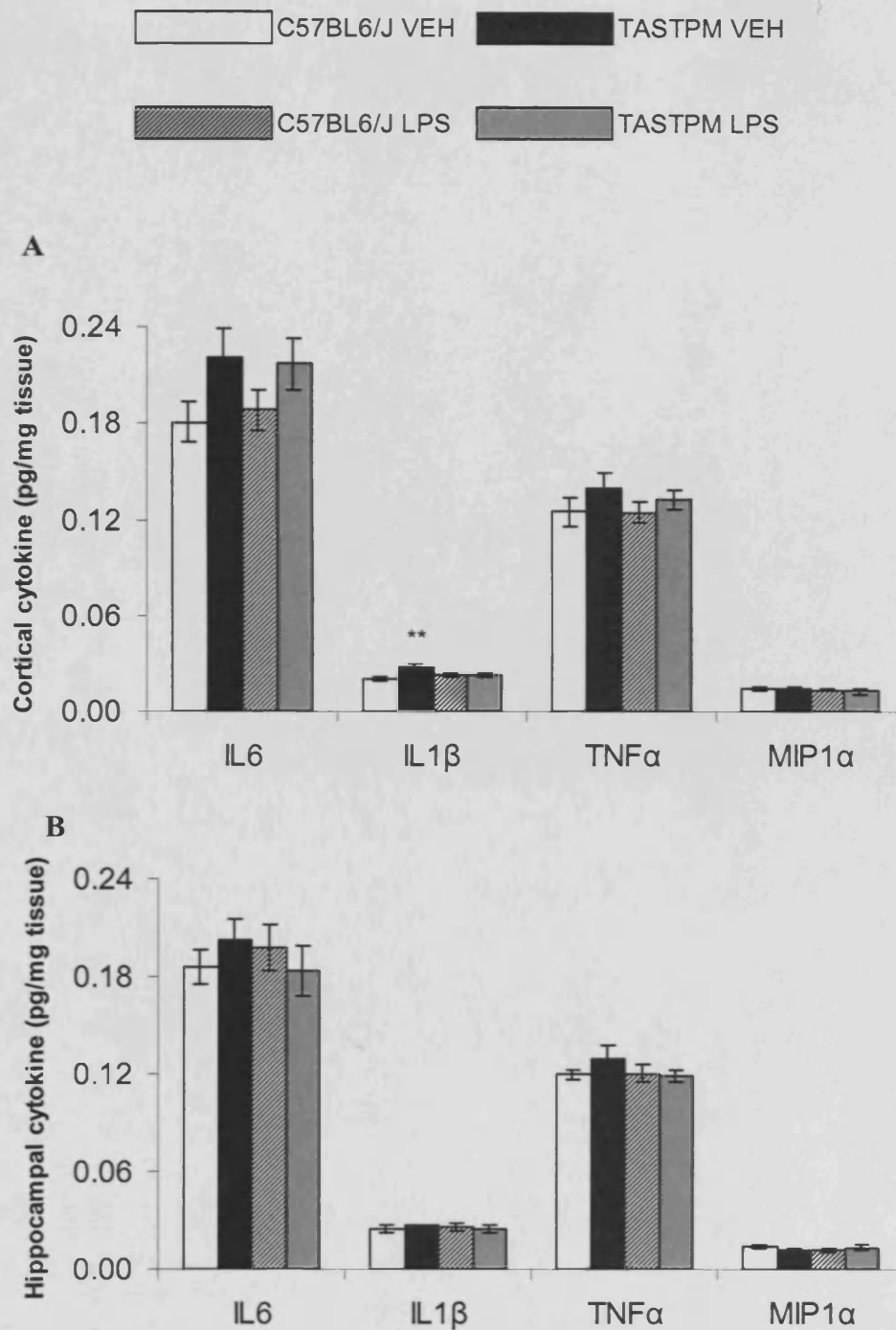


Figure 5.9: Effect of repeated IP administration of LPS on cytokine protein in the cortex (A), hippocampus (B) of C57BL6/J and TASTPM mice (n=10-12 per group) by 48 hours post the last IP LPS administration, data represented as cytokine protein (pg) per milligram of tissue and shows mean  $\pm$  SEM. \*\*  $p \leq 0.01$  vs. vehicle (repeated measures ANOVA followed by planned comparisons)

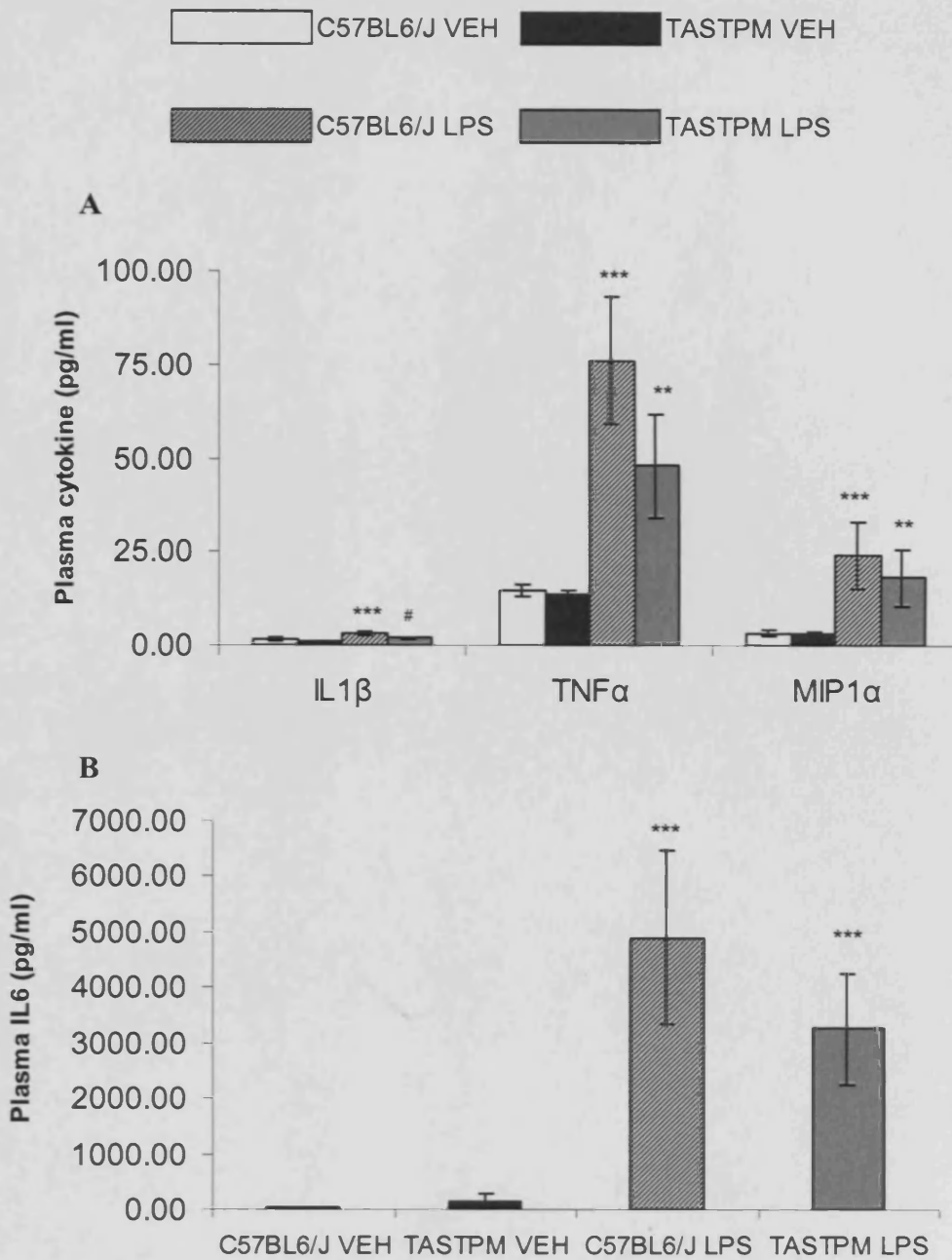


Figure 5.10: Effect of repeated IP administration of LPS on plasma IL1 $\beta$ , TNF $\alpha$ , and MIP1 $\alpha$  protein (A) and plasma IL6 protein (B) of C57BL6/J and TASTPM mice (n=10-12 per group) by 2.5 hours post the last IP LPS administration, data represented as cytokine protein (pg) per millilitre of sample and shows mean  $\pm$  SEM. \*  $p \leq 0.05$ , \*\*  $p \leq 0.01$ , \*\*\*  $p \leq 0.001$  vs. vehicle, #  $p \leq 0.05$  vs. C57BL6/J LPS (univariate ANOVA followed by planned comparisons)

### 5.4.2.3 Cytokine protein in plasma at 48hrs

Univariate analysis of cytokine production by 48 hours following the last IP LPS administration revealed no overall effect of treatment on plasma IL-6,  $F_{(1,46)} = 3.19$ ,  $p = 0.08$ , IL-1 $\beta$ ,  $F_{(1,46)} = 0.08$ ,  $p = 0.77$ , TNF- $\alpha$ ,  $F_{(1,49)} = 1.50$ ,  $p = 0.31$  or MIP-1 $\alpha$ ,  $F_{(1,49)} = 0.49$ ,  $p = 0.49$  and no overall effect of genotype on plasma IL-6,  $F_{(1,46)} = 2.80$ ,  $p = 0.10$ , IL-1 $\beta$ ,  $F_{(1,46)} = 0.02$ ,  $p = 0.90$ , TNF- $\alpha$ ,  $F_{(1,49)} = 0.11$ ,  $p = 0.74$  or MIP-1 $\alpha$ ,  $F_{(1,49)} = 0.16$ ,  $p = 0.69$ , cytokine protein (fig 5.11).

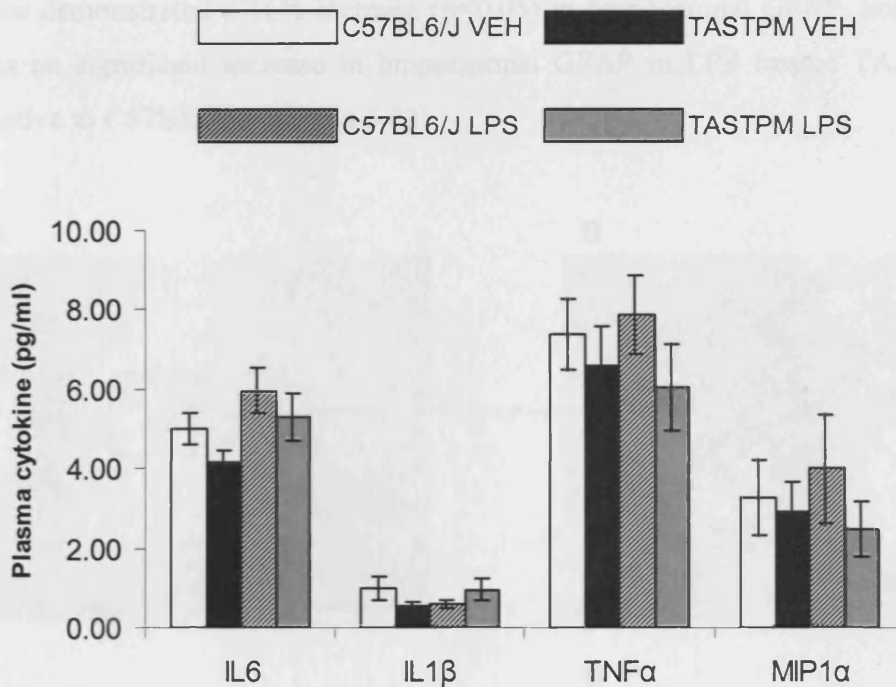


Figure 5.11: Effect of repeated IP administration of LPS on plasma IL6, IL1 $\beta$ , TNF $\alpha$ , and MIP1 $\alpha$  protein of C57BL6/J and TASTPM mice (n=10-12 per group) by 48 hours post the last IP LPS administration, data represented as cytokine protein (pg) per millilitre of sample and shows mean  $\pm$  SEM (univariate ANOVA followed by planned comparisons)

#### 5.4.2.4 Cell-mediated neuroinflammation

Repeated measures ANOVA revealed a significant effect of genotype,  $F_{(1, 46)} = 50.00$ ,  $p < 0.001$  (fig 5.12). There were also significant effects of brain region,  $F_{(1, 46)} = 485.82$ ,  $p < 0.001$  and a significant brain region\*genotype interaction,  $F_{(3, 46)} = 22.19$ ,  $p < 0.001$ . LPS treatment of both C57BL6/J control and TASTPM transgenic mice failed to induce a significant increase in GFAP. Vehicle treated and LPS treated TASTPM mice exhibited a 635% and a 198% increase in cortical GFAP respectively relative to C57BL6/J controls ( $p < 0.001$ , both groups). Vehicle treated TASTPM mice demonstrated a 16% increase ( $p < 0.05$ ) in hippocampal GFAP, however, there was no significant increase in hippocampal GFAP in LPS treated TASTPM mice relative to C57BL6/J mice (fig 5.13).

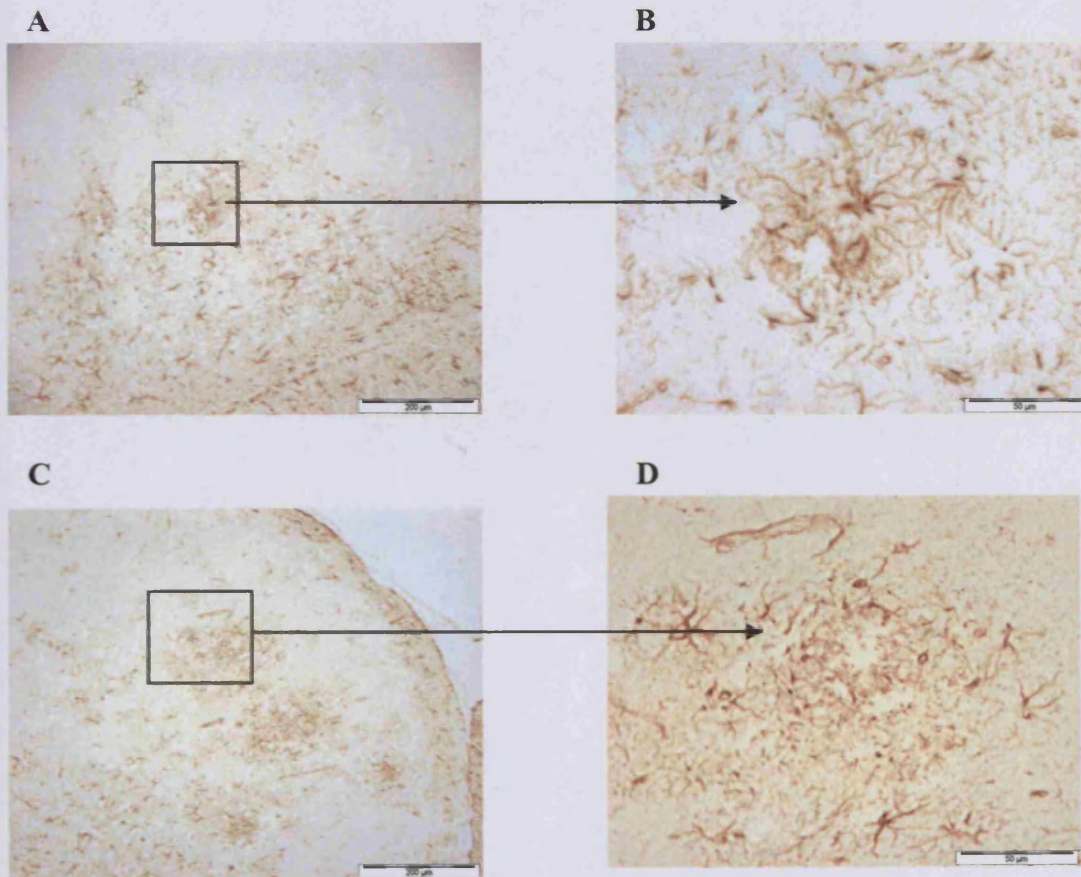


Figure 5.12: Representative photomicrographs of coronal sections of the hippocampus and cortex stained for GFAP in vehicle TASTPM (A, B) and LPS TASTPM (C, D) mice ( $n=10-12$  per group) following repeated IP administration of LPS, scale bar represents 200µmetres and 50µmetres

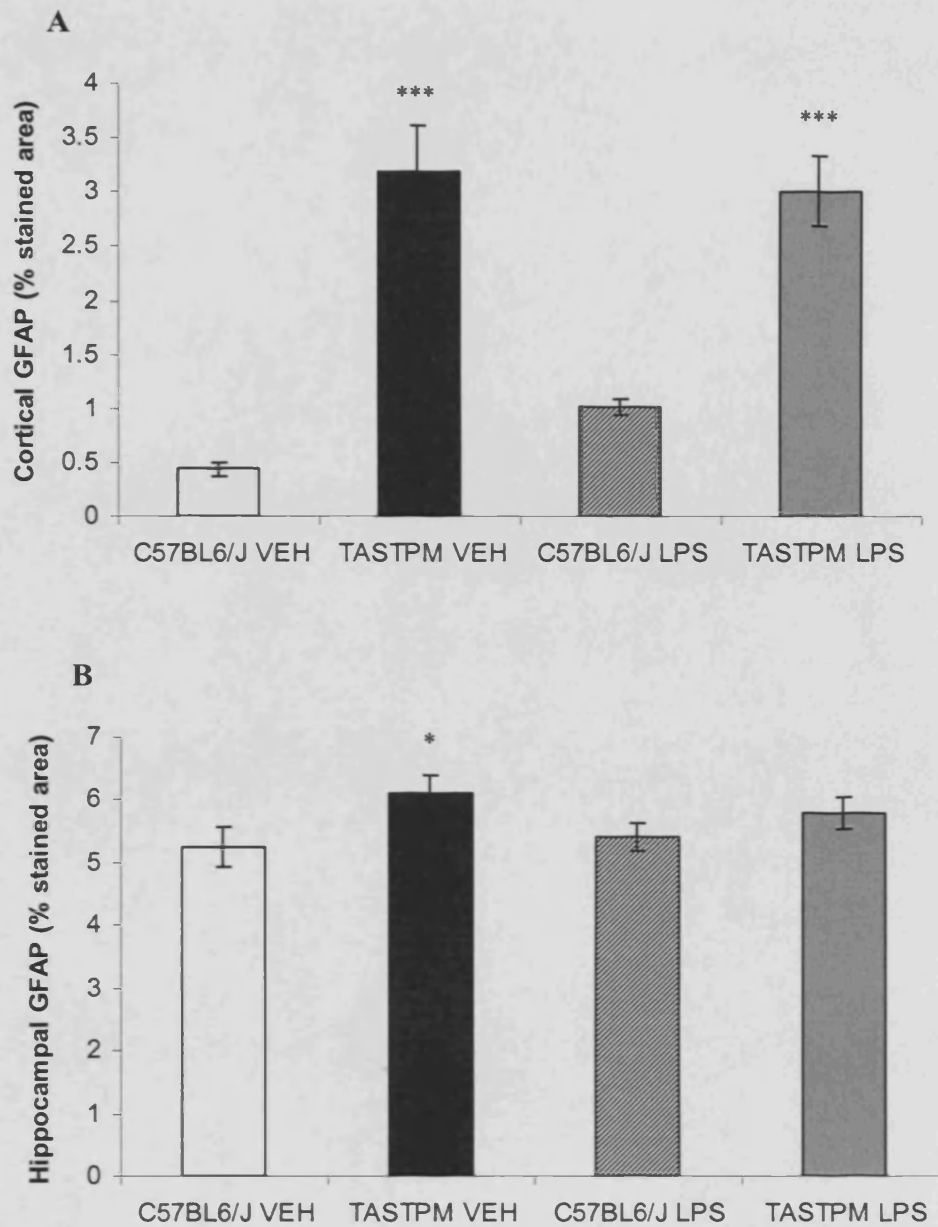


Figure 5.13: Effect of repeated IP administration of LPS on GFAP in the cortex (A) and hippocampus (B) in C57BL6/J or TASTPM mice (n=10-12 per group), data represented as percentage stained area and shows mean  $\pm$  SEM. \*  $p \leq 0.05$ , \*\*\*  $p \leq 0.001$  vs. vehicle (univariate ANOVA followed by planned comparisons)

Qualitative analysis of the presence of microglia in brain tissue indicated no obvious differences in numbers or size of CD68 positive cells (fig 5.14). There was no activated microglia present in the C57BL6/J mice.

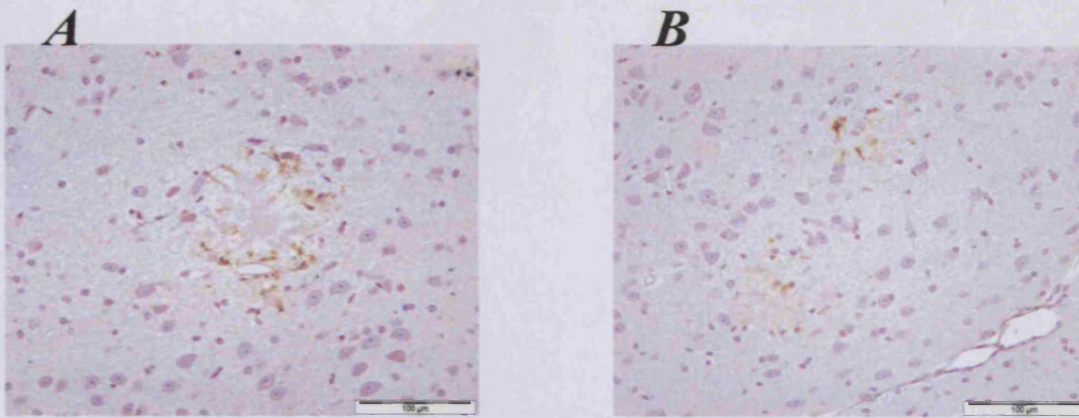


Figure 5.14: Representative photomicrographs of coronal sections of the hippocampus and cortex stained for CD68 in vehicle TASTPM (A) and LPS TASTPM (B) mice (n=10-12 per group) following repeated IP administration of LPS, scale bar represents 100µmetres

#### 5.4.2.5 $A\beta$ load

Analysis of  $A\beta$  load in the brain of LPS TASTPM mice revealed an overall effect of genotype on  $A\beta$ 1-40,  $F_{(1, 21)} = 299.48$ ,  $p < 0.001$ , and  $A\beta$ 1-42,  $F_{(1, 21)} = 145.00$ ,  $p < 0.001$  (fig. 5.15). TASTPM mice exhibited significantly higher  $A\beta$  load than C57BL6/J mice, regardless of treatment. There was no overall effect of treatment on  $A\beta$ 1-40,  $F_{(1, 21)} = 0.57$ ,  $p = 0.46$ , or  $A\beta$ 1-42,  $F_{(1, 21)} = 1.76$ ,  $p = 0.199$ . There was also no difference in numbers of  $A\beta$  plaques observed by immunohistochemistry between vehicle and LPS treated TASTPM mice (fig 5.16 & 5.17).

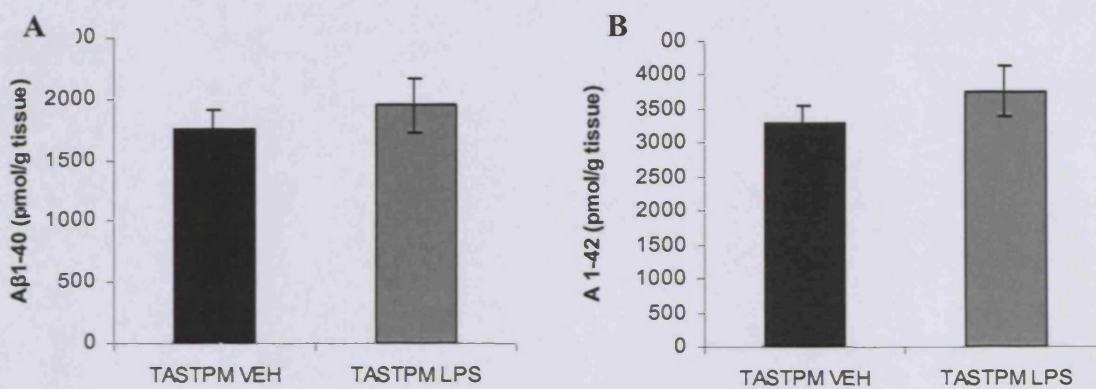


Figure 5.15: Effect of repeated IP administration of LPS on brain  $A\beta$ 1-40 (A) and  $A\beta$ 1-42 (B) in TASTPM mice (n=10-12), data represented as pmol of  $A\beta$  per gram of tissue and shows mean  $\pm$  SEM (univariate ANOVA followed by planned comparisons)

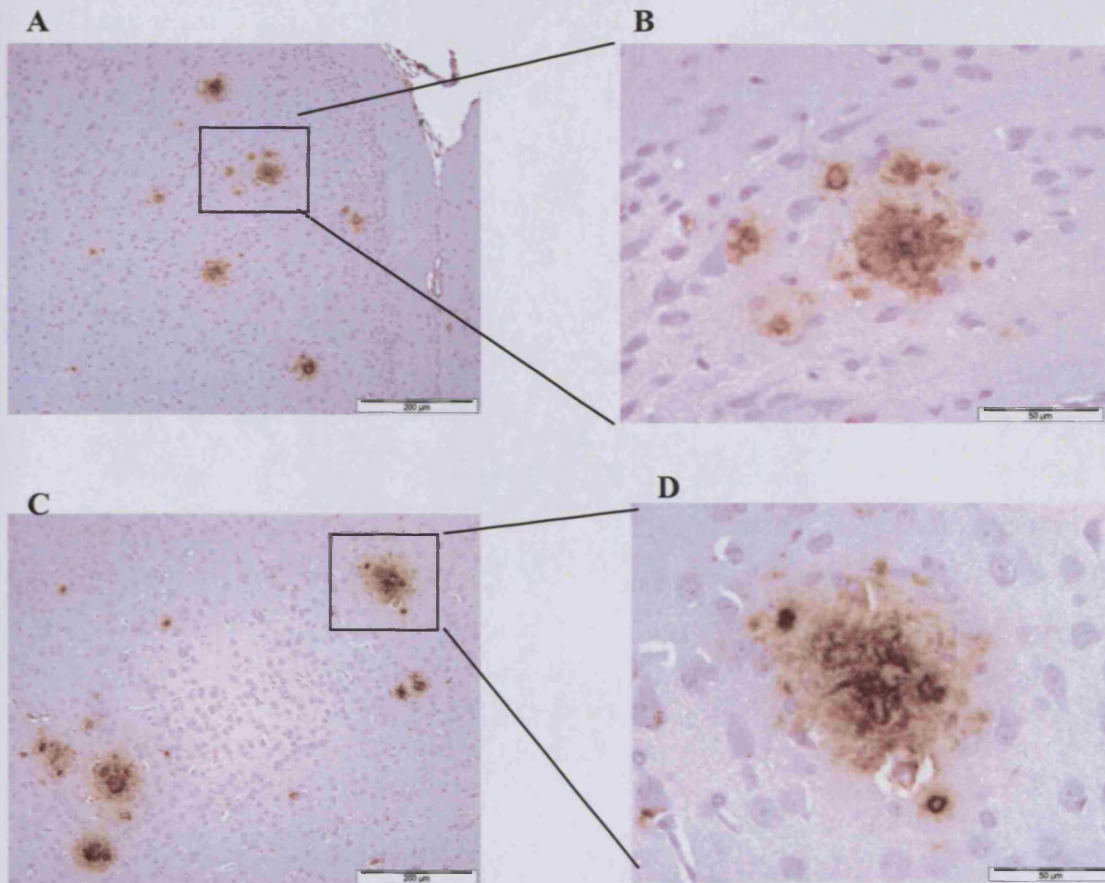


Figure 5.16: Representative photomicrographs of coronal sections of the cortex stained for A $\beta$  deposits in vehicle TASTPM (A, B) and LPS TASTPM (C, D) mice (n=10-12 per group) following repeated IP administration of LPS, scale bar represents 100 $\mu$ metres

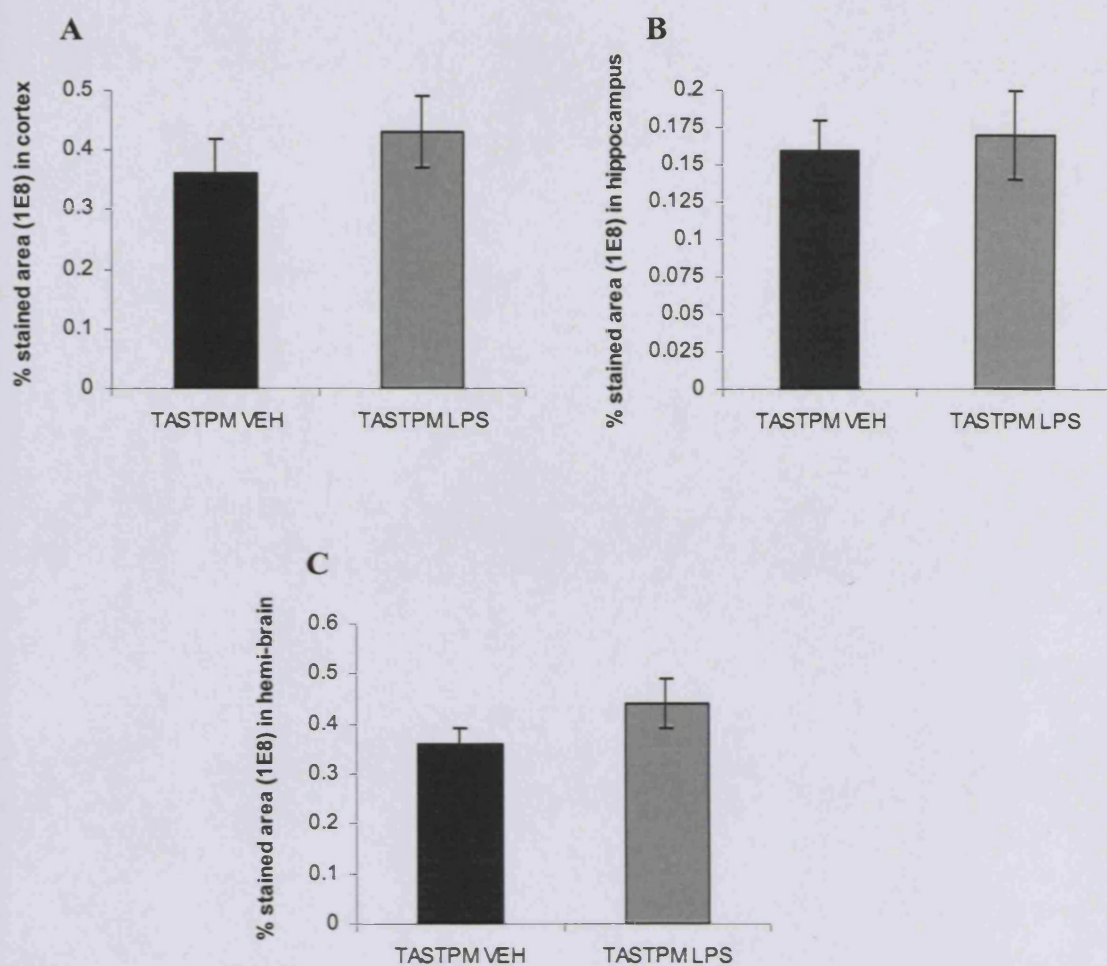


Figure 5.17: Effect of repeated IP administration of LPS on A $\beta$  load in the cortex (A), hippocampus (B) and whole brain (C) of C57BL6J and TASTPM mice (n=10-12 per group), data represented as percentage stained area and shows mean  $\pm$  SEM (univariate ANOVA followed by planned comparisons)

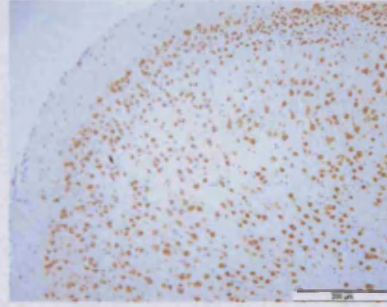
#### 5.4.2.6 *NeuN*

There was no effect of genotype,  $F_{(1, 47)} = 0.00$ ,  $p=0.95$  or LPS treatment,  $F_{(1, 47)} = 0.18$ ,  $p=0.68$  (fig. 5.18) on neurons as quantified by an assessment of the percentage area covered by NeuN positive stained cells in cortical and hippocampal regions (fig 5.19).

**A VEHICLE C57BL6/J**



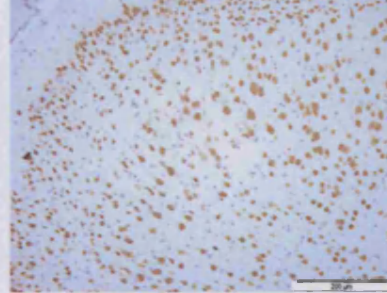
**B VEHICLE C57BL6/J**



**C VEHICLE TASTPM**



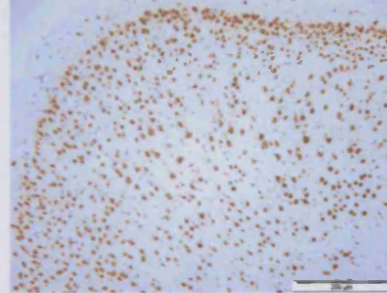
**D VEHICLE TASTPM**



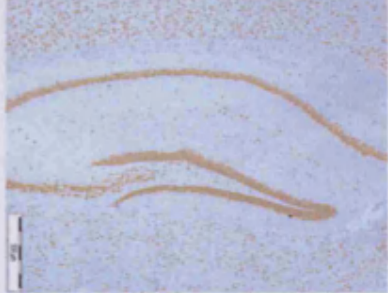
**E LPS C57BL6/J**



**F LPS C57BL6/J**



**G LPS TASTPM**



**H LPS TASTPM**

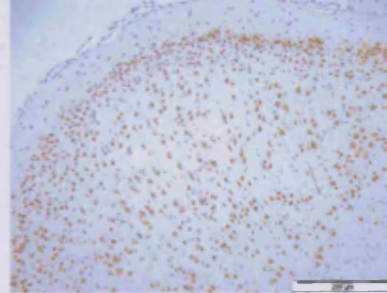


Figure 5.18: Representative photomicrographs of coronal sections of the hippocampus and cortex stained for NeuN positive cells in vehicle C57BL6/J (A, B) and TASTPM (C, D) mice and LPS treated C57BL6/J (E, F) and TASTPM (G, H) TASTPM mice (n=10-12 per group), scale bar represents 500µmetres (A, C, E, G) and (B, D, F, H) 200µmetres

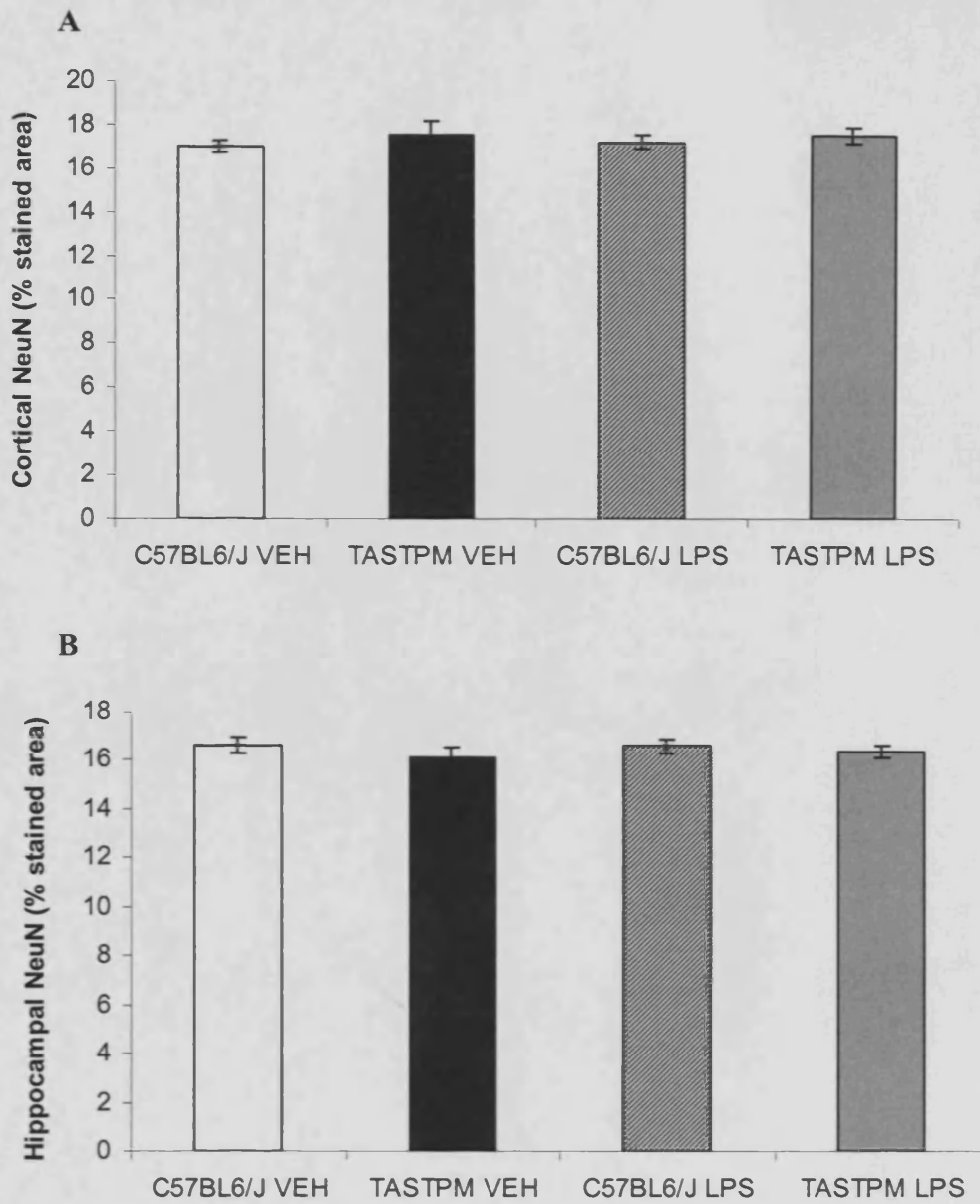


Figure 5.19: Effect of repeated IP administration of LPS on NeuN staining in the cortex (A) and hippocampus (B) of C57BL6J and TASTPM mice (n=10-12 per group), data represented as percentage stained area and shows mean  $\pm$  SEM (univariate ANOVA followed by planned comparisons)

## 5.5 Discussion

### 5.5.1 *LPS induced neuroinflammation - APP/PS1 transgenic mice*

Administration of a single dose of LPS shown to induce a small increase in central cytokine protein in C57BL6/J controls resulted in alteration of the neuroinflammatory profile of TASTPM APP/PS1 mutant mice. Interestingly, the primary effect of LPS was evident on the chemokine, MIP-1 $\alpha$ . Cortical and hippocampal MIP-1 $\alpha$  was increased in vehicle treated TASTPM relative to vehicle treated C57BL6/J mice by 10 months of age (fig 5.4). Cortical and hippocampal MIP-1 $\alpha$  was increased by 5 months and 10 months in LPS treated TASTPM relative to LPS treated C57BL6/J mice (fig 5.4). Central MIP-1 $\alpha$  remained unaltered in C57BL6/J mice, regardless of treatment or age, indicating a genotype-specific increase of MIP-1 $\alpha$  in TASTPM brain tissue. This supports previous literature describing the increase of pre-existing MIP-1 $\alpha$  mRNA expression in brain tissue following IP administration of LPS, at an age when A $\beta$  plaques and associated activated microglia were evident in the brains of APP overexpressing mice (Tg2576) (Quinn et al, 2003). Earlier onset of increased MIP-1 $\alpha$  expression following LPS treatment to TASTPM mice may suggest the presence of peripheral inflammation can exacerbate a pre-existing neuroinflammatory profile in APP or APP/PS1 overexpressing mice, particularly since MIP-1 $\alpha$  was the only cytokine altered in vehicle treated TASTPM versus C57BL6/J mice. Repeated IP injection of LPS to TASTPM mice from 4 through to 7 months of age did not alter MIP-1 $\alpha$  protein expression in brain tissue, despite evidence that, following repeated LPS treatment, plasma MIP-1 $\alpha$  was increased relative to vehicle treated TASTPM mice (fig 5.8). The importance of increased MIP-1 $\alpha$  protein in the brain of APP and APP/PS1 overexpressing mice is unclear but it was suggested by Quinn et al, 2003 that it might not be linked to A $\beta$  plaque load. Acute IP injection of LPS to 2 month TASTPM mice failed to increase central MIP-1 $\alpha$  protein expression relative to LPS treated C57BL6/J mice, indicating that peripheral inflammation initiated before onset of significant fibrillar A $\beta$  plaque deposition does not cause a genotype-specific increase in cytokine expression in brain tissue. This suggests an interaction between A $\beta$  neuropathology and peripheral inflammation is required to enhance the response of the brain to peripheral infection.

Acute LPS injection increased the protein expression of one other cytokine in brain tissue. Cortical and hippocampal IL-6 in both C57BL6/J (consistent with validation studies) and TASTPM mice at 2, 5 and 10 months of age, was increased following a single IP LPS injection (fig 5.1). This indicates central IL-6 expression; unlike MIP-1 $\alpha$ , was not genotype specific. Reasons for the increase in hippocampal IL-6 evident in 5 month LPS treated TASTPM versus LPS treated C57BL6/J mice are unclear. The alteration may be in response to the rapid deposition of A $\beta$  occurring at this age and may warrant further investigation by characterising central IL-6 expression at ages in between the 2 and 5 month timepoints assessed in the current study.

Following acute IP LPS administration, although by 2 months of age, LPS treatment significantly increased plasma IL-1 $\beta$  in LPS treated TASTPM versus vehicle treated TASTPM mice, plasma IL-1 $\beta$  was attenuated relative to LPS treated C57BL6/J mice at this age with a non-significant trend for plasma IL-1 $\beta$  reduction by 5 and 10 months (fig 5.6). Plasma IL-1 $\beta$  was also decreased in LPS treated TASTPM relative to LPS treated C57BL6/J mice following repeated LPS injection (fig 5.10). The reason for an abrogation of a peripheral pro-inflammatory response to LPS in TASTPM mice is uncertain and is not reported in the current literature so it is difficult to determine how this change relates to other APP or APP/PS1 mutant transgenic mouse lines. Since the reduction of plasma IL-1 $\beta$  was already evident in TASTPM transgenic mice by 2 months of age, before the onset of plaque deposition, it is likely that the difference in peripheral immune response between C57BL6/J and TASTPM mice following IP LPS injection is due to underlying differences in their development rather than an effect of A $\beta$  load.

It cannot be discounted that the lack of detectable changes in the expression of other cytokines in TASTPM brain tissue following LPS treatment may be due to the method of cytokine detection. Previous literature has documented the increase in central cytokine mRNA in APP overexpressing mice (Abbas et al, 2002; Lim et al, 2000; Sly et al, 2001). However, much of the evidence has relied on the immunohistochemical detection of cytokine expression, associated with microglia and astrocytes, in brain tissue (Abbas et al., 2002; Apelt and Schliebs, 2001; Benzing et al., 1999; Mehlhorn et al., 2000). Cytokine production by immune cells is localised to A $\beta$  plaques thus, homogenisation of discrete brain regions may cause

dilution of the cytokine signal due to the presence of surrounding healthy tissue (Quinn et al, 2003). Fold changes in mRNA expression of some cytokines may be small, limiting the successful detection of cytokine expression at the protein level by Luminex<sup>®</sup> or ELISA techniques.

Immunohistochemical analysis of GFAP positive astrocytes and CD68 positive microglia/macrophage in vehicle treated TASTPM versus vehicle treated C57BL6/J mice indicated no change in the morphology or number of microglial cells in brain tissue (fig 5.14) but a significant increase in cortical and hippocampal GFAP positive astrocytes (fig 5.13). Repeated LPS IP injection had no effect on either CD68 or GFAP staining by 48 hours following the last LPS injection, indicating the peripheral inflammation did not influence cell-mediated neuroinflammation. Previous reports of enhanced GFAP expression in APP overexpressing mice following LPS treatment are variable. At 1 through to 18 hours, following peripheral LPS injection, GFAP mRNA was increased in brain tissue of aged (4 months after A $\beta$  plaque onset) Tg2576, (Sly et al, 2001). It is unclear whether this rapid increase in GFAP mRNA expression is transient and decreases back to basal levels by later timepoints. A more in-depth characterisation investigating GFAP mRNA and protein expression in brain tissue at acute (1-24 hours) and chronic timepoints following peripheral LPS injection may provide more insight into whether increased GFAP mRNA is a transient event. Activation of microglia in brain tissue following peripheral LPS injection has also been reported in APP overexpressing mice (Sheng et al, 2003), however, the effect of LPS on microglia in wildtype mice was not described so it is uncertain how this relates to a basal reaction to LPS and whether this was a genotype specific change. Certainly, the morphology and numbers of activated microglia following repeated LPS injection in the current study suggests peripheral inflammation does not affect the chronic cellular neuroinflammatory response.

### **5.5.2 Modulation of A $\beta$ load by LPS – APP/PS1 transgenic mice**

Previous studies report alterations of A $\beta$  load following peripheral (Quinn et al, 2003; Sheng et al, 2003) and central injection of LPS (Qiao et al, 2001; DiCarlo et al, 2001; Herber et al, 2004) and suggest modulation of A $\beta$  load depends largely on the protocol of LPS administration. Typically, LPS injection after onset of A $\beta$  plaque

deposition results in a reduction in A $\beta$  load. Analysis of A $\beta$ 1-40 or A $\beta$ 1-42 load and A $\beta$  plaque deposition in brain tissue using ELISA and immunohistochemical techniques revealed that LPS treatment had no effect following repeated IP injection of LPS to TASTPM mice (fig 5.15). This is in contrast to published literature, primarily reporting the use of APP overexpressing mice, demonstrating the reduction (Quinn et al, 2003; DiCarlo et al, 2001) and increase (Sheng et al, 2003; Sly et al, 2001) in A $\beta$  load, particularly increased intracellular A $\beta$ , following IP LPS treatment. The lack of A $\beta$  modulation following LPS treatment in TASTPM APP/PS1 overexpressing mice may be a result of the significantly more rapid A $\beta$  deposition evident in APP/PS1 models, hence A $\beta$  load is already substantial and further modulation of A $\beta$  levels may be difficult.

### **5.5.3 LPS induced neurodegeneration – APP/PS1 transgenic mice**

Cortical and hippocampal NeuN positive cells were quantified in C57BL6/J and TASTPM brain tissue following repeated IP LPS treatment. LPS had no effect on percentage NeuN staining in either cortex or hippocampus (fig 5.18 & 5.19). As discussed in section 5.4.2, repeated administration of LPS also failed to modulate A $\beta$  load in TASTPM brain tissue. Neurodegeneration in AD brain is associated with A $\beta$  plaques in the entorhinal cortex and hippocampus (Scott et al, 1991; Armstrong, 2006). A high level of A $\beta$  deposition in TASTPM animals does not cause overt neurodegeneration and, as LPS treatment did not increase A $\beta$  load, A $\beta$ -mediated neurodegeneration was unlikely. Previously, increased plasma IL-1 $\beta$  levels and peripheral infection has been suggested to exacerbate the progression of AD (Holmes et al, 2003). The exacerbation of a pre-existing neuroinflammatory profile in TASTPM tissue following repeated LPS injection may indicate that the presence of a peripheral infection after onset of A $\beta$  plaque deposition could exacerbate pre-existing pathology. Importantly, peripheral infections occur in AD patients during later stages of the neurodegenerative pathology suggesting peripheral inflammation may exacerbate rather than initiate neurodegeneration. Therefore, it may be difficult to induce cell death via a peripherally administered inflammatory insult considering the absence of neurodegeneration in vehicle treated TASTPM mice. The induction of neuronal cell loss in brain tissue of APP/PS1 overexpressing mice could be further investigated via a more chronic injection of LPS either centrally or peripherally. An

extended duration of treatment may be a more sufficient insult for causing neurodegeneration in APP/PS1 overexpressing mice.

In summary, the initial use of A $\beta$  peptide to cause neuroinflammation and neurodegeneration in rat brain tissue resulted in a variable window of cell death unsuitable in a model of A $\beta$ -induced neurodegeneration, despite the significant increase in neuroinflammation. This prompted an investigation of the use of LPS to exacerbate neuroinflammation and possibly induce onset of neurodegeneration in APP/PS1 overexpressing TASTPM mice that exhibit robust A $\beta$  neuropathology. Peripheral LPS administration exacerbated MIP-1 $\alpha$ , a chemokine evident in the brain tissue of vehicle treated TASTPM mice, suggesting peripheral inflammation may enhance a pre-existing neuroinflammatory profile rather than initiate extensive neuroinflammation or induce neurodegeneration. Although a longer duration of LPS treatment may lead to different results, the repeated peripheral administration of an inflammatory stimulus to TASTPM mice is unlikely to provide a robust in vivo model of neuroinflammation and neurodegeneration, despite relevance to the chronic neurodegenerative disease, AD. The idea that a peripheral inflammatory or specific neurotoxic challenge may enhance neuroinflammation in TASTPM mice will be further investigated in the following chapter. Chapter 6 will describe use of the noradrenergic neurotoxin DSP-4 in exacerbating neuroinflammation and potentially causing neurodegeneration in TASTPM brain tissue.

## **CHAPTER 6**

### ***Repeated DSP-4 administration to TASTPM APP/PS1 transgenic mice***

#### **6.1 Introduction**

Degeneration of central noradrenergic neurons projecting from the locus coeruleus (LC) to terminal regions including the cortex and hippocampus (Mann et al, 1982; Mann & Yates, 1983) correlates with duration of illness (Zarow et al, 2003), A $\beta$  plaque deposition and duration and severity of dementia (Bondareff et al, 1987) in AD. Noradrenaline (NA) acts via adrenoceptors and  $\alpha$ 2 adrenoceptors are significantly reduced in the hippocampus of AD patients (Szot et al, 2006). Previous reports describe the anti-inflammatory and neuroprotective properties of NA including the attenuation of pro-inflammatory cytokine expression and increased release of neurotrophic factors (reviewed by Galea et al, 2003; Marien et al, 2004). In addition, previous chapters in this thesis have described the anti-inflammatory activity of the  $\alpha$ 2 antagonist, fluparoxan on LPS-mediated pro-inflammatory cytokine expression in rodent brain tissue (sections 2.5.3.2 & 3.5.2.2). Hence, reduction of NA in brain tissue may exacerbate neuroinflammation in double mutant APP/PS1 transgenic TASTPM mice.

#### **6.1.1 Role of NA in neuroinflammation & neurodegeneration**

NA negatively regulates the expression and release of pro-inflammatory cytokines (Kaneko et al, 2005; Hu et al, 1991; Dello Russo et al, 2004) and inhibits microglial activation (Lee et al, 1992; Loughlin et al, 1993; Chang & Liu, 2000). LPS (i.p) administration causes a significant increase in NA in the brain of rats indicating a response of NA to an inflammatory stimulus (Linthorst et al, 1998). NA has been shown to inhibit the microglial induced cell death of cortical neurons by reducing IL-1 $\beta$  release from microglia (Madrigal et al, 2005).  $\alpha$ 2 adrenoceptor antagonists that act to increase extracellular NA have been reported to have anti-inflammatory actions in vivo (Hasko et al, 1998) and data presented earlier in this thesis (section 2.5.3.2) also demonstrated the in vivo anti-inflammatory activity of the  $\alpha$ 2-

adrenoceptor antagonist, fluparoxan in brain tissue. Low doses of the noradrenergic neurotoxin N - (2-chloroethyl)-N-ethyl-2-bromobenzylamine (DSP-4) (50µg/kg) potentiated Aβ induced neuroinflammation (Heneka et al, 2002 & 2003a) and exacerbated microglial activation and inflammatory gene expression (Feinstein et al., 2004) in APP over expressing mice. Compromising the NA system by DSP-4 appears to render the brain tissue more susceptible to the pro-inflammatory effects of Aβ protein (Heneka et al., 2002; Heneka et al., 2003a). NA can protect neurons and promote recovery from neurotoxic stimuli including inflammatory and excitotoxic insults by enhancing the release of neurotrophic factors and acting as an anti-oxidant (Marien et al, 2004). More recent studies published since the completion of the work described in this chapter reported increased neuroinflammation and neuronal cell death in the hippocampus and cortex of APP23 mice following the peripheral injection of DSP-4 (Heneka et al, 2006). Reduction in central NA also increased Aβ plaque number in the brain tissue of APPV717F (H6) overexpressing mice (Kalinin et al, 2006).

### **6.1.2 Depletion of NA following DSP4 administration**

DSP-4, a tertiary haloalkylamine that can cross the blood-brain barrier, causes marked depletion of endogenous NA via inhibition of uptake and decreased NA synthesis (Ross et al, 1976; Jaim-Etcheverry & Zieher, 1980). The response of central noradrenergic axons to DSP-4 occurs via two phases. The first phase involves massive NA depletion via irreversible uptake inhibition and depletion of endogenous NA via decreased NA synthesis (Fritschy et al, 1990). The second phase involves a reduction in the enzyme dopamine-β-hydroxylase (DβH) and degeneration of NA axons (Fritschy et al, 1990). Inhibition of NA uptake and depletion of endogenous neuronal NA occurs rapidly and in a dose dependent manner after DSP-4 administration. Storage and uptake of NA recovers quickly in the periphery but continues in the CNS for a long duration and recovery time differs between specific brain regions (Wolfman et al, 1994). The increased affinity of DSP-4 for the NA uptake carrier in synaptosomes from LC terminal areas may explain the actions of DSP-4 on neuronal projections specifically originating in the LC (Fritschy & Grzanna, 1991). Areas innervated by the LC, such as the cortex and hippocampus, also demonstrate the greatest NA depletion due to increased NA turnover rate

relative to other regions (Logue et al, 1985). Degeneration of terminals is associated with a gradual loss of noradrenergic cell bodies in the LC with approximately a 30% loss of LC neurons within 2 months after a single DSP-4 injection suggesting terminal loss induces retrograde degeneration. Six months after DSP-4 administration, surviving LC neurons were observed to regenerate resulting in the reinnervation of specific brain regions including the forebrain, in contrast to a lack of regenerative neuronal sprouting in the brainstem and cerebellum (Fritschy & Grzanna, 1992).

### **6.1.3 Chapter Aims**

The primary purpose of this investigation was to determine the effect of noradrenergic depletion on A $\beta$  plaque deposition and neuroinflammation in TASTPM transgenic brain tissue. TASTPM mice exhibit high levels of circulating A $\beta$  protein, A $\beta$  plaque deposition, neuroinflammation and cognitive and behavioural deficits (Howlett et al., 2004) but lack overt neuronal cell death. Depletion of NA may exacerbate some of the features of AD and hence the effects of noradrenergic depletion on neurodegeneration, normally absent in the TASTPM model, was also examined.

## **6.2 Materials & Methods**

### **6.2.1 Animals**

Male TASTPM mice (5 months old) were obtained from GlaxoSmithKline, UK and specific, pathogen free male C57BL6/J mice (25g, approx 10 weeks of age) were ordered from Charles River, UK or as aged (5 months) animals from Harlan, UK. All mice were singly housed (GlaxoSmithKline, Harlow, UK) under controlled conditions (temperature: 21-24°C, 12-h light/dark cycle (7am lights on) and provided with Global Rodent Maintained Diet (Harlan Teklad) and water *ad libitum*. Analysis of DNA isolated from tail tips removed at termination confirmed genotype status. All experimental procedures were conducted in accordance with the GlaxoSmithKline local ethics committee and conformed to the UK Animals (Scientific Procedures) Act 1986.

### **6.2.2 Materials**

Saline and DSP-4 were obtained from VWR International, UK and Sigma, UK respectively. 4% paraformaldehyde was prepared in-house (GSK, UK). All materials for HPLC analyses were obtained from VWR International, UK unless otherwise stated. Immunostaining machines, PAP pens, proteinase K, peroxidase blocking solution and diaminobenzidine substrate kit were all obtained from DakoCytomation, UK. Optimax buffer was obtained from A. Menarini, UK. Gills haematoxylin stain was purchased from HD Supplies, UK. The sources of additional materials are individually stated.

### **6.2.3 Treatment**

Mice were IP injected with either filtered PBS or DSP-4 (5 or 50mg/kg) dissolved in filtered PBS (5ml/kg dose volume). DSP-4 in solution is relatively unstable and was administered immediately after preparation (Ross, 1976). A number of previous reports describe the reduction of NA and loss of LC neurons following a single injection of 50mg/kg DSP-4 (Hallman & Jonsson, 1984; Fritschy & Grzanna, 1989; Prieto & Giralt, 2001; Fritschy et al, 1990; Fritschy & Grzanna, 1991). A much lower dose of 50µg/kg has been previously shown to potentiate A $\beta$  induced neuroinflammation (Heneka et al, 2002; Heneka et al, 2003) and previous unpublished studies highlighted increased incidence of mortality in APP overexpressing mice following administration of 50mg/kg DSP-4 (personal communication; D. Feinstein, University of Illinois, Chicago, USA). A recent publication by Heneka et al, 2006 details the use of 5mg/kg DSP-4 to modulate A $\beta$  deposition in the brain tissue of APP overexpressing mice.

### **6.2.4 Sample collection**

Mice were deeply anaesthetised with sodium pentobarbital (Euthatal<sup>®</sup> 100mg kg<sup>-1</sup> i.p, Rhône Mérieux, Harlow, UK).

**Study 15:** cortex, hippocampus and cerebellum were microdissected and placed in prelabelled 2ml eppendorfs (VWR International, UK) and stored at -80°C for HPLC analysis of NA. The cortex and hippocampus were hemi-dissected to allow the assessment of potential differences in the effect of DSP-4 on NA between left and right brain hemispheres.

**Study 16:** The brain was microdissected: half brain (right), cortex and hippocampal (left) samples. Half brain was immersed fixed in 4% paraformaldehyde, left cortex samples from 5 animals were placed into sterile biopur<sup>®</sup> (RNase-free) safe-lock eppendorfs (VWR International, UK) and stored at -80°C for RNA quantification. Cortex samples from remaining animals and hippocampus from all mice were stored into prelabelled 2ml eppendorfs (VWR International, UK) and stored at -80°C for high performance liquid chromatography (HPLC) analysis of NA.

### 6.2.5 *Ex-vivo neurochemistry- HPLC*

#### 6.2.5.1 *Tissue Preparation*

Samples were weighed and homogenised in 0.4 M perchloric acid containing sodium metabisulphate (0.1% wv<sup>-1</sup>), EDTA (ethylene diamine tetra acetate 0.01% wv<sup>-1</sup>) and L-cysteine (0.1% wv<sup>-1</sup>) at a ratio of 100µl homogenising buffer per mg of tissue (giving a tissue concentration of 0.01 g/ml). All samples were centrifuged on 10,000g at 4°C for 10 minutes and supernatant decanted.

#### 6.2.5.2 *High Performance Liquid Chromatography (HPLC)-ECD analysis*

Aliquots (30µl) of supernatant were transferred into micro-volume glass vials for HPLC-ECD analysis. The HPLC-ECD protocol was based on previous published literature (Lacroix et al, 2004) and in-house validation. Mobile phase consisted of 0.07M KH<sub>2</sub>PO<sub>4</sub>, containing 1.5 mM sodium octylsulphonate and 0.1 mM EDTA.Na<sub>2</sub>, MeOH, tetrahydrofuran (87.5:12:0.5%, wv<sup>-1</sup>). Flow rates for optimal separation and detection varied between 2.2 to 2.5 ml/min. Sample aliquots of 10µl each were automatically injected onto the columns. Separation was performed using two Chromolith Performance columns connected in series (100 × 4.6 mm i.d., Lutterworth UK). Eluates were detected using a Decade electrochemical detector fitted with a glassy carbon cell (Antec, Leyden, The Netherlands) set at +0.65V versus *in situ* Ag/AgCl reference electrode. Data were collected using Empower software (Waters, Milford, MA). The chromatograms were compared with internally run NA standard calibrations (concentrations between 1 and 100ng/ml) to identify and quantify components. HPLC analysis was kindly completed by Tracey Ashmeade, GSK, Harlow, UK.

### **6.2.6 Immunohistochemistry**

Hemisected brains immersed fixed in 4% paraformaldehyde for 3 days at room temperature were processed and embedded into paraffin wax as described in section 5.2.7 and semi-serial sections (5 $\mu$ M thick) taken throughout the LC (bregma -4 to -7) and cortical and hippocampal regions (bregma -1 to -4). Sections (2 sections unless otherwise stated) were stained for neurons (NeuN) (6 sections), glial fibrillary acid protein (GFAP), microglia (CD68) and A $\beta$  as described in section 5.2.7. Additionally sections were stained for tyrosine hydroxylase (TH). Sections were microwaved (Sanyo Showerwave, 1000W) in tris-borate-EDTA buffer, pH 8.3 (Sigma-Aldrich, UK) for 2.5 minutes at 1000W, 10 minutes at 450W and allowed to cool for 20 minutes. Sections received peroxidase block for 5 minutes, primary antibody rabbit anti TH, affinity purified (1/500 in antibody diluent, 30 minutes) (Chemicon International, UK), biotinylated goat anti rabbit (1/200 in optimax buffer, 30 minutes) (Vector Laboratories, UK), peroxidase ABC kit (Vector Laboratories, UK) for 45 minutes and diaminobenzidine substrate kit for 10 minutes. Sections were counter-stained using Gills haematoxylin (3 seconds followed by running tap water), dehydrated in IMS (70 to 100%), cleared in HistoClear and mounted in DPX (VWR, UK). Sections were viewed using a Colourview digital camera (x10 objective for TH sections, x4 objective for 1E8 sections) attached to an Olympus BX41 microscope. Photomicrographs for NeuN, GFAP, CD68 and TH were captured and analysed using image analysis software (AnalySIS, Soft Imaging Systems, UK). Sections stained for 1E8 were viewed using a Leica DC100 camera attached to a Leitz DMRB microscope. Photomicrographs were captured and percentage area stained by 1E8 was analysed using Leica Qwin software (Leica systems, Buckinghamshire, UK). Immunohistochemical staining and analysis was kindly completed by Martin Vidgeon-Hart, GSK, Harlow, UK.

### **6.2.7 TaqMan analyses**

Total RNA was isolated from cortex tissues from WT and TASTPM mice using TRIZOL<sup>®</sup> reagent (Invitrogen, USA). Cortical mRNA was quantified following the protocol described in section 2.3.8. Primer (F and R) and probe (P) sets were designed from sequences in the Genbank database using Primer Express software (Perkin-Elmer, UK) (table 6.1). Taqman analysis was kindly completed by Ainsley

Culbert and Florence Guillot, GSK, Harlow, UK.

Gene	Reagent Sequences
<b>GFAP</b>	F; GGAGCTCAATGACCGCTTTG R; AGCGCCTTGTTTTGCTGCTC P; CAGCTACATCGAGAAGGTTTCG
<b>TNF<math>\alpha</math></b>	F; TCCAGGCGGTGCCTATGT R; GAGCGTGGTGGCCCC P; TCAGCCTCTTCTCATTCTGCTTGTGG
<b>MIP-1<math>\alpha</math></b>	F; AGCTGACACCCCGACTGC R; GTCAACGATGAATTGGCGTG P; TGCTGCTTCTCCTACAGCCGGAAGAT
<b>RANTES</b>	F; TCTTGCAGTCGTGTTTGTCCAC R; TCTTGAACCCACTTCTTCTCT P; AGGAACCGCCAAGTGTGTGC
<b>IL-1<math>\beta</math></b>	F; TTGGGCCTCAAAGGAAAGAAT R; TCTCCAGCTGCAGGGTGG P; TATACCTGTCTGTGTAATGAAAGACGGCA CA
<b>I<math>\kappa</math>B<math>\alpha</math></b>	F; CGGAGGACGGAGGACTCGTT R; ACTTCCATGGTCAGCGGCT P; TGCACCTGGCAATCATCCACGAAGA

Table 6.1: TaqMan reagent sequences

### 6.2.8 Data Analysis

A general linear mixed model approach using the Proc Mixed procedure in SAS<sup>®</sup> Version 8 (SAS<sup>®</sup> Institute, UK) assessed the effect of DSP-4 treatment on central NA levels within C57BL6/J subjects using brain region as a repeated measure. Separate ANOVA analyses at each age point were used to calculate the overall effect and interactions between genotype and treatment on cortical and hippocampal NA in

C57BL6/J and TASTPM mice, using brain region as a repeated measure. Separate univariate ANOVAs (Statistica™ Version 6.1 (Statsoft, USA)) at each age point calculated the overall effect of DSP-4 treatment on each mRNA marker, plaque load and LC degeneration. Post hoc planned comparisons assessed individual treatment effects for study 15 and individual differences between groups at each age following repeated DSP-4 injection to C57BL6/J and TASTPM subjects. Outliers (data points outside 2 standard deviations of the mean) were omitted from statistical analysis and graphical representation.

### **6.3 Protocols**

#### **6.3.1 Study 15: Acute DSP-4 effects on NA (5mg/kg and 50mg/kg)**

24 male C57BL6/J mice (n=8) (Charles River, UK) were IP administered with 0.9% saline, 5mg/kg DSP-4 or 50mg/kg DSP-4 dissolved in 0.9% saline (5ml/kg) were euthanased 24 hours post treatment via anaesthetic overdose. Since brain tissue would be hemidissected in order to provide tissue for a multitude of analyses including immunohistochemistry, taqman and HPLC analysis, I compared left and right side cortex and hippocampus to investigate the effect of hemisphere on NA quantification using HPLC analysis.

#### **6.3.2 Study 16: Repeated administration of DSP-4 to TASTPM mice**

Male TASTPM mice aged 5 months (n=46) (GSK, Harlow, UK) and age matched C57BL6/J controls (n=46) (Harlan, UK) were IP administered with 0.9% saline or 5mg/kg DSP-4 dissolved in 0.9% saline (5ml/kg) monthly. Half of each treatment group were euthanased at 8 months of age whilst remaining animals continued treatment and were euthanased at 11 months of age via anaesthetic overdose. Brain tissue was hemidissected for half whole brain (right) for immunohistochemical analysis and the remaining half brain (left) was microdissected for cortex for either taqman or HPLC analysis or hippocampus for HPLC analysis alone.

## 6.4 Results

### 6.4.1 *Study 15: acute DSP-4 effects on NA (5mg/kg and 50mg/kg)*

Repeated measures ANOVA indicated an overall effect of DSP-4 treatment,  $F_{(2, 8)} = 128.66$ ,  $p < 0.001$ , brain region,  $F_{(4, 32)} = 7.78$ ,  $p < 0.001$  and a significant interaction between brain region\*treatment,  $F_{(8, 32)} = 2.88$ ,  $p < 0.05$ . Acute administration of 5mg/kg DSP-4 significantly reduced cortical NA by 21% ( $p = 0.01$ ) and 16% ( $p < 0.01$ ) in left (fig 6.1A) and right cortex (fig 6.1B) respectively whilst 50mg/kg DSP-4 treatment induced a 90% (left cortex;  $p < 0.001$ ) and 87% (right cortex;  $p < 0.001$ ) NA reduction. DSP-4 (5mg/kg) also significantly reduced left hippocampal NA (fig 6.1C) by 22% ( $p < 0.01$ ) but failed to significantly reduce right hippocampal NA (fig 6.1D). Treatment of 50mg/kg DSP-4 significantly reduced left ( $p < 0.001$ ) and right ( $p < 0.001$ ) hippocampal NA by 74% and 89% respectively. 5mg/kg and 50mg/kg DSP-4 treatment significantly reduced NA levels in the cerebellum by 12% ( $p < 0.05$ ) and 48% ( $p < 0.001$ ) (fig 6.1E).

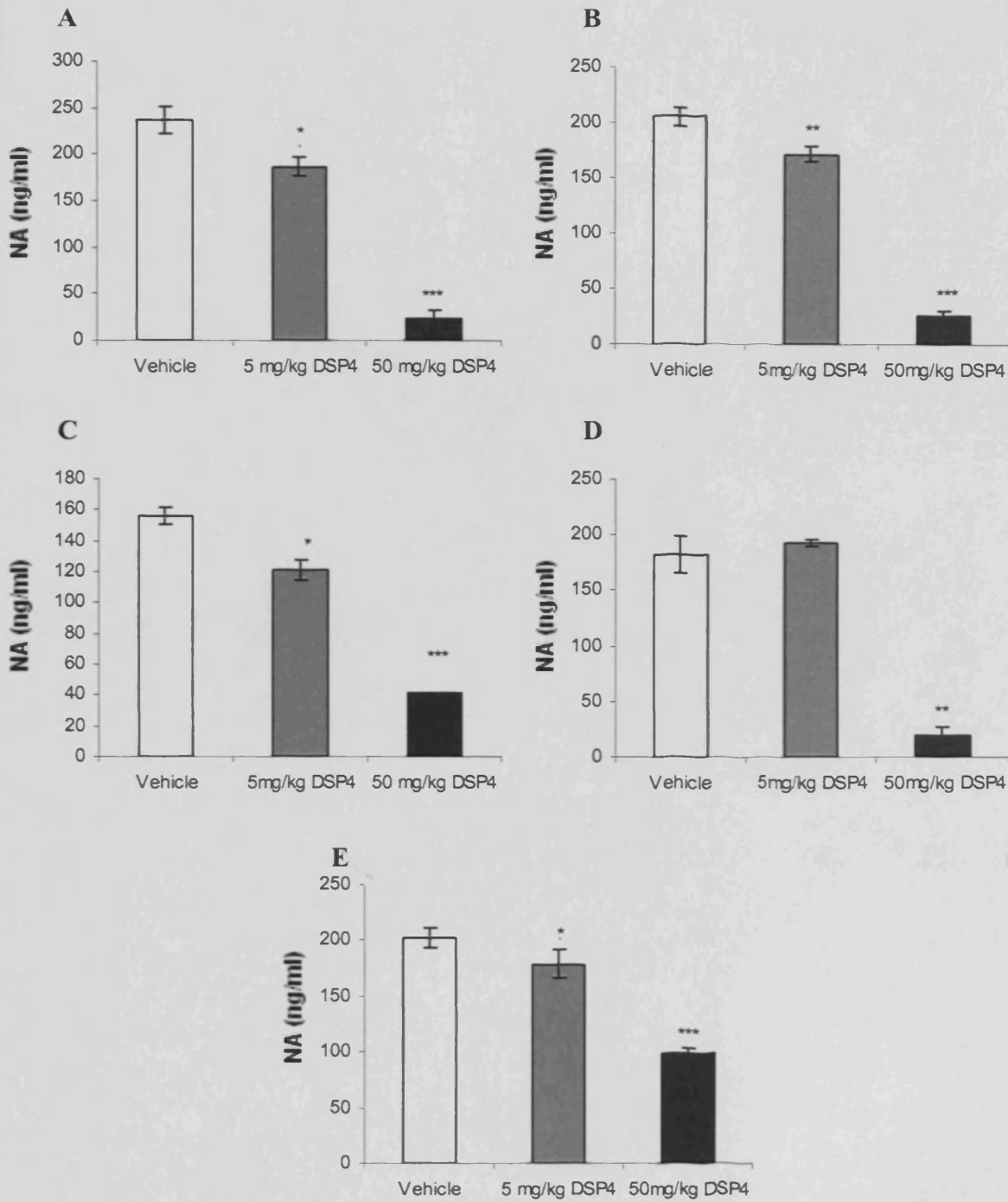


Figure 6.1: Comparison of 5mg/kg and 50mg/kg DSP-4 on NA in left cortex (A), right cortex (B), left hippocampus (C), right hippocampus (D) and whole cerebellum (E) in male C57BL6/J mice (n=8 per group), data represented as noradrenaline (NA) in ng/ml and shows mean  $\pm$  SEM. \*  $p \leq 0.05$ , \*\*  $p \leq 0.01$ , \*\*\*  $p \leq 0.001$  significantly different vs. vehicle (repeated measures ANOVA followed by planned comparisons)

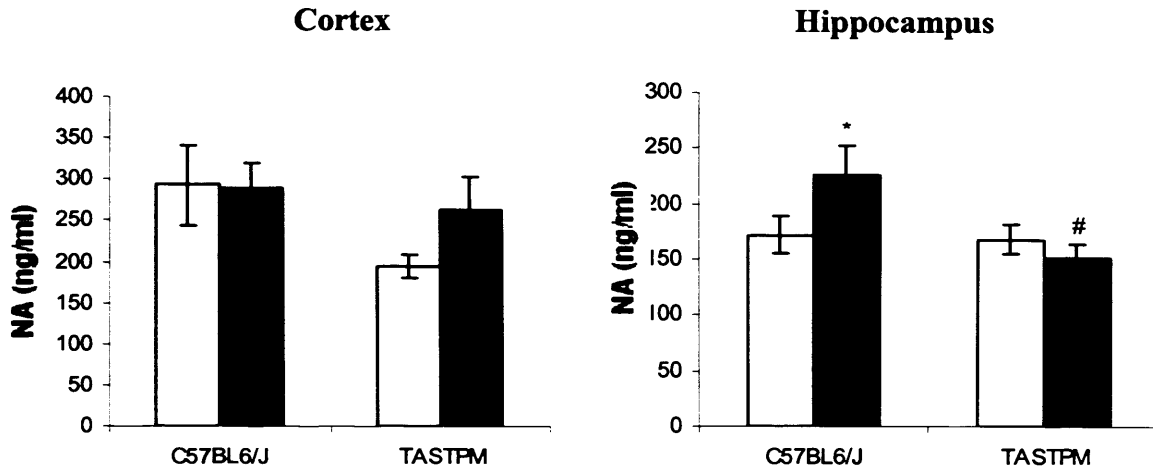
## 6.4.2 *Study 16: Repeated administration of DSP-4 to TASTPM mice*

### 6.4.2.1 *NA depletion following chronic DSP4 treatment*

Repeated measures ANOVA analysis on mice at 8 months revealed no significant effect of genotype,  $F_{(1,34)} = 3.85$ ,  $p = 0.058$ , or treatment,  $F_{(1,34)} = 3.56$ ,  $p = 0.067$ , on NA (fig 6.2). There was a non-significant trend for DSP-4 treated groups to exhibit elevated NA levels, particularly in cortical tissue of TASTPM mice (35% increase relative to vehicle TASTPM). There was also a significant elevation of NA in hippocampal tissue of C57BL6/J mice (31% increase relative to vehicle C57BL6/J). At 11 months, repeated measures ANOVA revealed an overall effect of genotype,  $F_{(1,36)} = 50.82$ ,  $p < 0.001$ , brain region,  $F_{(1,26)} = 8.71$ ,  $p < 0.01$ , and a significant genotype\*treatment interaction,  $F_{(1,36)} = 5.9$ ,  $p < 0.01$ . Post hoc planned comparisons revealed a significant reduction in cortical ( $p < 0.01$ ) and hippocampal ( $p < 0.05$ ) NA levels in vehicle treated TASTPM transgenic mice relative to vehicle treated C57BL6/J mice. Also a significant reduction in cortical ( $p < 0.01$ ) and hippocampal ( $p < 0.001$ ) NA levels in DSP-4 treated TASTPM transgenic mice versus DSP-4 treated C57BL6/J mice. DSP-4 treatment did not significantly affect C57BL6/J mice, however, there was a reduction of cortical ( $p = 0.01$ ) and hippocampal ( $p < 0.05$ ) NA levels by 57% and 45% respectively in DSP-4 treated TASTPM transgenic mice relative to vehicle treated TASTPM transgenic mice.

Vehicle
  DSP4

**NA – 8 months:**



**NA – 11 months:**

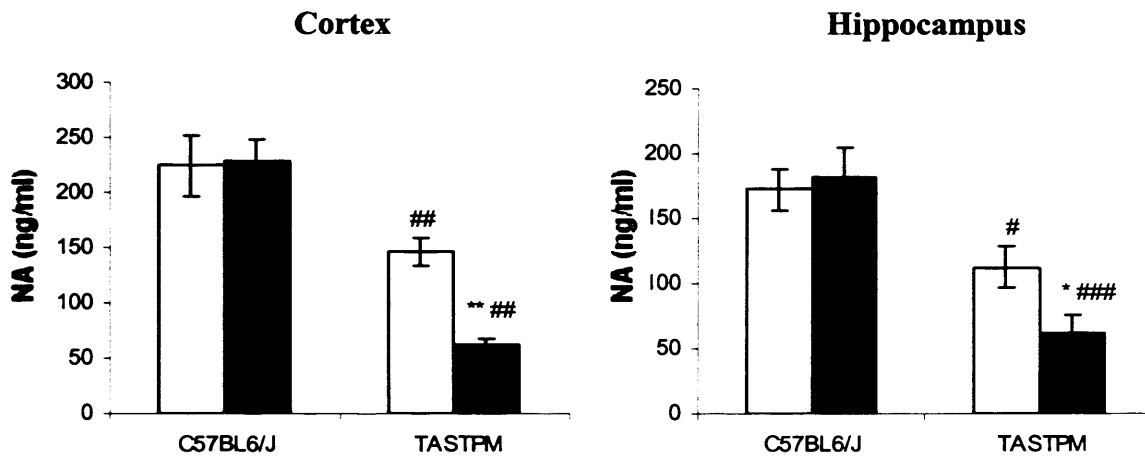


Figure 6.2: NA depletion in cortex and hippocampus of 8 month and 11 month DSP-4 and vehicle treated C57BL6/J and TASTPM mice (n=12 per group), data represented as noradrenaline (NA) in ng/ml and shows mean ± SEM. \*  $p \leq 0.05$ , \*\*  $p \leq 0.01$  significantly different vs. vehicle treatment, #  $p \leq 0.05$ , ##  $p \leq 0.01$ , ###  $p \leq 0.001$  significantly different vs. C57BL6/J (repeated measures ANOVA followed by planned comparisons at each age point)

#### 6.4.2.2 Neuroinflammation following chronic DSP-4 treatment

##### A. Taqman

Taqman PCR was used to analyse mRNA expression of a number of neuroinflammatory markers in hemidissected cortical tissue (fig 6.3 & fig 6.4). Univariate ANOVA analysis on mRNA expression in 8 month cortex revealed a significant effect of genotype on GFAP,  $F_{(1,17)} = 114.68$ ,  $p < 0.001$ , TNF- $\alpha$ ,  $F_{(1,16)} = 13.18$ ,  $p < 0.01$ , MIP-1 $\alpha$ ,  $F_{(1,17)} = 682.48$ ,  $p < 0.001$  and RANTES,  $F_{(1,17)} = 61.24$ ,  $p < 0.001$ . There was also a significant genotype\*treatment interaction on TNF- $\alpha$ ,  $F_{(1,16)} = 6.87$ ,  $p < 0.05$ , MIP-1 $\alpha$ ,  $F_{(1,17)} = 9.43$ ,  $p < 0.01$  and RANTES,  $F_{(1,17)} = 8.05$ ,  $p < 0.05$ . Post hoc planned comparisons revealed significantly increased GFAP, MIP-1 $\alpha$ , and RANTES in TASTPM relative to C57BL6/J mice regardless of treatment (TASTPM versus C57BL6/J,  $p < 0.001$  all groups). TNF- $\alpha$  mRNA expression was also increased in TASTPM versus C57BL6/J mice after vehicle treatment ( $p < 0.001$ ). There was also a trend towards a reduction of GFAP ( $p = 0.15$ ), TNF- $\alpha$  ( $p = 0.06$ ) and RANTES with a significant reduction of MIP-1 $\alpha$  ( $p < 0.05$ ) in DSP-4 treated TASTPM relative to vehicle treated TASTPM mice.

Univariate ANOVA analysis on mRNA expression in 11 month cortex revealed significant genotype effects on GFAP,  $F_{(1,16)} = 204.24$ ,  $p < 0.001$ , TNF- $\alpha$ ,  $F_{(1,15)} = 39.05$ ,  $p < 0.001$ , MIP-1 $\alpha$ ,  $F_{(1,16)} = 1539.18$ ,  $p < 0.001$ , RANTES,  $F_{(1,16)} = 82.36$ ,  $p < 0.001$ , IL-1 $\beta$ ,  $F_{(1,16)} = 6.60$ ,  $p < 0.05$ , and I $\kappa$ B $\alpha$ ,  $F_{(1,16)} = 24.69$ ,  $p < 0.001$ . There was also an overall treatment effect on IL-1 $\beta$ ,  $F_{(1,16)} = 9.63$ ,  $p < 0.01$ , and I $\kappa$ B $\alpha$ ,  $F_{(1,16)} = 8.96$ ,  $p < 0.01$ . GFAP ( $p < 0.01$ , both groups), TNF- $\alpha$  ( $p < 0.001$ , both groups), MIP-1 $\alpha$  ( $p < 0.01$ , both groups), RANTES ( $p < 0.001$ , both groups) were increased in TASTPM relative to C57BL6/J mice, regardless of treatment. There was also a significant potentiation of IL-1 $\beta$  ( $p < 0.05$ ) in DSP-4 treated TASTPM relative to vehicle treated TASTPM and DSP-4 treated C57BL6/J mice at 11 months. There was a non-significant decrease in I $\kappa$ B $\alpha$  ( $p = 0.06$ ) in DSP-4 treated TASTPM relative to vehicle treated TASTPM mice and a significant reduction in I $\kappa$ B $\alpha$  ( $p < 0.05$ ) in DSP-4 treated C57BL6/J relative to vehicle treated C57BL6/J mice at 11 months.

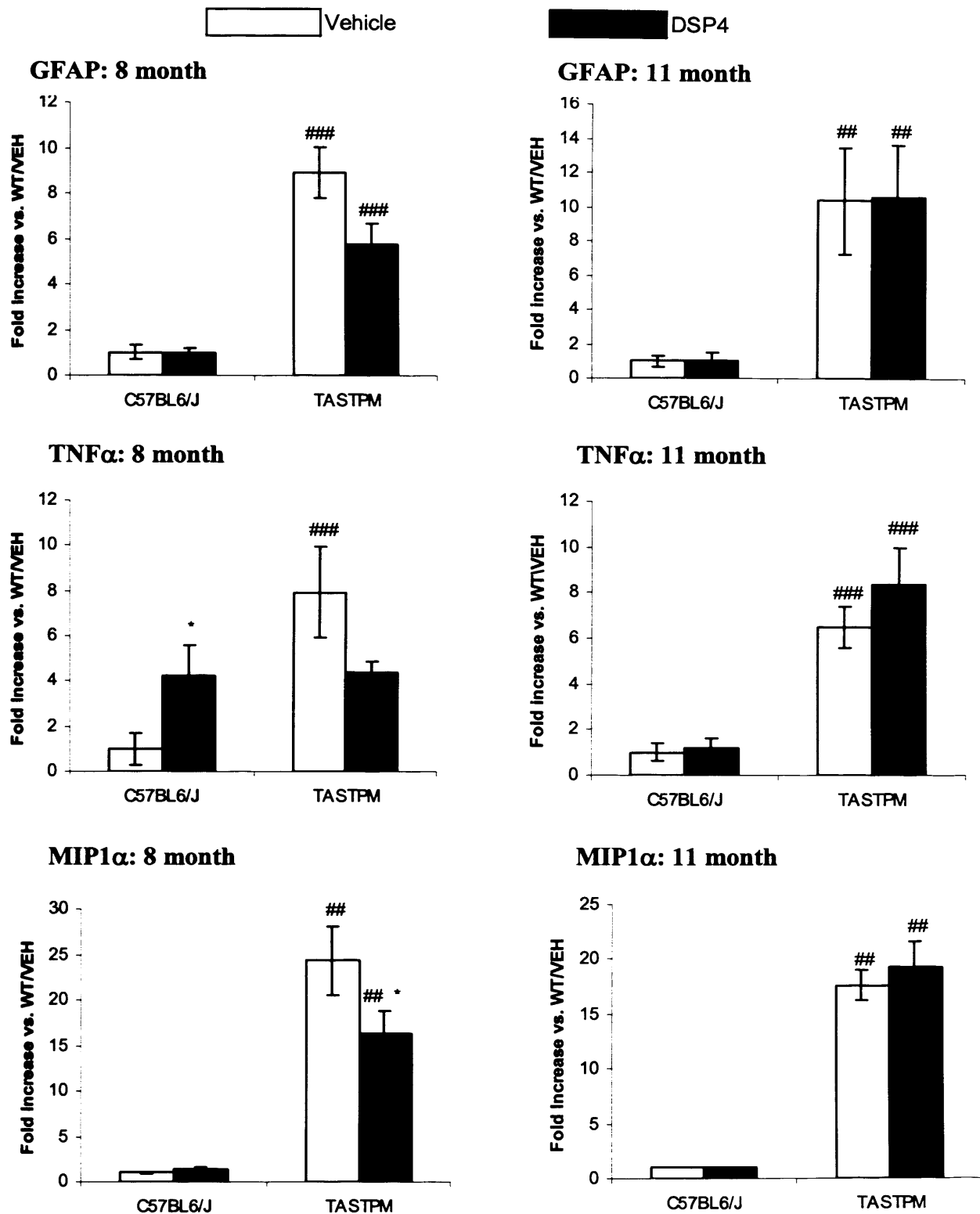
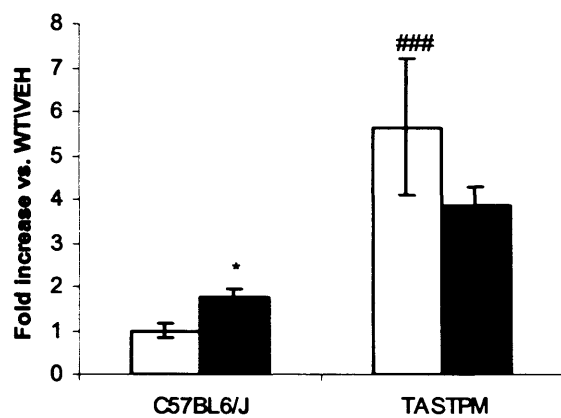
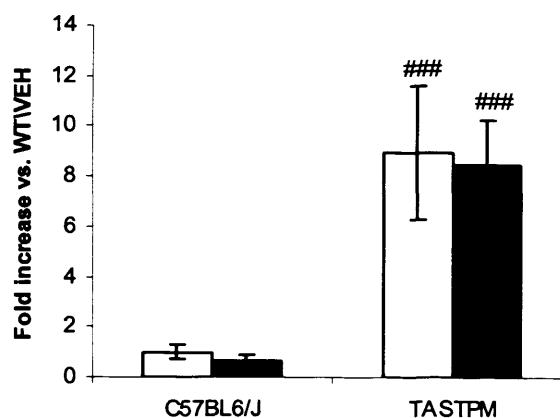


Figure 6.3: Cortical inflammatory mRNA markers in 8 month and 11 month vehicle and DSP-4 treated C57BL6/J and TASTPM transgenic mice (n=12 per group), data represented as fold increase relative to GAPDH and shows mean  $\pm$  SEM. \*  $p \leq 0.05$ , \*\*  $p \leq 0.01$  vs. vehicle treatment, #  $p \leq 0.05$ , ##  $p \leq 0.01$ , ###  $p \leq 0.001$  vs. C57BL6/J (univariate ANOVA followed by planned comparisons)

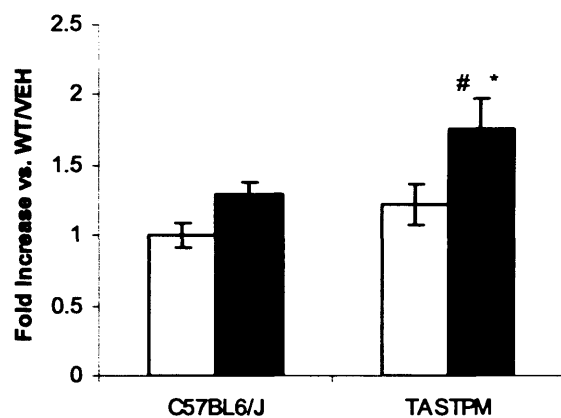
### RANTES: 8 month



### RANTES: 11 month



### IL1 $\beta$ : 11 month



### IkB $\alpha$ : 11 month

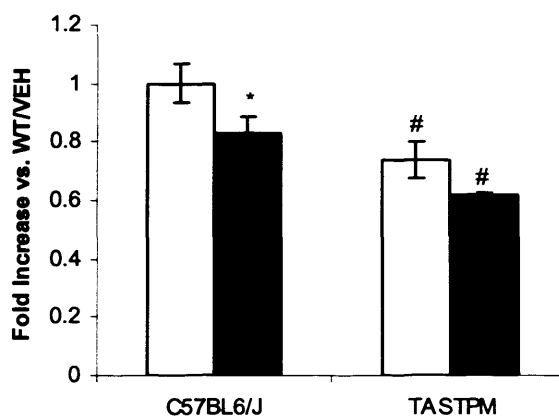


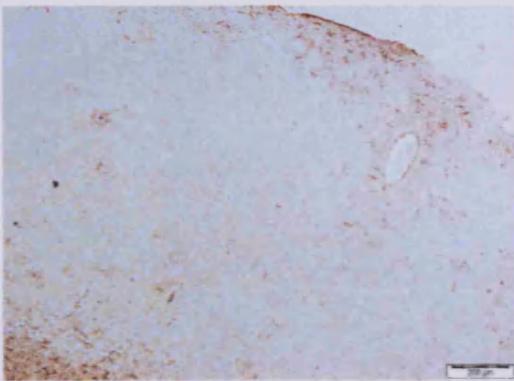
Figure 6.4: Cortical inflammatory mRNA markers in 8 month and 11 month vehicle and DSP-4 treated C57BL6/J and TASTPM transgenic mice (n=12 per group), data represented as fold increase relative to GAPDH and shows mean  $\pm$  SEM. \*  $p \leq 0.05$  significantly different vs. vehicle treatment, #  $p \leq 0.05$ , ###  $p \leq 0.001$  significantly different vs. C57BL6/J (univariate ANOVA followed by planned comparisons)

*B. Immunohistochemistry (IHC)*

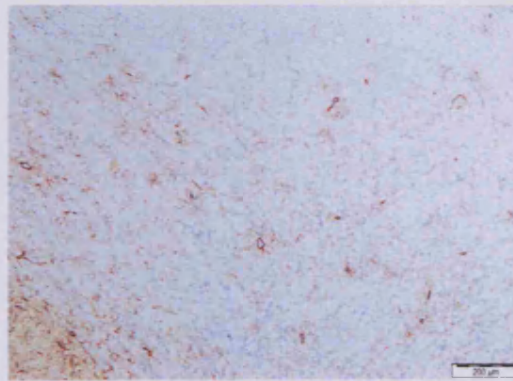
Brains were immunohistochemically processed to identify reactive astrocytes (GFAP) (figs 6.5 & 6.6) and activated microglia (CD68) (fig 6.7), as markers of neuroinflammation. There was no effect of DSP-4 treatment on the area of microglial stain in cortex of TASTPM mice at 8 or 11 months; however, cortical GFAP staining for reactive astrocytes was patchy and less dense in DSP4 treated relative to vehicle treated TASTPM mice at 8 months. This was supported at the transcriptional level by a reduction in cortical GFAP mRNA of DSP-4 treated TASTPM mice at 8 months of age (fig 6.3). By 11 months of age, there was no difference in GFAP staining between DSP4 treated and vehicle treated TASTPM mice.

**GFAP:**

**8 month DSP-4 C57BL6/J**

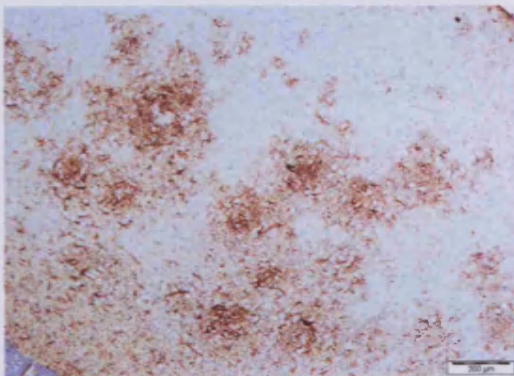


**8 month VEH C57BL6/J**



**GFAP:**

**8 month DSP-4 TASTPM**



**8 month VEH TASTPM**

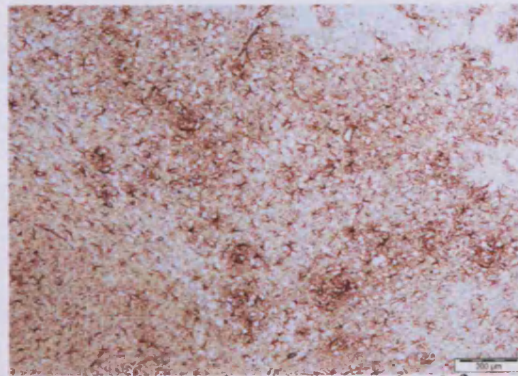
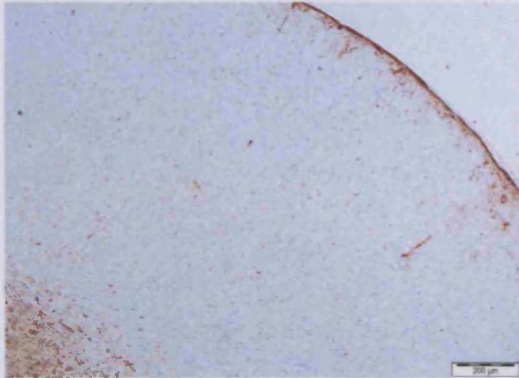


Figure 6.5: Representative photomicrographs of sagittal sections of the cortex stained for GFAP from 8 month vehicle and DSP-4 treated C57BL6/J and TASTPM transgenic mice (n=12 per group), scale bar represents 200µmetres

**GFAP:**

**11 month DSP-4 C57BL6/J**

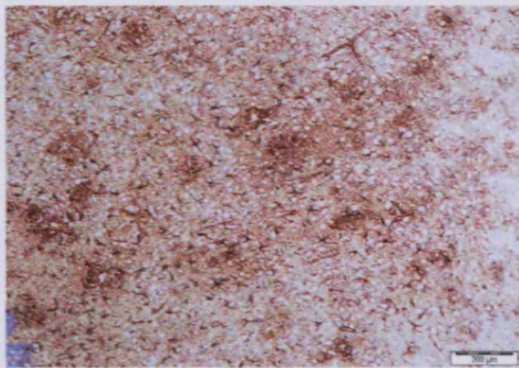


**11 month VEH C57BL6/J**



**GFAP:**

**11 month DSP-4 TASTPM**



**11 month VEH TASTPM**

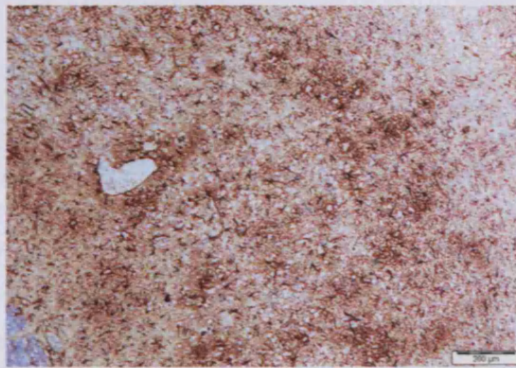
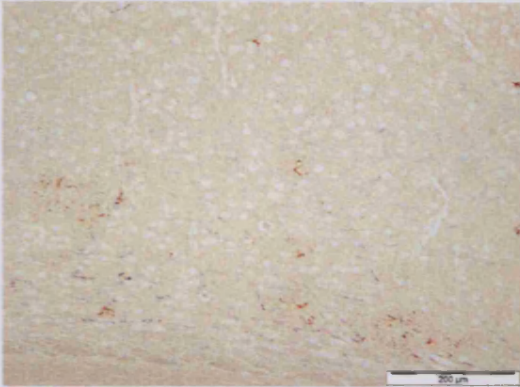


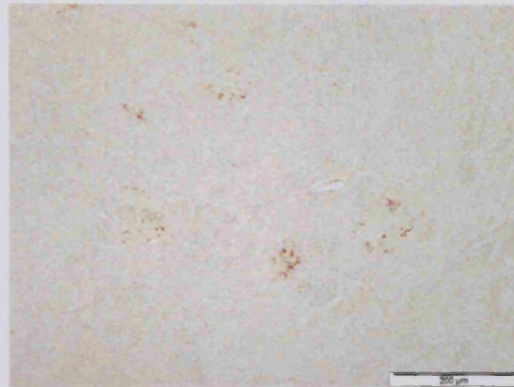
Figure 6.6: Representative photomicrographs of sagittal sections of the cortex stained for GFAP from 11 month vehicle and DSP-4 treated C57BL6/J and TASTPM transgenic mice (n=12 per group), scale bar represents 200μmetres

**CD68:**

**8 month DSP-4 TASTPM**



**8 month VEH TASTPM**



**CD68:**

**11 month DSP-4 TASTPM**



**11 month VEH TASTPM**

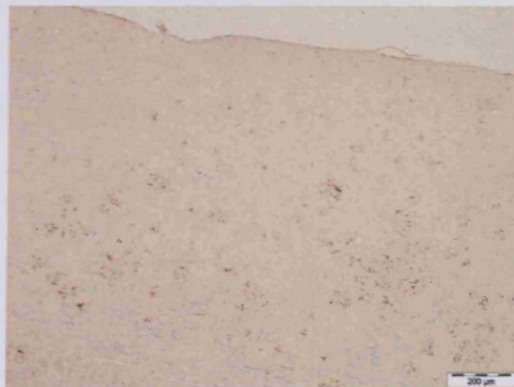


Figure 6.7: Representative photomicrographs of sagittal sections of the cortex stained for CD68 from 8 and 11 month vehicle and DSP-4 treated TASTPM transgenic mice (n=12 per group), scale bar represents 200µmetres

#### 6.4.2.3 Amyloid plaque load

Brains were immunohistochemically processed to identify A $\beta$  plaques (fig 6.8 & 6.9). At 8 months of age, repeated measures ANOVA of A $\beta$  plaque number at the 8 month timepoint revealed a significant effect of treatment,  $F_{(1,38)} = 14.01$ ,  $p < 0.001$ , genotype,  $F_{(1,38)} = 209.30$ ,  $p < 0.001$  and a significant treatment\*genotype interaction,  $F_{(1,38)} = 14.01$ ,  $p < 0.001$ . Post hoc planned comparisons indicated a significant reduction in percentage area of A $\beta$  in cortex in DSP-4 treated relative to

vehicle treated TASTPM mice ( $p < 0.01$ ) (fig 6.10). There was no significant difference in percentage hippocampal A $\beta$  plaque deposition in DSP-4 treated TASTPM versus vehicle treated TASTPM mice.

At 11 months, repeated measures ANOVA revealed an overall effect of genotype,  $F_{(1,39)} = 231.54$ ,  $p < 0.001$ , but no effect of treatment,  $F_{(1,39)} = 2.22$ ,  $p = 0.14$ , on cortical A $\beta$  plaques. There was also an overall effect of genotype,  $F_{(1,39)} = 464.53$ ,  $p < 0.001$ , but no effect of treatment,  $F_{(1,39)} = 0.74$ ,  $p = 0.40$ , on hippocampal A $\beta$  plaques. TASTPM transgenic mice had significantly greater A $\beta$  plaques than C57BL6.J mice irrespective of treatment ( $p < 0.001$ , all groups).

**Amyloid – 8 month:**

**DSP-4 C57BL6/J**



**VEH C57BL6/J**



**Amyloid – 8 month:**

**DSP-4 TASTPM**



**VEH TASTPM**

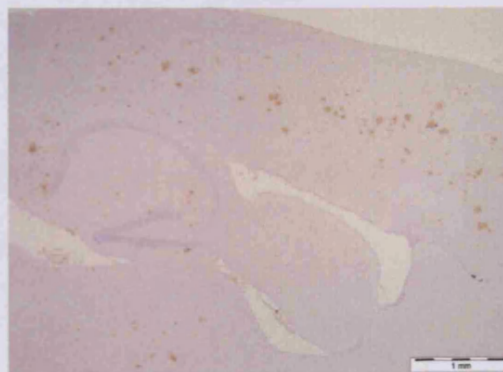


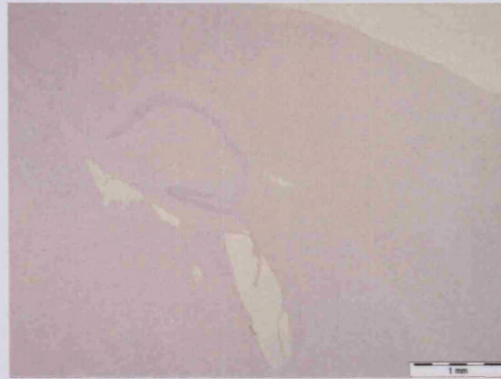
Figure 6.8: Representative photomicrographs of sagittal sections of the cortex and hippocampus stained for amyloid from 8 month vehicle and DSP-4 treated C57BL6/J and TASTPM transgenic mice ( $n=12$  per group), scale bar represents 1mm

**Amyloid – 11 month:**

**DSP-4 C57BL6/J**

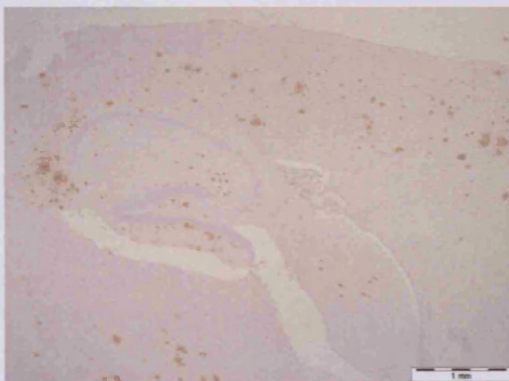


**VEH C57BL6/J**



**Amyloid – 11 month:**

**DSP-4 TASTPM**



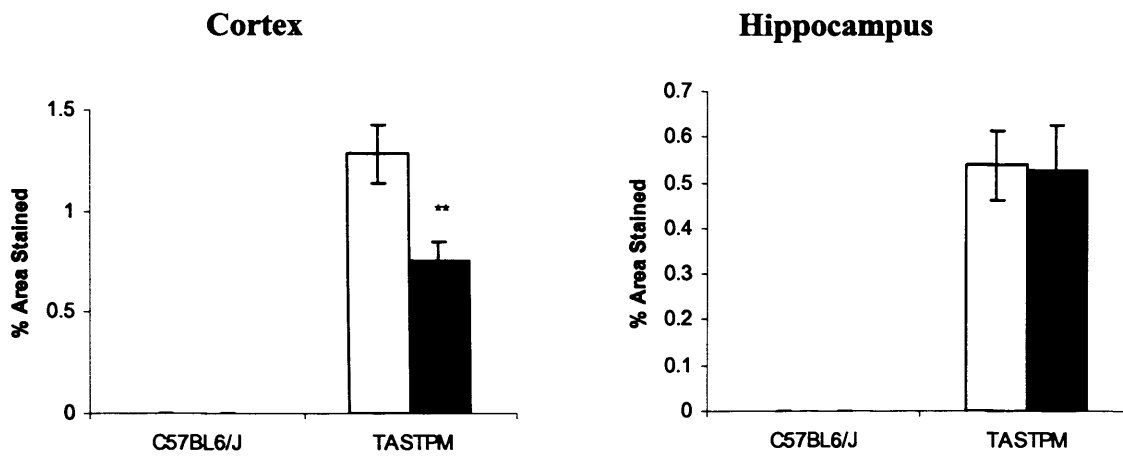
**VEH TASTPM**



Figure 6.9: Representative photomicrographs of sagittal sections of the cortex and hippocampus stained for amyloid from 11 month vehicle and DSP-4 treated C57BL6/J and TASTPM transgenic mice (n=12 per group), scale bar represents 1mm



**Amyloid – 8 month:**



**Amyloid – 11 month:**

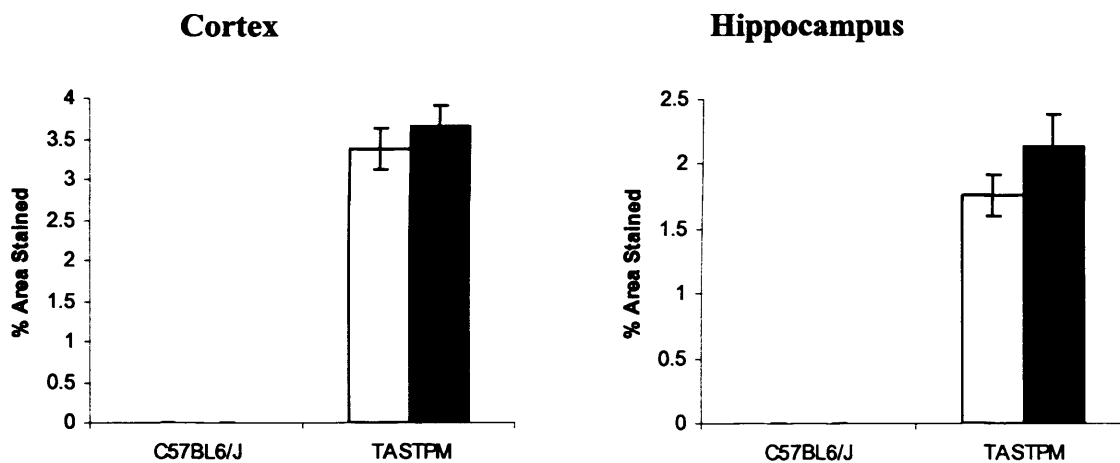


Figure 6.10: Percentage of amyloid stained area in cortex and hippocampus of 8 month and 11 month vehicle and DSP-4 treated C57BL6/J and TASTPM transgenic mice, data represented as percentage stained area and shows mean  $\pm$  SEM. \*\*  $p \leq 0.01$  significantly different vs. vehicle TASTPM (univariate ANOVA followed by planned comparisons)

**6.4.2.4 Neurodegeneration following chronic DSP-4 treatment**

**A. Noradrenergic depletion in the LC**

Brains were immunohistochemically processed to identify tyrosine hydroxylase (TH) as a marker of noradrenergic depletion (fig 6.11 & 6.12). At 8 months of age, there was no overall effect of treatment,  $F_{(1,39)} = 0.13$ ,  $p = 0.72$ , or genotype,  $F_{(1,39)} = 0.31$ ,

$p = 0.58$  on TH cell count. A separate univariate ANOVA revealed a significant effect of treatment,  $F_{(1,38)} = 4.47$ ,  $p = 0.05$  at 11 months of age. Post hoc planned comparisons indicated a significant reduction (19% vs. vehicle TASTPM,  $p < 0.05$ ) in TH staining within the LC (fig 6.13). There was no difference in TH staining of the LC between vehicle and DSP-4 treated C57BL6/J control mice.

**TH – 11 month:**

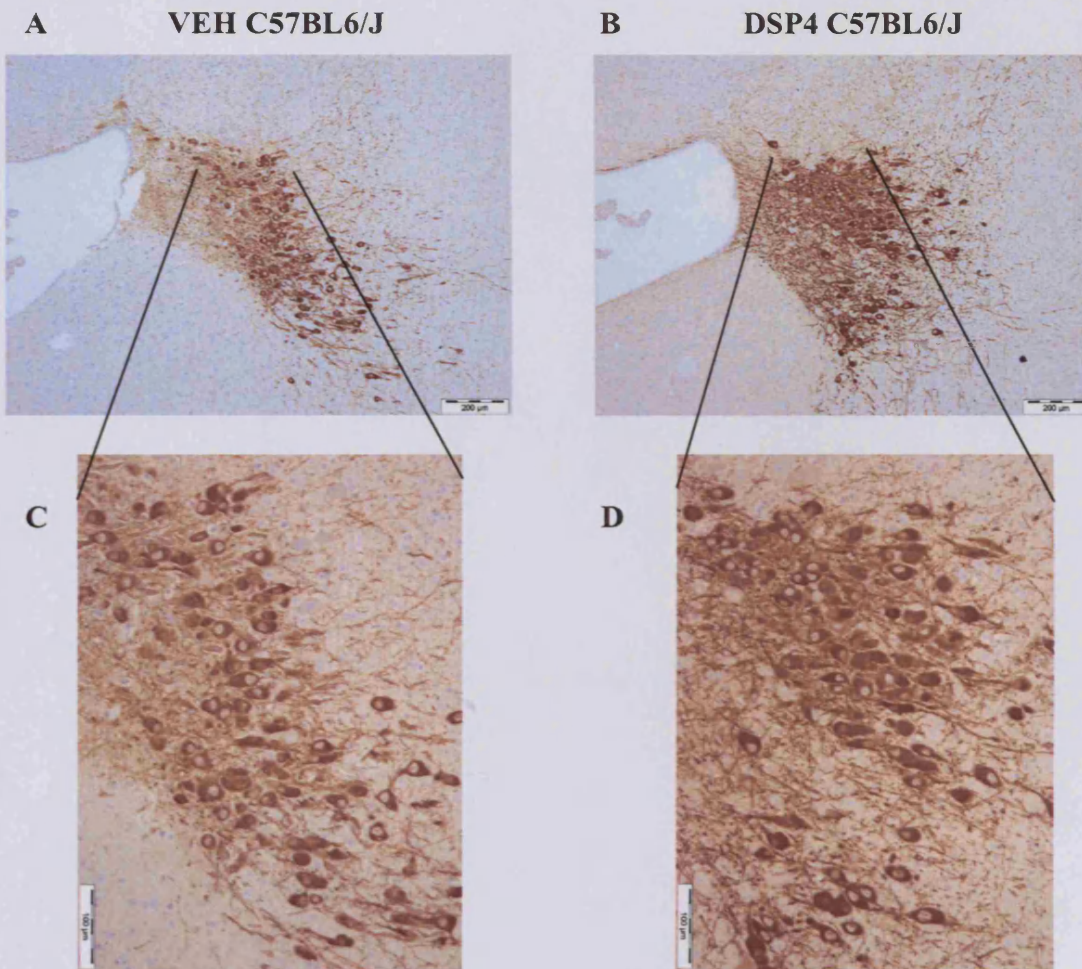


Figure 6.11: Representative photomicrographs of sagittal sections of the locus coeruleus stained for tyrosine hydroxylase (TH) from 11 month vehicle and DSP-4 treated C57BL6/J mice (n=12 per group), scale bar represents 200µmetres (A, B) and 100µmetres (C, D)

TH – 11 month:

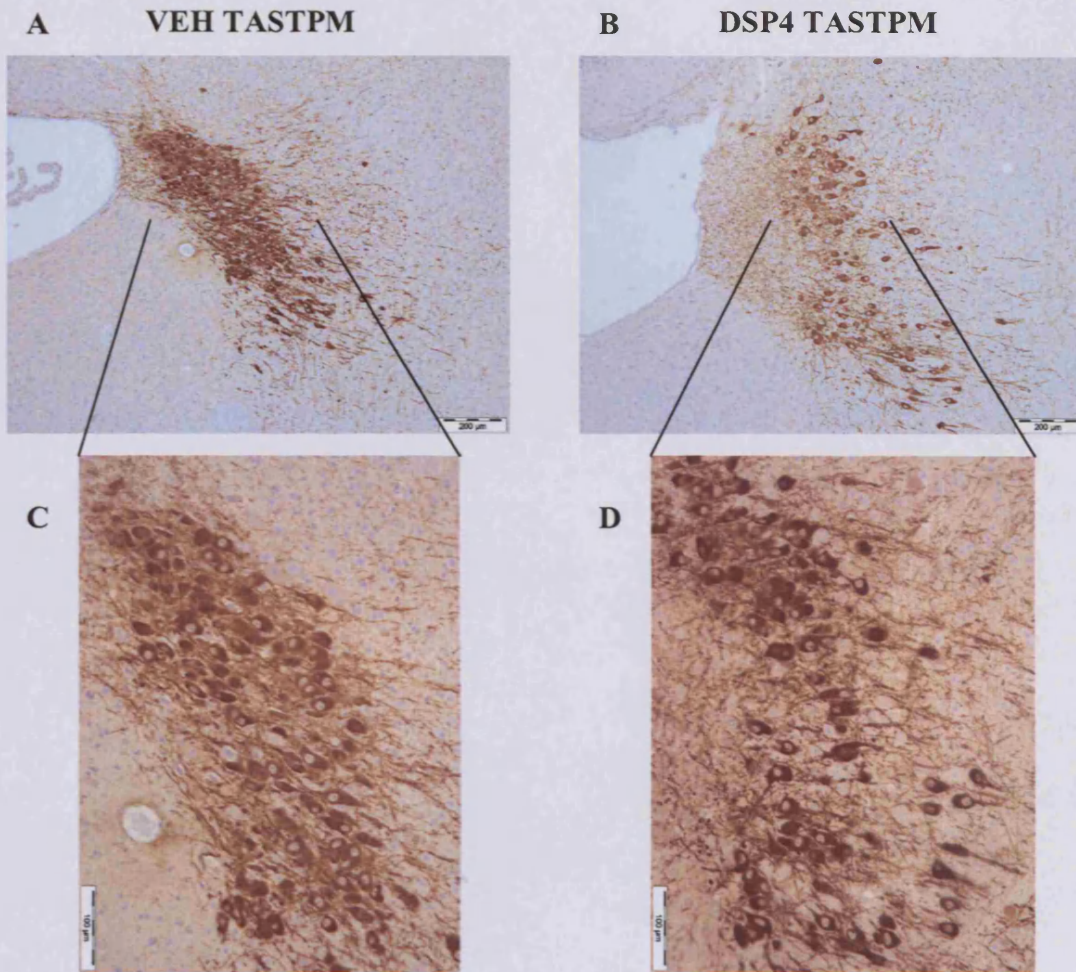


Figure 6.12: Representative photomicrographs of sagittal sections of the locus coeruleus stained for tyrosine hydroxylase (TH) from 11 month vehicle and DSP-4 treated TASTPM transgenic mice (n=12 per group), scale bar represents 200µmetres (A, B) and 100µmetres (C, D)

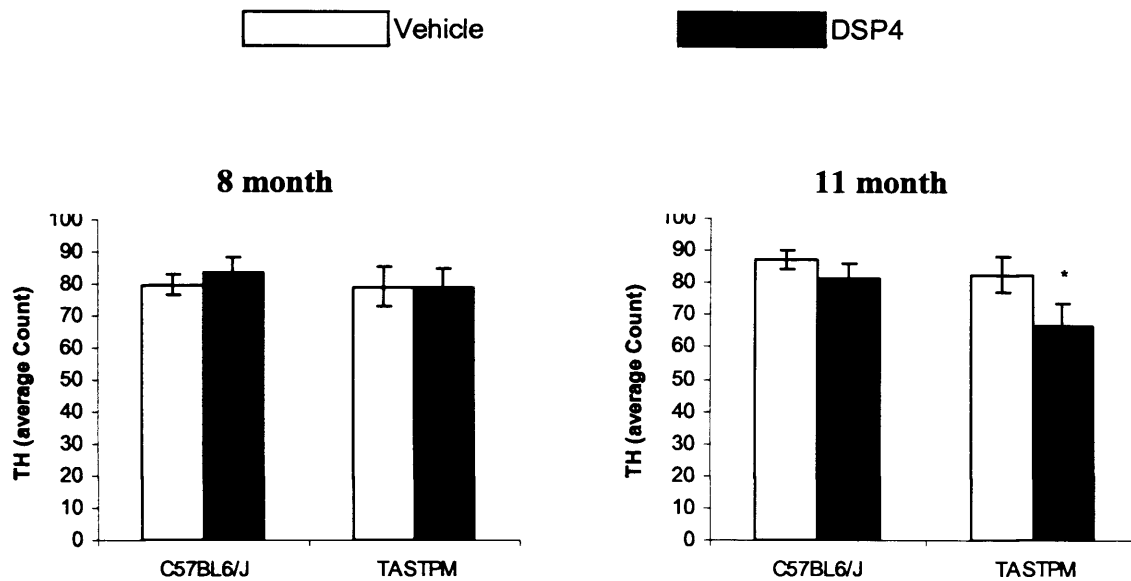


Figure 6.13: TH cell count in the locus coeruleus (LC) of 8 month and 11 month vehicle and DSP-4 treated C57BL6/J and TASTPM transgenic mice (n=12 per group), data represented as count of tyrosine hydroxylase positive stained cells and shows mean  $\pm$  SEM. \*  $p \leq 0.05$  significantly different vs. vehicle TASTPM (univariate ANOVA followed by planned comparisons)

### B. Neurodegeneration in hippocampus

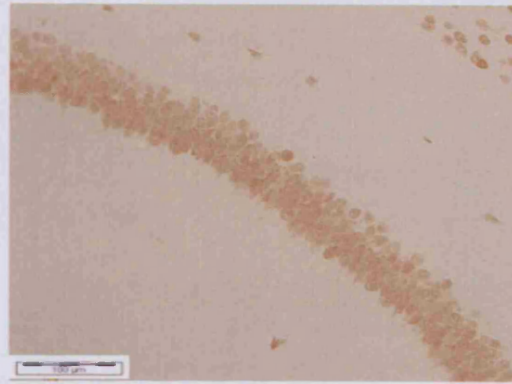
A univariate ANOVA demonstrated an overall effect of age,  $F_{(1,64)} = 33.69$ ,  $p < 0.001$ , on hippocampal NeuN cell count (fig 6.14). There was no overall effect of genotype,  $F_{(1,64)} = 2.49$ ,  $p = 0.12$ , treatment,  $F_{(1,64)} = 3.16$ ,  $p = 0.09$ , or any interaction between treatment\*genotype,  $F_{(1,64)} = 0.00$ ,  $p = 0.99$ . Post hoc planned comparisons revealed that there was a significant difference in cell count between 8 month and 11 month mice within all treatment groups ( $p \leq 0.01$ , all groups) (fig 6.15).

**NeuN:**

**8 month DSP-4 TASTPM**



**8 month VEH TASTPM**



**NeuN:**

**11 month DSP-4 TASTPM**



**11 month VEH TASTPM**

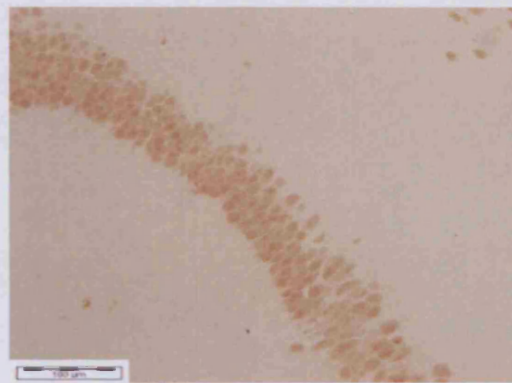


Figure 6.14: Representative photomicrographs of sagittal sections of the hippocampus stained for NeuN from 8 and 11 month vehicle and DSP-4 treated TASTPM transgenic mice (n=12 per group), scale bar represents and 100μmetres

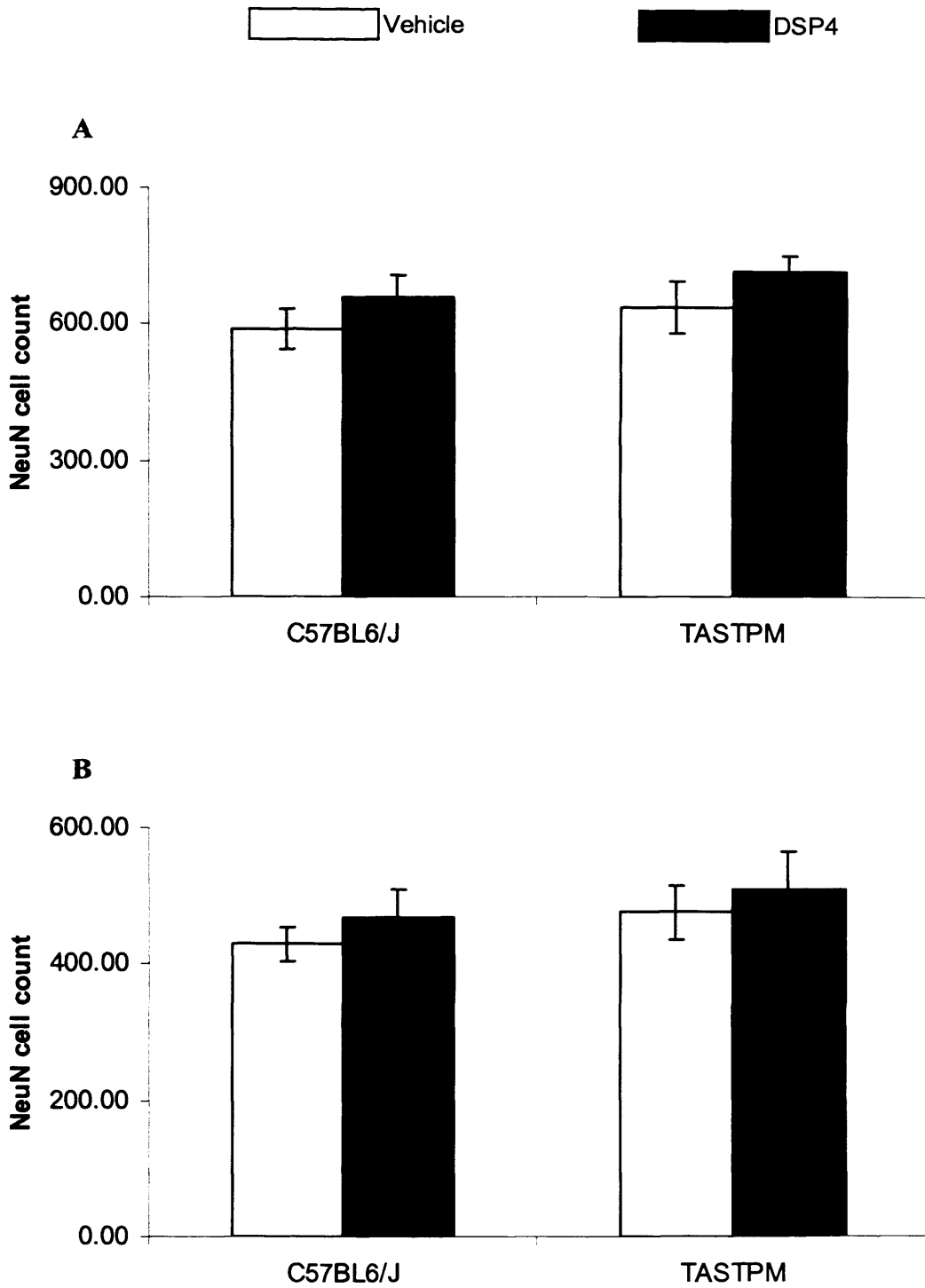


Figure 6.15: NeuN cell count in the hippocampus of 8 month (A) and 11 month (B) vehicle and DSP-4 treated C57BL6/J and TASTPM transgenic mice (n=12 per group), data represented as count of NeuN stained positive cells and shows mean  $\pm$  SEM

## 6.5 Discussion

### 6.5.1 *Acute effect of DSP-4 on NA (5mg/kg and 50mg/kg)*

The reduction of central NA by high doses (50mg/kg) of the noradrenergic specific neurotoxin DSP-4 has been reported in detail (Jonsson et al, 1981; Hallman & Jonsson, 1984; Prieto & Giralt, 2001) and appears specific to axons originating from the locus coeruleus (LC) (Fritschy & Grzanna, 1991). DSP-4 treatment subsequently causes an acute and selective degeneration of central NA axonal terminals (Fritschy et al, 1990) leading to a loss of NA cell bodies in the LC (Fritschy & Grzanna,).

The data described in this experiment confirms that DSP-4 can cause an acute reduction of NA in the main LC terminal regions i.e. hippocampus, cortex and cerebellum (fig 6.1) using a well-published dose of 50mg/kg DSP-4 (Hallman & Jonsson, 1984; Fritschy & Grzanna, 1989; Prieto & Giralt, 2001; Fritschy et al, 1990; Fritschy & Grzanna, 1991). As detailed in the methods section of this chapter, previous literature revealed multiple IP injections of 50µg/kg DSP-4 was sufficient to potentiate neuroinflammation in rats cortically injected with Aβ1-42 (Heneka et al, 2002; Heneka et al, 2003). Through personal communication with Dr D Feinstein, a dose of 5mg/kg was considered appropriate to enhance neuroinflammation but minimise the incidence of mortality of TASTPM mice. An acute administration of 5mg/kg DSP-4 significantly reduced cortical, hippocampal and cerebellar NA concentrations (fig 6.1) indicating chronic treatment at this dose would successfully lower NA levels in TASTPM mice. A cortical NA reduction induced by both DSP-4 doses was evident irrespective of hemisphere; however, although a significant reduction was elicited by 50mg/kg DSP-4 in both sides of the hippocampus a decrease in NA in the right hand side using 5mg/kg DSP4 was absent. This may be due to a lower hippocampal NA concentration apparent in vehicle treated animals relative to other brain regions and the increased variance evident in right hand side hippocampal samples.

### 6.5.2 *Repeated administration of DSP-4 to TASTPM mice*

The most prominent neuronal loss evident in AD occurs in the LC (Zarow et al, 2003) and correlates with the duration and severity of dementia (Bondareff et al, 1987). Previous literature also describes the potentiation of neuroinflammation in

vivo following noradrenergic depletion by administration of DSP-4 (Heneka et al, 2002; Heneka et al, 2003; Feinstein et al, 2002; Song et al, 1999; Feinstein et al, 2004; Wenk et al, 2003). This evidence suggests NA depletion may exacerbate the neuroinflammatory actions of amyloid and subsequently enhance neurodegeneration. Hence, I investigated the effects of NA depletion elicited by repeated peripheral injection of DSP-4 on neuroinflammation, amyloid plaque load and neurodegeneration.

#### 6.5.2.1 *Neuroinflammation*

The anti-inflammatory actions of NA are mediated through the modulation of the pro-inflammatory cytokine expression and release from microglia (Russo et al, 2004; Loughlin et al, 1993) and can protect cortical neurons against microglial induced cell death by inhibiting the release of IL-1 $\beta$  (Madrigal et al, 2005). In contrast, low doses of the noradrenergic neurotoxin N - (2-chloroethyl)-N-ethyl-2-bromobenzylamine (DSP-4) (50 $\mu$ g/kg) have been reported to exacerbate microglial activation and inflammatory gene expression (Feinstein et al., 2004) in APP over expressing mice.

The present studies demonstrate that modulation of the NA system by repeated peripheral administration of the noradrenergic neurotoxin DSP-4 can influence the expression of neuroinflammatory markers in APP/PS1 mice. At 8 months of age, vehicle treated TASTPM mice displayed an increased neuroinflammatory profile demonstrated by a trend for increased cortical mRNA expression of the pro-inflammatory cytokine TNF- $\alpha$  and the chemokine MIP-1 $\alpha$  relative to DSP-4 treated TASTPM mice (fig 6.3). There was also a trend towards increased GFAP ( $p = 0.15$ ) in vehicle treated TASTPM relative to DSP-4 treated TASTPM mice (fig 6.3). The reduction in GFAP cortical mRNA expression in DSP-4 treated TASTPM mice was further supported by patchy cortical GFAP staining relative to strong staining evident in C57BL6/J mice (fig 6.5). Interestingly, the trend for an increased neuroinflammatory profile in vehicle versus DSP-4 treated TASTPM mice may relate to the prevention of a natural decline in cortical extracellular NA observed in the vehicle TASTPM transgenic group as a trend towards a reduction in cortical NA levels (fig 6.2). A 3 month treatment of 5 mg/kg DSP-4, administered once a month, did not decrease extracellular cortical or hippocampal NA levels (fig 6.2) in TASTPM mice and did not cause the degeneration of TH-immunopositive cell

bodies in the LC (fig 6.13). The effect of low (5mg/kg) doses of DSP-4 on NA levels in brain tissue has not been reported but the administration of a high dose of DSP-4 (50mg/kg) causes significant reduction in NA levels (Hallman & Jonsson, 1984). It is relevant to the current studies that a 50mg/kg dose of DSP-4 has also been shown to result in the acute increase of extracellular NA efflux in rat brain (Hughes & Stanford, 1998). Hence, the short term (3 months) repeated peripheral administration of DSP-4 at a 5mg/kg dose may not result in a reduction of central NA levels in the brain tissue of DSP-4 treated TASTPM mice. Furthermore, since NA exerts anti-inflammatory actions (Hu et al, 1991), the short term increases in cortical NA levels, in the absence of LC damage, may explain the reduction of neuroinflammatory markers evident in DSP-4 versus vehicle treated TASTPM brain tissue.

Continued administration of DSP-4 resulted in a significant reduction of TH-positive cells in the LC by 11 months (fig 6.13) associated with a significant reduction in cortical and hippocampal NA levels relative to vehicle treated TASTPM mice (fig 6.2). There was no reduction in NA levels in C57BL6/J control mice at any timepoint. The noradrenergic depletion caused by repeated injection of 5mg/kg DSP4 for 6 months to TASTPM mice resulted in the potentiation of cortical IL-1 $\beta$  mRNA expression (fig 6.4) and a reduction in I $\kappa$ B $\alpha$  mRNA (fig 6.4), an intracellular inhibitory kinase responsible for regulating translocation of the transcription factor NF- $\kappa$ B, important in mediating transcription of target genes. Repeated administration of DSP-4 for 6 months did not increase IL-1 $\beta$  mRNA in C57BL6/J control mice. Long-term (6 months) administration of DSP-4 at a low dose (5mg/kg) results in the exacerbation of A $\beta$ -induced neuroinflammation evident in APP/PS1 transgenic mice via the reduction in extracellular cortical and hippocampal NA levels and the loss of TH-positive cell bodies in the LC. The current data support evidence that sufficient depletion of the noradrenergic system by DSP-4 treatment can increase inflammatory gene expression and particularly that of IL-1 $\beta$  (Heneka et al, 2002; Feinstein et al., 2004). Neuroinflammation is associated with A $\beta$  plaques in AD brain tissue (McGeer et al, 1994). The acute increase in cortical NA levels (fig 6.2) in DSP-4 treated TASTPM mice by 8 months of age also resulted in a significant reduction in cortical amyloid plaque load (fig 6.10), which correlates with the significant decrease in cortical GFAP staining (fig 6.5) and mRNA expression (fig 6.3). Recent literature published after completion of the current study demonstrated that twice monthly

dosing of 5mg/kg DSP-4 to mutant V717F APP mice over a 6 month period exacerbated A $\beta$  plaque burden and GFAP staining in brain tissue (Kalinin et al, 2006). These data described here support evidence that NA can modulate A $\beta$  deposition and associated neuroinflammation.

#### 6.5.2.2 *Neurodegeneration*

Recent data has revealed a significant exacerbation of neuronal cell death in the hippocampus, cortex and subiculum of APP23 mice following 50mg/kg DSP4 (Heneka et al, 2006). Here, using a lower 5mg/kg DSP-4 dose repeatedly administered monthly for 3 or 6 months, neurodegeneration in the hippocampus, quantified as NeuN cell count, was not evident (fig 6.15). It is difficult to compare between the study described in this chapter and that reported by Heneka et al, 2006 since a different DSP-4 protocol and transgenic line was used. The lack of neuronal cell death in TASTPM mice following DSP-4 treatment may be explained by the difference in DSP-4 dose and protocol reported by Heneka et al, 2006 to that used in this study. Heneka et al, 2006 reported a 50-60% reduction in TH staining in the LC following two doses of 50mg/kg DSP-4 in contrast to the 19% observed following repeated administration of 5mg/kg DSP4 in the current study. A greater magnitude of noradrenergic depletion in the LC is subsequently more likely to affect terminal regions such as the hippocampus. It is also interesting, however, that control APP23 mice exhibited significant neurodegeneration in the brain regions studied relative to wildtype controls. Hence, DSP-4 treatment significantly exacerbated pre-existing cell death in the brain tissue of APP23 mice. A lack of quantifiable neurodegeneration in the brain tissue of TASTPM transgenic mice prior to the administration of DSP-4 may suggest that peripheral injection of DSP-4 exacerbates pre-existing cell death rather than initiating the occurrence of neurodegeneration in the rodent brain. To address this issue, further work should directly compare the occurrence and magnitude of cell death in brain tissue following DSP-4 administration (using the same protocol) in APP transgenic lines that usually exhibit or fail to exhibit pre-existing neurodegeneration. The injection of DSP-4 prior to and after the occurrence of pre-existing cell death in APP transgenic animals may also further elucidate the role of noradrenergic depletion in initiating or exacerbating neurodegeneration.

Overall, the current studies provide novel information regarding the effects of NA modulation on neuroinflammation, amyloid load and neurodegeneration in APP/PS1 transgenic mice, particularly following the short-term treatment of DSP-4 at relatively low doses (5mg/kg). Altering the DSP-4 protocol to induce a more significant loss of TH staining in the LC, similar to that reported by Heneka et al, 2006, may enhance the possibility of increasing A $\beta$  plaque deposition and neuroinflammation and causing neurodegeneration in TASTPM brain tissue. I have been able to begin a further study at GSK, Harlow to investigate modulation of neuroinflammation and the occurrence of neurodegeneration in TASTPM brain tissue. I am using the DSP-4 protocol described by Heneka et al, 2006. This will clarify further the potential of noradrenergic depletion in TASTPM transgenic mice to provide markers of neuroinflammation and neurodegeneration.

# CHAPTER 7

## *General Discussion & Conclusions*

### 7.1 Discussion

The progression of Alzheimer's disease (AD) is characterised by A $\beta$  plaque formation, neuroinflammation and neurodegeneration. Current therapies for AD are restricted to symptomatic relief and do not, at present, modulate the pathological progression of the disorder. Putative anti-inflammatory and neuroprotective agents for AD need to be tested preclinically in rodent in vivo models that demonstrate robust and reproducible markers of neuroinflammation and neurodegeneration. This thesis explored the development of rodent in vivo models of neuroinflammation and neurodegeneration and investigated markers of neuroinflammation and neurodegeneration in brain tissue. This involved using a range of in vivo and in vitro techniques including IP or ICV injection of LPS, intranuclear injection of A $\beta$ , western blotting to assess the presence of different A $\beta$  forms, oral administration of anti-inflammatory agents, immunohistochemical analysis of A $\beta$  deposits, neurons and immune cells in rodent brain, Luminex<sup>®</sup> analysis of cytokine and other intracellular proteins in brain tissue and lastly, the colorimetric assessment of plasma iNOS activity.

#### 7.1.1 *Luminex<sup>®</sup> - cytokine detection in plasma and brain tissue*

Cytokines are key mediators of inflammation (reviewed by Cohen & Cohen, 1996) and are present in AD brain tissue (Griffin et al, 1995; Grammas et al, 2001; Luterman et al, 2000). Thus, the detection and quantification of cytokine expression, particularly in brain tissue, is an important readout for in vivo models of neuroinflammation. Although the detection of mRNA expression can provide information on gene activity, the post transcriptional events leading to protein production are not taken into account (reviewed by Lockhart & Winzeler, 2000). Hence, the simultaneous detection of cytokine protein is more informative than relying on quantification of mRNA expression. The advantage of analysing a wide range of cytokines within a single sample via Luminex<sup>®</sup> ensures that the balance

between pro- and anti-inflammatory responses can be clearly identified within each individual animal. For example, treatment with a putative anti-inflammatory agent may increase anti-inflammatory readouts as well as decrease pro-inflammatory cytokine expression.

There are currently only two published papers, by the same author, reporting the detection of cytokine protein in rodent (mouse) tissue (Goujon et al, 1996; 1997). A majority of the published literature relies on the quantification of cytokine mRNA expression in brain tissue following IP LPS injection (Gayle et al, 1998; Castanon et al, 2004). Since the completion of this current thesis, Roche et al, 2006 have reported the detection, by ELISA, of significantly increased IL-1 $\beta$  protein associated with a small increase in TNF- $\alpha$  protein in rat brain tissue following IP LPS injection. This recent study supports the data that I have obtained using Luminex<sup>®</sup>. I report a significant increase in IL-1 $\beta$  protein throughout rat brain tissue and an inconsistent increase in TNF- $\alpha$  and IL-1 $\alpha$  within various brain regions including the hippocampus, cortex and hypothalamus (fig 2.3). Roche et al (2006) investigated TNF- $\alpha$  protein at a 2 hour timepoint. The present studies described within this thesis focus primarily on a 6 hour timepoint, suggesting that the detection of various cytokine proteins is dependent upon the timepoint chosen for study as the time-dependant profile of protein production will differ between cytokines. This also has implications on the cytokine protein changes evident in brain tissue following ICV LPS injection. Administration of LPS via ICV injection significantly increased the expression of TNF- $\alpha$ , IL-1 $\alpha$  and IL-1 $\beta$  protein in brain tissue (fig 3.1 & 3.5). At the 2 hour timepoint studied, hippocampal cytokine protein was of a greater magnitude than cortical cytokine protein. LPS initially activates microglia in hippocampal and thalamic areas (Nicholson & Renton, 2001) following ICV administration so that, by 2 hours post LPS, higher levels of cytokine protein are observed in the hippocampus relative to the cortex. In contrast to the wide range of plasma cytokines increased by IP LPS including IFN- $\gamma$ , IL-10, IL-1 $\alpha$ , IL-1 $\beta$ , IL-6 and TNF- $\alpha$  by 6 hours (fig 2.3), ICV LPS increased production of IL-1 $\beta$ , IL-6 and TNF- $\alpha$  only (fig 3.3. & 3.6). Disparity between the range and levels of plasma cytokine protein induced by IP or ICV LPS injection may also relate to differences in the timepoints investigated for each administration route.

### 7.1.2 *Communication of inflammation between the brain and periphery*

I adapted the Luminex<sup>®</sup> system to detect changes in phosphorylated I $\kappa$ B $\alpha$ , p38 and JNK in brain tissue following IP LPS, providing the first report of the detection of phosphorylated intracellular proteins by Luminex<sup>®</sup>. The phosphorylation of intracellular proteins involved in LPS-mediated signalling pathways in brain tissue suggests a centrally derived response to peripherally administered LPS. Previous literature has reported the possible mechanism by which LPS circulating in blood may elicit neuroinflammation (Nadeau & Rivest, 1999). The receptor for LPS, TLR4, is located on microglia found at areas of weak blood brain barrier (BBB) including the circumventricular organs (CVOs), leptomeninges and choroid plexus (ChP) of the brain (Vallieres & Rivest, 1997). Activation of TLR4 causes translocation of NF- $\kappa$ B and activation of MAPK pathways resulting in transcription of target genes within microglia, firstly at the CVOs, and subsequently throughout the brain tissue (Herkenham et al, 1998). Following IP LPS, Luminex<sup>®</sup> detection of intracellular protein phosphorylation revealed that, in agreement with the literature, the LPS-mediated inflammatory response occurred through early NF- $\kappa$ B activation via phosphorylation of the inhibitory factor, I $\kappa$ B $\alpha$  in hippocampal brain tissue at 2 hours following IP LPS (fig 2.8) (Krappmann et al, 2004). NF- $\kappa$ B activation also resulted in decreased cortical JNK phosphorylation by 2 hours following IP LPS (fig 2.8). This supports recent published data indicating NF- $\kappa$ B has anti-apoptotic properties by suppressing JNK activity (Bubici et al, 2006). Phosphorylation of p38 kinase was increased by 6 hours following IP LPS (fig 2.8) indicating that this is a late event in relation to LPS-mediated NF- $\kappa$ B activation within the IP LPS model, which, as is discussed later, has implications on the efficacy of p38 inhibitors in this model. To my knowledge, this is the first report describing the utilisation of Luminex<sup>®</sup> suspension bead arrays for detecting intracellular protein phosphorylation in rodent brain tissue and illustrates the broader application of this technology for detection of proteins in ex vivo tissue. It cannot be discounted that LPS-mediated activation of NF- $\kappa$ B and MAPK pathways in the brain following peripheral LPS administration may be due to entry of LPS into the brain through the BBB and the subsequent action of LPS on immune cells in brain tissue rather than those localised at CVOs. Although there is a molecular weight dependent breakdown of the BBB following IP LPS this is limited to access of molecules approximately <340Da in

size (Singh et al, 2004). Interestingly, following an ICV injection of LPS there is rapid diffusion of LPS across the BBB into blood (Chen et al, 2000). There is a possibility that the indwelling cannula implanted in the brain tissue, necessary for ICV administration of LPS, may damage blood vessels within the brain adequately for LPS to diffuse into blood quickly. This warrants further investigation by assessing the transport across the BBB of dextran molecules more akin to the molecular weight of LPS. This will help establish whether entry of LPS into the brain following IP or out of the brain following ICV LPS is possible and how much the central and peripheral profiles resulting from IP or ICV LPS injection are influenced by diffusion of LPS through the BBB.

### **7.1.3 *LPS models of neuroinflammation – utility for compound screening***

Cytokine protein can be detected in rat brain tissue following IP LPS injection but since the inflammatory response is communicated from blood to brain, any reduction in the peripheral immune response caused by an anti-inflammatory agent may have a knock-on effect to the brain, preventing central cytokine production. Hence, although anti-inflammatory activity of a novel agent can be assessed following IP LPS injection, the central efficacy of anti-inflammatory agents is difficult to determine. The ICV LPS model provides a central inflammatory response evidenced by increased protein production of several cytokines. The ICV model is low throughput because, in rat; stereotaxic surgery is needed to fix an indwelling cannula or to directly inject LPS via Hamilton syringe. The IP and ICV LPS models should be used in conjunction to assess putative anti-inflammatory compounds. I assessed the effects of the glucocorticoid dexamethasone (DEX), the  $\alpha_2$  adrenoceptor antagonist, fluparoxan and the p38 inhibitor, GW569293 on LPS-induced cytokine protein production.

Glucocorticoids modulate cytokine production by numerous mechanisms as previously described in section 1.4.2 of this thesis. DEX is a standard glucocorticoid drug used routinely in preclinical models of inflammation and has been reported to attenuate plasma cytokine expression following IP LPS injection (Mengozi et al, 1994). DEX can reduce LPS-induced cytokine mRNA expression within brain tissue; however, the subsequent effect of DEX on cytokine protein readouts had not yet been quantified (Satta et al, 1998; Jacobs et al, 1997; Kakizaki et al, 1999). Pre-

treatment with DEX significantly inhibited the central and peripheral production of pro-inflammatory cytokines following IP LPS administration (fig 2.5 & 2.6). Since the central efficacy of glucocorticoid was difficult to assess in the IP LPS model, I analysed the efficacy of DEX further using the ICV LPS model. This indicated peripheral pre-treatment with DEX could fully inhibit hippocampal IL-1 $\beta$  and attenuate cortical and hippocampal IL-1 $\alpha$  and TNF- $\alpha$  following ICV administration of 5 $\mu$ g LPS (fig 3.5).

The LPS models have demonstrated peripheral treatment of DEX can inhibit both peripheral and centrally derived inflammation. The efficacy of DEX in both the IP and ICV LPS models also indicates that, used in conjunction, both models can provide valuable information on anti-inflammatory agents.

I further assessed the utilisation of these models using the  $\alpha$ 2-adrenoceptor antagonist, fluparoxan. The role of NA in AD and the action of NA on adrenoceptors was described in section 1.8 of this thesis. NA can down-regulate pro-inflammatory cytokines (Kaneko et al, 2005).  $\alpha$ 2 adrenoceptor antagonists act as anti-inflammatory agents by increasing NA levels. Pre-treatment with fluparoxan prior to IP LPS caused a significant reduction in LPS-induced plasma TNF- $\alpha$  and IL-1 $\beta$  (fig 2.14) and attenuated hippocampal IL-1 $\beta$  and cortical IL-1 $\alpha$  (fig 2.11). This significant anti-inflammatory effect of fluparoxan pre-treatment led to the further assessment of fluparoxan in the ICV LPS model. Peripherally administered fluparoxan significantly attenuated ICV LPS-induced cortical and hippocampal IL-1 $\beta$  and TNF- $\alpha$  and reduced cortical IL-1 $\alpha$  (fig 3.7). These data are the first to demonstrate the anti-inflammatory properties of a  $\alpha$ 2-adrenoceptor antagonist fluparoxan, on IL-1 $\alpha$ , IL-1 $\beta$  and TNF- $\alpha$  protein in both plasma and brain tissue. It also indicates the importance of NA in the modulation of neuroinflammation. This may have important implications in the search for efficacious anti-inflammatory agents suitable for the treatment of inflammatory based neurological disorders including AD.

Previous literature describes the anti-inflammatory actions of p38 $\alpha$  inhibitors in numerous in vivo models of inflammation (Barone et al, 2001; Legos et al, 2001; reviewed by Kaminska, 2005). MAP kinase pathways, particularly, p38 kinase, are also thought to be involved in LPS-mediated intracellular signalling (Lee & Young, 1996; Nolan et al, 2003). I had previously demonstrated that, at timepoints used to assess cytokine readouts, p38 phosphorylation in cortex occurred by 6 hours

following IP LPS (fig 2.8). This event was later than I $\kappa$ B $\alpha$  phosphorylation which occurred in hippocampus by 2 hours. Hence, involvement of MAP kinase pathways may occur as a late event in brain tissue during LPS-induced transcription of target genes following IP LPS injection. These data are consistent with a report by Nolan et al, 2003 that described the increased phosphorylation in cortex and hippocampus of p38 kinase, detected by western blot. The p38 pathway may have a greater contribution to the long-term effects of LPS-induced inflammation since the early increase in I $\kappa$ B $\alpha$  phosphorylation reveals acute effects in brain tissue caused by the peripheral injection of LPS are mediated via NF- $\kappa$ B. Agonism of  $\alpha$ 2 adrenoceptors can induce NF- $\kappa$ B transcriptional activity suggesting an  $\alpha$ 2 adrenoceptor antagonist may inhibit NF- $\kappa$ B transcription of target genes (Lymperopoulos et al, 2006). Dexamethasone has also been reported to inhibit NF- $\kappa$ B translocation (Quan et al, 2000), providing further evidence that agents that can affect the activity of LPS-mediated NF- $\kappa$ B activity may subsequently influence the production of pro- and anti-inflammatory cytokines. It was interesting that subsequent studies demonstrated that p38 $\alpha$  inhibition failed to modulate cytokine protein production in both the IP and ICV LPS models, leading to the hypothesis that, in models demonstrating phosphorylation of p38 kinase as a late event and the main transcription of cytokines occurring via NF- $\kappa$ B activation, p38 inhibitors fail to influence cytokine expression. Previous literature also indicates that p38 activity may be cell-specific, differentially affecting cytokine release between different cell types (Van den Blink et al, 2001; Zhang et al, 1997). Further investigation to establish the specific immune cells activated in plasma and brain tissue following IP LPS injection and a correlation with known p38 activity on different cell types is required. It is important to consider the mechanism of action of anti-inflammatory agents when investigating their activity using LPS models. Agents that may affect cytokine protein production by altering gene transcription may not be efficacious in IP or ICV LPS models if they are unable to modulate NF- $\kappa$ B activity.

#### **7.1.4 Injection of exogenous A $\beta$ in vivo**

There are many in vivo models described in the literature that involve the use of a variety of A $\beta$  fragments, A $\beta$  preparations and methods of delivering A $\beta$  into rodent brain tissue (Miguel-Hidalgo et al, 1998; Craft et al, 2004; Nakagawa et al, 2004;

Ryu et al, 2004). This huge variation in the literature has led to conflicting reports regarding the neuroinflammatory and neurotoxic effects following injection of A $\beta$  into rodent brain. At low (100 $\mu$ M) concentrations of A $\beta$ 1-42, it was revealed that ICV tubing with a metal injector attachment was unlikely to be a suitable method for A $\beta$  delivery (fig 4.2). In contrast, A $\beta$ 1-42 (100 $\mu$ M) was successfully delivered as monomeric, oligomeric and aggregated forms via Hamilton syringe (fig 4.2). Previous literature indicates that most researchers prefer to use a Hamilton syringe when administering A $\beta$  into rodent brain tissue (Song et al, 2001; Ryu et al, 2004). A team led by Sally Frautschy routinely use minipumps to chronically infuse oligomeric A $\beta$  (Frautschy et al, 2001; Craft et al, 2004, Harris-white et al, 2004). The analysis of an oligomeric A $\beta$  solution expelled from the tubing of a minipump revealed that little A $\beta$ 1-42 solution was delivered, particularly in the presence of the metal cannula (fig 4.3). Oligomeric forms were present in the control sample and a sample removed from the minipump but the solution contained within the minipump also consisted of A $\beta$  aggregates. This suggests the oligomeric A $\beta$  solution may aggregate over time, which would have implications on the success of the oligomeric A $\beta$  delivery due to issues with the amount of oligomeric A $\beta$  available within the minipump and the potential blocking of the plastic minipump tubing by rapidly forming A $\beta$  aggregates. Interestingly, A $\beta$  solutions that had previously been shown to cause neurotoxicity in rodent brain tissue when injected via Hamilton syringe (Ryu et al, 2004, Miguel-Hidalgo et al, 1998) consisted of mostly monomeric and some oligomeric forms of A $\beta$ 1-42. Pre-aggregating A $\beta$ 1-42 solutions described in these reports resulted in the increased presence of aggregated A $\beta$  in a control sample; however, this could not be successfully expelled through a Hamilton syringe (fig 4.4). Hence, A $\beta$  aggregates appear difficult to expel successfully from any apparatus routinely used to apply agents into brain tissue *in vivo*. These current novel data implies that there are limitations to examining A $\beta$  mediated neuroinflammation or neurodegeneration *in vivo* as the direct injection via a Hamilton syringe is restricted to the delivery of soluble forms of A $\beta$ 1-42.

There is a further concern regarding the successful delivery of A $\beta$  into rodent brain *in vivo*. Some authors describe the deposition of injected A $\beta$  within brain tissue (Miguel-Hidalgo et al, 1998; Weldon et al, 1998); however, in contrast many do not

report whether the A $\beta$  solution injected has been successfully delivered into the brain (Jantaratnotai et al, 2003; Ryu et al, 2004; Heneka et al, 2002; Games et al, 1992). In agreement with previous literature, viewing Congo red stained A $\beta$  deposits under polarised light revealed that the A $\beta$  did not form fibrils once in the brain tissue (fig 4.18); therefore, neurotoxicity occurred in response to the presence of soluble A $\beta$  (Miguel-Hidalgo et al, 1998). Although A $\beta$  deposition in brain tissue is a prominent feature of AD, it is still unclear whether A $\beta$  plaques are causative for the disease. The current studies demonstrate that the delivery of A $\beta$ 1-42 into rodent brain tissue is restricted to soluble forms and that soluble A $\beta$ , by 7 days post injection, does not fibrillise in the tissue. This suggests it will be difficult to consistently assess the role of fibrillised A $\beta$  in vivo since it is difficult to achieve reliable delivery and the A $\beta$  deposit may not aggregate over a short study duration. The argument against a role for insoluble A $\beta$  in neurotoxicity includes evidence that A $\beta$  plaque load does not strongly correlate with the progression and severity of cognitive deficits in AD and does not cause significant neurodegeneration in mouse with mutant APP or APP and PS-1 overexpression (Games et al, 2006). More recently, the levels of soluble oligomeric forms of A $\beta$  have been shown to correlate with disease severity and induce neurotoxicity (Watson et al, 2005; De Felice et al, 2004).

### **7.1.5 *A $\beta$ models of neuroinflammation & neurodegeneration***

As stated previously, there is contradictory evidence regarding the neurotoxicity of A $\beta$  in vivo and much of the variability may result from differences between the A $\beta$  fragments and method of administration used. However, the solvent employed to dissolve and prepare the A $\beta$  can also vary widely (Winkler et al, 1994; O'Hare et al, 1999; Waite et al, 1992, Ryu et al, 2004). In the current studies, A $\beta$  was dissolved in PBS which caused approximately a 25% hippocampal cell loss (fig 4.13) and 69% mediolateral damage (fig 4.14) relative to vehicle treated animals. This effect was similar to that achieved by Ryu et al, 2004 in which Ryu et al described the comparison of A $\beta$  injected rats with non injected shams. In contrast to Ryu et al, 2004, the current studies revealed that A $\beta$ 1-42 dissolved in acetonitrile, at either 0.35 or 0.035%, caused toxicity that was similar to the neurotoxic effect of acetonitrile injection alone (fig 4.7 & 4.13). This highlights the importance of comparing an A $\beta$  injected animal to vehicle injection rather than non injected sham rats. The data

described in this thesis suggests that A $\beta$ 1-42 does not exacerbate acetonitrile driven cell death and that acetonitrile causes significant neurotoxicity in vivo, even when administered in relatively small quantities. This disagrees with a previous report suggesting that A $\beta$  may potentiate the toxicity of 35% acetonitrile in vivo (Waite et al, 1992) but this study described the injection of 3nmol human A $\beta$ 1-40 or rat A $\beta$ 1-42 in contrast to the 1nmol human A $\beta$ 1-42 used in these current studies. Acetonitrile is believed to cause calcium driven neurotoxicity and due to the nature of this in vivo model, direct application of an acetonitrile based vehicle onto hippocampal cells in vivo is likely to cause a large degree of neurotoxicity (Waite et al, 1992).

In contrast to the variable and inconsistent neurotoxicity induced by injection of A $\beta$ , significant neuroinflammation was observed around the injection site. Quantification of microglial and macrophage staining revealed a clear increase in neuroinflammation following injection of A $\beta$ 1-42 when using either PBS alone or acetonitrile/PBS as a vehicle (fig 4.16). This indicates that A $\beta$ 1-42 causes significant neuroinflammation whilst acetonitrile elicits neurotoxicity via an alternative mechanism (i.e. calcium-mediated neurotoxicity). The macrophage and microglia were surrounding the extracellular deposit and cell loss was evident only adjacent to the deposit (fig 4.15). This is similar to that seen in AD brain tissue since activated microglia surround extracellular senile plaques (McGeer et al, 1994). The role of microglia in mediating A $\beta$ -induced cell death is unclear. Activated microglia phagocytose extracellular A $\beta$  deposits and may attack the surrounding healthy tissue. Microglia can also release neurotoxic reactive species that cause further damage (Minager et al, 2002). It is possible that the toxicity evident in an exogenous A $\beta$  injection model occurs via an inflammatory-driven mechanism comprising the release of toxic agents by microglia and macrophage surrounding the A $\beta$  deposit. Certainly, the direct injection of soluble A $\beta$  primarily caused robust and quantifiable neuroinflammation with a small window of neurodegeneration. In vitro evidence suggests that the presence of microglia and the corresponding release of reactive oxygen species enhance A $\beta$  neurotoxicity, particularly when cells are incubated with low concentrations of A $\beta$  (Qin et al, 2002). Ryu et al, 2004 reported that minocycline, an antibiotic with anti-inflammatory properties in vivo, attenuated neuroinflammation and neurodegeneration following intra-hippocampal injection of soluble A $\beta$ 1-42 into rat brain tissue lending support that extracellular A $\beta$  induced

neurotoxicity may be mediated by an inflammatory mechanism. In addition, intracellular soluble A $\beta$  pools have also been suggested to significantly contribute to cell death (Wirhth et al, 2004). Recent evidence suggests a role for microglia in converting extracellular soluble A $\beta$  deposits, originally released from intraneuronal soluble A $\beta$  stores, into fibrillar A $\beta$  (Nagele et al, 2004). The role of extracellular insoluble A $\beta$  in AD remains uncertain and whilst fibrillised A $\beta$  will contribute to neuronal cell death in brain tissue, some argue that core plaques may also be neuroprotective by sequestering toxic A $\beta$  from intracellular pools of soluble A $\beta$  (Yan et al, 1996). Recently generated transgenic models of APP/PS1 overexpression exhibit intraneuronal A $\beta$  that correlates with neuronal loss in brain tissue further supporting a role for intraneuronal A $\beta$  in neurodegeneration. Although intraneuronal A $\beta$  may increase the window of cell death observed in an in vivo model of A $\beta$  mediated cell death, it is unlikely that this will be achieved by injection of exogenous A $\beta$  into rodent brain. Furthermore, the nature of the direct injection procedure in vivo and the resulting variability in neurotoxicity may only provide inconsistent readouts of neuronal cell death that are unsuitable for compound screening. This is in contrast to the significant A $\beta$  mediated neurotoxicity seen in vitro as the incubation of neuronal cells with A $\beta$  has been reported to cause significant cell death (Yankner et al, 1990) and neuronal cell culture assays are used to assess the activity of putative neuroprotective agents (Ban et al, 2006). The disparity between in vitro and in vivo models investigating A $\beta$ -mediated neurotoxicity is likely to be due to a wide variety of factors including differences between the amount of A $\beta$  administered to cause cell death in vitro or in vivo, variation of the A $\beta$  aggregation rate between an in vitro and in vivo setting and, importantly, the lack of cell-cell interactions in vitro. Taken together, previous literature and the current studies suggest that the magnitude of neurotoxicity observed in vitro has yet to be consistently detected in rodent in vivo A $\beta$  injection/infusion models. An in vivo A $\beta$  injection rodent model is more likely to be useful in the screening of putative anti-inflammatory agents for AD since robust changes in neuroinflammation were evident in the current studies.

In addition to A $\beta$ , another feature of AD is the intracellular aggregation of the microtubule associated protein tau as neurofibrillary tangles (NFTs) (Blennow et al, 2006). This pathological characteristic is not considered in models of A $\beta$  induced

neuroinflammation or neurodegeneration but NFTs have been shown to correlate with neuronal cell loss (Gomez-Isla et al, 1997) in AD. Previous studies have been conducted to investigate the effect of A $\beta$  injection on NFT numbers in the brain tissue of tau transgenic mice (Gotz et al, 2001). Triple (APP/PS1/tau) transgenic mice have also been generated (Oddo et al, 2006) but interestingly, recent data using these mice suggests that the presence of intraneuronal A $\beta$  precedes evidence of A $\beta$  plaques or tau pathology and correlates with deficits in synaptic plasticity (Cole et al, 2006). Future studies using models that combine A $\beta$  and tau pathology will further elucidate the role of intracellular and extracellular A $\beta$  and NFTs in neurodegeneration and neuroinflammation.

#### **7.1.6 APP & APP/PS1 transgenic mouse models**

Cytokines are present in the plasma, cerebrospinal fluid and brain tissue of AD patients (McGeer & McGeer, 2002). It remains controversial whether this inflammatory response is causal or consequential in the pathology of the disease (Perry et al, 2004). It is, therefore, interesting that peripheral infection can enhance cognitive decline and increase signs of neuroinflammation in AD patients (Holmes et al, 2003) suggesting a role for peripheral infection in the exacerbation of AD brain pathology. Early reports of APP or APP/PS1 transgenic mouse models were useful for the assessment of cognition and behaviour, amyloid neuropathology and neuroinflammation but apart from the neurodegeneration exhibited in the APP23 mouse line, most fail to demonstrate any overt neuronal loss (Stein & Johnson, 2002; Higgins & Jacobsen, 2003). Challenging transgenic mice with peripherally administered inflammatory or neurotoxic agents is a relatively new approach supported by early evidence that IP LPS administration to animals injected with prion protein exacerbates neuropathology and behavioural endpoints (Cunningham et al, 2005). This demonstrates the use of LPS to enhance pathology in other models of neurodegeneration. There has been little comprehensive assessment of the effect of peripheral LPS in APP/PS1 transgenic models, particularly investigating the production of cytokine protein (Sly et al, 2001) rather than mRNA cytokine readouts (Abbas et al, 2002; Lim et al, 2000). Quantification of cytokine protein in plasma and brain tissue following an acute peripheral LPS challenge in the APP/PS1 model TASTPM revealed an exacerbation of a pre-existing neuroinflammatory profile. Vehicle treated TASTPM mice exhibited increased central MIP-1 $\alpha$  by 10 months of

age (fig 5.4). Following IP LPS challenge, increased central MIP-1 $\alpha$  became evident from 5 months of age and maintained at 10 months in TASTPM brain tissue (fig 5.4). Acute LPS challenge did not significantly cause any other alteration in the neuroinflammatory profile of the TASTPM mouse. Chronic LPS did not exacerbate neuroinflammation or cause neurodegeneration in the TASTPM model. It cannot be discounted that the lack of any overt effect of repeated administration of LPS peripherally may be due to the duration of the treatment or the dose of LPS chosen. Certainly, throughout the long duration of a chronic neurodegenerative disorder like AD, a persistent peripheral infection may eventually cause neurodegeneration or cause significant exacerbation of pre-existing pathology. The earlier detection of MIP-1 $\alpha$  in TASTPM brain tissue following a single acute dose of LPS would suggest that, providing the magnitude of the peripheral inflammatory response were sufficient, it can exacerbate pre-existing neuroinflammation.

In addition, administration of the noradrenergic neurotoxin DSP-4 to TASTPM mice resulted in the modulation of inflammatory endpoints (fig 6.3 & 6.4) and A $\beta$  deposition (fig 6.8 – 6.10). Unexpected increases in hippocampal and cortical NA levels (fig 6.2) in TASTPM mice after 3 monthly injections with DSP-4 was associated with a decrease in A $\beta$  plaque deposition and an attenuation of cytokine and chemokine mRNA expression in TASTPM brain tissue. This is consistent with previous reports describing the potentiation of inflammation and A $\beta$  deposition following significant noradrenergic depletion (Heneka et al, 2002; Kalinin et al, 2006). Since the completion of this current study, Heneka et al 2006 reported that DSP-4 administration exacerbated cell loss and neuroinflammation in the brain tissue of APP23 mice. The APP23 mouse line has been previously reported to demonstrate significant neurodegeneration (Bondolfi et al, 2002). The TASTPM model does not demonstrate significant overt cell death. This implies that for a toxic peripheral challenge to induce a significant effect on cell death, a transgenic model must be chosen that has significant pre-existing neurodegenerative pathology.

### **7.1.7 Conclusion and future studies**

This thesis has presented studies investigating the development of rodent in vivo models comprising markers of neuroinflammation and neurodegeneration pertinent

to AD. Although a single acute injection of A $\beta$  or LPS or the administration of a peripheral insult to APP/PS1 overexpressing transgenic mice does not constitute a model of AD, particularly since these are relatively short duration studies in contrast to the chronic progressive nature of AD, the data described here have strong implications on the future development of in vivo models for screening putative therapeutic strategies for AD.

These data and more recent published studies suggest that administering a peripheral inflammatory or neurotoxic insult to mice with overexpression of mutant APP or APP/PS1 may provide robust and quantifiable markers of neuroinflammation and neurodegeneration suitable for screening novel agents. Heneka et al (2006) reported that the administration of a higher dose of DSP-4 (50mg/kg) to APP23 mice that exhibit neurodegeneration correlating with the presence of intraneuronal A $\beta$  exacerbates neuroinflammation and neurodegeneration. As a consequence of this recent publication and the data reported in this thesis, access to TASTPM mice has allowed me to continue this line of research. I will be investigating neuroinflammation (by immunohistochemistry and Luminex<sup>®</sup>) and neurodegeneration in TASTPM brain tissue at 8 and 11 months of age following IP administration of two 50mg/kg doses of DSP-4 (given a week apart) at 5 months of age. It will be interesting to determine whether administration of DSP-4 (50mg/kg), to an APP/PS1 transgenic mouse line that does not exhibit pre-existing neurodegeneration or significant intraneuronal A $\beta$ , results in the potentiation of neuroinflammation and initiates neurodegeneration. The novel data described in this thesis will focus the development of in vivo models to approaches most likely to provide robust markers of neuroinflammation and neurodegeneration in the future for the successful screening of novel disease modifying agents for AD.

## ***Publications***

### *Articles Published*

**P L Pugh**, M P Vidgeon-Hart, T Ashmeade, A Culbert, Z Seymour, M Perren, F Joyce, ST Bate, A Babin, D Virley, J Richardson, N Upton, D Sunter. Repeated administration of the noradrenergic neurotoxin *N*-(2-chloroethyl)-*N*-ethyl-2-bromobenzylamine (DSP-4) modulates neuroinflammation and amyloid plaque load in mice bearing amyloid precursor protein and presenilin-1 mutant transgenes. *Journal of Neuroinflammation* 2007 4:8

### *Articles in Preparation*

**Pugh PL**, Virley D, Culbert A, Guillot F, Leeson G, Upton N, Sunter D. Cytokine protein detection in rat brain tissue and plasma by a Luminex-100 system; modulation of innate immunity in the CNS by dexamethasone.

*For submission to Journal of Neuroimmunology*

**P Pugh**, D Virley, N Upton, D Sunter. Application of Luminex for the measurement of phosphoproteins in rat brain tissue following intraperitoneal LPS administration.

*For submission to Pharmacological Research*

**P Pugh**, D Virley, N Upton, D Sunter. Alpha 2 antagonism attenuates LPS-induced cytokine protein production in plasma and brain of rats. *For submission to Neuropharmacology*

**P Pugh**, T Jelliss, D Virley, N Upton, D Sunter. Development of rodent models of neuroinflammation and neurodegeneration: Can exogenously administered A1-42 induce neurotoxicity in vivo?

## *Poster Presentations*

**Pugh PL**, Virley, D, Jelliss, T, Upton, N, Sunter, D. Development of rodent models of neuroinflammation and neurodegeneration: Can exogenously administered A1-42 induce neurotoxicity in vivo? 5<sup>th</sup> Forum of European Neuroscience, 8<sup>th</sup> – 12<sup>th</sup> July, 2006, Vienna, Austria.

D Sunter, **PL Pugh**, MP Vidgeon-Hart, T Ashmeade, A Culbert, Z Seymour, M Perren, F Joyce, ST Bate, A Babin, D Virley, J Richardson, N Upton. Assessment of the consequences of noradrenaline manipulation in the APP/PS1 mutant TASTPM mouse. 10<sup>th</sup> International Conference on Alzheimer's Disease and Related Disorders, Madrid, 2006.

**PL Pugh**, Ian C Marshall, Isobel Boyfield, Ream Al-Hasani, Simon T Bate, Neil Upton, David J Virley, David Sunter. LPS-induced cytokine responses in the rat. AD/PD, 7<sup>th</sup> International Conference 2005, Sorrento, Italy, 2005.

**PL Pugh**, Ian C Marshall, Isobel Boyfield, Ream Al-Hasani, Simon T Bate, Neil Upton, David J Virley and David Sunter. Central and peripheral administration of LPS induces cytokine responses in the rat: Modulation by a PPAR gamma agonist. 18<sup>th</sup> National Meeting of the British Neuroscience Association, 3<sup>rd</sup> – 6<sup>th</sup> April, 2005, Brighton, U.K.

**Pugh PL**, Swales AG, Vidgeon-Hart MP, Marshall IC, Smith MI, Al-Hasani R, Brown M, Wadsworth G, Tilling LC, Virley DJ, Upton N, Sunter D. Development of In-Vivo Models of LPS-Induced Neuroinflammation and Neurodegeneration. *Journal of Neuroimmunology* 154 : p203. 7<sup>th</sup> International Congress of Neuroimmunology. Venice, Italy. Sep 28<sup>th</sup>- Oct 2<sup>nd</sup> 2004.

## *Abstracts*

**Pugh PL**, Virley, D, Jelliss, T, Al-Hasani, R, Upton, N, Sunter, D. Development of rodent models of neuroinflammation and neurodegeneration: Can exogenously administered A1-42 induce neurotoxicity in vivo? 5<sup>th</sup> Forum of European

Neuroscience, 8<sup>th</sup> – 12<sup>th</sup> July, 2006, Vienna, Austria.

**PL Pugh**, Ian C Marshall, Isobel Boyfield, Ream Al-Hasani, Simon T Bate, Neil Upton, David J Virley and David Sunter. Central and peripheral administration of LPS induces cytokine responses in the rat: Modulation by a PPAR gamma agonist. 18<sup>th</sup> National Meeting of the British Neuroscience Association, 3<sup>rd</sup> – 6<sup>th</sup> April, 2005, Brighton, U.K.

**Pugh PL**, Swales AG, Vidgeon-Hart MP, Marshall IC, Smith MI, Al-Hasani R, Brown M, Wadsworth G, Tilling LC, Virley DJ, Upton N, Sunter D. Development of In-Vivo Models of LPS-Induced Neuroinflammation and Neurodegeneration. *Journal of Neuroimmunology* 154 : p203. 7<sup>th</sup> International Congress of Neuroimmunology. Venice, Italy. Sep 28<sup>th</sup>- Oct 2<sup>nd</sup> 2004.

## References

- Abbas,N., Bednar,I., Mix,E., Marie,S., Paterson,D., Ljungberg,A., Morris,C., Winblad,B., Nordberg,A. & Zhu,J. (2002) Up-regulation of the inflammatory cytokines IFN-gamma and IL-12 and down-regulation of IL-4 in cerebral cortex regions of APP(SWE) transgenic mice. *J.Neuroimmunol.*, 126, 50-57.
- Abramov,A.Y., Canevari,L. & Duchen,M.R. (2003) Changes in intracellular calcium and glutathione in astrocytes as the primary mechanism of amyloid neurotoxicity. *J.Neurosci.*, 23, 5088-5095.
- Adams,J.L., Badger,A.M., Kumar,S. & Lee,J.C. (2001) p38 MAP kinase: molecular target for the inhibition of pro-inflammatory cytokines. *Prog.Med.Chem.*, 38, 1-60.
- Aisen,P.S. (2002) Evaluation of selective COX-2 inhibitors for the treatment of Alzheimer's disease. *J.Pain Symptom.Manage.*, 23, S35-S40.
- Akama,K.T., Albanese,C., Pestell,R.G. & Van Eldik,L.J. (1998) Amyloid beta-peptide stimulates nitric oxide production in astrocytes through an NFkappaB-dependent mechanism. *Proc.Natl.Acad.Sci.U.S.A*, 95, 5795-5800.
- Akiyama,H., Arai,T., Kondo,H., Tanno,E., Haga,C. & Ikeda,K. (2000) Cell mediators of inflammation in the Alzheimer disease brain. *Alzheimer Dis.Assoc.Disord.*, 14 Suppl 1, S47-S53.
- Akundi,R.S., Candelario-Jalil,E., Hess,S., Hull,M., Lieb,K., Gebicke-Haerter,P.J. & Fiebich,B.L. (2005) Signal transduction pathways regulating cyclooxygenase-2 in lipopolysaccharide-activated primary rat microglia. *Glia*, 51, 199-208.
- Alvarez,V., Mata,I.F., Gonzalez,P., Lahoz,C.H., Martinez,C., Pena,J., Guisasola,L.M. & Coto,E. (2002) Association between the TNFalpha-308 A/G polymorphism and the onset-age of Alzheimer disease. *Am.J.Med.Genet.*, 114, 574-577.

- Alzheimer,A., Stelzmann,R.A., Schnitzlein,H.N. & Murtagh,F.R. (1995) An English translation of Alzheimer's 1907 paper, "Uber eine eigenartige Erkankung der Hirnrinde". *Clin.Anat.*, 8, 429-431.
- Ambrosini,A., Louin,G., Croci,N., Plotkine,M. & Jafarian-Tehrani,M. (2005) Characterization of a rat model to study acute neuroinflammation on histopathological, biochemical and functional outcomes. *J.Neurosci.Methods*, 144, 183-191.
- Angeli,A., Masera,R.G., Sartori,M.L., Fortunati,N., Racca,S., Dovio,A., Staurenghi,A. & Frairia,R. (1999) Modulation by cytokines of glucocorticoid action. *Ann.N.Y.Acad.Sci.*, 876 , 210-220.
- Antzutkin,O.N., Leapman,R.D., Balbach,J.J. & Tycko,R. (2002) Supramolecular structural constraints on Alzheimer's beta-amyloid fibrils from electron microscopy and solid-state nuclear magnetic resonance. *Biochemistry*, 41, 15436-15450.
- Aoki,C., Go,C.G., Venkatesan,C. & Kurose,H. (1994) Perikaryal and synaptic localization of alpha 2A-adrenergic receptor-like immunoreactivity. *Brain Res.*, 650, 181-204.
- Apelt,J. & Schliebs,R. (2001) Beta-amyloid-induced glial expression of both pro- and anti-inflammatory cytokines in cerebral cortex of aged transgenic Tg2576 mice with Alzheimer plaque pathology. *Brain Res.*, 894, 21-30.
- Argellati,F., Massone,S., d' Abramo,C., Marinari,U.M., Pronzato,M.A., Domenicotti,C., & Ricciarelli,R. (2006) Evidence against the overexpression of APP in Down syndrome. *IUBMB Life.*, 58, 103-106.
- Armstrong,R.A. (2006) Plaques and tangles and the pathogenesis of Alzheimer's disease. *Folia Neuropathol.*, 44, 1-11.
- Arzt,E., Sauer,J., Pollmacher,T., Labeur,M., Holsboer,F., Reul,J.M. & Stalla,G.K. (1994) Glucocorticoids suppress interleukin-1 receptor antagonist synthesis following induction by endotoxin. *Endocrinology*, 134, 672-677.

- Asadullah,K., Sterry,W. & Trefzer,U. (2002) Cytokine therapy in dermatology. *Exp.Dermatol.*, 11, 97-106.
- Aschner,M. (1998) Immune and inflammatory responses in the CNS: modulation by astrocytes. *Toxicol.Lett.*, 102-103, 283-287.
- Aslan,M. & Ozben,T. (2004) Reactive oxygen and nitrogen species in Alzheimer's disease. *Curr.Alzheimer Res.*, 1, 111-119.
- Ayroldi,E., Migliorati,G., Bruscoli,S., Marchetti,C., Zollo,O., Cannarile,L., D'Adamio,F. & Riccardi,C. (2001) Modulation of T-cell activation by the glucocorticoid-induced leucine zipper factor via inhibition of nuclear factor kappaB. *Blood*, 98, 743-753.
- Bailey,J.M. (1991) New mechanisms for effects of anti-inflammatory glucocorticoids. *Biofactors*, 3, 97-102.
- Baldi,I., Lebailly,P., Mohammed-Brahim,B., Letenneur,L., Dartigues,J.F. & Brochard,P. (2003) Neurodegenerative diseases and exposure to pesticides in the elderly. *Am.J.Epidemiol.*, 157, 409-414.
- Bamberger,M.E. & Landreth,G.E. (2001) Microglial interaction with beta-amyloid: implications for the pathogenesis of Alzheimer's disease. *Microsc.Res.Tech.*, 54, 59-70.
- Ban,J,Y., Cho,S,O., Koh,S,B., Song,K,S., Bae,K. & Seong,Y,H. (2006) Protection of amyloid beta protein (25-35)-induced neurotoxicity by methanol extract of *Smilacis chinae* rhizome in cultured rat cortical neurons. *J.Ethnopharmacol.*, 106, 230-237.
- Barger,S.W. & Harmon,A.D. (1997) Microglial activation by Alzheimer amyloid precursor protein and modulation by apolipoprotein E. *Nature*, 388, 878-881.
- Barone,F.C., Irving,E.A., Ray,A.M., Lee,J.C., Kassis,S., Kumar,S., Badger,A.M., Legos,J.J., Erhardt,J.A., Ohlstein,E.H., Hunter,A.J., Harrison,D.C., Philpott,K., Smith,B.R., Adams,J.L. & Parsons,A.A. (2001) Inhibition of p38 mitogen-activated protein kinase provides neuroprotection in cerebral focal

- ischemia. *Med.Res.Rev.*, 21, 129-145.
- Barranco-Quintana,J.L., Allam,M.F., Del Castillo,A.S. & Navajas,R.F. (2005) [Risk factors for Alzheimer's disease]. *Rev.Neurol.*, 40, 613-618.
- Bazil,V., Baudys,M., Hilgert,I., Stefanova,I., Low,M.G., Zbrozek,J. & Horejsi,V. (1989) Structural relationship between the soluble and membrane-bound forms of human monocyte surface glycoprotein CD14. *Mol.Immunol.*, 26, 657-662.
- Beckmann,M.P. & Morrissey,P.J. (1991) Assays for lymphokines, cytokines and their receptors. *Curr.Opin.Immunol.*, 3, 247-251.
- Behl,C. & Holsboer,F. (1998) [Oxidative stress in the pathogenesis of Alzheimer's disease and antioxidant neuroprotection]. *Fortschr.Neurol.Psychiatr.*, 66, 113-121.
- Beishuizen,A. & Thijs,L.G. (2003) Endotoxin and the hypothalamo-pituitary-adrenal (HPA) axis. *J.Endotoxin.Res.*, 9, 3-24.
- Benzing,W.C., Wujek,J.R., Ward,E.K., Shaffer,D., Ashe,K.H., Younkin,S.G. & Brunden,K.R. (1999) Evidence for glial-mediated inflammation in aged APP(SW) transgenic mice. *Neurobiol.Aging*, 20, 581-589.
- Bertini,R., Bianchi,M., Mengozzi,M. & Ghezzi,P. (1989) Protective effect of chlorpromazine against the lethality of interleukin 1 in adrenalectomized or actinomycin D-sensitized mice. *Biochem.Biophys.Res.Commun.*, 165, 942-946.
- Betancur,C., Borrell,J. & Guaza,C. (1995) Cytokine regulation of corticosteroid receptors in the rat hippocampus: effects of interleukin-1, interleukin-6, tumor necrosis factor and lipopolysaccharide. *Neuroendocrinology*, 62, 47-54.
- Bhattacharya,S.K., Das,N. & Rao,P.J. (1988) Brain monoamines during carrageenan-induced acute paw inflammation in rats. *J.Pharm.Pharmacol.*, 40, 518-520.
- Biber,K., de Jong,E.K., van Weering,H.R. & Boddeke,H.W. (2006) Chemokines and

their receptors in central nervous system disease. *Curr. Drug Targets.*, 7, 29-46.

Bishop, G.M. & Robinson, S.R. (2003) Deposits of fibrillar A beta do not cause neuronal loss or ferritin expression in adult rat brain. *J. Neural Transm.*, 110, 381-400.

Blach-Olszewska, Z. (2005) Innate immunity: cells, receptors, and signaling pathways. *Arch. Immunol. Ther. Exp. (Warsz.)*, 53, 245-253.

Blacker, D. (1997) The genetics of Alzheimer's disease: progress, possibilities, and pitfalls. *Harv. Rev. Psychiatry*, 5, 234-237.

Blennow, K., de Leon, M.J. & Zetterberg, H. (2006) Alzheimer's disease. *Lancet*, 368, 387-403.

Bobrowski, W.F., McDuffie, J.E., Sobocinski, G., Chupka, J., Olle, E., Bowman, A. & Albassam, M. (2005) Comparative methods for multiplex analysis of cytokine protein expression in plasma of lipopolysaccharide-treated mice. *Cytokine*, 32, 194-198.

Boissiere, F., Lehericy, S., Strada, O., Agid, Y. & Hirsch, E.C. (1996) Neurotrophin receptors and selective loss of cholinergic neurons in Alzheimer disease. *Mol. Chem. Neuropathol.*, 28, 219-223.

Bondareff, W., Mountjoy, C.Q., Roth, M., Rossor, M.N., Iversen, L.L., Reynolds, G.P. & Hauser, D.L. (1987) Neuronal degeneration in locus ceruleus and cortical correlates of Alzheimer disease. *Alzheimer Dis. Assoc. Disord.*, 1, 256-262.

Bondolfi, L., Calhoun, M., Ermini, F., Kuhn, H.G., Wiederhold, K.H., Walker, L., Staufenbiel, M. & Jucker, M. (2002) Amyloid-associated neuron loss and gliogenesis in the neocortex of amyloid precursor protein transgenic mice. *J. Neurosci.*, 22, 515-522.

Boyd, R.E. (2001) Alpha2-adrenergic receptor agonists as analgesics. *Curr. Top. Med. Chem.*, 1, 193-197.

Brattsand, R. & Linden, M. (1996) Cytokine modulation by glucocorticoids:

mechanisms and actions in cellular studies. *Aliment.Pharmacol.Ther.*, 10 Suppl 2, 81-90.

Breitner,J.C. (1996) Inflammatory processes and antiinflammatory drugs in Alzheimer's disease: a current appraisal. *Neurobiol.Aging*, 17, 789-794.

Brostjan,C., Anrather,J., Csizmadia,V., Stroka,D., Soares,M., Bach,F.H. & Winkler,H. (1996) Glucocorticoid-mediated repression of NFkappaB activity in endothelial cells does not involve induction of IkappaBalpha synthesis. *J.Biol.Chem.*, 271, 19612-19616.

Brown,R., Li,Z., Vriend,C.Y., Nirula,R., Janz,L., Falk,J., Nance,D.M., Dyck,D.G. & Greenberg,A.H. (1991) Suppression of splenic macrophage interleukin-1 secretion following intracerebroventricular injection of interleukin-1 beta: evidence for pituitary-adrenal and sympathetic control. *Cell Immunol.*, 132, 84-93.

Brown,R.C., Lockwood,A.H. & Sonawane,B.R. (2005) Neurodegenerative diseases: an overview of environmental risk factors. *Environ.Health Perspect.*, 113, 1250-1256.

Brugg,B., Dubreuil,Y.L., Huber,G., Wollman,E.E., Delhay-Bouchaud,N. & Mariani,J. (1995) Inflammatory processes induce beta-amyloid precursor protein changes in mouse brain. *Proc.Natl.Acad.Sci.U.S.A*, 92, 3032-3035.

Bubici,C., Papa,S., Pham,C.G., Zazzeroni,F. & Franzoso,G. (2006) The NF-kappaB-mediated control of ROS and JNK signaling. *Histol.Histopathol.*, 21, 69-80.

Buckingham,J.C., Loxley,H.D., Taylor,A.D. & Flower,R.J. (1994) Cytokines, glucocorticoids and neuroendocrine function. *Pharmacol.Res.*, 30, 35-42.

Burdick,D., Soreghan,B., Kwon,M., Kosmoski,J., Knauer,M., Henschen,A., Yates,J., Cotman,C. & Glabe,C. (1992) Assembly and aggregation properties of synthetic Alzheimer's A4/beta amyloid peptide analogs. *J.Biol.Chem.*, 267, 546-554.

Busciglio,J., Lorenzo,A. & Yankner,B.A. (1992) Methodological variables in the

- assessment of beta amyloid neurotoxicity. *Neurobiol.Aging*, 13, 609-612.
- Bush,A.I., Masters,C.L. & Tanzi,R.E. (2003) Copper, beta-amyloid, and Alzheimer's disease: tapping a sensitive connection. *Proc.Natl.Acad.Sci.U.S.A*, 100, 11193-11194.
- Buttini,M., Mir,A., Appel,K., Wiederhold,K.H., Limonta,S., Gebicke-Haerter,P.J. & Boddeke,H.W. (1997) Lipopolysaccharide induces expression of tumour necrosis factor alpha in rat brain: inhibition by methylprednisolone and by rolipram. *Br.J.Pharmacol.*, 122, 1483-1489.
- Cacquevel,M., Lebeurrier,N., Cheenne,S. & Vivien,D. (2004) Cytokines in neuroinflammation and Alzheimer's disease. *Curr.Drug Targets.*, 5, 529-534.
- Caldenhoven,E., Liden,J., Wissink,S., Van de,S.A., Raaijmakers,J., Koenderman,L., Okret,S., Gustafsson,J.A. & Van der Saag,P.T. (1995) Negative cross-talk between RelA and the glucocorticoid receptor: a possible mechanism for the antiinflammatory action of glucocorticoids. *Mol.Endocrinol.*, 9, 401-412.
- Calignano,A., Carnuccio,R., Di Rosa,M., Ialenti,A. & Moncada,S. (1985) The anti-inflammatory effect of glucocorticoid-induced phospholipase inhibitory proteins. *Agents Actions*, 16, 60-62.
- Cambroner,J.C., Rivas,F.J., Borrell,J. & Guaza,C. (1992) Release of corticotropin-releasing factor from superfused rat hypothalami induced by interleukin-1 is not dependent on adrenergic mechanism. *Eur.J.Pharmacol.*, 219, 75-80.
- Campbell,J., Ciesielski,C.J., Hunt,A.E., Horwood,N.J., Beech,J.T., Hayes,L.A., Denys,A., Feldmann,M., Brennan,F.M. & Foxwell,B.M. (2004) A novel mechanism for TNF-alpha regulation by p38 MAPK: involvement of NF-kappa B with implications for therapy in rheumatoid arthritis. *J.Immunol.* , 173, 6928-6937.
- Campeau,S., Day,H.E., Helmreich,D.L., Kollack-Walker,S. & Watson,S.J. (1998) Principles of psychoneuroendocrinology. *Psychiatr.Clin.North Am.*, 21, 259-276.

- Campion,D., Dumanchin,C., Hannequin,D., Dubois,B., Belliard,S., Puel,M., Thomas-Anterion,C., Michon,A., Martin,C., Charbonnier,F., Raux,G., Camuzat,A., Penet,C., Mesnage,V., Martinez,M., Clerget-Darpoux,F., Brice,A. & Frebourg,T. (1999) Early-onset autosomal dominant Alzheimer disease: prevalence, genetic heterogeneity, and mutation spectrum. *Am.J.Hum.Genet.*, 65, 664-670.
- Canevari,L., Abramov,A.Y. & Duchen,M.R. (2004) Toxicity of amyloid beta peptide: tales of calcium, mitochondria, and oxidative stress. *Neurochem.Res.*, 29, 637-650.
- Caroff,M., Karibian,D., Cavaillon,J.M. & Haeffner-Cavaillon,N. (2002) Structural and functional analyses of bacterial lipopolysaccharides. *Microbes.Infect.*, 4, 915-926.
- Casas,C., Sergeant,N., Itier,J.M., Blanchard,V., Wirths,O., van der,K.N., Vingtdoux,V., van de,S.E., Ret,G., Canton,T., Drobecq,H., Clark,A., Bonici,B., Delacourte,A., Benavides,J., Schmitz,C., Tremp,G., Bayer,T.A., Benoit,P. & Pradier,L. (2004) Massive CA1/2 neuronal loss with intraneuronal and N-terminal truncated Abeta42 accumulation in a novel Alzheimer transgenic model. *Am.J.Pathol.*, 165, 1289-1300.
- Castanon,N., Medina,C., Mormede,C. & Dantzer,R. (2004) Chronic administration of tianeptine balances lipopolysaccharide-induced expression of cytokines in the spleen and hypothalamus of rats. *Psychoneuroendocrinology*, 29, 778-790.
- Chan-Palay,V. & Asan,E. (1989) Alterations in catecholamine neurons of the locus coeruleus in senile dementia of the Alzheimer type and in Parkinson's disease with and without dementia and depression. *J.Comp Neurol.*, 287, 373-392.
- Chang,J.Y. & Liu,L.Z. (2000) Catecholamines inhibit microglial nitric oxide production. *Brain Res.Bull.*, 52, 525-530.
- Chauhan,N.B., Siegel,G.J. & Feinstein,D.L. (2004) Effects of lovastatin and pravastatin on amyloid processing and inflammatory response in TgCRND8

brain. *Neurochem.Res.*, 29, 1897-1911.

Chen,G., McCuskey,R.S. & Reichlin,S. (2000) Blood interleukin-6 and tumor necrosis factor-alpha elevation after intracerebroventricular injection of Escherichia coli endotoxin in the rat is determined by two opposing factors: peripheral induction by LPS transferred from brain to blood and inhibition of peripheral response by a brain-mediated mechanism. *Neuroimmunomodulation.*, 8, 59-69.

Chromy,B.A., Nowak,R.J., Lambert,M.P., Viola,K.L., Chang,L., Velasco,P.T., Jones,B.W., Fernandez,S.J., Lacor,P.N., Horowitz,P., Finch,C.E., Krafft,G.A. & Klein,W.L. (2003) Self-assembly of Abeta(1-42) into globular neurotoxins. *Biochemistry*, 42, 12749-12760.

Cleary,J., Hittner,J.M., Semotuk,M., Mantyh,P. & O'Hare,E. (1995) Beta-amyloid(1-40) effects on behavior and memory. *Brain Res.*, 682, 69-74.

Coelho,A.L., Hogaboam,C.M. & Kunkel,S.L. (2005) Chemokines provide the sustained inflammatory bridge between innate and acquired immunity. *Cytokine Growth Factor Rev.*, 16, 553-560.

Cohen,M.C. & Cohen,S. (1996) Cytokine function: a study in biologic diversity. *Am.J.Clin.Pathol.*, 105, 589-598.

Cole,G. (2006) A transgenic triple scores a home run. *Nat Med.*, 12, 762-53.

Combarros,O., Alvarez-Arcaya,A., Sanchez-Guerra,M., Infante,J. & Berciano,J. (2002) Candidate gene association studies in sporadic Alzheimer's disease. *Dement.Geriatr.Cogn Disord.*, 14, 41-54.

Combarros,O., Sanchez-Guerra,M., Infante,J., Llorca,J. & Berciano,J. (2002) Gene dose-dependent association of interleukin-1A [-889] allele 2 polymorphism with Alzheimer's disease. *J.Neurol.*, 249, 1242-1245.

Combrinck,M.I., Perry,V.H. & Cunningham,C. (2002) Peripheral infection evokes exaggerated sickness behaviour in pre-clinical murine prion disease. *Neuroscience*, 112, 7-11.

- Cornett,C.R., Ehmann,W.D., Wekstein,D.R. & Markesbery,W.R. (1998) Trace elements in Alzheimer's disease pituitary glands. *Biol.Trace Elem.Res.*, 62, 107-114.
- Cotman,C.W. & Anderson,A.J. (1995) A potential role for apoptosis in neurodegeneration and Alzheimer's disease. *Mol.Neurobiol.*, 10, 19-45.
- Cotman,C.W. & Su,J.H. (1996) Mechanisms of neuronal death in Alzheimer's disease. *Brain Pathol.*, 6, 493-506.
- Craft,J.M., Watterson,D.M., Frautschy,S.A. & Van Eldik,L.J. (2004) Aminopyridazines inhibit beta-amyloid-induced glial activation and neuronal damage in vivo. *Neurobiol.Aging*, 25, 1283-1292.
- Cruts,M. & Van Broeckhoven,C. (1998) Molecular genetics of Alzheimer's disease. *Ann.Med.*, 30, 560-565.
- Cunningham,C., Wilcockson,D.C., Campion,S., Lunnon,K. & Perry,V.H. (2005) Central and systemic endotoxin challenges exacerbate the local inflammatory response and increase neuronal death during chronic neurodegeneration. *J.Neurosci.*, 25, 9275-9284.
- da Silva,C.J. & Ulevitch,R.J. (2002) MD-2 and TLR4 N-linked glycosylations are important for a functional lipopolysaccharide receptor. *J.Biol.Chem.*, 277, 1845-1854.
- De Bosscher,K., Schmitz,M.L., Vanden Berghe,W., Plaisance,S., Fiers,W. & Haegeman,G. (1997) Glucocorticoid-mediated repression of nuclear factor-kappaB-dependent transcription involves direct interference with transactivation. *Proc.Natl.Acad.Sci.U.S.A.*, 94, 13504-13509.
- De Felice,F.G., Vieira,M.N., Saraiva,L.M., Figueroa-Villar,J.D., Garcia-Abreu,J., Liu,R., Chang,L., Klein,W.L. & Ferreira,S.T. (2004) Targeting the neurotoxic species in Alzheimer's disease: inhibitors of Abeta oligomerization. *FASEB J.*, 18, 1366-1372.
- De Simoni,M.G., Del Bo,R., De Luigi,A., Simard,S. & Forloni,G. (1995) Central

endotoxin induces different patterns of interleukin (IL)-1 beta and IL-6 messenger ribonucleic acid expression and IL-6 secretion in the brain and periphery. *Endocrinology*, 136, 897-902.

Dean, J.L., Brook, M., Clark, A.R. & Saklatvala, J. (1999) p38 mitogen-activated protein kinase regulates cyclooxygenase-2 mRNA stability and transcription in lipopolysaccharide-treated human monocytes. *J. Biol. Chem.*, 274, 264-269.

Del Bo, R., Angeretti, N., Lucca, E., De Simoni, M.G. & Forloni, G. (1995) Reciprocal control of inflammatory cytokines, IL-1 and IL-6, and beta-amyloid production in cultures. *Neurosci. Lett.*, 188, 70-74.

Delarche, C. & Chollet-Martin, S. (1999) Plasma cytokines: what we are measuring. *Curr. Opin. Clin. Nutr. Metab Care*, 2, 475-479.

Dello Russo, C., Boullerne, A.I., Gavrilyuk, V., Feinstein, D.L. (2004) Inhibition of microglial inflammatory responses by norepinephrine: effects on nitric oxide and interleukin-1 beta production. *J. Neuroinflamm.*, 1, 9.

DeWitt, D.A., Perry, G., Cohen, M., Doller, C. & Silver, J. (1998) Astrocytes regulate microglial phagocytosis of senile plaque cores of Alzheimer's disease. *Exp. Neurol.*, 149, 329-340.

Di Santo, E., Sironi, M., Pozzi, P., Gnocchi, P., Isetta, A.M., Delvaux, A., Goldman, M., Marchant, A. & Ghezzi, P. (1995) Interleukin-10 inhibits lipopolysaccharide-induced tumor necrosis factor and interleukin-1 beta production in the brain without affecting the activation of the hypothalamus-pituitary-adrenal axis. *Neuroimmunomodulation.*, 2, 149-154.

DiCarlo, G., Wilcock, D., Henderson, D., Gordon, M. & Morgan, D. (2001) Intrahippocampal LPS injections reduce A beta load in APP+PS1 transgenic mice. *Neurobiol. Aging*, 22, 1007-1012.

Dickson, D.W., Lee, S.C., Mattiace, L.A., Yen, S.H. & Brosnan, C. (1993) Microglia and cytokines in neurological disease, with special reference to AIDS and Alzheimer's disease. *Glia*, 7, 75-83.

- Dixon,D.R. & Darveau,R.P. (2005) Lipopolysaccharide heterogeneity: innate host responses to bacterial modification of lipid a structure. *J.Dent.Res.*, 84, 584-595.
- Dobrovolskaia,M.A., Medvedev,A.E., Thomas,K.E., Cuesta,N., Toshchakov,V., Ren,T., Cody,M.J., Michalek,S.M., Rice,N.R. & Vogel,S.N. (2003) Induction of in vitro reprogramming by Toll-like receptor (TLR)2 and TLR4 agonists in murine macrophages: effects of TLR "homotolerance" versus "heterotolerance" on NF-kappa B signaling pathway components. *J.Immunol.*, 170, 508-519.
- Dominguez,C., Powers,D.A. & Tamayo,N. (2005) p38 MAP kinase inhibitors: many are made, but few are chosen. *Curr.Opin.Drug Discov.Devel.*, 8, 421-430.
- Dong,C., Davis,R.J. & Flavell,R.A. (2001) Signaling by the JNK group of MAP kinases. c-jun N-terminal Kinase. *J.Clin.Immunol.*, 21, 253-257.
- Dong,C., Davis,R.J. & Flavell,R.A. (2002) MAP kinases in the immune response. *Annu.Rev.Immunol.*, 20, 55-72.
- Douglas L.Feinstein, Michael T.Heneka, Sergey Kalinin, Neelima Chauhan, and Vitaliy Gavriilyuk. Cortical noradrenergic depletion accelerates pathology in TGAPP mice. *Neurobiology of Aging* 25[2], S60. 1-7-2004.
- Du,Y.S., Zhu,H., Fu,J., Yan,S.F., Roher,A., Tourtellotte,W.W., Rajavashisth,T., Chen,X., Godman,G.C., Stern,D. & Schmidt,A.M. (1997) Amyloid-beta peptide-receptor for advanced glycation endproduct interaction elicits neuronal expression of macrophage-colony stimulating factor: a proinflammatory pathway in Alzheimer disease. *Proc.Natl.Acad.Sci.U.S.A.*, 94, 5296-5301.
- Dumitru,C.D., Ceci,J.D., Tsatsanis,C., Kontoyiannis,D., Stamatakis,K., Lin,J.H., Patriotis,C., Jenkins,N.A., Copeland,N.G., Kollias,G. & Tschlis,P.N. (2000) TNF-alpha induction by LPS is regulated posttranscriptionally via a Tpl2/ERK-dependent pathway. *Cell*, 103, 1071-1083.
- Dunn,A.J. (2000) Cytokine activation of the HPA axis. *Ann.N.Y.Acad.Sci.*, 917, 608-

- Dykens, J.A., Moos, W.H. & Howell, N. (2005) Development of 17alpha-estradiol as a neuroprotective therapeutic agent: rationale and results from a phase I clinical study. *Ann.N.Y.Acad.Sci.*, 1052, 116-135.
- Emre, M., Geula, C., Ransil, B.J. & Mesulam, M.M. (1992) The acute neurotoxicity and effects upon cholinergic axons of intracerebrally injected beta-amyloid in the rat brain. *Neurobiol.Aging*, 13, 553-559.
- Ericsson, A., Liu, C., Hart, R.P. & Sawchenko, P.E. (1995) Type 1 interleukin-1 receptor in the rat brain: distribution, regulation, and relationship to sites of IL-1-induced cellular activation. *J.Comp Neurol.*, 361, 681-698.
- Esche, C., Stellato, C. & Beck, L.A. (2005) Chemokines: key players in innate and adaptive immunity. *J.Invest Dermatol.*, 125, 615-628.
- Eskay, R.L., Grino, M. & Chen, H.T. (1990) Interleukins, signal transduction, and the immune system-mediated stress response. *Adv.Exp.Med.Biol.*, 274, 331-343.
- Farmer, P. & Pugin, J. (2000) beta-adrenergic agonists exert their "anti-inflammatory" effects in monocytic cells through the IkappaB/NF-kappaB pathway. *Am.J.Physiol Lung Cell Mol.Physiol.*, 279, L675-L682.
- Feinstein, D.L., Heneka, M.T., Kalinin, S., Chauhan N & Gavrilyuk, V. (2004) Cortical noradrenergic depletion accelerates pathology in TGAPP mice. *Neurobiol. Aging*, 25 Suppl 12, S60.
- Felten, D.L., Felten, S.Y., Bellinger, D.L. & Lorton, D. (1992) Noradrenergic and peptidergic innervation of secondary lymphoid organs: role in experimental rheumatoid arthritis. *Eur.J.Clin.Invest*, 22 Suppl 1, 37-41.
- Fenton, M.J. & Golenbock, D.T. (1998) LPS-binding proteins and receptors. *J.Leukoc.Biol.*, 64, 25-32.
- Fernandez-Vizarra, P., Fernandez, A.P., Castro-Blanco, S., Serrano, J., Bentura, M.L., Martinez-Murillo, R., Martinez, A. & Rodrigo, J. (2004) Intra- and extracellular Abeta and PHF in clinically evaluated cases of Alzheimer's

- disease. *Histol.Histopathol.*, 19, 823-844.
- Fernandez-Vizarra,P., Fernandez,A.P., Castro-Blanco,S., Encinas,J.M., Serrano,J., Bentura,M.L., Munoz,P., Martinez-Murillo,R. & Rodrigo,J. (2004) Expression of nitric oxide system in clinically evaluated cases of Alzheimer's disease. *Neurobiol.Dis.*, 15, 287-305.
- Fessler,H.E., Otterbein,L., Chung,H.S. & Choi,A.M. (1996) Alpha-2 adrenoceptor blockade protects rats against lipopolysaccharide. *Am.J.Respir.Crit Care Med.*, 154, 1689-1693.
- Finck,B.N., Dantzer,R., Kelley,K.W., Woods,J.A. & Johnson,R.W. (1997) Central lipopolysaccharide elevates plasma IL-6 concentration by an alpha-adrenoreceptor-mediated mechanism. *Am.J.Physiol*, 272, R1880-R1887.
- Firuzi,O. & Pratico,D. (2006) Coxibs and Alzheimer's disease: should they stay or should they go? *Ann.Neurol.*, 59, 219-228.
- Folin,M., Baiguera,S., Conconi,M.T., Pati,T., Grandi,C., Parnigotto,P.P. & Nussdorfer,G.G. (2003) The impact of risk factors of Alzheimer's disease in the Down syndrome. *Int.J.Mol.Med.*, 11, 267-270.
- Forloni,G., Demicheli,F., Giorgi,S., Bendotti,C. & Angeretti,N. (1992) Expression of amyloid precursor protein mRNAs in endothelial, neuronal and glial cells: modulation by interleukin-1. *Brain Res.Mol.Brain Res.*, 16, 128-134.
- Foti,M., Granucci,F. & Ricciardi-Castagnoli,P. (2004) A central role for tissue-resident dendritic cells in innate responses. *Trends Immunol.*, 25, 650-654.
- Frautschy,S.A., Baird,A. & Cole,G.M. (1991) Effects of injected Alzheimer beta-amyloid cores in rat brain. *Proc.Natl.Acad.Sci.U.S.A*, 88, 8362-8366.
- Frautschy,S.A., Yang,F., Calderon,L. & Cole,G.M. (1996) Rodent models of Alzheimer's disease: rat A beta infusion approaches to amyloid deposits. *Neurobiol.Aging*, 17, 311-321.
- Frautschy,S.A., Hu,W., Kim,P., Miller,S.A., Chu,T., Harris-White,M.E. & Cole,G.M. (2001) Phenolic anti-inflammatory antioxidant reversal of Abeta-

induced cognitive deficits and neuropathology. *Neurobiol.Aging*, 22, 993-1005.

Freeman,J.J. & Hayes,E.P. (1988) Microsomal metabolism of acetonitrile to cyanide. Effects of acetone and other compounds. *Biochem.Pharmacol.*, 37, 1153-1159.

Freeman,P.K. & Haugen,C.M. (1998) Differential photohydrodehalogenation reactivity of bromobenzenes (1,2,4-tribromobenzene, 1,2,3,5-tetrabromobenzene) and pentachlorobenzene: sunlight-based remediation. *J.Chem.Technol.Biotechnol.*, 72, 45-49.

Frevel,M.A., Bakheet,T., Silva,A.M., Hissong,J.G., Khabar,K.S. & Williams,B.R. (2003) p38 Mitogen-activated protein kinase-dependent and -independent signaling of mRNA stability of AU-rich element-containing transcripts. *Mol.Cell Biol.*, 23, 425-436.

Fritschy,J.M., Geffard,M. & Grzanna,R. (1990) The response of noradrenergic axons to systemically administered DSP-4 in the rat: an immunohistochemical study using antibodies to noradrenaline and dopamine-beta-hydroxylase. *J.Chem.Neuroanat.*, 3, 309-321.

Fritschy,J.M. & Grzanna,R. (1991) Selective effects of DSP-4 on locus coeruleus axons: are there pharmacologically different types of noradrenergic axons in the central nervous system? *Prog.Brain Res.*, 88, 257-268.

Fujimoto,T., Yamazaki,S., Eto-Kimura,A., Takeshige,K. & Muta,T. (2004) The amino-terminal region of toll-like receptor 4 is essential for binding to MD-2 and receptor translocation to the cell surface. *J.Biol.Chem.*, 279, 47431-47437.

Galea,E., Heneka,M.T., Dello,R.C. & Feinstein,D.L. (2003) Intrinsic regulation of brain inflammatory responses. *Cell Mol.Neurobiol.*, 23, 625-635.

Gallay,P., Barras,C., Tobias,P.S., Calandra,T., Glauser,M.P. & Heumann,D. (1994) Lipopolysaccharide (LPS)-binding protein in human serum determines the tumor necrosis factor response of monocytes to LPS. *J.Infect.Dis.*, 170, 1319-

1322.

- Games,D., Khan,K.M., Soriano,F.G., Keim,P.S., Davis,D.L., Bryant,K. & Lieberburg,I. (1992) Lack of Alzheimer pathology after beta-amyloid protein injections in rat brain. *Neurobiol.Aging*, 13, 569-576.
- Games,D., Buttini,M., Kobayashi,D., Schenk,D. & Seubert,P. (2006) Mice as models: Transgenic approaches and Alzheimer's disease. *J.Alzheimers.Dis.*, 9, 133-149.
- Garzon-Rodriguez,W., Vega,A., Sepulveda-Becerra,M., Milton,S., Johnson,D.A., Yatsimirsky,A.K. & Glabe,C.G. (2000) A conformation change in the carboxyl terminus of Alzheimer's A $\beta$  (1-40) accompanies the transition from dimer to fibril as revealed by fluorescence quenching analysis. *J.Biol.Chem.*, 275, 22645-22649.
- Gauthier,E., Fortier,I., Courchesne,F., Pepin,P., Mortimer,J. & Gauvreau,D. (2000) Aluminum forms in drinking water and risk of Alzheimer's disease. *Environ.Res.*, 84, 234-246.
- GayKema,R.P.A., Dijkstra,I. & Tilders,F.J.H. (1995) Subdiaphragmic vagotomy suppresses endotoxin-induced activation of hypothalamic corticotrophin-releasing hormones neurons and ACTH secretion. *Endocrinology.*, 136, 4717-20.
- Gayle,D., Ilyin,S.E., Flynn,M.C. & Plata-Salaman,C.R. (1998) Lipopolysaccharide (LPS)- and muramyl dipeptide (MDP)-induced anorexia during refeeding following acute fasting: characterization of brain cytokine and neuropeptide systems mRNAs. *Brain Res.*, 795, 77-86.
- Gayle,D., Ilyin,S.E. & Plata-Salaman,C.R. (1999) Feeding status and bacterial LPS-induced cytokine and neuropeptide gene expression in hypothalamus. *Am.J.Physiol*, 277, R1188-R1195.
- George-Hyslop,P.H., Tanzi,R.E., Polinsky,R.J., Haines,J.L., Nee,L., Watkins,P.C., Myers,R.H., Feldman,R.G., Pollen,D., Drachman,D. & . (1987) The genetic defect causing familial Alzheimer's disease maps on chromosome 21.

*Science*, 235, 885-890.

Ghezzi,P., Sacco,S., Agnello,D., Marullo,A., Caselli,G. & Bertini,R. (2000) Lps induces IL-6 in the brain and in serum largely through TNF production. *Cytokine*, 12, 1205-1210.

Gillis,S. (1991) Cytokine receptors. *Curr.Opin.Immunol.*, 3, 315-319.

Ginham,R., Harrison,D.C., Facci,L., Skaper,S. & Philpott,K.L. (2001) Upregulation of death pathway molecules in rat cerebellar granule neurons undergoing apoptosis. *Neurosci.Lett.*, 302, 113-116.

Giordano,T., Pan,J.B., Monteggia,L.M., Holzman,T.F., Snyder,S.W., Krafft,G., Ghanbari,H. & Kowall,N.W. (1994) Similarities between beta amyloid peptides 1-40 and 40-1: effects on aggregation, toxicity in vitro, and injection in young and aged rats. *Exp.Neurol.*, 125, 175-182.

Giovannelli,L., Scali,C., Fausson-Pellegrini,M.S., Pepeu,G. & Casamenti,F. (1998) Long-term changes in the aggregation state and toxic effects of beta-amyloid injected into the rat brain. *Neuroscience*, 87, 349-357.

Gitter,B.D., Cox,L.M., Rydel,R.E. & May,P.C. (1995) Amyloid beta peptide potentiates cytokine secretion by interleukin-1 beta-activated human astrocytoma cells. *Proc.Natl.Acad.Sci.U.S.A.*, 92, 10738-10741.

Giulian,D., Haverkamp,L.J., Yu,J.H., Karshin,W., Tom,D., Li,J., Kirkpatrick,J., Kuo,L.M. & Roher,A.E. (1996) Specific domains of beta-amyloid from Alzheimer plaque elicit neuron killing in human microglia. *J.Neurosci.*, 16, 6021-6037.

Glenner,G.G. & Wong,C.W. (1984) Alzheimer's disease: initial report of the purification and characterization of a novel cerebrovascular amyloid protein. *Biochem.Biophys.Res.Commun.*, 120, 885-890.

Goedert,M. (1987) Neuronal localization of amyloid beta protein precursor mRNA in normal human brain and in Alzheimer's disease. *EMBO J.*, 6, 3627-3632.

Goldgaber,D., Harris,H.W., Hla,T., Maciag,T., Donnelly,R.J., Jacobsen,J.S.,

- Vitek,M.P. & Gajdusek,D.C. (1989) Interleukin 1 regulates synthesis of amyloid beta-protein precursor mRNA in human endothelial cells. *Proc.Natl.Acad.Sci.U.S.A*, 86, 7606-7610.
- Gomez-Isla,T., Price,J.L., McKeel,D.W., Jr., Morris,J.C., Growdon,J.H. & Hyman,B.T. (1996) Profound loss of layer II entorhinal cortex neurons occurs in very mild Alzheimer's disease. *J.Neurosci.*, 16, 4491-4500.
- Gomez-Isla,T., Hollister,R., West,H., Mui,S., Growden,J.H., Petersen,R.C., Parisi,J.E., & Hyman,B.T. (1997) Neuronal loss correlates with but exceeds neurofibrillary tangles in Alzheimer's disease. *Ann.Neurol.*, 41, 17-24.
- Goodman,Y. & Mattson,M.P. (1994) Secreted forms of beta-amyloid precursor protein protect hippocampal neurons against amyloid beta-peptide-induced oxidative injury. *Exp.Neurol.*, 128, 1-12.
- Goodridge,H.S. & Harnett,M.M. (2005) Introduction to immune cell signalling. *Parasitology*, 130 Suppl, S3-S9.
- Gordon,S. (1998) The role of the macrophage in immune regulation. *Res.Immunol.*, 149, 685-688.
- Gordon,S. (2002) Pattern recognition receptors: doubling up for the innate immune response. *Cell*, 111, 927-930.
- Gottschall,P.E., Komaki,G. & Arimura,A. (1992) Increased circulating interleukin-1 and interleukin-6 after intracerebroventricular injection of lipopolysaccharide. *Neuroendocrinology*, 56, 935-938.
- Gotz,J., Chen,F., van Dorpe,J. & Nitsch,R.M. (2001) Formation of neurofibrillary tangles in P301I tau transgenic mice induced by Abeta 42 fibrils. *Science*, 293, 1491-5.
- Goujon,E., Parnet,P., Laye,S., Combe,C., Kelley,K.W. & Dantzer,R. (1995) Stress downregulates lipopolysaccharide-induced expression of proinflammatory cytokines in the spleen, pituitary, and brain of mice. *Brain Behav.Immun.*, 9, 292-303.

- Goujon,E., Parnet,P., Laye,S., Combe,C. & Dantzer,R. (1996) Adrenalectomy enhances pro-inflammatory cytokines gene expression, in the spleen, pituitary and brain of mice in response to lipopolysaccharide. *Brain Res.Mol.Brain Res.*, 36, 53-62.
- Goujon,E., Laye,S., Parnet,P. & Dantzer,R. (1997) Regulation of cytokine gene expression in the central nervous system by glucocorticoids: mechanisms and functional consequences. *Psychoneuroendocrinology*, 22 Suppl 1, S75-S80.
- Grammas,P. & Ovasse,R. (2001) Inflammatory factors are elevated in brain microvessels in Alzheimer's disease. *Neurobiol.Aging* , 22, 837-842.
- Gray,E. & Ferrell,W.R. (1992) Acute joint inflammation alters the adrenoceptor profile of synovial blood vessels in the knee joints of rabbits. *Ann.Rheum.Dis.*, 51, 1129-1133.
- Green,K.N. & Peers,C. (2001) Amyloid beta peptides mediate hypoxic augmentation of Ca(2+) channels. *J.Neurochem.*, 77, 953-956.
- Griffin,W.S., Stanley,L.C., Ling,C., White,L., MacLeod,V., Perrot,L.J., White,C.L., III & Araoz,C. (1989) Brain interleukin 1 and S-100 immunoreactivity are elevated in Down syndrome and Alzheimer disease. *Proc.Natl.Acad.Sci.U.S.A*, 86, 7611-7615.
- Griffin,W.S., Sheng,J.G., Roberts,G.W. & Mrak,R.E. (1995) Interleukin-1 expression in different plaque types in Alzheimer's disease: significance in plaque evolution. *J.Neuropathol.Exp.Neurol.*, 54, 276-281.
- Griffin,W.S. (2006) Inflammation and neurodegenerative diseases. *Am.J.Clin.Nutr.*, 83, 470S-474S.
- Grilli,M., Goffi,F., Memo,M. & Spano,P. (1996) Interleukin-1beta and glutamate activate the NF-kappaB/Rel binding site from the regulatory region of the amyloid precursor protein gene in primary neuronal cultures. *J.Biol.Chem.*, 271, 15002-15007.
- Guzik,T.J., Korbout,R. & Adamek-Guzik,T. (2003) Nitric oxide and superoxide in

- inflammation and immune regulation. *J.Physiol Pharmacol.*, 54, 469-487.
- Gwosdow,A.R., O'Connell,N.A., Spencer,J.A., Kumar,M.S., Agarwal,R.K., Bode,H.H. & Abou-Samra,A.B. (1992) Interleukin-1-induced corticosterone release occurs by an adrenergic mechanism from rat adrenal gland. *Am.J.Physiol*, 263, E461-E466.
- Gyure,K.A., Durham,R., Stewart,W.F., Smialek,J.E. & Troncoso,J.C. (2001) Intraneuronal abeta-amyloid precedes development of amyloid plaques in Down syndrome. *Arch.Pathol.Lab Med.*, 125, 489-492.
- Hailman,E., Lichenstein,H.S., Wurfel,M.M., Miller,D.S., Johnson,D.A., Kelley,M., Busse,L.A., Zukowski,M.M. & Wright,S.D. (1994) Lipopolysaccharide (LPS)-binding protein accelerates the binding of LPS to CD14. *J.Exp.Med.*, 179, 269-277.
- Hallenbeck,J.M., Dutka,A.J., Vogel,S.N., Heldman,E., Doron,D.A. & Feuerstein,G. (1991) Lipopolysaccharide-induced production of tumor necrosis factor activity in rats with and without risk factors for stroke. *Brain Res.*, 541, 115-120.
- Halliday,C.A., Jones,B.J., Skingle,M., Walsh,D.M., Wise,H. & Tyers,M.B. (1991) The pharmacology of fluparoxan: a selective alpha 2-adrenoceptor antagonist. *Br.J.Pharmacol.*, 102, 887-895.
- Hallman,H. & Jonsson,G. (1984) Pharmacological modifications of the neurotoxic action of the noradrenaline neurotoxin DSP4 on central noradrenaline neurons. *Eur.J.Pharmacol.*, 103 , 269-278.
- Hardy,J. & Allsop,D. (1991) Amyloid deposition as the central event in the aetiology of Alzheimer's disease. *Trends Pharmacol.Sci.*, 12, 383-388.
- Hardy,J. (1997) Amyloid, the presenilins and Alzheimer's disease. *Trends Neurosci.*, 20, 154-159.
- Harris-White,M.E., Balverde,Z., Lim,G.P., Kim,P., Miller,S.A., Hammer,H., Galasko,D. & Frautschy,S.A. (2004) Role of LRP in TGFbeta2-mediated

neuronal uptake of Abeta and effects on memory. *J.Neurosci.Res.*, 77, 217-228.

Harrison,D.C., Medhurst,A.D., Bond,B.C., Campbell,C.A., Davis,R.P. & Philpott,K.L. (2000) The use of quantitative RT-PCR to measure mRNA expression in a rat model of focal ischemia--caspase-3 as a case study. *Brain Res.Mol.Brain Res.*, 75, 143-149.

Hartley,D.M., Walsh,D.M., Ye,C.P., Diehl,T., Vasquez,S., Vassilev,P.M., Teplow,D.B. & Selkoe,D.J. (1999) Protofibrillar intermediates of amyloid beta-protein induce acute electrophysiological changes and progressive neurotoxicity in cortical neurons. *J.Neurosci.*, 19, 8876-8884.

Hasko,G., Elenkov,I.J., Kvetan,V. & Vizi,E.S. (1995) Differential effect of selective block of alpha 2-adrenoreceptors on plasma levels of tumour necrosis factor-alpha, interleukin-6 and corticosterone induced by bacterial lipopolysaccharide in mice. *J.Endocrinol.*, 144, 457-462.

Heine,H., El Samalouti,V.T., Notzel,C., Pfeiffer,A., Lentschat,A., Kusumoto,S., Schmitz,G., Hamann,L. & Ulmer,A.J. (2003) CD55/decay accelerating factor is part of the lipopolysaccharide-induced receptor complex. *Eur.J.Immunol.*, 33, 1399-1408.

Heneka,M.T., Galea,E., Gavriluyk,V., Dumitrescu-Ozimek,L., Daeschner,J., O'Banion,M.K., Weinberg,G., Klockgether,T. & Feinstein,D.L. (2002) Noradrenergic depletion potentiates beta -amyloid-induced cortical inflammation: implications for Alzheimer's disease. *J.Neurosci.*, 22, 2434-2442.

Heneka,M.T., Sastre,M., Dumitrescu-Ozimek,L., Dewachter,I., Walter,J., Klockgether,T. & Van Leuven,F. (2005) Focal glial activation coincides with increased BACE1 activation and precedes amyloid plaque deposition in APP[V717I] transgenic mice. *J.Neuroinflammation.*, 2, 22.

Heneka,M.T., Ramanathan,M., Jacobs,A.H., Dumitrescu-Ozimek,L., Bilkei-Gorzo,A., Debeir,T., Sastre,M., Galldiks,N., Zimmer,A., Hoehn,M.,

- Heiss,W.D., Klockgether,T. & Staufenbiel,M. (2006) Locus ceruleus degeneration promotes Alzheimer pathogenesis in amyloid precursor protein 23 transgenic mice. *J.Neurosci.*, 26, 1343-1354.
- Hensley,K., Carney,J.M., Mattson,M.P., Aksenova,M., Harris,M., Wu,J.F., Floyd,R.A. & Butterfield,D.A. (1994) A model for beta-amyloid aggregation and neurotoxicity based on free radical generation by the peptide: relevance to Alzheimer disease. *Proc.Natl.Acad.Sci.U.S.A*, 91, 3270-3274.
- Herber,D.L., Roth,L.M., Wilson,D., Wilson,N., Mason,J.E., Morgan,D. & Gordon,M.N. (2004) Time-dependent reduction in A $\beta$  levels after intracranial LPS administration in APP transgenic mice. *Exp.Neurol.*, 190, 245-253.
- Herkenham,M., Lee,H.Y. & Baker,R.A. (1998) Temporal and spatial patterns of c-fos mRNA induced by intravenous interleukin-1: a cascade of non-neuronal cellular activation at the blood-brain barrier. *J.Comp Neurol.*, 400, 175-196.
- Herlaar,E. & Brown,Z. (1999) p38 MAPK signalling cascades in inflammatory disease. *Mol.Med.Today*, 5, 439-447.
- Heumann,D. & Roger,T. (2002) Initial responses to endotoxins and Gram-negative bacteria. *Clin.Chim.Acta*, 323, 59-72.
- Higgins,G.A. & Jacobsen,H. (2003) Transgenic mouse models of Alzheimer's disease: phenotype and application. *Behav.Pharmacol.*, 14, 419-438.
- Ho,L., Luterman,J.D., Aisen,P.S., Pasinetti,G.M., Montine,T.J. & Morrow,J.D. (2000) Elevated CSF prostaglandin E2 levels in patients with probable AD. *Neurology*, 55, 323.
- Hoebe,K., Janssen,E. & Beutler,B. (2004) The interface between innate and adaptive immunity. *Nat.Immunol.*, 5, 971-974.
- Holmes,C., El Okl,M., Williams,A.L., Cunningham,C., Wilcockson,D. & Perry,V.H. (2003) Systemic infection, interleukin 1 $\beta$ , and cognitive decline in Alzheimer's disease. *J.Neurol.Neurosurg.Psychiatry*, 74, 788-789.

- Holscher,C. (2005) Development of beta-amyloid-induced neurodegeneration in Alzheimer's disease and novel neuroprotective strategies. *Rev.Neurosci.*, 16, 181-212.
- Hoogendijk,W.J., Feenstra,M.G., Botterblom,M.H., Gilhuis,J., Sommer,I.E., Kamphorst,W., Eikelenboom,P. & Swaab,D.F. (1999) Increased activity of surviving locus ceruleus neurons in Alzheimer's disease. *Ann.Neurol.*, 45, 82-91.
- Hosoi,T., Okuma,Y. & Nomura,Y. (2000) Electrical stimulation of afferent vagus nerve induces IL-1beta expression in the brain and activates HPA axis. *Am.J.Physiol Regul.Integr.Comp Physiol*, 279, R141-R147.
- Howlett,D.R., Jennings,K.H., Lee,D.C., Clark,M.S., Brown,F., Wetzal,R., Wood,S.J., Camilleri,P. & Roberts,G.W. (1995) Aggregation state and neurotoxic properties of Alzheimer beta-amyloid peptide. *Neurodegeneration.*, 4, 23-32.
- Howlett,D.R., Richardson,J.C., Austin,A., Parsons,A.A., Bate,S.T., Davies,D.C. & Gonzalez,M.I. (2004) Cognitive correlates of Abeta deposition in male and female mice bearing amyloid precursor protein and presenilin-1 mutant transgenes. *Brain Res.*, 1017, 130-136.
- Hu,J., Akama,K.T., Krafft,G.A., Chromy,B.A. & Van Eldik,L.J. (1998) Amyloid-beta peptide activates cultured astrocytes: morphological alterations, cytokine induction and nitric oxide release. *Brain Res.*, 785, 195-206.
- Hu,J. & Van Eldik,L.J. (1999) Glial-derived proteins activate cultured astrocytes and enhance beta amyloid-induced glial activation. *Brain Res.*, 842, 46-54.
- Hu,X.X., Goldmuntz,E.A. & Brosnan,C.F. (1991) The effect of norepinephrine on endotoxin-mediated macrophage activation. *J.Neuroimmunol.*, 31, 35-42.
- Huang,X., Cuajungco,M.P., Atwood,C.S., Hartshorn,M.A., Tyndall,J.D., Hanson,G.R., Stokes,K.C., Leopold,M., Multhaup,G., Goldstein,L.E., Scarpa,R.C., Saunders,A.J., Lim,J., Moir,R.D., Glabe,C., Bowden,E.F., Masters,C.L., Fairlie,D.P., Tanzi,R.E. & Bush,A.I. (1999) Cu(II) potentiation

- of alzheimer abeta neurotoxicity. Correlation with cell-free hydrogen peroxide production and metal reduction. *J.Biol.Chem.*, 274, 37111-37116.
- Hughes,Z.A. & Stanford,S.C. (1998) Evidence from microdialysis and synaptosomal studies of rat cortex for noradrenaline uptake sites with different sensitivities to SSRIs. *Br.J.Pharmacol.*, 124, 1141-1148.
- Hulse,R.E., Kunkler,P.E., Fedynyshyn,J.P. & Kraig,R.P. (2004) Optimization of multiplexed bead-based cytokine immunoassays for rat serum and brain tissue. *J.Neurosci.Methods*, 136 , 87-98.
- Huttunen,H.J., Fages,C. & Rauvala,H. (1999) Receptor for advanced glycation end products (RAGE)-mediated neurite outgrowth and activation of NF-kappaB require the cytoplasmic domain of the receptor but different downstream signaling pathways. *J.Biol.Chem.*, 274, 19919-19924.
- In,'t Veld,B.A., Launer,L.J., Hoes,A.W., Ott,A., Hofman,A., Breteler,M.M. & Stricker,B.H. (1998) NSAIDs and incident Alzheimer's disease. The Rotterdam Study. *Neurobiol.Aging*, 19, 607-611.
- Ingalls,R.R. & Golenbock,D.T. (1995) CD11c/CD18, a transmembrane signaling receptor for lipopolysaccharide. *J.Exp.Med.*, 181, 1473-1479.
- Iravani,M.M., Leung,C.C., Sadeghian,M., Haddon,C.O., Rose,S. & Jenner,P. (2005) The acute and the long-term effects of nigral lipopolysaccharide administration on dopaminergic dysfunction and glial cell activation. *Eur.J.Neurosci.*, 22, 317-330.
- Ishizuka,Y., Ishida,Y., Kunitake,T., Kato,K., Hanamori,T., Mitsuyama,Y., & Kannan,H. (1997) Effects of area postrema lesion and abdominal vagotomy on interleukin-1 $\beta$ -induced norepinephrine release in the hypothalamic paraventricular nucleus region in the rat. *Neurosci.Lett.*, 223, 57-60.
- Itagaki,S., McGeer,P.L., Akiyama,H., Zhu,S. & Selkoe,D. (1989) Relationship of microglia and astrocytes to amyloid deposits of Alzheimer disease. *J.Neuroimmunol.*, 24, 173-182.

- Iversen,L.L., Mortishire-Smith,R.J., Pollack,S.J. & Shearman,M.S. (1995) The toxicity in vitro of beta-amyloid protein. *Biochem.J.*, 311 ( Pt 1), 1-16.
- Jacobs,R.A., Satta,M.A., Dahia,P.L., Chew,S.L. & Grossman,A.B. (1997) Induction of nitric oxide synthase and interleukin-1beta, but not heme oxygenase, messenger RNA in rat brain following peripheral administration of endotoxin. *Brain Res.Mol.Brain Res.*, 49, 238-246.
- Jaim-Etcheverry,G. & Zieher,L.M. (1980) DSP-4: a novel compound with neurotoxic effects on noradrenergic neurons of adult and developing rats. *Brain Res.*, 188, 513-523.
- Janeway,C.A., Jr. (1989) Approaching the asymptote? Evolution and revolution in immunology. *Cold Spring Harb.Symp.Quant.Biol.*, 54 Pt 1, 1-13.
- Jansson,E.T. (2005) Alzheimer disease is substantially preventable in the United States -- review of risk factors, therapy, and the prospects for an expert software system. *Med.Hypotheses*, 64, 960-967.
- Jantaratnotai,N., Ryu,J.K., Kim,S.U. & McLarnon,J.G. (2003) Amyloid beta peptide-induced corpus callosum damage and glial activation in vivo. *Neuroreport*, 14, 1429-1433.
- Jarrett,J.T., Berger,E.P. & Lansbury,P.T., Jr. (1993) The C-terminus of the beta protein is critical in amyloidogenesis. *Ann.N.Y.Acad.Sci.*, 695, 144-148.
- Johnson,A.K. & Epstein,A.N. (1975) The cerebral ventricles as the avenue for the dipsogenic action of intracranial angiotensin. *Brain Res.*, 86, 399-418.
- Jonsson,G., Hallman,H., Ponzio,F. & Ross,S. (1981) DSP4 (N-(2-chloroethyl)-N-ethyl-2-bromobenzylamine)--a useful denervation tool for central and peripheral noradrenaline neurons. *Eur.J.Pharmacol.*, 72, 173-188.
- Kagan,B.L., Hirakura,Y., Azimov,R., Azimova,R. & Lin,M.C. (2002) The channel hypothesis of Alzheimer's disease: current status. *Peptides*, 23, 1311-1315.
- Kakizaki,Y., Watanobe,H., Kohsaka,A. & Suda,T. (1999) Temporal profiles of interleukin-1beta, interleukin-6, and tumor necrosis factor-alpha in the

- plasma and hypothalamic paraventricular nucleus after intravenous or intraperitoneal administration of lipopolysaccharide in the rat: estimation by push-pull perfusion. *Endocr.J.*, 46, 487-496.
- Kalaria,R.N. & Hedera,P. (1995) Differential degeneration of the cerebral microvasculature in Alzheimer's disease. *Neuroreport*, 6, 477-480.
- Kalaria,R.N. (1999) Microglia and Alzheimer's disease. *Curr.Opin.Hematol.*, 6, 15-24.
- Kalehua,A.N., Taub,D.D., Baskar,P.V., Hengemihle,J., Munoz,J., Trambadia,M., Speer,D.L., De Simoni,M.G. & Ingram,D.K. (2000) Aged mice exhibit greater mortality concomitant to increased brain and plasma TNF-alpha levels following intracerebroventricular injection of lipopolysaccharide. *Gerontology*, 46, 115-128.
- Kalinin,S., Gavriyuk,V., Polak,P.E., Heneka,M.T. & Feinstein,D.L. (2006) Noradrenaline deficiency in brain increases beta-amyloid plaque burden in an animal model of Alzheimer's disease. *Neurobiol.Aging*. In Press.
- Kaminska,B. (2005) MAPK signalling pathways as molecular targets for anti-inflammatory therapy--from molecular mechanisms to therapeutic benefits. *Biochim.Biophys.Acta*, 1754, 253-262.
- Kaneko,Y.S., Mori,K., Nakashima,A., Sawada,M., Nagatsu,I. & Ota,A. (2005) Peripheral injection of lipopolysaccharide enhances expression of inflammatory cytokines in murine locus coeruleus: possible role of increased norepinephrine turnover. *J.Neurochem.*, 94 , 393-404.
- Kapcala,L.P., Chautard,T. & Eskay,R.L. (1995) The protective role of the hypothalamic-pituitary-adrenal axis against lethality produced by immune, infectious, and inflammatory stress. *Ann.N.Y.Acad.Sci.*, 771, 419-437.
- Karas,G.B., Burton,E.J., Rombouts,S.A., van Schijndel,R.A., O'Brien,J.T., Scheltens,P., McKeith,I.G., Williams,D., Ballard,C. & Barkhof,F. (2003) A comprehensive study of gray matter loss in patients with Alzheimer's disease using optimized voxel-based morphometry. *Neuroimage.*, 18, 895-907.

- Karin,M. (2004) Mitogen activated protein kinases as targets for development of novel anti-inflammatory drugs. *Ann.Rheum.Dis.*, 63 Suppl 2, ii62-ii64.
- Karin,M. (2005) Inflammation-activated protein kinases as targets for drug development. *Proc.Am.Thorac.Soc.*, 2, 386-390.
- Kasparova,J., Lisa,V., Tucek,S. & Dolezal,V. (2001) Chronic exposure of NG108-15 cells to amyloid beta peptide (A beta(1-42)) abolishes calcium influx via N-type calcium channels. *Neurochem.Res.*, 26, 1079-1084.
- Kellar,K.L. & Iannone,M.A. (2002) Multiplexed microsphere-based flow cytometric assays. *Exp.Hematol.*, 30, 1227-1237.
- Kelly,A., Vereker,E., Nolan,Y., Brady,M., Barry,C., Loscher,C.E., Mills,K.H. & Lynch,M.A. (2003) Activation of p38 plays a pivotal role in the inhibitory effect of lipopolysaccharide and interleukin-1 beta on long term potentiation in rat dentate gyrus. *J.Biol.Chem.*, 278, 19453-19462.
- Kennedy,M.N., Mullen,G.E., Leifer,C.A., Lee,C., Mazzoni,A., Dileepan,K.N. & Segal,D.M. (2004) A complex of soluble MD-2 and lipopolysaccharide serves as an activating ligand for Toll-like receptor 4. *J.Biol.Chem.*, 279, 34698-34704.
- Kim,J.H., Kim,J.H., Park,J.A., Lee,S.W., Kim,W.J., Yu,Y.S. & Kim,K.W. (2006) Blood-neural barrier: intercellular communication at glio-vascular interface. *J.Biochem.Mol.Biol.*, 39, 339-345.
- Kim,S.H., Kim,J. & Sharma,R.P. (2004) Inhibition of p38 and ERK MAP kinases blocks endotoxin-induced nitric oxide production and differentially modulates cytokine expression. *Pharmacol.Res.*, 49, 433-439.
- Kimbrell,D.A. & Beutler,B. (2001) The evolution and genetics of innate immunity. *Nat.Rev.Genet.*, 2, 256-267.
- Kobayashi,S.D., Voyich,J.M., Burlak,C. & DeLeo,F.R. (2005) Neutrophils in the innate immune response. *Arch.Immunol.Ther.Exp.(Warsz.)*, 53, 505-517.
- Kopec,K.K. & Carroll,R.T. (1998) Alzheimer's beta-amyloid peptide 1-42 induces a

- phagocytic response in murine microglia. *J.Neurochem.*, 71, 2123-2131.
- Kosik,K.S. (1994) Alzheimer's disease: which way is forward? *Neurobiol.Aging*, 15 Suppl 2, S91-S92.
- Kotlyarov,A., Neiningen,A., Schubert,C., Eckert,R., Birchmeier,C., Volk,H.D. & Gaestel,M. (1999) MAPKAP kinase 2 is essential for LPS-induced TNF-alpha biosynthesis. *Nat.Cell Biol.*, 1, 94-97.
- Kovalovsky,D., Paez,P.M., Sauer,J., Perez,C.C., Nahmod,V.E., Stalla,G.K., Holsboer,F. & Arzt,E. (1998) The Th1 and Th2 cytokines IFN-gamma and IL-4 antagonize the inhibition of monocyte IL-1 receptor antagonist by glucocorticoids: involvement of IL-1. *Eur.J.Immunol.*, 28, 2075-2085.
- Kowall,N.W., Beal,M.F., Busciglio,J., Duffy,L.K. & Yankner,B.A. (1991) An in vivo model for the neurodegenerative effects of beta amyloid and protection by substance P. *Proc.Natl.Acad.Sci.U.S.A*, 88, 7247-7251.
- Kowalska,A. (2004) [The beta-amyloid cascade hypothesis: a sequence of events leading to neurodegeneration in Alzheimer's disease]. *Neurol.Neurochir.Pol.*, 38, 405-411.
- Krappmann,D., Wegener,E., Sunami,Y., Esen,M., Thiel,A., Mordmuller,B. & Scheidereit,C. (2004) The IkappaB kinase complex and NF-kappaB act as master regulators of lipopolysaccharide-induced gene expression and control subordinate activation of AP-1. *Mol.Cell Biol.*, 24, 6488-6500.
- Kril,J.J., Hodges,J. & Halliday,G. (2004) Relationship between hippocampal volume and CA1 neuron loss in brains of humans with and without Alzheimer's disease. *Neurosci.Lett.*, 361, 9-12.
- Kuiper,M.A., Visser,J.J., Bergmans,P.L., Scheltens,P. & Wolters,E.C. (1994) Decreased cerebrospinal fluid nitrate levels in Parkinson's disease, Alzheimer's disease and multiple system atrophy patients. *J.Neurol.Sci.*, 121, 46-49.
- Kunzi,M.S. & Pitha,P.M. (2005) Interferon research: a brief history. *Methods*

*Mol.Med.*, 116, 25-35.

- Kusiak,J.W., Izzo,J.A. & Zhao,B. (1996) Neurodegeneration in Alzheimer disease. Is apoptosis involved? *Mol.Chem.Neuropathol.* , 28, 153-162.
- Lacor,P.N., Buniel,M.C., Chang,L., Fernandez,S.J., Gong,Y., Viola,K.L., Lambert,M.P., Velasco,P.T., Bigio,E.H., Finch,C.E., Krafft,G.A. & Klein,W.L. (2004) Synaptic targeting by Alzheimer's-related amyloid beta oligomers. *J.Neurosci.*, 24, 10191-10200.
- Lacroix,L.P., Dawson,L.A., Hagan,J.J. & Heidebreder,C.A. (2004) 5-HT<sub>6</sub> receptor antagonist SB-271046 enhances extracellular levels of monoamines in the rat medial prefrontal cortex. *Synapse.*, 51, 158-164.
- Lacroix,S., Feinstein,D. & Rivest,S. (1998) The bacterial endotoxin lipopolysaccharide has the ability to target the brain in upregulating its membrane CD14 receptor within specific cellular populations. *Brain Pathol.*, 8, 625-640.
- Lai,Y., Feldman,K.L. & Clark,R.S. (2005) Enzyme-linked immunosorbent assays (ELISAs). *Crit Care Med.*, 33, S433-S434.
- Laye,S., Parnet,P., Goujon,E. & Dantzer,R. (1994) Peripheral administration of lipopolysaccharide induces the expression of cytokine transcripts in the brain and pituitary of mice. *Brain Res.Mol.Brain Res.*, 27, 157-162.
- Laye,S., Gheusi,G., Cremona,S., Combe,C., Kelley,K., Dantzer,R. & Parnet,P. (2000) Endogenous brain IL-1 mediates LPS-induced anorexia and hypothalamic cytokine expression. *Am.J.Physiol Regul.Integr.Comp Physiol*, 279, R93-R98.
- Lee,J.C., Laydon,J.T., McDonnell,P.C., Gallagher,T.F., Kumar,S., Green,D., McNulty,D., Blumenthal,M.J., Heys,J.R., Landvatter,S.W. & . (1994) A protein kinase involved in the regulation of inflammatory cytokine biosynthesis. *Nature*, 372, 739-746.
- Lee,J.C. & Young,P.R. (1996) Role of CSB/p38/RK stress response kinase in LPS

and cytokine signaling mechanisms. *J.Leukoc.Biol.*, 59, 152-157.

- Lee,J.C., Kumar,S., Griswold,D.E., Underwood,D.C., Votta,B.J. & Adams,J.L. (2000) Inhibition of p38 MAP kinase as a therapeutic strategy. *Immunopharmacology*, 47, 185-201.
- Lee,M.R. & Dominguez,C. (2005) MAP kinase p38 inhibitors: clinical results and an intimate look at their interactions with p38alpha protein. *Curr.Med.Chem.*, 12, 2979-2994.
- Lee,S.C., Collins,M., Vanguri,P. & Shin,M.L. (1992) Glutamate differentially inhibits the expression of class II MHC antigens on astrocytes and microglia. *J.Immunol.*, 148, 3391-3397.
- Legos,J.J., Erhardt,J.A., White,R.F., Lenhard,S.C., Chandra,S., Parsons,A.A., Tuma,R.F. & Barone,F.C. (2001) SB 239063, a novel p38 inhibitor, attenuates early neuronal injury following ischemia. *Brain Res.*, 892, 70-77.
- Lehnardt,S., Massillon,L., Follett,P., Jensen,F.E., Ratan,R., Rosenberg,P.A., Volpe,J.J. & Vartanian,T. (2003) Activation of innate immunity in the CNS triggers neurodegeneration through a Toll-like receptor 4-dependent pathway. *Proc.Natl.Acad.Sci.U.S.A*, 100 , 8514-8519.
- Li,G., Sun,S., Cao,X., Zhong,J. & Tong,E. (2004) LPS-induced degeneration of dopaminergic neurons of substantia nigra in rats. *J.Huazhong.Univ.Sci.Technolog.Med.Sci.*, 24, 83-86.
- Licastro,F., Grimaldi,L.M., Bonafe,M., Martina,C., Olivieri,F., Cavallone,L., Giovanietti,S., Masliah,E. & Franceschi,C. (2003) Interleukin-6 gene alleles affect the risk of Alzheimer's disease and levels of the cytokine in blood and brain. *Neurobiol.Aging*, 24, 921-926.
- Liew,F.Y. & McInnes,I.B. (2002) The role of innate mediators in inflammatory response. *Mol.Immunol.*, 38, 887-890.
- Lim,G.P., Yang,F., Chu,T., Chen,P., Beech,W., Teter,B., Tran,T., Ubeda,O., Ashe,K.H., Frautschy,S.A. & Cole,G.M. (2000) Ibuprofen suppresses plaque

- pathology and inflammation in a mouse model for Alzheimer's disease. *J.Neurosci.*, 20, 5709-5714.
- Lim,G.P., Yang,F., Chu,T., Gahtan,E., Ubeda,O., Beech,W., Overmier,J.B., Hsiao-Ashec,K., Frautschy,S.A. & Cole,G.M. (2001) Ibuprofen effects on Alzheimer pathology and open field activity in APPsw transgenic mice. *Neurobiol.Aging*, 22, 983-991.
- Lim,G.P., Chu,T., Yang,F., Beech,W., Frautschy,S.A. & Cole,G.M. (2001) The curry spice curcumin reduces oxidative damage and amyloid pathology in an Alzheimer transgenic mouse. *J.Neurosci.*, 21, 8370-8377.
- Ling,E.A., Kaur,C. & Lu,J. (1998) Origin, nature, and some functional considerations of intraventricular macrophages, with special reference to the epiplexus cells. *Microsc.Res.Tech.*, 41, 43-56.
- Linthorst,A.C. & Reul,J.M. (1998) Brain neurotransmission during peripheral inflammation. *Ann.N.Y.Acad.Sci.*, 840, 139-152.
- Lio,D., Licastro,F., Scola,L., Chiappelli,M., Grimaldi,L.M., Crivello,A., Colonna-Romano,G., Candore,G., Franceschi,C. & Caruso,C. (2003) Interleukin-10 promoter polymorphism in sporadic Alzheimer's disease. *Genes Immun.*, 4, 234-238.
- Lockhart,D.J. & Winzeler,E.A. (2000) Genomics, gene expression and DNA arrays. *Nature*, 405, 827-836.
- Logue,M.P., Growdon,J.H., Coviella,I.L. & Wurtman,R.J. (1985) Differential effects of DSP-4 administration on regional brain norepinephrine turnover in rats. *Life Sci.*, 37, 403-409.
- Lorton,D., Schaller,J., Lala,A. & De Nardin,E. (2000) Chemotactic-like receptors and Abeta peptide induced responses in Alzheimer's disease. *Neurobiol.Aging*, 21, 463-473.
- Loughlin,A.J., Woodroffe,M.N. & Cuzner,M.L. (1993) Modulation of interferon-gamma-induced major histocompatibility complex class II and Fc receptor

- expression on isolated microglia by transforming growth factor-beta 1, interleukin-4, noradrenaline and glucocorticoids. *Immunology*, 79, 125-130.
- Lowenstein,C.J., Dinerman,J.L. & Snyder,S.H. (1994) Nitric oxide: a physiologic messenger. *Ann.Intern.Med.*, 120, 227-237.
- Luchsinger,J.A. & Mayeux,R. (2004) Dietary factors and Alzheimer's disease. *Lancet Neurol.*, 3, 579-587.
- Lue,L.F., Walker,D.G., Brachova,L., Beach,T.G., Rogers,J., Schmidt,A.M., Stern,D.M. & Yan,S.D. (2001) Involvement of microglial receptor for advanced glycation endproducts (RAGE) in Alzheimer's disease: identification of a cellular activation mechanism. *Exp.Neurol.*, 171, 29-45.
- Lustbader,J.W., Cirilli,M., Lin,C., Xu,H.W., Takuma,K., Wang,N., Caspersen,C., Chen,X., Pollak,S., Chaney,M., Trinchese,F., Liu,S., Gunn-Moore,F., Lue,L.F., Walker,D.G., Kuppusamy,P., Zewier,Z.L., Arancio,O., Stern,D., Yan,S.S. & Wu,H. (2004) ABAD directly links Abeta to mitochondrial toxicity in Alzheimer's disease. *Science*, 304, 448-452.
- Luterman,J.D., Haroutunian,V., Yemul,S., Ho,L., Purohit,D., Aisen,P.S., Mohs,R. & Pasinetti,G.M. (2000) Cytokine gene expression as a function of the clinical progression of Alzheimer disease dementia. *Arch.Neurol.*, 57, 1153-1160.
- Luth,H.J., Munch,G. & Arendt,T. (2002) Aberrant expression of NOS isoforms in Alzheimer's disease is structurally related to nitrotyrosine formation. *Brain Res.*, 953, 135-143.
- Lymperopoulos,A., Karkoulas,G., Koch,W.J. & Flordellis,C.S. (2006) Alpha2-adrenergic receptor subtype-specific activation of NF-kappaB in PC12 cells. *Neurosci.Lett.*, 402, 210-215.
- Lyness,S.A., Zarow,C. & Chui,H.C. (2003) Neuron loss in key cholinergic and aminergic nuclei in Alzheimer disease: a meta-analysis. *Neurobiol.Aging*, 24, 1-23.
- Mackenzie,I.R., Hao,C. & Munoz,D.G. (1995) Role of microglia in senile plaque

- formation. *Neurobiol.Aging*, 16, 797-804.
- Madrigal,J.L., Feinstein,D.L., & Russo,C.D. (2005) Norepinephrine protects cortical neurons against microglial-induced cell death. *J. Neurosci. Res*, 81, 390-396.
- Maes,M., Lin,A., Kenis,G., Egyed,B. & Bosmans,E. (2000) The effects of noradrenaline and alpha-2 adrenoceptor agents on the production of monocytic products. *Psychiatry Res.*, 96, 245-253.
- Mann,D.M., Yates,P.O. & Hawkes,J. (1982) The noradrenergic system in Alzheimer and multi-infarct dementias. *J.Neurol.Neurosurg.Psychiatry*, 45, 113-119.
- Mann,D.M. & Yates,P.O. (1983) Pathological basis for neurotransmitter changes in Parkinson's disease. *Neuropathol.Appl.Neurobiol.*, 9, 3-19.
- Marien,M.R., Colpaert,F.C. & Rosenquist,A.C. (2004) Noradrenergic mechanisms in neurodegenerative diseases: a theory. *Brain Res.Brain Res.Rev.*, 45, 38-78.
- Masters,C.L., Multhaup,G., Simms,G., Pottgiesser,J., Martins,R.N. & Beyreuther,K. (1985) Neuronal origin of a cerebral amyloid: neurofibrillary tangles of Alzheimer's disease contain the same protein as the amyloid of plaque cores and blood vessels. *EMBO J.*, 4, 2757-2763.
- Masters,C.L. & Beyreuther,K. (1995) Molecular neuropathology of Alzheimer's disease. *Arzneimittelforschung.*, 45, 410-412.
- Matsuoka,Y., Picciano,M., Malester,B., LaFrancois,J., Zehr,C., Daeschner,J.M., Olschowka,J.A., Fonseca,M.I., O'Banion,M.K., Tenner,A.J., Lemere,C.A. & Duff,K. (2001) Inflammatory responses to amyloidosis in a transgenic mouse model of Alzheimer's disease. *Am.J.Pathol.*, 158, 1345-1354.
- Matsuzawa,A. & Ichijo,H. (2005) Stress-responsive protein kinases in redox-regulated apoptosis signaling. *Antioxid.Redox.Signal.*, 7, 472-481.
- Mattson,M.P., Cheng,B., Davis,D., Bryant,K., Lieberburg,I. & Rydel,R.E. (1992) beta-Amyloid peptides destabilize calcium homeostasis and render human cortical neurons vulnerable to excitotoxicity. *J.Neurosci.*, 12, 376-389.

- Mattson, M.P., Tomaselli, K.J. & Rydel, R.E. (1993) Calcium-destabilizing and neurodegenerative effects of aggregated beta-amyloid peptide are attenuated by basic FGF. *Brain Res.*, 621, 35-49.
- Mattson, M.P., Mark, R.J., Furukawa, K. & Bruce, A.J. (1997) Disruption of brain cell ion homeostasis in Alzheimer's disease by oxy radicals, and signaling pathways that protect therefrom. *Chem. Res. Toxicol.*, 10, 507-517.
- McDowell, I. (2001) Alzheimer's disease: insights from epidemiology. *Aging (Milano.)*, 13, 143-162.
- McGeer, P.L., Rogers, J. & McGeer, E.G. (1994) Neuroimmune mechanisms in Alzheimer disease pathogenesis. *Alzheimer Dis. Assoc. Disord.*, 8, 149-158.
- McGeer, P.L., Schulzer, M. & McGeer, E.G. (1996) Arthritis and anti-inflammatory agents as possible protective factors for Alzheimer's disease: a review of 17 epidemiologic studies. *Neurology*, 47, 425-432.
- McGeer, P.L. & McGeer, E.G. (1998) Glial cell reactions in neurodegenerative diseases: pathophysiology and therapeutic interventions. *Alzheimer Dis. Assoc. Disord.*, 12 Suppl 2, S1-S6.
- McGeer, P.L. & McGeer, E.G. (2001) Polymorphisms in inflammatory genes and the risk of Alzheimer disease. *Arch. Neurol.*, 58, 1790-1792.
- McGeer, P.L. & McGeer, E.G. (2002) Innate immunity, local inflammation, and degenerative disease. *Sci. Aging Knowledge Environ.*, 2002, re3.
- Meda, L., Cassatella, M.A., Szendrei, G.I., Otvos, L., Jr., Baron, P., Villalba, M., Ferrari, D. & Rossi, F. (1995) Activation of microglial cells by beta-amyloid protein and interferon-gamma. *Nature*, 374, 647-650.
- Meda, L., Baron, P., Prat, E., Scarpini, E., Scarlato, G., Cassatella, M.A. & Rossi, F. (1999) Proinflammatory profile of cytokine production by human monocytes and murine microglia stimulated with beta-amyloid[25-35]. *J. Neuroimmunol.*, 93, 45-52.
- Medhurst, A.D., Harrison, D.C., Read, S.J., Campbell, C.A., Robbins, M.J. &

- Pangalos,M.N. (2000) The use of TaqMan RT-PCR assays for semiquantitative analysis of gene expression in CNS tissues and disease models. *J.Neurosci.Methods*, 98, 9-20.
- Mehlhorn,G., Hollborn,M. & Schliebs,R. (2000) Induction of cytokines in glial cells surrounding cortical beta-amyloid plaques in transgenic Tg2576 mice with Alzheimer pathology. *Int.J.Dev.Neurosci.*, 18, 423-431.
- Mengozi,M., Fantuzzi,G., Faggioni,R., Marchant,A., Goldman,M., Orencole,S., Clark,B.D., Sironi,M., Benigni,F. & Ghezzi,P. (1994) Chlorpromazine specifically inhibits peripheral and brain TNF production, and up-regulates IL-10 production, in mice. *Immunology*, 82, 207-210.
- Meyer,M.R., Tschanz,J.T., Norton,M.C., Welsh-Bohmer,K.A., Steffens,D.C., Wyse,B.W. & Breitner,J.C. (1998) APOE genotype predicts when--not whether--one is predisposed to develop Alzheimer disease. *Nat.Genet.*, 19, 321-322.
- Miesfeld,R.L. (1990) Molecular genetics of corticosteroid action. *Am.Rev.Respir.Dis.*, 141, S11-S17.
- Miguel-Hidalgo,J.J. & Cacabelos,R. (1998) Beta-amyloid(1-40)-induced neurodegeneration in the rat hippocampal neurons of the CA1 subfield. *Acta Neuropathol.(Berl)*, 95, 455-465.
- Miguel-Hidalgo,J.J., Alvarez,X.A., Cacabelos,R. & Quack,G. (2002) Neuroprotection by memantine against neurodegeneration induced by beta-amyloid(1-40). *Brain Res.*, 958, 210-221.
- Milatovic,D., Zaja-Milatovic,S., Montine,K.S., Horner,P.J. & Montine,T.J. (2003) Pharmacologic suppression of neuronal oxidative damage and dendritic degeneration following direct activation of glial innate immunity in mouse cerebrum. *J.Neurochem.*, 87, 1518-1526.
- Minagar,A., Shapshak,P., Fujimura,R., Ownby,R., Heyes,M. & Eisdorfer,C. (2002) The role of macrophage/microglia and astrocytes in the pathogenesis of three neurologic disorders: HIV-associated dementia, Alzheimer disease, and

- multiple sclerosis. *J.Neurol.Sci.*, 202, 13-23.
- Mire-Sluis,A.R., Gaines-Das,R. & Thorpe,R. (1995) Immunoassays for detecting cytokines: what are they really measuring? *J.Immunol.Methods*, 186, 157-160.
- Mire-Sluis,A.R. (1999) Cytokine and growth factor standardization: the need for research to answer modern issues. *Dev.Biol.Stand.*, 100, 83-93.
- Miyake,K. (2004) Innate recognition of lipopolysaccharide by Toll-like receptor 4-MD-2. *Trends Microbiol.*, 12, 186-192.
- Miyake,K. (2004) Endotoxin recognition molecules MD-2 and toll-like receptor 4 as potential targets for therapeutic intervention of endotoxin shock. *Curr.Drug Targets.Inflamm.Allergy*, 3, 291-297.
- Moller,A.S., Ovstebo,R., Haug,K.B., Joo,G.B., Westvik,A.B. & Kierulf,P. (2005) Chemokine production and pattern recognition receptor (PRR) expression in whole blood stimulated with pathogen-associated molecular patterns (PAMPs). *Cytokine*, 32, 304-315.
- Montine,T.J., Sidell,K.R., Crews,B.C., Markesbery,W.R., Marnett,L.J., Roberts,L.J. & Morrow,J.D. (1999) Elevated CSF prostaglandin E2 levels in patients with probable AD. *Neurology*, 53, 1495-1498.
- Montine,T.J., Milatovic,D., Gupta,R.C., Valyi-Nagy,T., Morrow,J.D. & Breyer,R.M. (2002) Neuronal oxidative damage from activated innate immunity is EP2 receptor-dependent. *J.Neurochem.*, 83, 463-470.
- Morand,E.F. & Leech,M. (1999) Glucocorticoid regulation of inflammation: the plot thickens. *Inflamm.Res.*, 48, 557-560.
- Morishima-Kawashima,M. & Ihara,Y. (2002) Alzheimer's disease: beta-Amyloid protein and tau. *J.Neurosci.Res.*, 70, 392-401.
- Mrak,R.E., Sheng,J.G. & Griffin,W.S. (1995) Glial cytokines in Alzheimer's disease: review and pathogenic implications. *Hum.Pathol.*, 26, 816-823.

- Mrak,R.E. & Griffin,W.S. (2001) Interleukin-1, neuroinflammation, and Alzheimer's disease. *Neurobiol.Aging*, 22, 903-908.
- Munoz,F.J., Sole,M. & Coma,M. (2005) The protective role of vitamin E in vascular amyloid beta-mediated damage. *Subcell.Biochem.*, 38, 147-165.
- Muramami,N., Fukata,J., Tsukada,T., Kobayashi,H., Ebisui,O., Segawa,H., Muro,S., Imura,H. & Nakao,K. (1993) Bacterial lipopolysaccharide-induced expression of interleukin-6 messenger ribonucleic acid in the rat hypothalamus, pituitary, adrenal gland, and spleen. *Endocrinology*, 133, 2574-2578.
- Murphy,M.P., Hickman,L.J., Eckman,C.B., Uljon,S.N., Wang,R. & Golde,T.E. (1999) gamma-Secretase, evidence for multiple proteolytic activities and influence of membrane positioning of substrate on generation of amyloid beta peptides of varying length. *J.Biol.Chem.*, 274, 11914-11923.
- Mutter,J., Naumann,J., Sadaghiani,C., Schneider,R. & Walach,H. (2004) Alzheimer disease: mercury as pathogenetic factor and apolipoprotein E as a moderator. *Neuro.Endocrinol.Lett.*, 25, 331-339.
- Nabeshima,T. & Nitta,A. (1994) Memory impairment and neuronal dysfunction induced by beta-amyloid protein in rats. *Tohoku J.Exp.Med.*, 174, 241-249.
- Naccari,C. (2003) Non-steroidal anti-inflammatory drug users possibly have a decreased risk of Alzheimer's disease. *CNS.Spectr.*, 8, 336.
- Nadeau,S. & Rivest,S. (1999) Effects of circulating tumor necrosis factor on the neuronal activity and expression of the genes encoding the tumor necrosis factor receptors (p55 and p75) in the rat brain: a view from the blood-brain barrier. *Neuroscience*, 93, 1449-1464.
- Nadeau,S. & Rivest,S. (2003) Glucocorticoids play a fundamental role in protecting the brain during innate immune response. *J.Neurosci.*, 23, 5536-5544.
- Nagele,R.G., Wegiel,J., Venkataraman,V., Imaki,H., Wang,K.C. & Wegiel,J. (2004) Contribution of glial cells to the development of amyloid plaques in

- Alzheimer's disease. *Neurobiol.Aging*, 25, 663-674.
- Nakagawa,Y., Yuzuriha,T. & Iwaki,T. (2004) Active clearance of human amyloid beta 1-42 peptide aggregates from the rat ventricular system. *Neuropathology.*, 24, 194-200.
- Nakamura,S., Murayama,N., Noshita,T., Annoura,H. & Ohno,T. (2001) Progressive brain dysfunction following intracerebroventricular infusion of beta(1-42)-amyloid peptide. *Brain Res.*, 912, 128-136.
- Navarro,J.A., Molina,J.A., Jimenez-Jimenez,F.J., Benito-Leon,J., Orti-Pareja,M., Gasalla,T., Cabrera-Valdivia,F., Vargas,C., de Bustos,F. & Arenas,J. (1996) Cerebrospinal fluid nitrate levels in patients with Alzheimer's disease. *Acta Neurol.Scand.*, 94, 411-414.
- Neininger,A., Kontoyiannis,D., Kotlyarov,A., Winzen,R., Eckert,R., Volk,H.D., Holtmann,H., Kollias,G. & Gaestel,M. (2002) MK2 targets AU-rich elements and regulates biosynthesis of tumor necrosis factor and interleukin-6 independently at different post-transcriptional levels. *J.Biol.Chem.*, 277, 3065-3068.
- Nicholson,T.E. & Renton,K.W. (2001) Role of cytokines in the lipopolysaccharide-evoked depression of cytochrome P450 in the brain and liver. *Biochem.Pharmacol.*, 62, 1709-1717.
- Nilsson,M.R. (2004) Techniques to study amyloid fibril formation in vitro. *Methods*, 34, 151-160.
- Nitta,A., Itoh,A., Hasegawa,T. & Nabeshima,T. (1994) beta-Amyloid protein-induced Alzheimer's disease animal model. *Neurosci.Lett.*, 170, 63-66.
- Nolan,Y., Vereker,E., Lynch,A.M. & Lynch,M.A. (2003) Evidence that lipopolysaccharide-induced cell death is mediated by accumulation of reactive oxygen species and activation of p38 in rat cortex and hippocampus. *Exp.Neurol.*, 184, 794-804.
- O'Connor,G.M., Hart,O.M. & Gardiner,C.M. (2006) Putting the natural killer cell in

its place. *Immunology*, 117, 1-10.

O'Garra,A. & Vieira,P. (1992) Polymerase chain reaction for detection of cytokine gene expression. *Curr.Opin.Immunol.*, 4, 211-215.

O'Hare,E., Weldon,D.T., Mantyh,P.W., Ghilardi,J.R., Finke,M.P., Kuskowski,M.A., Maggio,J.E., Shephard,R.A. & Cleary,J. (1999) Delayed behavioral effects following intrahippocampal injection of aggregated A beta (1-42). *Brain Res.*, 815, 1-10.

Oddo,S., Caccamo,A., Tran,L., Lambert,M.P., Glabe,C.G., Klein,W.L., & LaFerla,F.M. (2006) Temporal profile of amyloid-beta (Abeta) oligomerization in an in vivo model of Alzheimer disease. A link between Abeta and tau pathology. *J. Biol. chem.*, 281, 1599-604.

Ono,K. & Han,J. (2000) The p38 signal transduction pathway: activation and function. *Cell Signal.*, 12, 1-13.

Palsson-McDermott,E.M. & O'Neill,L.A. (2004) Signal transduction by the lipopolysaccharide receptor, Toll-like receptor-4. *Immunology*, 113, 153-162.

Panza,F., Solfrizzi,V., D'Introno,A., Capurso,C., Colacicco,A.M., Torres,F., Altomare,E. & Capurso,A. (2002) [Genetics of late-onset Alzheimer's disease: vascular risk and beta-amyloid metabolism]. *Recenti Prog.Med.*, 93, 489-497.

Pavlov,V.A., Wang,H., Czura, C.J., Friedman,S.G. & Tracey,K.J. (2003) The cholinergic anti-inflammatory pathway: a missing link in neuroimmunomodulation. *Mol.Medicine.*, 9, 125-134.

Payne,L.C., Weigent,D.A. & Blalock,J.E. (1994) Induction of pituitary sensitivity to interleukin-1: a new function for corticotropin-releasing hormone. *Biochem.Biophys.Res.Comm.*, 198, 480-484.

Pericak-Vance,M.A., Bebout,J.L., Gaskell,P.C., Jr., Yamaoka,L.H., Hung,W.Y., Alberts,M.J., Walker,A.P., Bartlett,R.J., Haynes,C.A., Welsh,K.A. & . (1991) Linkage studies in familial Alzheimer disease: evidence for chromosome 19

- linkage. *Am.J.Hum.Genet.*, 48, 1034-1050.
- Perretti,M., Becherucci,C., Scapigliati,G. & Parente,L. (1989) The effect of adrenalectomy on interleukin-1 release in vitro and in vivo. *Br.J.Pharmacol.*, 98, 1137-1142.
- Perry,V.H., Newman,T.A. & Cunningham,C. (2003) The impact of systemic infection on the progression of neurodegenerative disease. *Nat.Rev.Neurosci.*, 4, 103-112.
- Perry,V.H. (2004) The influence of systemic inflammation on inflammation in the brain: implications for chronic neurodegenerative disease. *Brain Behav.Immun.*, 18, 407-413.
- Pezeshki,G., Pohl,T. & Schobitz,B. (1996) Corticosterone controls interleukin-1 beta expression and sickness behavior in the rat. *J.Neuroendocrinol.*, 8, 129-135.
- Pike,C.J., Burdick,D., Walencewicz,A.J., Glabe,C.G. & Cotman,C.W. (1993) Neurodegeneration induced by beta-amyloid peptides in vitro: the role of peptide assembly state. *J.Neurosci.*, 13, 1676-1687.
- Pitossi,F., del Rey,A., Kabiersch,A. & Besedovsky,H. (1997) Induction of cytokine transcripts in the central nervous system and pituitary following peripheral administration of endotoxin to mice. *J.Neurosci.Res.*, 48, 287-298.
- Plackett,T.P., Boehmer,E.D., Faunce,D.E. & Kovacs,E.J. (2004) Aging and innate immune cells. *J.Leukoc.Biol.*, 76, 291-299.
- Plata-Salaman,C.R., Ilyin,S.E., Gayle,D. & Flynn,M.C. (1998) Gram-negative and gram-positive bacterial products induce differential cytokine profiles in the brain: analysis using an integrative molecular-behavioral in vivo model. *Int.J.Mol.Med.*, 1, 387-397.
- Pocock,J.M. & Liddle,A.C. (2001) Microglial signalling cascades in neurodegenerative disease. *Prog.Brain Res.*, 132, 555-565.
- Podlisny,M.B., Stephenson,D.T., Frosch,M.P., Lieberburg,I., Clemens,J.A. & Selkoe,D.J. (1992) Synthetic amyloid beta-protein fails to produce specific

- neurotoxicity in monkey cerebral cortex. *Neurobiol.Aging*, 13, 561-567.
- Poirier,J. (2000) Apolipoprotein E and Alzheimer's disease. A role in amyloid catabolism. *Ann.N.Y.Acad.Sci.*, 924, 81-90.
- Price,D.L. & Sisodia,S.S. (1998) Mutant genes in familial Alzheimer's disease and transgenic models. *Annu.Rev.Neurosci.*, 21, 479-505.
- Price,D.L., Wong,P.C., Markowska,A.L., Lee,M.K., Thinakaran,G., Cleveland,D.W., Sisodia,S.S. & Borchelt,D.R. (2000) The value of transgenic models for the study of neurodegenerative diseases. *Ann.N.Y.Acad.Sci.*, 920, 179-191.
- Prieto,M. & Giralt,M.T. (2001) Effects of N-(2-chloroethyl)-N-ethyl-2-bromobenzylamine (DSP4) on alpha2-adrenoceptors which regulate the synthesis and release of noradrenaline in the rat brain. *Pharmacol.Toxicol.*, 88, 152-158.
- Purswani,M.U., Eckert,S.J., Arora,H.K. & Noel,G.J. (2002) Effect of ciprofloxacin on lethal and sublethal challenge with endotoxin and on early cytokine responses in a murine in vivo model. *J.Antimicrob.Chemother.*, 50, 51-58.
- Qiao,X., Cummins,D.J. & Paul,S.M. (2001) Neuroinflammation-induced acceleration of amyloid deposition in the APPV717F transgenic mouse. *Eur.J.Neurosci.*, 14, 474-482.
- Qin,L., Liu,Y., Cooper,C., Liu,B., Wilson,B. & Hong,J. (2002) Microglia enhance  $\beta$ -amyloid peptide-induced toxicity in cortical and mesencephalic neurons by producing reactive oxygen species. *J.Neurochem.*, 83, 973-983.
- Quan,N., Sundar,S.K. & Weiss,J.M. (1994) Induction of interleukin-1 in various brain regions after peripheral and central injections of lipopolysaccharide. *J.Neuroimmunol.*, 49, 125-134.
- Quan,N., Whiteside,M. & Herkenham,M. (1998) Time course and localization patterns of interleukin-1beta messenger RNA expression in brain and pituitary after peripheral administration of lipopolysaccharide. *Neuroscience*, 83, 281-293.

- Quan,N., Stern,E.L., Whiteside,M.B. & Herkenham,M. (1999) Induction of pro-inflammatory cytokine mRNAs in the brain after peripheral injection of subseptic doses of lipopolysaccharide in the rat. *J.Neuroimmunol.*, 93, 72-80.
- Quan,N., He,L., Lai,W., Shen,T. & Herkenham,M. (2000) Induction of IkappaBalpha mRNA expression in the brain by glucocorticoids: a negative feedback mechanism for immune-to-brain signaling. *J.Neurosci.*, 20, 6473-6477.
- Quinn,J., Montine,T., Morrow,J., Woodward,W.R., Kulhanek,D. & Eckenstein,F. (2003) Inflammation and cerebral amyloidosis are disconnected in an animal model of Alzheimer's disease. *J.Neuroimmunol.*, 137, 32-41.
- Raetz,C.R. & Whitfield,C. (2002) Lipopolysaccharide endotoxins. *Annu.Rev.Biochem.*, 71, 635-700.
- Ralay,R.H., Craft,J.M., Hu,W., Guo,L., Wing,L.K., Van Eldik,L.J. & Watterson,D.M. (2006) Glia as a therapeutic target: selective suppression of human amyloid-beta-induced upregulation of brain proinflammatory cytokine production attenuates neurodegeneration. *J.Neurosci.*, 26, 662-670.
- Rao,K.M., Meighan,T. & Bowman,L. (2002) Role of mitogen-activated protein kinase activation in the production of inflammatory mediators: differences between primary rat alveolar macrophages and macrophage cell lines. *J.Toxicol.EnvIRON.Health A*, 65, 757-768.
- Ravaglia,G., Paola,F., Maioli,F., Martelli,M., Montesi,F., Bastagli,L., Bianchin,M., Chiappelli,M., Tumini,E., Bolondi,L. & Licastro,F. (2006) Interleukin-1beta and interleukin-6 gene polymorphisms as risk factors for AD: a prospective study. *Exp.Gerontol.*, 41, 85-92.
- Ray,A., LaForge,K.S. & Sehgal,P.B. (1990) On the mechanism for efficient repression of the interleukin-6 promoter by glucocorticoids: enhancer, TATA box, and RNA start site (Inr motif) occlusion. *Mol.Cell Biol.*, 10, 5736-5746.
- Ray,A. & Sehgal,P.B. (1992) Cytokines and their receptors: molecular mechanism of interleukin-6 gene repression by glucocorticoids. *J.Am.Soc.Nephrol.*, 2, S214-

S221.

- Refojo,D., Liberman,A.C., Holsboer,F. & Arzt,E. (2001) Transcription factor-mediated molecular mechanisms involved in the functional cross-talk between cytokines and glucocorticoids. *Immunol.Cell Biol.*, 79, 385-394.
- Refojo,D., Liberman,A.C., Giacomini,D., Carbia,N.A., Graciarena,M., Echenique,C., Paez,P.M., Stalla,G., Holsboer,F. & Arzt,E. (2003) Integrating systemic information at the molecular level: cross-talk between steroid receptors and cytokine signaling on different target cells. *Ann.N.Y.Acad.Sci.*, 992, 196-204.
- Reichlin,S. (2004) Neuroendocrinology of acute immunity. *J.Endocrinol.Invest*, 27, 48-61.
- Reuben,P.M. & Cheung,H.S. (2006) Regulation of matrix metalloproteinase (MMP) gene expression by protein kinases. *Front Biosci.*, 11, 1199-1215.
- Richardson,J.C., Kendal,C.E., Anderson,R., Priest,F., Gower,E., Soden,P., Gray,R., Topps,S., Howlett,D.R., Lavender,D., Clarke,N.J., Barnes,J.C., Haworth,R., Stewart,M.G. & Rupniak,H.T. (2003) Ultrastructural and behavioural changes precede amyloid deposition in a transgenic model of Alzheimer's disease. *Neuroscience*, 122, 213-228.
- Rivest,S., Lacroix,S., Vallieres,L.,Nadeau,S., Xhang,J. & Laflamme,N. (2000) How the blood talks to the brain parenchyma and the paraventricular nucleus of the hypothalamus during systemic inflammatory and infectious stimuli. *Proc.Soc.Exp.Biol.Med.*, 223, 222-38.
- Rocca,W.A., van Duijn,C.M., Clayton,D., Chandra,V., Fratiglioni,L., Graves,A.B., Heyman,A., Jorm,A.F., Kokmen,E., Kondo,K. & . (1991) Maternal age and Alzheimer's disease: a collaborative re-analysis of case-control studies. EURODEM Risk Factors Research Group. *Int.J.Epidemiol.*, 20 Suppl 2, S21-S27.
- Rocchi,A., Pellegrini,S., Siciliano,G. & Murri,L. (2003) Causative and susceptibility genes for Alzheimer's disease: a review. *Brain Res.Bull.*, 61, 1-24.

- Roche,M., Diamond,M., Kelly,J.P. & Finn,E.P. (2006) In vivo modulation of LPS-induced alterations in brain and peripheral cytokines and HPA axis activity by cannabinoids. *J.Neuroimmunol.*, ARTICLE IN PRESS.
- Rockenstein,E., Mante,M., Alford,M., Adame,A., Crews,L., Hashimoto,M., Esposito,L., Mucke,L. & Masliah,E. (2005) High beta-secretase activity elicits neurodegeneration in transgenic mice despite reductions in amyloid-beta levels: implications for the treatment of Alzheimer disease. *J.Biol.Chem.*, 280, 32957-32967.
- Rogers,J., Kirby,L.C., Hempelman,S.R., Berry,D.L., McGeer,P.L., Kaszniak,A.W., Zalinski,J., Cofield,M., Mansukhani,L., Willson,P. & . (1993) Clinical trial of indomethacin in Alzheimer's disease. *Neurology*, 43, 1609-1611.
- Rogers,J.T., Leiter,L.M., McPhee,J., Cahill,C.M., Zhan,S.S., Potter,H. & Nilsson,L.N. (1999) Translation of the alzheimer amyloid precursor protein mRNA is up-regulated by interleukin-1 through 5'-untranslated region sequences. *J.Biol.Chem.*, 274, 6421-6431.
- Roses,A.D. (1996) Apolipoprotein E in neurology. *Curr.Opin.Neurol.*, 9, 265-270.
- Ross,S.B. & Renyl,A.L. (1976) On the long-lasting inhibitory effect of N-(2-chloroethyl)-N-ethyl-2-bromobenzylamine (DSP 4) on the active uptake of noradrenaline. *J.Pharm.Pharmacol.*, 28, 458-459.
- Rossi,M. & Young,J.W. (2005) Human dendritic cells: potent antigen-presenting cells at the crossroads of innate and adaptive immunity. *J.Immunol.*, 175, 1373-1381.
- Rossor,M.N. (1993) Molecular pathology of Alzheimer's disease. *J.Neurol.Neurosurg.Psychiatry*, 56, 583-586.
- Roumestan,C., Gougat,C., Jaffuel,D. & Mathieu,M. (2004) [Glucocorticoids and their receptor: mechanisms of action and clinical implications]. *Rev.Med.Interne*, 25, 636-647.
- Rovira,C., Arbez,N. & Mariani,J. (2002) Aβ(25-35) and Aβ(1-40) act on

- different calcium channels in CA1 hippocampal neurons. *Biochem.Biophys.Res.Commun.*, 296, 1317-1321.
- Russo,C., Schettini,G., Saido,T.C., Hulette,C., Lippa,C., Lannfelt,L., Ghetti,B., Gambetti,P., Tabaton,M. & Teller,J.K. (2000) Presenilin-1 mutations in Alzheimer's disease. *Nature*, 405, 531-532.
- Ryu,J.K., Franciosi,S., Sattayaprasert,P., Kim,S.U. & McLarnon,J.G. (2004) Minocycline inhibits neuronal death and glial activation induced by beta-amyloid peptide in rat hippocampus. *Glia*, 48, 85-90.
- Ryu,J.K. & McLarnon,J.G. (2006) Minocycline or iNOS inhibition block 3-nitrotyrosine increases and blood-brain barrier leakiness in amyloid beta-peptide-injected rat hippocampus. *Exp.Neurol.*, 198, 552-557.
- Saklatvala,J., Dean,J. & Clark,A. (2003) Control of the expression of inflammatory response genes. *Biochem.Soc.Symp.*, 95-106.
- Saklatvala,J. (2004) The p38 MAP kinase pathway as a therapeutic target in inflammatory disease. *Curr.Opin.Pharmacol.*, 4, 372-377.
- Salmon,R.A., Guo,X., Teh,H.S. & Schrader,J.W. (2001) The p38 mitogen-activated protein kinases can have opposing roles in the antigen-dependent or endotoxin-stimulated production of IL-12 and IFN-gamma. *Eur.J.Immunol.*, 31, 3218-3227.
- Sandbrink,R., Hartmann,T., Masters,C.L. & Beyreuther,K. (1996) Genes contributing to Alzheimer's disease. *Mol.Psychiatry*, 1, 27-40.
- Sanna,P.P., Weiss,F., Samson,M.E., Bloom,F.E. & Pich,E.M. (1995) Rapid induction of tumor necrosis factor alpha in the cerebrospinal fluid after intracerebroventricular injection of lipopolysaccharide revealed by a sensitive capture immuno-PCR assay. *Proc.Natl.Acad.Sci.U.S.A.*, 92, 272-275.
- Sasaki,A., Yamaguchi,H., Ogawa,A., Sugihara,S. & Nakazato,Y. (1997) Microglial activation in early stages of amyloid beta protein deposition. *Acta Neuropathol.(Berl)*, 94, 316-322.

- Sasaki,N., Toki,S., Chowei,H., Saito,T., Nakano,N., Hayashi,Y., Takeuchi,M. & Makita,Z. (2001) Immunohistochemical distribution of the receptor for advanced glycation end products in neurons and astrocytes in Alzheimer's disease. *Brain Res.*, 888, 256-262.
- Satta,M.A., Jacobs,R.A., Kaltsas,G.A. & Grossman,A.B. (1998) Endotoxin induces interleukin-1beta and nitric oxide synthase mRNA in rat hypothalamus and pituitary. *Neuroendocrinology*, 67, 109-116.
- Scali,C., Prosperi,C., Giovannelli,L., Bianchi,L., Pepeu,G. & Casamenti,F. (1999) Beta(1-40) amyloid peptide injection into the nucleus basalis of rats induces microglia reaction and enhances cortical gamma-aminobutyric acid release in vivo. *Brain Res.*, 831, 319-321.
- Scheinin,M., Lomasney,J.W., Hayden-Hixson,D.M., Schambra,U.B., Caron,M.G., Lefkowitz,R.J. & Fremeau,R.T., Jr. (1994) Distribution of alpha 2-adrenergic receptor subtype gene expression in rat brain. *Brain Res.Mol.Brain Res.*, 21, 133-149.
- Schieven,G.L. (2005) The biology of p38 kinase: a central role in inflammation. *Curr.Top.Med.Chem.*, 5, 921-928.
- Schleimer,R.P. (1993) An overview of glucocorticoid anti-inflammatory actions. *Eur.J.Clin.Pharmacol.*, 45 Suppl 1, S3-S7.
- Schmidt,T.J. & Meyer,A.S. (1994) Autoregulation of corticosteroid receptors. How, when, where, and why? *Receptor*, 4, 229-257.
- Schmitz,C., Rutten,B.P., Pielen,A., Schafer,S., Wirths,O., Tremp,G., Czech,C., Blanchard,V., Multhaup,G., Rezaie,P., Korr,H., Steinbusch,H.W., Pradier,L. & Bayer,T.A. (2004) Hippocampal neuron loss exceeds amyloid plaque load in a transgenic mouse model of Alzheimer's disease. *Am.J.Pathol.*, 164, 1495-1502.
- Sciacca,F.L., Ferri,C., Licastro,F., Veglia,F., Biunno,I., Gavazzi,A., Calabrese,E., Martinelli,B.F., Sorbi,S., Mariani,C., Franceschi,M. & Grimaldi,L.M. (2003) Interleukin-1B polymorphism is associated with age at onset of Alzheimer's

disease. *Neurobiol.Aging*, 24, 927-931.

Scott,S.A., DeKosky,S.T. & Scheff,S.W. (1991) Volumetric atrophy of the amygdala in Alzheimer's disease: quantitative serial reconstruction. *Neurology*, 41, 351-356.

Seger,R. & Krebs,E.G. (1995) The MAPK signaling cascade. *FASEB J.*, 9, 726-735.

Selkoe,D.J. (1993) Physiological production of the beta-amyloid protein and the mechanism of Alzheimer's disease. *Trends Neurosci.*, 16, 403-409.

Selkoe,D.J. (1998) The cell biology of beta-amyloid precursor protein and presenilin in Alzheimer's disease. *Trends Cell Biol.*, 8, 447-453.

Selkoe,D.J. (2000) Toward a comprehensive theory for Alzheimer's disease. Hypothesis: Alzheimer's disease is caused by the cerebral accumulation and cytotoxicity of amyloid beta-protein. *Ann.N.Y.Acad.Sci.* , 924, 17-25.

Semmler,A., Okulla,T., Sastre,M., Dumitrescu-Ozimek,L. & Heneka,M.T. (2005) Systemic inflammation induces apoptosis with variable vulnerability of different brain regions. *J.Chem.Neuroanat.*, 30, 144-157.

Shaffer,L.M., Dority,M.D., Gupta-Bansal,R., Frederickson,R.C., Younkin,S.G. & Brunden,K.R. (1995) Amyloid beta protein (A beta) removal by neuroglial cells in culture. *Neurobiol.Aging*, 16, 737-745.

Shaw,K.T., Utsuki,T., Rogers,J., Yu,Q.S., Sambamurti,K., Brossi,A., Ge,Y.W., Lahiri,D.K. & Greig,N.H. (2001) Phenserine regulates translation of beta - amyloid precursor protein mRNA by a putative interleukin-1 responsive element, a target for drug development. *Proc.Natl.Acad.Sci.U.S.A*, 98, 7605-7610.

Shen,C.L. & Murphy,R.M. (1995) Solvent effects on self-assembly of beta-amyloid peptide. *Biophys.J.*, 69, 640-651.

Sheng,J.G., Mrak,R.E. & Griffin,W.S. (1995) Microglial interleukin-1 alpha expression in brain regions in Alzheimer's disease: correlation with neuritic plaque distribution. *Neuropathol.Appl.Neurobiol.*, 21, 290-301.

- Sheng,J.G., Bora,S.H., Xu,G., Borchelt,D.R., Price,D.L. & Koliatsos,V.E. (2003) Lipopolysaccharide-induced-neuroinflammation increases intracellular accumulation of amyloid precursor protein and amyloid beta peptide in APPswe transgenic mice. *Neurobiol.Dis.*, 14, 133-145.
- Sherrington,R., Froelich,S., Sorbi,S., Campion,D., Chi,H., Rogaeva,E.A., Levesque,G., Rogaev,E.I., Lin,C., Liang,Y., Ikeda,M., Mar,L., Brice,A., Agid,Y., Percy,M.E., Clerget-Darpoux,F., Piacentini,S., Marcon,G., Nacmias,B., Amaducci,L., Frebourg,T., Lannfelt,L., Rommens,J.M. & George-Hyslop,P.H. (1996) Alzheimer's disease associated with mutations in presenilin 2 is rare and variably penetrant. *Hum.Mol.Genet.*, 5, 985-988.
- Shimazu,R., Akashi,S., Ogata,H., Nagai,Y., Fukudome,K., Miyake,K. & Kimoto,M. (1999) MD-2, a molecule that confers lipopolysaccharide responsiveness on Toll-like receptor 4. *J.Exp.Med.*, 189, 1777-1782.
- Shin,R.W., Ogino,K., Kondo,A., Saido,T.C., Trojanowski,J.Q., Kitamoto,T. & Tateishi,J. (1997) Amyloid beta-protein (Abeta) 1-40 but not Abeta1-42 contributes to the experimental formation of Alzheimer disease amyloid fibrils in rat brain. *J.Neurosci.*, 17, 8187-8193.
- Siman,R., Card,J.P., Nelson,R.B. & Davis,L.G. (1989) Expression of beta-amyloid precursor protein in reactive astrocytes following neuronal damage. *Neuron*, 3, 275-285.
- Simmons,L.K., May,P.C., Tomaselli,K.J., Rydel,R.E., Fuson,K.S., Brigham,E.F., Wright,S., Lieberburg,I., Becker,G.W., Brems,D.N. & . (1994) Secondary structure of amyloid beta peptide correlates with neurotoxic activity in vitro. *Mol.Pharmacol.*, 45, 373-379.
- Singh,A.K. & Jiang,Y. (2004) How does peripheral lipopolysaccharide induce gene expression in the brain of rats? *Toxicology*, 201, 197-207.
- Sironi,M., Gadina,M., Kankova,M., Riganti,F., Mantovani,A., Zandalasini,M. & Ghezzi,P. (1992) Differential sensitivity of in vivo TNF and IL-6 production to modulation by anti-inflammatory drugs in mice. *Int.J.Immunopharmacol.*,

14, 1045-1050.

Skullerud, K. (1985) Variations in the size of the human brain. Influence of age, sex, body length, body mass index, alcoholism, Alzheimer changes, and cerebral atherosclerosis. *Acta Neurol. Scand. Suppl*, 102, 1-94.

Sly, L.M., Krzesicki, R.F., Brashler, J.R., Buhl, A.E., McKinley, D.D., Carter, D.B. & Chin, J.E. (2001) Endogenous brain cytokine mRNA and inflammatory responses to lipopolysaccharide are elevated in the Tg2576 transgenic mouse model of Alzheimer's disease. *Brain Res. Bull.*, 56, 581-588.

Smith, J.B., Nguyen, T.T., Hughes, H.J., Herschman, H.R., Widney, D.P., Bui, K.C. & Rovai, L.E. (2002) Glucocorticoid-attenuated response genes induced in the lung during endotoxemia. *Am. J. Physiol Lung Cell Mol. Physiol*, 283, L636-L647.

Smyth, M.D., Kesslak, J.P., Cummings, B.J. & Cotman, C.W. (1994) Analysis of brain injury following intrahippocampal administration of beta-amyloid in streptozotocin-treated rats. *Neurobiol. Aging*, 15, 153-159.

Song, D.K., Im, Y.B., Jung, J.S., Suh, H.W., Huh, S.O., Park, S.W., Wie, M.B. & Kim, Y.H. (1999) Differential involvement of central and peripheral norepinephrine in the central lipopolysaccharide-induced interleukin-6 responses in mice. *J. Neurochem.*, 72, 1625-1633.

Song, D.K., Im, Y.B., Jung, J.S., Cho, J., Suh, H.W. & Kim, Y.H. (2001) Central beta-amyloid peptide-induced peripheral interleukin-6 responses in mice. *J. Neurochem.*, 76, 1326-1335.

Soreghan, B., Kosmoski, J. & Glabe, C. (1994) Surfactant properties of Alzheimer's A beta peptides and the mechanism of amyloid aggregation. *J. Biol. Chem.*, 269, 28551-28554.

Soulet, D. & Rivest, S. (2003) Polyamines play a critical role in the control of the innate immune response in the mouse central nervous system. *J. Cell Biol.*, 162, 257-268.

- Spengler,R.N., Allen,R.M., Remick,D.G., Strieter,R.M. & Kunkel,S.L. (1990) Stimulation of alpha-adrenergic receptor augments the production of macrophage-derived tumor necrosis factor. *J.Immunol.*, 145, 1430-1434.
- Stein,T.D. & Johnson,J.A. (2002) Lack of neurodegeneration in transgenic mice overexpressing mutant amyloid precursor protein is associated with increased levels of transthyretin and the activation of cell survival pathways. *J.Neurosci.*, 22, 7380-7388.
- Stein,T.D., Anders,N.J., DeCarli,C., Chan,S.L., Mattson,M.P. & Johnson,J.A. (2004) Neutralization of transthyretin reverses the neuroprotective effects of secreted amyloid precursor protein (APP) in APPSW mice resulting in tau phosphorylation and loss of hippocampal neurons: support for the amyloid hypothesis. *J.Neurosci.*, 24, 7707-7717.
- Stephan,A., Laroche,S. & Davis,S. (2001) Generation of aggregated beta-amyloid in the rat hippocampus impairs synaptic transmission and plasticity and causes memory deficits. *J.Neurosci.*, 21, 5703-5714.
- Stewart,W.F., Kawas,C., Corrada,M. & Metter,E.J. (1997) Risk of Alzheimer's disease and duration of NSAID use. *Neurology*, 48, 626-632.
- Su,J.H., Anderson,A.J., Cummings,B.J. & Cotman,C.W. (1994) Immunohistochemical evidence for apoptosis in Alzheimer's disease. *Neuroreport*, 5, 2529-2533.
- Sumbayev,V.V. & Yasinska,I.M. (2006) Role of MAP kinase-dependent apoptotic pathway in innate immune responses and viral infection. *Scand.J.Immunol.*, 63, 391-400.
- Sweep,F., Rijnkels,C. & Hermus,A. (1991) Activation of the hypothalamus-pituitary-adrenal axis by cytokines. *Acta Endocrinol.(Copenh)*, 125 Suppl 1, 84-91.
- Szczepanik,A.M., Rampe,D. & Ringheim,G.E. (2001) Amyloid-beta peptide fragments p3 and p4 induce pro-inflammatory cytokine and chemokine production in vitro and in vivo. *J.Neurochem.*, 77, 304-317.

- Szczepanik,A.M. & Ringheim,G.E. (2003) IL-10 and glucocorticoids inhibit Abeta(1-42)- and lipopolysaccharide-induced pro-inflammatory cytokine and chemokine induction in the central nervous system. *J.Alzheimers.Dis.*, 5, 105-117.
- Szelenyi,J., Kiss,J.P., Puskas,E., Szelenyi,M. & Vizi,E.S. (2000) Contribution of differently localized alpha 2- and beta-adrenoceptors in the modulation of TNF-alpha and IL-10 production in endotoxemic mice. *Ann.N.Y.Acad.Sci.*, 917, 145-153.
- Szelenyi,J. (2001) Cytokines and the central nervous system. *Brain Res. Bull.*, 54, 329-459.
- Szot,P., White,S.S., Greenup,J.L., Leverenz,J.B., Peskind,E.R. & Raskind,M.A. (2006) Compensatory changes in the noradrenergic nervous system in the locus ceruleus and hippocampus of postmortem subjects with Alzheimer's disease and dementia with Lewy bodies. *J.Neurosci.*, 26, 467-478.
- Tabaton,M., Nunzi,M.G., Xue,R., Usiak,M., Autilio-Gambetti,L. & Gambetti,P. (1994) Soluble amyloid beta-protein is a marker of Alzheimer amyloid in brain but not in cerebrospinal fluid. *Biochem.Biophys.Res.Comm.*, 200, 1598-1603.
- Tabaton,M. & Gambetti,P. (2006) Soluble amyloid-beta in the brain: The scarlet pimpernel. *J.Alzheimers.Dis.*, 9, 127-132.
- Tabet,N., Mantle,D. & Orrell,M. (2000) Free radicals as mediators of toxicity in Alzheimer's disease: a review and hypothesis. *Adverse Drug React.Toxicol.Rev.*, 19, 127-152.
- Tabet,N. & Feldman,H. (2002) Indomethacin for the treatment of Alzheimer's disease patients. *Cochrane.Database.Syst.Rev.*, CD003673.
- Takata,K., Kitamura,Y., Tsuchiya,D., Kawasaki,T., Taniguchi,T. & Shimohama,S. (2004) High mobility group box protein-1 inhibits microglial Abeta clearance and enhances Abeta neurotoxicity. *J.Neurosci.Res.* , 78, 880-891.

- Tamagno,E., Bardini,P., Guglielmotto,M., Danni,O. & Tabaton,M. (2006) The various aggregation states of beta-amyloid 1-42 mediate different effects on oxidative stress, neurodegeneration, and BACE-1 expression. *Free Radic.Biol.Med.*, 41, 202-212.
- Tanaka,J., Toku,K., Zhang,B., Ishihara,K., Sakanaka,M. & Maeda,N. (1999) Astrocytes prevent neuronal death induced by reactive oxygen and nitrogen species. *Glia*, 28, 85-96.
- Tanzi,R.E., Gusella,J.F., Watkins,P.C., Bruns,G.A., George-Hyslop,P., Van Keuren,M.L., Patterson,D., Pagan,S., Kurnit,D.M. & Neve,R.L. (1987) Amyloid beta protein gene: cDNA, mRNA distribution, and genetic linkage near the Alzheimer locus. *Science*, 235, 880-884.
- Tarkowski,E., Blennow,K., Wallin,A. & Tarkowski,A. (1999) Intracerebral production of tumor necrosis factor-alpha, a local neuroprotective agent, in Alzheimer disease and vascular dementia. *J.Clin.Immunol.*, 19, 223-230.
- Tarkowski,E., Liljeroth,A.M., Nilsson,A., Ricksten,A., Davidsson,P., Minthon,L. & Blennow,K. (2000) TNF gene polymorphism and its relation to intracerebral production of TNFalpha and TNFbeta in AD. *Neurology*, 54, 2077-2081.
- ten Hove,T., van den,B.B., Pronk,I., Drillenburger,P., Peppelenbosch,M.P. & van Deventer,S.J. (2002) Dichotomous role of inhibition of p38 MAPK with SB 203580 in experimental colitis. *Gut*, 50, 507-512.
- Thorpe,R., Wadhwa,M., Bird,C.R. & Mire-Sluis,A.R. (1992) Detection and measurement of cytokines. *Blood Rev.*, 6, 133-148.
- Tibbles,L.A. & Woodgett,J.R. (1999) The stress-activated protein kinase pathways. *Cell Mol.Life Sci.*, 55, 1230-1254.
- Tohgi,H., Abe,T., Yamazaki,K., Murata,T., Ishizaki,E. & Isobe,C. (1999) Alterations of 3-nitrotyrosine concentration in the cerebrospinal fluid during aging and in patients with Alzheimer's disease. *Neurosci.Lett.*, 269, 52-54.
- Tol,J., Roks,G., Slooter,A.J. & van Duijn,C.M. (1999) Genetic and environmental

- factors in Alzheimer's disease. *Rev.Neurol.(Paris)*, 155 Suppl 4, S10-S16.
- Tonelli,L.H., Maeda,S., Rapp,K.L. & Sternberg,E.M. (2003) Differential induction of interleukin-I beta mRNA in the brain parenchyma of Lewis and Fischer rats after peripheral injection of lipopolysaccharides. *J.Neuroimmunol.*, 140, 126-136.
- Triantafilou,M., Miyake,K., Golenbock,D.T. & Triantafilou,K. (2002) Mediators of innate immune recognition of bacteria concentrate in lipid rafts and facilitate lipopolysaccharide-induced cell activation. *J.Cell Sci.*, 115, 2603-2611.
- Tsang,M.L. & Weatherbee,J.A. (1996) Cytokine assays and their limitations. *Aliment.Pharmacol.Ther.*, 10 Suppl 2, 55-61.
- Turnbull,A.V. & Rivier,C.L. (1999) Regulation of the hypothalamic-pituitary-adrenal axis by cytokines: actions and mechanisms of action. *Physiol Rev.*, 79, 1-71.
- Turrin,N.P., Gayle,D., Ilyin,S.E., Flynn,M.C., Langhans,W., Schwartz,G.J. & Plata-Salaman,C.R. (2001) Pro-inflammatory and anti-inflammatory cytokine mRNA induction in the periphery and brain following intraperitoneal administration of bacterial lipopolysaccharide. *Brain Res.Bull.*, 54, 443-453.
- Uchihara,T., Akiyama,H., Kondo,H. & Ikeda,K. (1997) Activated microglial cells are colocalized with perivascular deposits of amyloid-beta protein in Alzheimer's disease brain. *Stroke*, 28, 1948-1950.
- Uehara,A., Gottschall,P.E., Dahl,R.R. & Arimura,A. (1987) Interleukin-1 stimulates ACTH release by an indirect action which requires endogenous corticotropin releasing factor. *Endocrinology*, 121, 1580-1582.
- Ulevitch,R.J. & Tobias,P.S. (1995) Receptor-dependent mechanisms of cell stimulation by bacterial endotoxin. *Annu.Rev.Immunol.*, 13, 437-457.
- Urakami,K., Wakutani,Y., Wada-Isoe,K., Yamagata,K., Adachi,Y. & Nakashima,K. (2001) [Analysis of causative genes and genetic risk factor in Alzheimer's disease]. *Nippon Ronen Igakkai Zasshi*, 38, 769-771.

- Vallieres,L. & Rivest,S. (1997) Regulation of the genes encoding interleukin-6, its receptor, and gp130 in the rat brain in response to the immune activator lipopolysaccharide and the proinflammatory cytokine interleukin-1beta. *J.Neurochem.*, 69, 1668-1683.
- van Dam,A.M., Poole,S., Schultzberg,M., Zavala,F. & Tilders,F.J. (1998) Effects of peripheral administration of LPS on the expression of immunoreactive interleukin-1 alpha, beta, and receptor antagonist in rat brain. *Ann.N.Y.Acad.Sci.*, 840, 128-138.
- van den,B.B., Juffermans,N.P., ten Hove,T., Schultz,M.J., van Deventer,S.J., van der,P.T. & Peppelenbosch,M.P. (2001) p38 mitogen-activated protein kinase inhibition increases cytokine release by macrophages in vitro and during infection in vivo. *J.Immunol.*, 166, 582-587.
- Van der Saag,P.T., Caldenhoven,E. & Van de,S.A. (1996) Molecular mechanisms of steroid action: a novel type of cross-talk between glucocorticoids and NF-kappa B transcription factors. *Eur.Respir.J.Suppl*, 22, 146s-153s.
- van Rossum,D., Hanisch,U.K. & Quirion,R. (1997) Neuroanatomical localization, pharmacological characterization and functions of CGRP, related peptides and their receptors. *Neurosci.Biobehav.Rev.*, 21, 649-678.
- van Rossum,D. & Hanisch,U.K. (2004) Microglia. *Metab Brain Dis.*, 19, 393-411.
- Vanden Berghe,W., Francesconi,E., De Bosscher,K., Resche-Rigon,M. & Haegeman,G. (1999) Dissociated glucocorticoids with anti-inflammatory potential repress interleukin-6 gene expression by a nuclear factor-kappaB-dependent mechanism. *Mol.Pharmacol.*, 56, 797-806.
- Varadarajan,S., Yatin,S., Aksenova,M. & Butterfield,D.A. (2000) Review: Alzheimer's amyloid beta-peptide-associated free radical oxidative stress and neurotoxicity. *J.Struct.Biol.*, 130, 184-208.
- Velazquez,P., Cribbs,D.H., Poulos,T.L. & Tenner,A.J. (1997) Aspartate residue 7 in amyloid beta-protein is critical for classical complement pathway activation: implications for Alzheimer's disease pathogenesis. *Nat.Med.*, 3, 77-79.

- Verhoeckx,K.C., Doornbos,R.P., van der,G.J., Witkamp,R.F. & Rodenburg,R.J. (2005) Inhibitory effects of the beta-adrenergic receptor agonist zilpaterol on the LPS-induced production of TNF-alpha in vitro and in vivo. *J.Vet.Pharmacol.Ther.*, 28, 531-537.
- Verhoeff,N.P. (2005) Acetylcholinergic neurotransmission and the beta-amyloid cascade: implications for Alzheimer's disease. *Expert.Rev.Neurother.*, 5, 277-284.
- Viel,J.J., McManus,D.Q., Smith,S.S. & Brewer,G.J. (2001) Age- and concentration-dependent neuroprotection and toxicity by TNF in cortical neurons from beta-amyloid. *J.Neurosci.Res.*, 64, 454-465.
- Vignali,D.A. (2000) Multiplexed particle-based flow cytometric assays. *J.Immunol.Methods*, 243, 243-255.
- Visintin,A., Mazzoni,A., Spitzer,J.A. & Segal,D.M. (2001) Secreted MD-2 is a large polymeric protein that efficiently confers lipopolysaccharide sensitivity to Toll-like receptor 4. *Proc.Natl.Acad.Sci.U.S.A*, 98, 12156-12161.
- Vogels,O.J., Broere,C.A., ter Laak,H.J., ten Donkelaar,H.J., Nieuwenhuys,R. & Schulte,B.P. (1990) Cell loss and shrinkage in the nucleus basalis Meynert complex in Alzheimer's disease. *Neurobiol.Aging*, 11, 3-13.
- Waite,J., Cole,G.M., Frautschy,S.A., Connor,D.J. & Thal,L.J. (1992) Solvent effects on beta protein toxicity in vivo. *Neurobiol.Aging*, 13, 595-599.
- Walsh,D.M. & Selkoe,D.J. (2004) Oligomers on the brain: the emerging role of soluble protein aggregates in neurodegeneration. *Protein Pept.Lett.*, 11, 213-228.
- Wang,Z., Liu,R.H., Reddy,V.K. & Barnes,C.D. (1994) Hippocampal beta-amyloid reduces locus coeruleus glutamate and tyrosine hydroxylase. *Brain Res.Bull.*, 35, 485-491.
- Watson,D., Castano,E., Kokjohn,T.A., Kuo,Y.M., Lyubchenko,Y., Pinsky,D., Connolly,E.S., Jr., Esh,C., Luehrs,D.C., Stine,W.B., Rowse,L.M.,

- Emmerling,M.R. & Roher,A.E. (2005) Physicochemical characteristics of soluble oligomeric Abeta and their pathologic role in Alzheimer's disease. *Neurol.Res.*, 27, 869-881.
- Weggen,S., Eriksen,J.L., Das,P., Sagi,S.A., Wang,R., Pietrzik,C.U., Findlay,K.A., Smith,T.E., Murphy,M.P., Bulter,T., Kang,D.E., Marquez-Sterling,N., Golde,T.E. & Koo,E.H. (2001) A subset of NSAIDs lower amyloidogenic Abeta42 independently of cyclooxygenase activity. *Nature*, 414, 212-216.
- Wegiel,J., Wang,K.C., Imaki,H., Rubenstein,R., Wronska,A., Osuchowski,M., Lipinski,W.J., Walker,L.C. & LeVine,H. (2001) The role of microglial cells and astrocytes in fibrillar plaque evolution in transgenic APP(SW) mice. *Neurobiol.Aging*, 22, 49-61.
- Weiner,M.F., Hynan,L.S., Bret,M.E. & White,C., III (2005) Early behavioral symptoms and course of Alzheimer's disease. *Acta Psychiatr.Scand.*, 111, 367-371.
- Weldon,D.T., Rogers,S.D., Ghilardi,J.R., Finke,M.P., Cleary,J.P., O'Hare,E., Esler,W.P., Maggio,J.E. & Mantyh,P.W. (1998) Fibrillar beta-amyloid induces microglial phagocytosis, expression of inducible nitric oxide synthase, and loss of a select population of neurons in the rat CNS in vivo. *J.Neurosci.*, 18, 2161-2173.
- Wenk,G.L., McGann,K., Hauss-Wegrzyniak,B. & Rosi,S. (2003) The toxicity of tumor necrosis factor-alpha upon cholinergic neurons within the nucleus basalis and the role of norepinephrine in the regulation of inflammation: implications for Alzheimer's disease. *Neuroscience*, 121, 719-729.
- Whicher,J. & Ingham,E. (1990) Cytokine measurements in body fluids. *Eur.Cytokine Netw.*, 1, 239-243.
- White,J.A., Manelli,A.M., Holmberg,K.H., Van Eldik,L.J. & Ladu,M.J. (2005) Differential effects of oligomeric and fibrillar amyloid-beta 1-42 on astrocyte-mediated inflammation. *Neurobiol.Dis.*, 18, 459-465.
- Wiegers,G.J. & Reul,J.M. (1998) Induction of cytokine receptors by glucocorticoids:

- functional and pathological significance. *Trends Pharmacol.Sci.*, 19, 317-321.
- Winkler,J., Connor,D.J., Frautschy,S.A., Behl,C., Waite,J.J., Cole,G.M. & Thal,L.J. (1994) Lack of long-term effects after beta-amyloid protein injections in rat brain. *Neurobiol.Aging*, 15, 601-607.
- Wirhns,O., Multhaup,G. & Bayer,T.A. (2004) A modified beta-amyloid hypothesis: intraneuronal accumulation of the beta-amyloid peptide--the first step of a fatal cascade. *J.Neurochem.*, 91, 513-520.
- Wolfman,C., Abo,V., Calvo,D., Medina,J., Dajas,F. & Silveira,R. (1994) Recovery of central noradrenergic neurons one year after the administration of the neurotoxin DSP4. *Neurochem.Int.*, 25, 395-400.
- Woodgett,J.R., Avruch,J. & Kyriakis,J. (1996) The stress activated protein kinase pathway. *Cancer Surv.*, 27, 127-138.
- Xia,M.Q. & Hyman,B.T. (1999) Chemokines/chemokine receptors in the central nervous system and Alzheimer's disease. *J.Neurovirol.*, 5, 32-41.
- Yamada,K., Tanaka,T., Han,D., Senzaki,K., Kameyama,T. & Nabeshima,T. (1999) Protective effects of idebenone and alpha-tocopherol on beta-amyloid-(1-42)-induced learning and memory deficits in rats: implication of oxidative stress in beta-amyloid-induced neurotoxicity in vivo. *Eur.J.Neurosci.*, 11, 83-90.
- Yan,Q., Zhang,J., Liu,H., Babu-Khan,S., Vassar,R., Biere,A.L., Citron,M. & Landreth,G. (2003) Anti-inflammatory drug therapy alters beta-amyloid processing and deposition in an animal model of Alzheimer's disease. *J.Neurosci.*, 23, 7504-7509.
- Yan,S.D., Chen,X., Fu,J., Chen,M., Zhu,H., Roher,A., Slattery,T., Zhao,L., Nagashima,M., Morser,J., Migheli,A., Nawroth,P., Stern,D. & Schmidt,A.M. (1996) RAGE and amyloid-beta peptide neurotoxicity in Alzheimer's disease. *Nature*, 382, 685-691.
- Yan,S.D., Fu,J., Soto,C., Chen,X., Zhu,H., Al Mohanna,F., Collison,K., Zhu,A.,

- Stern,E., Saido,T., Tohyama,M., Ogawa,S., Roher,A. & Stern,D. (1997) An intracellular protein that binds amyloid-beta peptide and mediates neurotoxicity in Alzheimer's disease. *Nature*, 389, 689-695.
- Yankner,B.A., Duffy,L.K. & Kirschner,D.A. (1990) Neurotrophic and neurotoxic effects of amyloid beta protein: reversal by tachykinin neuropeptides. *Science*, 250, 279-282.
- Yates,S.L., Burgess,L.H., Kocsis-Angle,J., Antal,J.M., Dority,M.D., Embury,P.B., Piotrkowski,A.M. & Brunden,K.R. (2000) Amyloid beta and amylin fibrils induce increases in proinflammatory cytokine and chemokine production by THP-1 cells and murine microglia. *J.Neurochem.*, 74, 1017-1025.
- Ye,R.D. (2000) beta-Adrenergic agonists regulate NF-kappaB activation through multiple mechanisms. *Am.J.Physiol Lung Cell Mol.Physiol*, 279, L615-L617.
- Zarow,C., Lyness,S.A., Mortimer,J.A. & Chui,H.C. (2003) Neuronal loss is greater in the locus coeruleus than nucleus basalis and substantia nigra in Alzheimer and Parkinson diseases. *Arch.Neurol.*, 60, 337-341.
- Zhang,C., Baumgartner,R.A., Yamada,K. & Beaven,M.A. (1997) Mitogen-activated protein (MAP) kinase regulates production of tumor necrosis factor-alpha and release of arachidonic acid in mast cells. Indications of communication between p38 and p42 MAP kinases. *J.Biol.Chem.*, 272, 13397-13402.
- Zhang,Y., McLaughlin,R., Goodyer,C. & LeBlanc,A. (2002) Selective cytotoxicity of intracellular amyloid beta peptide1-42 through p53 and Bax in cultured primary human neurons. *J.Cell Biol.*, 156, 519-529.
- Zhang,Z.Y., Zhou,B. & Xie,L. (2002) Modulation of protein kinase signaling by protein phosphatases and inhibitors. *Pharmacol.Ther.*, 93, 307-317.
- Zujovic,V., Schussler,N., Jourdain,D., Duverger,D. & Taupin,V. (2001) In vivo neutralization of endogenous brain fractalkine increases hippocampal TNFalpha and 8-isoprostane production induced by intracerebroventricular injection of LPS. *J.Neuroimmunol.*, 115 , 135-143.

